ივანე ჯავახიშვილის სახელობის თბილისის სახელმწიფო უნივერსიტეტის
პეტრე მელიქიშვილის სახელობის ფიზიკური და ორგანული ქიმიის ინსტიტუტი

IVANE JAVAKHISHVILI TBILISI STATE UNIVERSITY
PETRE MELIKISHVILI INSTITUTE OF PHYSICAL AND ORGANIC CHEMISTRY

პეტრე მელიქიშვილის სახელობის ფიზიკური და ორგანული ქიმიის ინსტიტუტის

შ რ ო მ ე ბ ი

T R A N S A C T I O N S

of Petre Melikishvili Institute of Physical and Organic Chemistry

2019

თბილისი – Tbilisi

ივანე ჯავახიშვილის სახ. თბილისის სახელმწიფო უნივერსიტეტის
პეტრე მელიქიშვილის სახ. ფიზიკური და ორგანული ქიმიის ინსტიტუტი

IVANE JAVAKHISHVILI TBILISI STATE UNIVERSITY
PETRE MELIKISHVILI INSTITUTE OF PHYSICAL AND ORGANIC CHEMISTRY

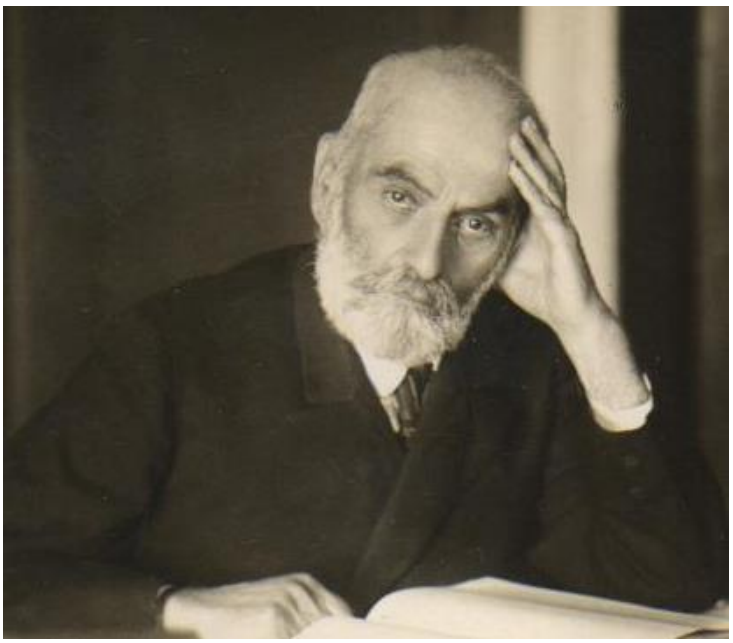

პეტრე მელიქიშვილის სახელობის ფიზიკური და ორგანული ქიმიის ინსტიტუტის

შ რ ო მ ე ბ ი

მიძღვნილი ინსტიტუტის დაარსების 90 წლისთავისადმი

T R A N S A C T I O N S

of Petre Melikishvili Institute of Physical and Organic Chemistry
Dedicated to the 90th anniversary of the Institute

თბილისი – Tbilisi
2019

პეტრე მელიქიშვილის სახელობის ქიმიის ინსტიტუტში შრომათა კრებულების გამოცემა მიმდინარეობდა 1935-63 წლებში, 2009 წელს კი, ინსტიტუტის დაარსებიდან 80 წლის იუბილესთან დაკავშირებით, მიღებული იყო გადაწყვეტილება ინსტიტუტის სამეცნიერო ნაშრომების კრებულის გამოცემის განახლების შესახებ. პირველი კრებული (2010) მიეძღვნა ინსტიტუტის საპატიო დირექტორის, საქართველოს მეცნიერებათა ეროვნული აკადემიის აკადემიკოსის გიორგი ციციშვილის დაბადების 95 წლისთავს, 2015 წლის კრებული კი მის ხსოვნას 100 წლისთავის იუბილესთან დაკავშირებით. წარმოდგენილი კრებული ეძღვნება ინსტიტუტის დაარსების 90 წლის იუბილეს და მასში განხილულია ინსტიტუტის თანამშრომლების მიერ ბოლო წლებში მიღებული სამეცნიერო შედეგები.

რედაქტორი ვლადიმერ ციციშვილი - საქართველოს მეცნიერებათა ეროვნული აკადემიის აკადემიკოსი, ინსტიტუტის სამეცნიერო საბჭოს თავმჯომარე

შემდგენლები : ქეთევან ებრალიძე - ინსტიტუტის დირექტორი
მანანა ბურჯანაძე - ინსტიტუტის სწავლული მდივანი

ივანე ჯავახიშვილის სახ. თბილისის სახელმწიფო უნივერსიტეტის
პეტრე მელიქიშვილის სახ. ფიზიკური და ორგანული ქიმიის ინსტიტუტი
0186 თბილისი, ა.პოლიტკოვსკაიას ქ. # 31; ტელ. 254-15-62

Transactions of the Petre Melikishvili Institute of Chemistry have been published in 1935/63, and decision to resume such edition was passed according to the jubulee of 80th anniversary of the Institute, in 2009. First renewed collection of 2010 was dedicated to 95th anniversary of Giorgi Tsitsishvili, Honorary Director of the Institute, Member of the Georgian National Academy of Sciences, and Transactions of 2015 were dedicated to his memory and 100th anniversary. Presented issue is dedicated to the 90th anniversary of the Institute and includes articles of its scientists results.

Editor Vladimer Tsitsishvili - Membar of Georgian National Academy of Scienses, Head of the Scientific Council

Compilers: Ketevan Ebralidze - Director of the Institute
Manana Burjanadze - Scientific Secretary of the Institute

Petre Melikishvili Institute of Physical and Organic Chemistry
at Ivane Javakhishvili Tbilisi State University
31 A.Politkovskaia str., Tbilisi 0186; tel.: 254-15-62

ISBN 978-9941-8-1656-7

CONTENTS

სტატიების ქართული რეზიუმეები

Recovery of valuable products from Georgian agro-industrial waste

Mzia Tsitsagi*, Imeda Rubashvili, Mariam Chkhaidze, Miranda Khachidze, Manana Buzariashvili, Ketevan Ebralidze, Vladimer Tsitsishvili

Ivane Javakhishvili Tbilisi State University, Petre Melikishvili Institute of Physical and Organic Chemistry, 31 Politkovskaya str., 0186, Tbilisi, Georgia
**E-mail and phone number of the corresponding author*

Abstract. Eco-friendly extraction procedures for the valuable compounds (oils, phenolics, carotenoids, flavonoids) from typical for Georgia agro-industrial waste materials – grape seeds, tomato and onion skin, tangerine and orange peels have been developed. Applying the supercritical fluid extraction, the ultrasound-assisted extraction and other techniques, the effect of the operating pressure, the temperature, the extraction time, the flow rate of supercritical fluid, the sample size, the ultrasound power and the solvent nature used was investigated. The optimal conditions for extraction were found. A rapid, effective and selective high performance liquid chromatographic methods for quantitative determination of extracted compounds were developed and validated with respect to robustness, specificity, linearity-range, accuracy, precision, limit of detection and quantitation as well.

Keywords: Supercritical fluid extraction, ultrasound- assisted extraction, grape seed, tomato onion skin, citrus peel, polyphenol, carotenoid, flavonoid.

INTRODUCTION

Georgia is a developing country, and over the past 15 years, the intensification of agricultural, livestock breeding, industrial and tourist activities has produced an immense increase in the production and accumulation of large amounts of wastes that increase disposal and pollution problems because of their high organic matter content. Generally, agro-industrial wastes are mainly composed of complex polysaccharide/proteins, carbohydrates, polyphenolic constituents, etc. [1].

Currently, different strategies of treatment are applied for the valorisation of the agro-industrial waste such as compost [2], animal feed [3] and bioethanol production [4]. Alternative strategies for the valorisation of agro-industry waste include their exploitation as growth media for biotechnologically useful microorganisms and their related enzymes [5] or as source of biopolymers [6] that should be used in food, cosmetic and pharmaceutical industries. Actually, agro-industrial residues represent a cheap chemical feedstock for extraction of useful products since they are rich in high value added compounds like lipids, fibres, natural pigments [7], carotenoids and antioxidants, as well as bioactive molecules such as polyphenolic compounds.

The basis of Georgia's agriculture is grapes, but citrus, tomato and onion are no less important. Some hundreds of compounds have been identified in grape [8], citrus peels contain essential oil and are very rich in antioxidant phenolic compounds [9], tomato and onion skin is a source of natural colorants [10].

The industrial scale process to obtain grape seed oil includes stages of seed conditioning (cleaning and drying), grinding and oil extraction. The following extraction methods are used: extraction by pressure (cold-pressed or hot pressed oil, the yield is 4-5%wt.), and solvent extraction conventionally using hexane, the yield is 7-8% [11]. The hot water extraction and supercritical fluid extraction (SFE) using carbon dioxide ($SC\text{-}CO_2$) have been proposed as an alternative to extraction with organic solvents [12]. Industrial extraction with supercritical carbon dioxide results in similar yields as the oil extraction through solvent and has a similar quality as cold-pressed product.

SFE eliminates the solvent removal process and subsequent stages of refinement, but this method is rarely used in oil production because the cost of the equipment is high when compared to the extraction with organic solvents or by pressure.

A broad spectrum of extraction techniques is widely used for the early purification of natural products from plant material and microorganisms. Traditional methods including Soxhlet extraction, maceration, percolation and turbo extraction (high speed mixing) are very often time-consuming and require relatively

large quantities of polluting solvents [13]. Nowadays, various pretreatment techniques followed by chromatographic analysis have been developed to extract natural colorants and biologically active compounds from different waste samples.

Accelerated solvent extraction (ASE), also known as pressurized liquid extraction (PLE), involves extraction at constant high pressure, facilitating improved cell permeability, intermolecular physical interactions and penetration of the extracting solvent, and thus improves the mass transfer of substances to be recovered. However, it is difficult to apply PLE to large volumes due to clogging caused by sugars and pectins of plant matrix [13].

Ultrasound-assisted extraction (UAE) is the removal and recovery of organic analytes from a permeable solid matrix by means of a solvent which is energized by sound energy. It is rapid, non-thermal and efficient process, but UAE requires small particle size (≈50 μm) of the sample [14].

Microwave-assisted extraction (MAE) is a simple, rapid and economic method for a large variety of matrices and compounds, requiring a very short extraction time with low amount of solvents, but electromagnetic waves can cause thermal degradation of target compound [13].

Pulsed electric field assisted (PEF) technology is a non- thermal method involving the application of repetitive short high voltage pulses of less than a few milliseconds to a cellular material placed between two electrodes [15]. The high cost of instrumentation prevents its implementation; PEF parameters depend on the electrical conductivity of the sample, and bubbles may cause technical problems.

The main goal of our studies [16] was to establish rational eco-friendly techniques and optimal conditions for the extraction of valuable products from the waste of the agro-industrial sector of Georgia. Grape pomace, orange and tangerine peel, tomato paste waste, and onion skin were the main subjects of research, and oils, phenolic antioxidants and colorants, carotenoids and flavonoids were target products.

MATERIALS & METHODS

A. Materials

Grape pomace has been provided by local wine factories and SMEs from the Kakheti and Imereti regions of Georgia. The raw material was dried at 50-60°C as described in [16] and [17], after which the peel was separated from the seeds by a fan. Separated grape skin was additionally dried in laboratory room under the controlled conditions (20-25°C, and the relative humidity – 30-60 %) and protected from direct sun light.

Ripe tangerine (Citrus Unshiu), orange and tomato were bought in the local agrarian market of Georgia. The peel and skin were manually removed from the selected fruit/vegetable and dried for 14 days in laboratory room under the controlled conditions (the temperature – 20-25°C, the relative humidity – 30-60%) and protected from direct sun light.

The certified analytical standards of cyanidin chloride, kuromanin chloride and β-carotene, the HPLC grade acetone, ethanol, ethyl acetate, acetonitrile, methanol, the analytical grade hydrochloric acid, formic acid and phosphoric acid were supplied by Sigma-Aldrich (Germany). The HPLC/GC grade acetonitrile, methanol, ethanol, acetone, ethyl acetate, acetic acid, dimethyl formamide, dimethyl sulfoxide, 1,2-dichloromethane, *n*-hexane were purchased from Sigma-Aldrich, Merck and Carl Roth (Germany).

The HPLC grade water was prepared using Milli Q Adventage A10 purification system (Merk-Millipore, France).

B. Soxhlet Extraction

The grape seed oil was extracted with the help of the Soxhlet equipped hubs. For each hub of the equipment, 10 g of grinded with an electrical grinder seeds, with the dimension of 1 mm have been used. The extraction was done with hexane and petrol ether at 50-60°C, and repeated 5 times for each variety of seeds.

C. SC-CO_2 Extraction

SC-CO_2 extraction was carried out on a home-built SFE system (Figure 1) including a 500 mL stainless steel extraction vessel (reactor), equipped with CO_2 high pressure pump PM 101 (Germany), and using conventional cylinders for transportation and supply of carbon dioxide.

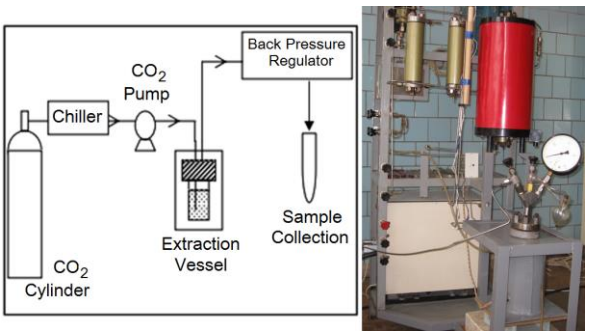

Fig. 1. The scheme and photograph of supercritical fluid extraction laboratory system.

The system operates in the following mode: the carbon dioxide is compressed and chilled at –5°C, liquefied CO_2 is pumped continuously into the extraction vessel in which the previously weighed sample is loaded; The extraction takes place under static equilibrium conditions, at constant temperature and pressure, for a certain time. Dynamic extraction is

carried out by feeding with a certain flow rate the liquefied CO_2 gas or its mixture with co-solvent.

D. UAE and MSE

Ultrasonic P 300 H bath (Elma Schmidbauer, Germany) was used for ultrasound-assisted extraction at 37 and 80 kHz, the temperature was controlled during ultrasonication. IKA C-MAG MS magnetic stirrer (IKA-Werke, Germany) was used for magnetic stirring extraction. The stirring speed was 100 – 1500 rpm and the temperature was 25 – 60°C.

E. Chromatographic analysis

Agilent Quadrupole GC-MS 790B1/5977A system (AG Technologies, USA) was used for the gas chromatography – mass spectrometry (GC-MS) analysis. The chromatographic conditions have been optimized using the fused silica capillary column – HP-5ms (30m × 0.32mm × 0.25μm) [16], [18]. The high performance liquid chromatography (HPLC) analysis was performed using Agilent 1260 Infinity HPLC system (AG Technologies, USA) and an LC-20AD Prominence HPLC system (Shimadzu, Japan). The chromatographic conditions have been optimized using the following columns - RP-18 endcapped Lichrocart 4 x250 mm, 5 μm (Merck-Millipore) and Agilent SB-C18 4.6x250 mm, 5 μm (AG Technologies, USA).

System control, data collection and data processing for GC-MS and HPLC were accomplished using Chemstation software (Hewlett-Packard).

Analytical balance ALX-210 (USA) was used for standard and sample preparation.

All the measuring equipment was appropriately calibrated and qualified.

F. Validation of Developed Methods

All developed methods for HPLC analysis of compounds [19]-[21] were validated according to guideline of the International Council for Harmonization of Technical Requirements for Pharmaceuticals for Human Use (ICH) [22] and other recommendations [23]-[24] with respect to robustness – standard solution stability and filter compatibility test, system suitability test, specificity, linearity-range, accuracy, precision, limit of detection (LOD) and quantitation (LOQ) as well.

RESULTS

Results should be clear and concise, this part of the text can be divided into sections.

A. Grape Pomace Products

According to the data from the Department of Statistics of Georgia, the annual harvest of grapes in the country varies between 170 and 220 thousand tons, out of about 60% is processed at wineries producing up to 25 thousand tons of grape pomace.

To establish the maximum possible yield of oil from Georgian grape seeds, control experiments were carried out by the Soxhlet (Table 1) and SC-CO_2 (Table 2) extraction.

Table 1. The yield of the oil after 8 hours of extraction with hexane and petroleum ether.

Sample #	Grape variety	Place & Manufacturer	Yield (%)
1	Saperavi	Manavi winery	15.8-16.0
2		Kakabeti SE	14.6-15.9
3		Telavi winery	14.5-15.3
4	Rkatsiteli	Manavi winery	14.5-15.6
5		Manavi SE	14.1-15.5
6	Aladasturi	SE in Kakheti region	10.9-11.2
7		SE in Imereti region	9.8-10.8

During the SC-CO_2 extraction, the temperature varied within 40-70°C, the equilibrium pressure from 150 to 300 atmospheres, the time from 15 to 60 minutes, the dynamic pressure from 250 to 300 atmospheres, and the time from 120 to 240 minutes. The maximum oil yield occurs at a dynamic pressure of 300 atmospheres, other optimal parameters are given in Table 2.

Table 2. The highest yield of oil after SC-CO_2 extraction.

Sample #	Tempe-rature (°C)	Equilibrium		Dynamic time (min)	Yield (%)
		Pressure (atm)	Time (min)		
1	60	150	15	180	15.6
2	60	250 – 300	15	240	15.4
3	60	150	15	300	14.7
4	65	150	60	180	14.8
5	60	150	60	180	14.6
6	65	150	60	180	10.5
7	65	150	60	120	9.8

The highest content of oil is revealed for seeds of red grapes of the Saperavi variety, the lowest – for the seeds of red grapes of the Aladasturi variety.

The obtained oil has a greenish-yellow color and a pleasant aroma. The density of the extracted grape seed oil measured at room temperature $d^{20}=928\pm1$ kg/m^3 is slightly higher than that of the olive, rapeseed, corn, coconut and other common oils, it is close to the density of the milkweed oil [25] and the density of the refined sunflower oil. The refractive index n_d^{20} measured at $\lambda=589$ nm and standard temperature varies from 1.4723 and 1.4726, and is typical for vegetable oils. The low-yield oil from the Aladasturi variety has the largest iodine (up to 144 g/100g) and acid (up to 4.1 mg/g) numbers, other samples are typical for vegetable oils indicators of unsaturation (126 – 131 g/100g) and the number of carboxylic acid groups (1.67 – 1.91 mg/g). According

to the saponification value as a measure of the average molecular weight, the oil isolated from grape seeds of the Rkatsiteli variety is characterized by long chain fatty acids. The average content of fatty acids in the extracted oil is given in Table 3.

Table 3. The composition of grape seed oil.

Fatty acid	Type	Content (%)
Linoleic	ω-6 unsaturated	72 – 76
Oleic	ω-9 unsaturated	15 – 16
Palmitic	Saturated	up to 7
Stearic	Saturated	up to 4
α-Linoleic	ω-3 unsaturated	up to 1
Palmitoleic	ω-7 unsaturated	up to 1

The oil extracted from the Georgian grape varieties in terms of its characteristics and composition can be used both in the food industry and in perfumery. Results of feasibility study on production of grape seed oil by eco-friendly non-solvent technologies (pressing and SFE extraction) including financial analysis of investment, the creation and operation of a SME with annual capacity up to 2 thousand tons is given in [16].

Grape pomace contains phenolics due to an incomplete extraction during the winemaking process. Phenolics are secondary plant metabolites with potential beneficial effects on human health because of their antioxidant activity and antimicrobial, antiviral, and anti-inflammatory properties.

The extraction of phenolic antioxidants [26] from the seeds of Georgian red grape varieties Saperavi (pomace samples 1-3) and Aladasturi (pomace samples 6,7) was performed using methanol, ethanol and mixture of ethanol to water 1:1 as solvents and under various conditions of pH, solvent to sample ratio and extraction period, at ambient temperature as described in [18], and the SFE was carried out using CO_2 – ethanol – water mixtures as solvents. Ethanol has a higher critical temperature (513.9K) and lower critical pressure (60.6 atm) than carbon dioxide, while the density of critical ethanol is almost two times lower.

Table 4. Content of polyphenols extracted from Georgian red grape seeds by different solvents.

Sample #	Methanol	Ethanol	Ethanol: water	SC-CO_2
1	17.5	20.5	21.3	19.1
2	19.0	21.4	22.0	20.5
3	21.5	24.2	24.2	25.5
6	8.75	14.6	14.4	15.0
7	9.0	15.0	15.0	15.4

Table 4 shows the highest phenol yields (mg/g GAE) obtained under optimal extraction conditions, the SC-CO_2 method (one hour static extraction at 60-65^{o}C and 150 atm, followed by 300 atm at a flow rate 2 mL/min during 2 hr) is effective for samples with a relatively low content of phenols.

In another series of experiments the recovery of polyphenols from the Saperavi SC-CO_2-deoiled grape seeds was carried out using SC-CO_2 modified with ethanol-water mixture (40%), varying temperature and extraction time. The maximum polyphenol yield, 285 mg/g GAE, was reached at the ethanol/water ratio 2:1, extraction time of 60 minute and temperature of 80^{o}C.

Polyphenols were also isolated from the skin of grape Saperavi, extraction with the ethanol : water mixture gives a slightly higher yield (~90 mg/g) than SFE (~80 mg/g).

B. Anthocyanins of Red Grape Saperavi

Anthocyanins attracted considerable attention because of their antioxidant activity [27],[28]. They protect against oxidative damage from radical reactive species by various mechanisms that ultimately result in the neutralization of free radicals. Owing to the anthocyanin's positive charge and aromatic hydroxyl groups (Figure 2), these compounds can easily donate protons to the free radicals [29]).

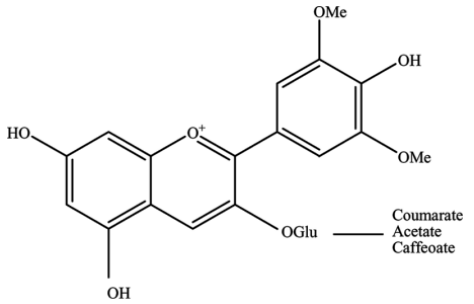

Fig. 2. Chemical structure of the major anthocyanins in red grape.

The objective of the study was to develop and validate extraction procedures of anthocyanins from grape skin using the ultrasound-assisted extraction (UAE), magnetic stirring extraction (MSE) and the supercritical fluid extraction (SFE) techniques.

The effect of the operating pressure and the temperature, extraction time, the flow rate of the SC-CO_2, the sample size and the nature of solvent used was investigated to develop the sequential extraction procedure and establish their optimal parameters.

The effect of pressure on the recovery of anthocyanins at a constant temperature is a function of amount of SC-CO_2. The solubility of target analytes increased with increase of pressure. The content of total antocyanins decreases at the higher extraction temperature at a constant pressure, also the recovery of target compounds increases with increase of the extraction time at a constant temperature as well. The use of co-solvent – ethanol/water (50:50 v/v) at pH 4 increases the recovery of antocyanins.

The optimal parameters for SC-CO_2 extraction with co-solvents (acetone/water, ethanol/water, and ethyl acetate/ water acidified by hydrochloric acid) are: the extraction pressure – 200 atm, temperature – 50°C, the equilibrium extraction time – 180 min, the dynamic extraction time – 60 min, the flow rate of SC-CO_2 – 2 mL/min.

Ultrasonocation and magnetic stirring result in exponential increase of antocyanins recovery, most of target products extracted during the $^2/_3$ of total extraction time. It was observed that the influence of composition of solvents mixture (acetone/water, ethyl acetate/water and ethanol/ water, from 50 : 50 to 90 :10 v/v) was important.

The optimal parameters for the three-step extraction UAE (37 kHz) and MSE procedures are as follows: the extraction time – 30 min, solvent mixtures – acetone/water (70 : 30 v/v) and ethanol/water (50 : 50 v/v) acidified by hydrochloric acid, the temperature of UAE is 25 and 50 °C, respectively, and 60 °C for both mixtures at MSE.

The content of total anthocyanins was determined by developed and validated HPLC analysis method [21], the results are given in Table 5, the Figure 3 shows typical chromatogram obtained with the extract sample solution containing target products, kuromanin and cyanindin chlorides.

Table 5. The content of anthocyanins in grape skin.

Extraction technique	Total anthocyanins (μg/g) in dried grape skin
UAE	2.50 – 51.81
SFE	2,70 – 70.78
MSE	4.06 – 56.00

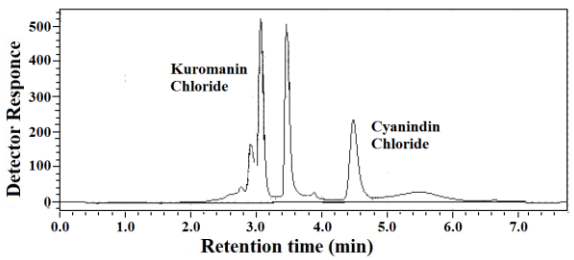

Fig. 3. Chromatogram of the extract sample solution.

Used eco-friendly separation procedures provide high quality of target compounds and can be used to develop a standard technological process for utilization of agro-industrial waste material – grape skin.

C. Bioactive Compounds of Tangerine Peel

Essential oil (D-limonene), carotenes and flavanones were extracted from tangerine peel by increasing the polarity of the supercritical fluid using different co-solvents with the carbon dioxide in stepwise SC-CO_2 extraction (Figure 4) followed by recovery of flavanone hesperidin ($C_{28}H_{34}O_{15}$) from extract and vegetable agglutinate hetero-polysaccharide pectin from dry residue [20].

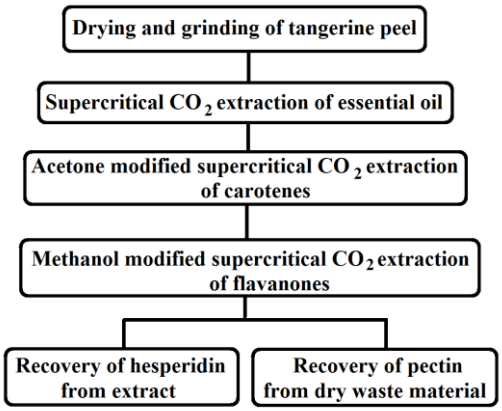

Fig. 4. The scheme of sequential stepwise processing of tangerine peel.

According to the GC-MS data, the yield of essential oil from dry tangerine peel at subcritical conditions is lowest, but most selective. As the temperature, pressure and extraction time increases, yield of oil increases, but selectivity drastically reduces. The essential oil found to extract carotenoids and imparting orange color to the extract. Optimal conditions for β-carotene free tangerine oil are 100 atm pressure and 35°C temperature at 15 min equilibrium time. The yield of the carotene free oil varies from 0.8%wt to 0.9%wt, the principal compound is D-limonene ($C_{10}H_{16}$).

Optimal parameters of the β-carotene isolation at the second stage are: 1 hr equilibrium extraction at 150 atm, 40°C, followed by 1 hr dynamic extraction at a flow rate of 2.0 mL/min. Colorless residue indicated complete extraction of target product, the content of β-carotene varies from 0.445 to 3.972 μg per 1 gram of the dried tangerine peel.

Optimal parameters for the SC-CO_2 extraction of hesperidin are: 1 hr at 250 atm pressure and 60°C temperature at static conditions, and 30 min of dynamic extraction at 2.0 mL/min flow rate. Extracts were collected in ice water pH-4.5, crude product was recrystallized in dimethyl sulfoxide, the yield of IR-identified hesperidin (melting point 252°C) – 1.6-1.8% wt.

Optimal operative conditions for recovery of pectin are pH=1.5, extraction time – 25 min, the temperature – 50°C. Purification of pectin was carried out via alcohol- precipitation procedure (APP) [30-31], and high quality product was obtained.

Alternative conventional low cost extraction procedure was developed for extraction of oil, pectin, hesperidin and carotene bioactive compounds from tangerin peel (Figure 5).

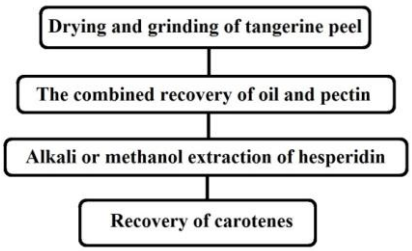

Fig. 5. The scheme of sequential stepwise processing of tangerine peel.

Pectin was extracted at the same time the hydrodistilation of oil from citrus peel took place. Citric acid was added for maintaining pH=1.5. Both alkali and methanol extraction method was used for recovery of hesperidin. Disadvantage of described method is low yield of carotenes in comparison to sequential supercritical CO_2 extraction method.

D. Major Carotenoids of Tomato and Citrus

The objective of the study was to develop sequential extraction procedures for the major carotenoids – beta- carotene and lycopene [32] (Figure 6) from agro-industrial waste materials – tomato skin, tangerine and orange peels using the ultrasound-assisted extraction and the supercritical fluid extraction techniques.

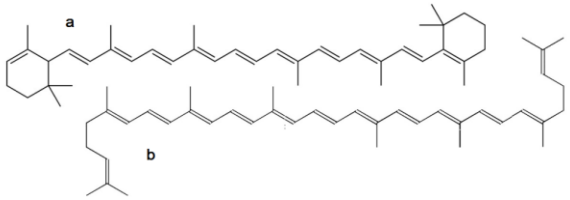

Fig. 6. Chemical structure of β-carotene (a) and lycopene (b).

The effect of pressure on the extraction of carotenoids was investigated in a range of 100 – 250 atm at constant flow rate of SC-CO_2 (2 mL/min) and low temperature (40^{o}C) selected to avoid thermal degradation of target analytes. The effect of temperature was studied up to 60^{o}C, the effect of flow rate – from 1 to 5 mL/min, the effect of sample size in a range of 10 – 50 g per 0.5 L reactor vessel.

The optimal parameters for the two-step extraction procedure are: extraction step I – the sample size 40-45 g, the extraction pressure 150 atm, the extraction temperature 40^{0}C, the dynamic extraction time 30 min, the flow rate of SC-CO_2 2 mL/min; for the extraction step II the extraction pressure is 100 atm, the extraction temperature 40^{0}C, the dynamic extraction time 60 min, the flow rate 2 mL/min, acetone (7%) was used as co-solvent. The obtained collorless residue indicates complete extraction of target compounds.

The results of UAE procedure indicate that the effects of the extraction time (30 – 90 min) and ultrasound power are significant for both analytes. As described above, the recovery of carotenoids increased exponentially in 5-10 minutes, then gradually in 25 minutes and then became constant. Thermal effect plays an important role, the high ultrasonic power (80 kHz) causes isomerization of thermally sensitive target substances. The optimal conditions for the three-step UAE procedure at 37 kHz are: extraction by acetone for 30 min (step I) and for 15 min (step II), extraction by ethyl acetate for 15 min (step III).

The organic extract solutions prepared using the developed supercritical fluid and sequential ultrasonic assisted extraction procedures and were analyzed using the validated HPLC method [19], results are given in Table 6, the Figure 7 shows typical chromatogram obtained with the extract sample solution.

Table 6. The content of beta-carotene and lycopene in dried agro-industrial waste material.

Material	Beta-carotene (mg/g)		Licopene (mg/g)	
	UAE	SC-CO_2	UAE	SC-CO_2
Tomato skin	9.06 – 10.7	8.4 – 12.8	165 – 174	166 – 180
Tangerine peel	26.8 – 31.6	25.6 – 32.2	12.2 – 16.0	11.1 – 17.9
Orange peel	42.0 – 54.6	41.7 – 59.2	8.4 – 9.9	9.6 – 10.6

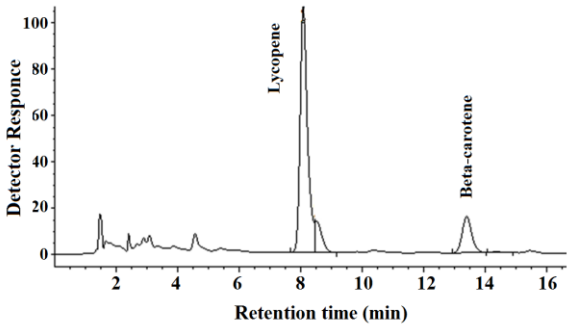

Fig. 7. Chromatogram of the extract sample solution.

E. Quercetin and Colorants from Red Onion Skin

Extraction of flavonol quercetin ($C_{15}H_{10}O_7$) from onion skin by supercritical fluids, modified carbon dioxide [33] and water [34], as well as by MAE and SPE technique [35] is described. Maximum product yield, 0.024 g per kg of dry raw material, was obtained by SC-CO_2 using ethanol as a co-solvent at 40-50^{o}C and 180 atm, microwave assisted extraction and solid-phase separation give ~0.021 g/kg.

UAE was carried out using acetone, ethyl acetate, ethanol, and methanol as a solvent, the acetone was found to be the best solvent for the extraction of

quercetin from the onion skin providing high yield (up to 0.030 g/kg) and best selectivity of target product.

Eco-friendly SC-CO_2 using 6-7% of acetone as a modifier at 40-50^{o}C and 140 – 150 atm gave a yield of 0.028 g/kg.

SC-CO_2 modified with ethanol/acetic acid (80:1) at a pressure of 300 atm and temperature 80^{o}C was used for extraction of anthocyanidin (Figure 7) colorants, listed in the Table 6. Total anthocyanins amount in onion skin quantified by Folin-Ciocalteu's method is in a range of 85 – 107 mg/g, in accordance with published results [36].

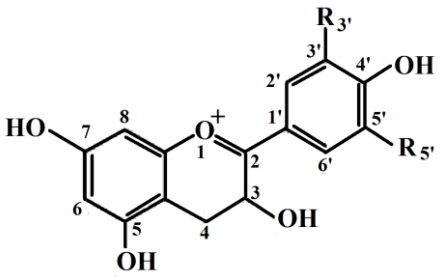

Fig. 7. Basic structure of extracted anthocyanidins.

Table 6. Anthocyanidins extracted from the red onion skin.

Anthocyanin	Color	$R^{3'}$	$R^{5'}$
Cyanidin	Violet (at pH 7-8)	–OH	–H
Delphidin	Blue-red	–OH	–OH
Pelargonidin	Orange	–H	–H
Malvidin	Blue	$–OCH_3$	$–OCH_3$
Peonidin	Purplish-red	$–OCH_3$	–H
Petunidin	Dark red	–OH	$–OCH_3$

CONCLUSION

In Georgia, it is possible to organize SMEs for the processing of agro-industrial wastes and their profitable operation; for the recovery of valuable products should be applied sequential stepwise schemes using various modern methods of extraction.

REFERENCES

[1] Mohd Y., "Agro-industrial waste materials and their recycled value-added applications: Review", in *Handbook of Ecomaterials*, (Ed. Martínez L. M. T.), Springer International Publishing, 2017, pp. 1-11

[2] Lopez-Real J. M., "Composting of agricultural wastes", in *The Science of Composting*, (ED. de Bertoldi M., Sequi P., Lemmes B., Papi T.), Springer: Dordrecht, South Holland, 1996, pp. 542-550.

[3] Venglovsky J., Martinez J., Placha I., "Hygienic and ecological risks connected with utilization of animal manures and biosolids in agriculture", *Livestock Science*, 2006, vol. 102, no. 3, pp. 197-203.

[4] Sarkar N., Ghosh S. K., Bannerjee S., Aikat K., "Bioethanol production from agricultural wastes: an overview", *Renewable Energy*, 2012, vol. 37, no. 1, pp. 19-27.

[5] Di Donato P., Fiorentino G., Anzelmo G., Tommonaro B., Nicolaus B., Poli A., "Re-use of vegetable wastes as cheap substrates for extremophile biomass production", *Waste and Biomass Valorization*, 2011, vol. 2, no. 2, pp. 103-111.

[6] Lemes A. C., Sala L., Ores J. D., Braga A. R., Egea M. B., Fernandes K. F., "A review of the latest advances in encrypted bioactive peptides from protein-rich waste", *International Journal of Molecular Sciences*, 2016, vol. 17, no. 6, pp. 950-574.

[7] Yusuf M., Shabbir M., Mohammad F., "Natural colorants: historical, processing and sustainable prospects". *Natural Prododucts and Bioprospecting*, 2017, vol. 7, no. 1, pp. 123-145.

[8] Iriti M., Vitalini S., "Chemical diversity of grape products, a complex blend of bioactive secondary metabolites", *Natural Products Journal*, 2011, vol. 1, no. 1, pp. 71-74.

[9] Al-Yuhaimi F. Y., "Citrus fruits by-products as sources of bioactive compounds with antioxidant potential", *Pakistan Journal of Botanics*, 2014. vol. 46, no. 4, pp. 1459-1462.

[10] Elbadrawy E., Sello A., "Evaluation of nutritional value and antioxidant activity of tomato peel extracts", *Arabian Journal of Chemistry*, 2016, vol. 9, no. 2, pp. S1010-S1018.

[11] Luque-Rodríguez J. M., Luque de Castro M. D., Pérez-Juan P., "Extraction of fatty acids from grape seed by superheated hexane", *Talanta*, 2005, vol. 68, pp. 126-130.

[12] Gómez A. M., López C. P., De la Ossa E. M., "Recovery of grape seed oil by liquid and supercritical carbon dioxide extraction: A comparison with conventional solvent extraction", *The Chemical Engineering Journal and the Biochemical Engineering Journal*, 1996, vol. 61, no. 3, pp. 227-232.

[13] Martino K. G., Guyer D., "Supercritical fluid extraction of quercetin from onion skins", *Journal of Food Process Engineering*, 2004. vol. 204, no, 27, pp. 7-28.

[14] Chemat F., Rombaut N., Sicaire A.-G., Meullemiestre A., Fabiano-Tixier A.-S., Abert-Vian M., "Ultrasound assisted extraction of food and natural products. Mechanisms, techniques, combinations, protocols and applications. A review", *Ultrasonics Sonochemistry*, 2017, vol. 34, pp. 540-560.

[15] Ricci A., Parpinello G. P., Versari A., "Review. Recent advances and applications of pulsed electric fields (PEF) to improve polyphenol extraction and color release during red winemaking", *Beverages*, 2018, vol. 4, no. 18, pp. 1-12.

[16] Tsitsishvili V., Tsitsagi M., Rubashvili I., Ebralidze K., *Extraction of valuable products from agro-industrial waste materials*, LAP LAMBERT Academic Publishing, 2018, 90 p.

[17] Kvartskhava G., Tsitsagi M., Chkhaidze M.. Khachidze M., Jinikashvili I., "Utilization of winery wastes by using supercritical CO_2", *Proceedings of the Georgian National Academy of Sciences, chemical series*, 2010, vol. 36, no. 2, pp. 149-152.

[18] Tsitsagi M., Chkhaidze M., Khachidze M., Buzariashvili M., Ebralidze K., Ramishvili Ts., Tsitsishvili V., "Sequential supercritical fluid extraction of essential oil, carotenoids and bioflavanoids from tangerine (Citrus Unshiu) peel". *Proceedings of the Georgian National Academy of Sciences, chemical series*, 2015, vol. 41, no. 3, pp. 248-250.

[19] Rubashvili I., Tsitsagi M., Ebralidze K., Tsitsishvili V., Eprikashvili L., Chkhaidze M., Zautashvili M., "Extraction and analysis of the major carotenoids of agro-industrial waste materials using sequential extraction techniques and high performance liquid chromatography", *Eurasian Journal of Analitical Chemistry*, 2018, vol. 13, no. 3, em06, pp. 1-14.

[20] Tsitsagi M.. Chkhaidze M., Ebralidze K., Rubashvili I., Tsitsishvili V., "Sequential extraction of bioactive compounds from tangerine (Citrus Unshiu) peel", *Annals of Agrarian Science*, 2018, vol. 16, no. 2, pp. 236-241.

[21] Rubashvili I., Tsitsagi M., Tsitsishvili V., Kordzakhia T., Ebralidze K., Buzariashvili M., Khachidze M., "Sequential extraction and HPLC analysis of total anthocyanins of grape skin", *The Chemist, Journal of the American Institute of Chemists*, 2019, vol. 91, no. 2, pp. 33-41.

[22] Harmonized Tripartite Guideline: Validation of Analytical Procedures: Text and Methodology, International Conference on Harmonization Q2(R1), Genova, November 2005, pp. 1-13.
[23] Guide for Evaluation of Uncertainty in Calibration, International accreditation service, Brea, CA, USA, January 2016, pp. 1-11.
[24] Validation of Compendial Procedures, first supplement to USP 40-NF 35, The U.S. Pharmacopeia national formulary, United Book Press, Baltimore, 2017, pp. <1225>1-6.
[25] Noureddini H., Teoh B. C., Davis Clements L., "Densities of vegetable oils and fatty acids", *Journal of the American Oil Chemists' Society*, 1992, vol. 69, no. 12, pp. 1884-1888.
[26] Lafka T.-I., Sinanoglou V., Lazos E. S., "On the extraction and antioxidant activity of phenolic compounds from winery wastes", *Food Chemisrtry*, 2007, vol. 104, no. 3, pp. 1206-1214.
[27] Wu X., Beecher G. R., Holden J. M., Haytowitz D. B., Gebhardt S. E., Prior R. L., "Concentrations of anthocyanins in common foods in the United States and estimation of normal consumption", *Journal of Agricultural and Food Chemistry*, 2006, vol. 54, no. 11, pp. 4069-4075.
[28] Ghassempour A., Heydari R., Talebpour Z., Fakhari A. R., Rassouli A., Davies N., Aboul-Enein H. Y., "Study of new extraction methods for separation of anthocyanins from red grape skins: Analysis by HPLC and LCMS/MS", *Journal of Liquid Chromatography and Related Technologies*, 2008, vol. 31, no. 17, pp. 2686-2703.
[29] Huang D., Ou B., Prior R. L., "The chemistry behind antioxidant capacity assays", *Journal of Agricultural and Food Chemistry*, 2005, vol. 53, no. 6, pp. 1841-1856.
[30] Shaha R.K., Punichevana Y.N.A.P., Afandi A., "Optimized extraction conditions and characterization of pectin from Kaffir lime (*Citrus hystrix*)", *Research Journal of Agriculture and Forestry Sciences*, 2013, vol. 1, no. 2, pp. 1-11.
[31] Devi W.E., Shukla R.N., Abraham A., Jarpula S., Kaushik U., "Optimized extraction condition and characterization of pectin from orange peel", *International Journal of Research in Engineering and Advanced Technology*, 2014, vol. 2, no. 2, pp. 1-9.
[32] Choksi P. M., Joshi V.Y., "A review on lycopene – extraction, purification, stability and applications", *International Journal of Food Properties*, 2007, vol. 10, no. 2, pp. 289-298.
[33] Martino K. G., Guyer D., "Supercritical fluid extraction of quercetin from onion skins", *Journal of Food Process Engineering*, 2007, vol. 27, pp. 7-28.
[34] Ko M.-J., Cheigh C.-I., Cho S.-W., Chung M.-S., "Subcritical water extraction of flavonol quercetin from onion skin", *Journal of Food Engineering*, 2011, vol. 102, no. 4, pp. 327-335.
[35] B. Kumar, K. Smita, B. Kumar, L. Cumbal, and G. Rosero, "Microwave-assisted extraction and solid-phase separation of quercetin from solid onion (Allium cepa L.)," *Separation Science and Technology*, vol. 49, no 16, pp. 2502-2509, 2014.
[36] Prior R., Wu X., Schaich K., "Standardized methods for the determination of antioxidant capacity and phenolics in foods and dietary supplements", *Journal of Agricultural and Food Chemistry*, 2005, vol. 53, no. 10, pp. 4290-4302.

საქართველოს აგროსამრეწველო ნარჩენებიდან სასარგებლო პროდუქტების გამოყოფა

მზია ციცაგი*, იმედა რუბაშვილი, მარიამ ჩხაიძე, მირანდა ხაჩიძე, მანანა ბუზარიაშვილი, ქეთევან ებრალიძე, ვლადიმერ ციციშვილი

ივანე ჯავახიშვილის სახ. თბილისის სახელმწიფო უნივერსიტეტის პეტრე მელიქიშვილის სახ. ფიზიკური და ორგანული ქიმიის ინსტიტუტი, ანა პოლიტკოვსკაიას ქ. 31, თბილისი 0186
**პასუხისმგებელი ავტორის ელექტრონული პოსტის მისამართი და ტელეფონი*

რეზიუმე. შემუშავებულია სასარგებლო ნივთიერებების (ზეთები, ფენოლური ნაერთები, კაროტინოიდები, ფლავანოიდები) გამოყოფა საქართველოს აგროსამრეწველო ნარჩენებიდან - როგორიცაა ყურძნის წიპწა, პომიდვრის და ხახვის კანი, მანდარინის და ფორთოხლის ქერქი - ეკო-მეგობრული ექსტრაქციის მეთოდებით. გამოყენებული იქნა სუპერკრიტიკული ფლუიდებით და ულტრაბგერითი ექსტრაქციის და სხვა ტრადიციული მეთოდები. შესწავლილია სუპერკრიტიკული ფლუიდების ოპერეტიული წნევის, ტემპერატურის, ექსტრაქციის დროის და დინების სიჩქარის, აღებული ნიმუშის ზომის, ულტრაბგერის სიმძლავრის და გამხსნელის ბუნების გავლენა ექსტრაქციის შედეგებზე და შემუშავებულია ექსტრაქციის ოპტიმალური პირობები. სწრაფი, სელექტიური და მაღალეფექტური სითხური ქრომატოგრაფიის მეთოდებით მოხდა ექსტრაგირებული ნივთიერებების რაოდენობის განსაზღვრა და დასაბუთდა მათი სიდიდე, სპეციფიურობა, სწორხაზოვნების დონე (არეალი), სიზუსტე , გამოვლენის საზღვრები.

Catalytic conversion of linalool and geraniol on micro-mesoporous BEA-type zeolites

Tsiuri Ramishvili[1], Vladimer Tsitsishvili[1*], Irina Ivanova[2], Irina Dobryakova[2]

[1] *Petre Melikishvili Institute of Physical and Organic Chemistry at Ivane Javakhishvili Tbilisi State University, 31 A.Politkovskaia str., Tbilisi 0186, Georgia*
[2] *Chemistry Department, Laboratory of Kinetics and Catalysis, Lomonosov Moscow State University, 1-3 Leninskiye Gory, 119991 Moscow, Russia*
**v.tsitsishvili@gmail.com +995 599 988198*

Abstract. The catalytic conversion of tertiary terpenic alcohols linalool and geraniol on samples of the BEA type microporous zeolites and on their modified micro-mesoporous forms has been studied. Conversion of linalool in inert atmosphere at 60–170 ˚C gives products of isomerization, dehydration, cyclization and condensation; the conversion degree and selectivity of the formation of nerol and geraniol are low. Mesopores lead to a significant increase in conversion of linalool and a slight growth in selectivity, mainly determined by weak acid sites in zeolite. Conversion of geraniol gives β-linalool, trans,trans-farnesol and (2E,6E)-6,11-dimethyl-2,6,10-dodecatrien-1-ol, as well as small quantities of β-myrcene, D-limonene, trans-β-ocymene, β-ocymene, α-terpineol, cis-geraniol (nerol), cis-isogeraniol, trans,trans,trans-geranylgeraniol, p- and m-camphorene (Dimircene), and unidentified isomer of trans-geranylgeraniol. It is established, that by one-pot method in "zeolitic reactor" it is possible not only to receive long-chain $C_{14} – C_{20}$ molecules, but to produce macrocycles.

Keywords: condensation, cyclization, dehydration, isomerization.

INTRODUCTION

Geraniol (3,7-dimethyl-trans-2,6-octadiene-1-ol) and and its cis-isomer nerol are valuable aromatic substances having subtle perfume of rose aroma and used in perfumery, as well as "building units" in syntheses of A, E and K vitamins, carotenoids, ionones and methyl-ionones [1,2]. About 10% of worldwide annual production of aromatics (10,000 tons) falls on geraniol [2].

Commercial production of geraniol and nerol generally is based on the catalytic liquid-phase isomerization of linalool (3,7-dimethyl-1,6-octadiene-3-ol), extracted from Lavandula flowers, Coriandrum sativum seeds, or α- and β–pinene obtained from coniferous wood, as well as received using multistage chemical ways. Both isomers – geraniol and nerol are obtained from linalool by 1,3-migration of the OH-group and appropriate shift (allylic rearrangement) of the double bond (Fig. 1).

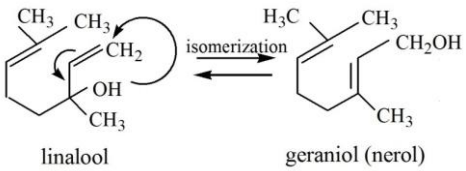

Fig. 1. Isomerization of linalool.

Today there are no catalysts for linalool regioselective isomerization; only the microbial transformation of linalool to geraniol without nerol formation is described [3]. Catalytic isomerization of linalool in the mixture of geraniol and its geometric isomer nerol is a reversible process; initially it was conducted in the presence of homogenous catalysts H_2SO_4, H_3PO_4 or gaseous HCI and HBr, or else in the presence of mixture of acetic acid and acetic anhydride; afterwards alyllic rearrangement was realized in the presence of oxo-compounds of transition metals (V,Mo,W,Re,Nb) [4], and catalytic system of alkyl orthovanadate $(RO)_3V=O$ and tetrabutylammonium hydroxide $[(Bu)_4N^+]$ OH was testified as the most stable and having high selectivity at 100-240˚C temperature [5]. In comparison with vanadium-containing catalysts, complexes of tungsten oxo (VI) alkoxides [6] are less toxic, but product yield is low and hydrolysis of catalysts easily occurs. In manufacturing process nerol is obtained via geraniol isomerization by heating with alkali.

Negative aspects of abovementioned catalytic processes of linalool isomerization reactions: namely, multistaging of processes, low regioselectivity, problem with products' separation, abundance of waste waters, excessive expenses for neutralization of alkalis and acids, difficulties related to preparations of catalysts and their multiuse, as well as their toxicity are among biggest challenges.

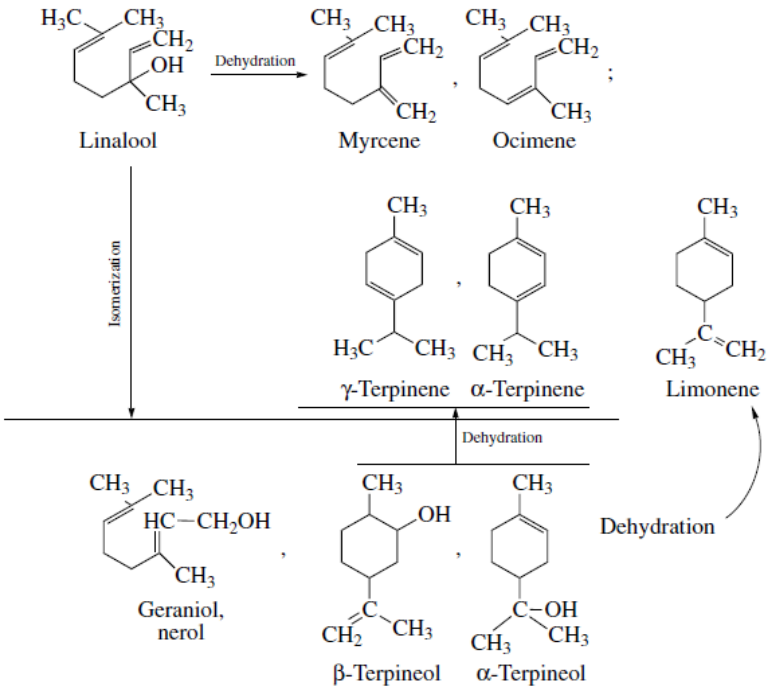

Fig. 1. Linalool conversion reactions on zeolites.

.

The allyl rearrangement of linalool on H- and dealuminated forms of zeolites FAU(Y), BEA, MOR, and OFF with large pores, as well as on mesoporous MCM-41 at 100–180 ˚C is complicated by linalool dehydratation, cyclization and condensation [7, Fig.2].

Low selectivity for geraniol and nerol on zeolitic catalysts is due to the fact that isomerization of linalool's bulky molecules (e.g., for linalool molecular sizes are 9.0 x ~5.8 Å) takes place mainly on the outer shell of the zeolites [7].

The wide-pore, high-silica zeolite beta, also called BEA type zeolite was first synthesized in 1967, today it is a commercial product and an excellent catalyst for a wide number of acid-catalyzed reactions. According to the data of the International Zeolite Association [8], crystal chemical formula of zeolite beta is $|Na_7|$ **[**$Al_7Si_{57}O_{128}$]-***BEA**, its microporous structure is a hybrid of two intergrowing polymorphs termed A and B [9] and having the three-dimensional 12-membered ring pore system with two straight channels, each with a cross section of 0.77 x 0.66 nm, parallel to [100] and [010], and a channel of 0.56 x 0.56 nm, which runs along the [001] direction. The polymorphs grow as two-dimensional sheets and the sheets randomly alternate between the two. The intergrowth of the polymorphs does not significantly affect the pores in X and Y dimensions, but in the Z direction of the faulting, the pore becomes tortuous, but not blocked. The hypothetical polymorph A is depicted in Fig. 2, where cross sections of channels are also shown.

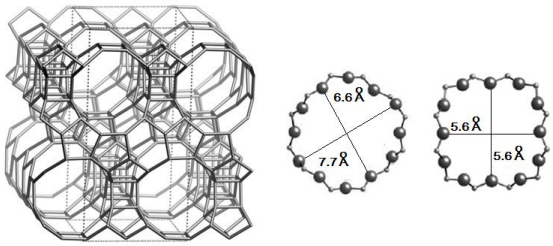

Fig. 2. The polymorph A of BEA framework viewed along [010] and cross sections of wide and tortuous channels [8].

It is known, that the catalyst is more effective when the crystals are small or when a secondary porous network exists in the material, thereby allowing shorter diffusion paths. Several studies have demonstrated the beneficial effect of steaming and acid leaching on the performance of zeolite beta, and it was concluded, that hydrothermal treatment of a macrocrystalline BEA results in the formation of secondary mesoporous structure [10,11].

We used the micro-mesoporous composite zeolite materials synthesized from the BEA type zeolites [12] for the catalytic conversion of tertiary terpene alcohol linalool (**(±)**-3,7-Dimethyl-1, 6-octadien-3-ol). The goal was to establish the relationship between the porosity and acidity and the selectivity of the formation of linalool isomerization products– primary alcohols geraniol and nerol [13].

Our next research [14] has been devoted to consideration of catalytic transformations of geraniol on the same zeolites characterized by different chemical (SiO_2/Al_2O_3 ratio, total acidity) and structural (surface area, micro and meso pore volumes, amount of weak and strong acid centers) properties. It has been established that along with products of isomerization-cyclisation ($C_{10}H_{18}O$) and dehydration ($C_{10}H_{16}$) some substances $C_{14} – C_{20}$ with higher molecular mass are formed. Discussion of opportunities of formation of long chains and macrocycles on micro- and micro-mesoporous BEA-type zeolite was a main objective of our subsequent article [15], and consideration of synergic actions of BEA-type zeolites and ultrasonic irradiation in the conversion of geraniol [16] completed our research.

The purpose of this contribution is to summarize our work on the study of catalytic conversion of linalool and geraniol on micro-mesoporous BEA-type zeolites.

MATERIALS & METHODS

A. Reagents

Racemic linalool (97-98%, FG containing 1.12% 1,2-dihydrolinalool), geraniol (97%), nerol (97%) and methanol (for HPLC, ≥99.9%) were purchased from Sigma-Aldrich. Argon and nitrogen (99.999 % pure) were used as the reaction medium.

B. Preparation and charactrization of catalysts

Zeolites BEA-25 and BEA-150 (Zeolyst International, batchs CP-814-E2200-19 and CP-811-E 1822-75) were used in NH_4- and H-forms, respectively. The micro-mesoporous materials named RBEA-25 and RBEA-150 have been synthesized by recrystallization of corresponding zeolites BEA-25 and BEA-150 in NaOH aqueous solution as described in [17, 18].

The chemical composition of the catalysts was determined using X-ray fluorescence analysis on a Thermo Scientific ARL Perform'X instrument equipped with a 3.5-kW rhodium tube.

Nitrogen adsorption-desorption isotherms were measured at 77 K on an automated porosimeter ASAP 2000 (Micromeritics, USA). Specific surface area was calculated by the Brunauer-Emmet-Teller (BET) method; the micropore volume was determined using the *t*-plot method. The pore volume, which takes into account adsorption in micropores and mesopores and on the external surface, was calculated from the amount of nitrogen adsorbed at a relative pressure of $p/p_0 = 0.95$.

The acid properties of catalysts were estimated using temperature-programmed desorption of ammonia (TPD NH_3) on a USGA-101 multipurpose sorption gas analyzer.

C. Catalytic activity and analyzes of products

Experiments have been carried out on the H-forms of BEA-zeolites preliminary calcined for 2 hours at 550˚C in a stream of purified air, and the NH_4-form ─ under the same conditions, but for 6 hours in the program mode.

Catalytic conversion of both terpene alcohols was performed in the liquid phase in a 50 ml three-necked round bottomed glass flask with a reflux condenser, thermometer and a port for input of an inert gas.

In the presence of solvents (methanol and ethanol), the conversion of terpene alcohol is complicated by side processes, so following experiments were carried out under solvent-free condition at temperatures in the range of 60 –170 °C and in an atmosphere of inert gases (nitrogen or argon); duration of run was from 0.5 – 3 h, the catalyst mass 0.010 – 0.050 g, mass ratio of catalyst : linalool was from $^1/_{129}$ to $^1/_{26}$ (0.84 – 0.17 mole of linalool per gram of catalyst). Reagent and catalyst were stirred by a magnetic stirrer with heater. Catalytic experiments on geraniol conversion were conducted at temperatures in the range of 27-150 °C and under ambient pressure; duration of run was 1-2 h, catalyst mass – 0.01-0. 07 g, mass ratio of catalyst: geraniol was 1/133 -1/19 respectively, i.e. 0.86-0.12 mol geraniol/g of catalyst.

The catalyst was separated from the reaction products using centrifugation. The catalytic properties were characterized by the conversion of linalool or geraniol and the selectivity of the formation of isomerization products.

The analysis of products of catalytic reactions was carried out by the gas chromatography – mass-spectrometry (GC-MS) methods (Agilent Technologies, 5890B/5977A, capillary column HP-5ms, Ultra Inert, 30 m x 0.32 mm x 0.25 μm), analyzed in program mode: hold at 80 ˚C for 5 min, ramp to 210 ˚C at 30˚/min, hold at 210˚C for 10 min. The amounts of linalool, geraniol and nerol was determined from the calibration data.

The relative content of the reaction products (C_i, %) was determined using geraniol as an internal standard, also the amount of linalool, geraniol, and nerol was determined from corresponding calibration curves. Conversion of geraniol was calculated by the formula: $C_{geraniol}=(\mathbf{m}_{initial\ geraniol} - \mathbf{m}_{unconverted\ geraniol})\times 100/\mathbf{m}_{initial\ geraniol}$; the yield ($Y_i$, %) and selectivity to products (S_i, %) were determined according to the following formulas, respectively: $Y_i=C_i\times M_{geraniol}\times 100/97\times M_i$, $S_i=100\times Y_i/C_{geraniol}$, where $M_{geraniol}$ is molar mass of geraniol, 97% – its initial concentration, **m** is the mass of substance.

RESULTS

The results include characterization of catalysts, their catalytic properties in linalool conversion reaction, and geraniol conversion data.

A. Characterization of catalysts

The adsorption-desorption isotherms of nitrogen for initial zeolites BEA-25 and BEA-150 (Fig. 3) represent a combination of type I and IV curves (according to IUPAC classification); at a low relative pressure ($p/p_0 \leq 0.2$) they are typical for adsorption in micropores; the hysteresis loop at $p/p_0 = 0.7$─1.0 is associated with the filling of the intercrystalline space [13, 14].

Isotherms of recrystallyzed samples RBEA-25 and RBEA-150 (Fig. 4) show a jump at $p/p_0 = 0.3$-0.4 indicating the presence of mesopores.

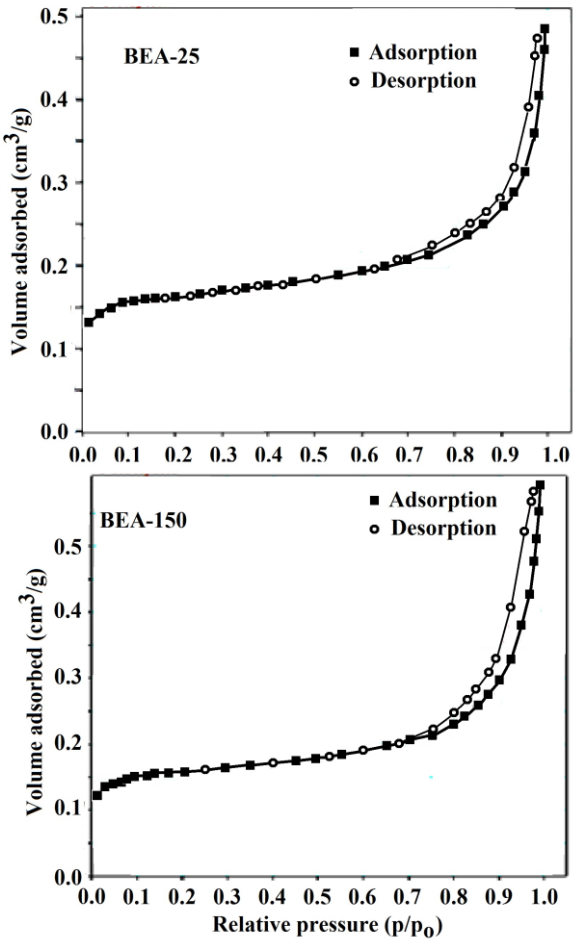

Fig. 3. N_2 adsorption-desorption isotherms on initial zeolites.

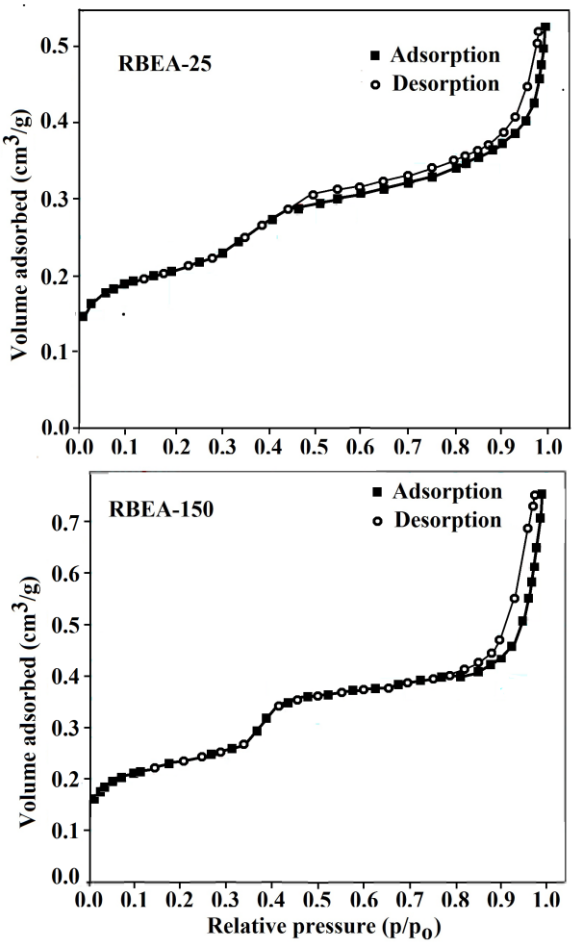

Fig. 4. N_2 adsorption-desorption isotherms on recrystallized zeolites.

The total acidity $a_0(NH_3)$ expressed as ammonia specific sorption capacity is 1200 and 180 μmol/g for BEA-25 and BEA-150, respectively, and as a result of recrystallization, this value changes slightly – decreases to 1179 and increases to 233 μmol/g for RBEA-25 and RBEA-150, respectively.

The thermo-programmed desorption (TPD) curves of ammonia in the temperature range 100 – 700 ˚C (Fig. 5) have two maxima, corresponding to the presence in the catalysts of two types of acid sites – maximum desorption of ammonia at a temperature of about 200˚C occurs from relatively weak acid sites, desorption of ammonia at temperatures above 300-350˚C occurs from stronger sites.

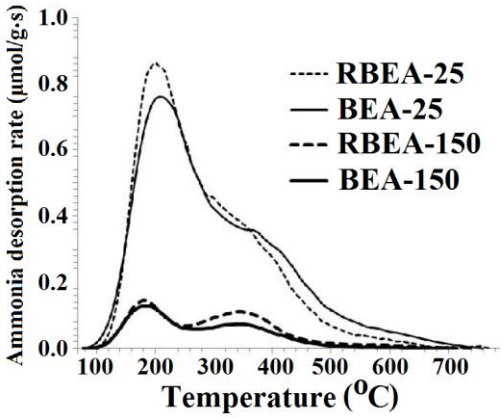

Fig. 5. Ammonia temperature desorption spectra.

Characteristics of initial (BEA) and recrystallized (RBEA) samples of beta-type zeolites are summarized in the Table 1, where [Si/Al] is molar ratio of SiO_2/Al_2O_3 in zeolite structure, S_{BET} (m^2/g) is specific surface area calculated by the BET method from the nitrogen adsorption isotherms, V (m^3/g) is total specific pore volume, $v_{micro} = V_{micro}/V$ is the micropore volume fraction, $v_{meso} = V_{meso}/V$ is the mesopore volume fraction, and a_0 (μmol/g) is total acidity including acidity of weak and strong acid sites, a_w (μmol/g) and a_s (μmol/g), respectively, evaluated from the ammonia desorption data.

Table 1. Characteristics of catalysts.

	Catalyst			
	BEA-25	RBEA-25	BEA-150	RBEA-150
[Si/Al]	25.0	23.8	150.0	176.4
S_{BET}	558	721	539	822
V	0.486	0.625	0.588	0.792
v_{micro}	0.34	0.2	0.26	0.18
v_{meso}	0.66	0.8	0.74	0.82
a_0	1200	1179	180	233
a_w	725	704	97	95
a_s	475	475	83	138

Chemical composition of the parent microporous and corresponding micromesoporous samples is nearly similar, recrystallization results both in decreasing (BEA-25) and increasing (BEA-150) of the silicon content.

The nitrogen adsorption-desorption isotherms for initial zeolites BEA-25 and BEA-150 represent a combination of type I and IV curves (according to IUPAC classification); at a low relative pressure ($p/p_0 \leq 0.2$) high adsorption of nitrogen in micropores is observed; in the range of p/p_0= 0.7-1.0 a long hysteresis loop begins, which is associated with the filling of the intercrystalline pores. On the isotherms of recrystallyzed samples RBEA-25 and RBEA-150 there is a jump (at p/p_0=0.3-0.4) indicating the presence of mesopores with average pore diameter of 3.47 and 3.85 nm, respectively. According to obtained results, the total pore volume and mesopore volume increase in recrystallized samples (micro-mesoporous materials), and the fraction of micropores decrease in comparison with the parent microporous zeolites.

The thermo-programmed desorption (TPD) curves of ammonia have two maxima, corresponding to the presence of two types of acid sites in the catalysts – weak acid sites with ammonia desorption temperature maximum approx. at 200 °C, and stronger sites with desorption temperature over 300 °C. Catalysts with high aluminum content (BEA-25 and RBEA-25) have a large number of weak acid sites, for catalysts with high silicon content (BEA-150 and RBEA-150) amount of weak and strong sites is nearly the same. The parent and the corresponding recrystallized samples differ little from each other in terms of their total acidity (a_0) and the strength of the acid sites.

B. Catalytic conversion of linalool

The catalytic reaction products were the light yellow liquids with a characteristic smell. After catalytic conversion the catalyst was separated from the reaction products by centrifugation. It contained in adsorbed form a significant part (up to 25-35% volumetric) of reaction products. Their washing was carried out with methanol and their composition was identical with the main reaction product.

Catalytic activity of surveyed catalysts was compared for their 0.05 g masses; for 0.04-0.05 g masses the catalytic activity for all surveyed catalysts is not depended on mass of the latter. Optimum time of reaction conduct – 1 hour was selected for the experiment.

It was shown that the nature of astehiometric components of reaction (nitrogen and argon) has no influence on running of the linalool conversion process on surveyed catalysts. Linalool conversion reaction runs in many, but identical routes on both microporous BEA-25 andmicro-mesoporous RBEA-25 catalysts with nearly the same values of total acidity ($a_0(NH_3)$ is 1200 and 1179 μmol/g, respectively).

These are basically the processes running on acid sites: reactions of dehydratation, cyclization and condensation, as well as isomerization; and the qualitative content of reaction products is identical.

Typical chromatogram of the products of linalool conversion on the investigated catalysts is shown in Fig. 6.

In conditions under study, linalool is mainly dehydrated and cyclized to form terpenic hydrocarbons (mircene, ocymene, terpinenes, d-limonene), converted into 3-Cycloxen-1-ol, 3,7-octadiene-2.6-diol, 2,6-dimethyl, $C_{10}H_{18}O_2$ (on BEA-25), trans-Geranylgeraniol, condensed to Squalene $C_{30}H_{50}$, cyclic alcohol Thunbergol ($C_{20}H_{34}O$), 2,6,10-Dodecatrien-1-ol ($C_{15}H_{26}O$), isomerized into ±-Terpineol (monoterpene alcohol), Geraniol, Nerol.

As is seen from Table 2, in case of identical loads on catalyst ($m_{catalysator}/m_{linalool}$ = 1/26), linalool conversion on micro-mesoporous RBEA-25 is higher than on microporous BEA-25, apparently due to bigger share of mesopores in the first one ($(V_{meso}/V_{micro}+V_{meso})$= 0.800). Product yields of linalool isomerization into geraniol/nerol are low (3-5%) and they do not depend on temperature, as well as on the mole ratio of geraniol/nerol, which approximately equals to 2. Product yields for other processes on BEA-25 and RBEA-25 are 7-17% and 19-39%, respectively, when linalool conversion is 10-42%. The same takes place in a case of BEA-150 and RBEA -50 (see Table 3), but linalool conversion and product yields of isomerization into geraniol and nerol are lower – 4-30% and 2-4%, respectively.

..

Table 2. Catalytic properties of microporous BEA-25 and micro-mesoporous RBEA-25 zeolites in linalool conversion reaction. Medium- Ar, $m_{catalyst}/m_{linalool}$= 1/26, catalyst mass - 0.05 g, run – 1 hour.

Catalyst	BEA-25			RBEA-25		
Temperature, °C	60	80	130	65	80	130
Conversion, %	10.4	12.9	22.5	22.9	28.0	42.0
Yield of geraniol, %	2.4	2.4	2.7	3.3	2.2	2.0
Yield of nerol, %	1.2	1.2	1.3	1.4	1.2	1.1
Selectivity of isomerization in geraniol, %	23.1	18.6	12.0	14.4	7.8	4.8
Selectivity of isomerization in nerol, %	11.5	9.3	5.8	6.4	4.3	2.6

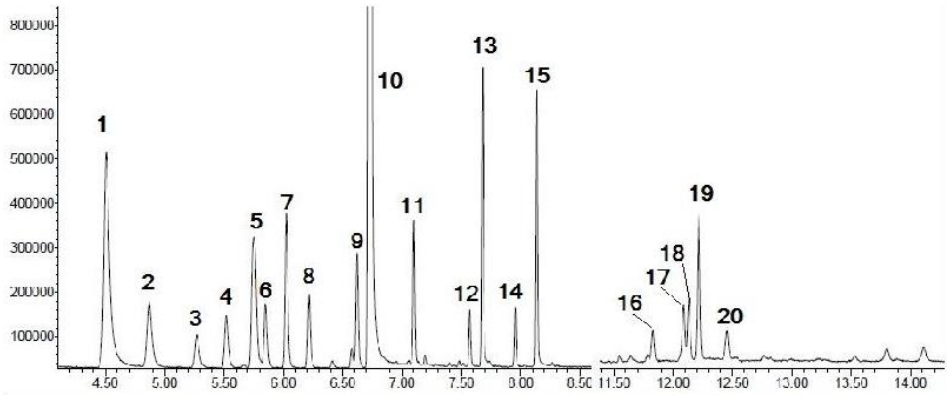

Fig. 6. Chromatogram of catalytic conversion products of linalool on micro-mesoporous zeolite R-BEA-150 (mcat/mlinalool =1/26, reaction carried out in a nitrogen atmosphere at 80 °C): 1 – Pinene, 2 – β-Mircene, 3 – α-Phellandrene, 4 – α-Terpinene, 5 – D-Limonene, 6 – trans-β–Ocymene, 7 – α-cis- Ocimene, 8 – γ-Terpinene, 9 – Terpinolene, 10 – Linalool, 11 – 1,2-dihydrolinalool (impurity in initial linalool), 12 – 3-Cyclohexen-1-ol, 13 – α-Terpineol, 14 – Nerol, 15 – Geraniol, 16 – trans-Geranyl geraniol, 17 – Squalene ($C_{30}H_{50}$), 18 – Thunbergol ($C_{20}H_{34}O$), 19 – 2,6,10-Dodecatrien-1-ol ($C_{15}H_{26}O$), 20 – ±-Springene ($C_{20}H_{32}$).

Table 3. Catalytic properties of microporous BEA-150 and micro-mesoporous RBEA-150 zeolites in linalool conversion reaction carried out in argon, $m_{catalyst}/m_{linalool}$= 1/26, catalyst mass - 0.05 g, run – 1 hour.

Catalyst	BEA-150				RBEA-150			
Temperature, °C	80	100	130	150	80	120	150	170
Conversion, %	3.7	5.1	7/0	10.0	15.5	18.0	26.4	28.9
Yield of geraniol, %	slight	1.5	1.0	1.0	2.1	2.4	2.7	2.7
Yield of nerol, %	slight	0.8	0.7	0.6	1.2	1.3	1.4	1.4
Selectivity of isomerization in geraniol, %	-	29.4	14.3	10.0	13.6	13.3	10.2	9.4
Selectivity of isomerization in nerol, %	-	15.6	10.0	6.0	7.8	7.2	5.3	4.9

Linalool conversion decreases in the RBEA-25 > RBEA-150 > BEA-25 > BEA-150 series starting with the micro-mesoporous samples RBEA-25 having the highest number of acid sites (1179 μmol/g, basically represented by weak acid centers); the high-silicon sample RBEA-150 has nearly identical specific volume of micropores (0.18) and mesopores (0.82), but lower acidity (233 μmol/g, shares of weak and strong acid sites are nearly equal). In both microporous and micromesoporous samples prevailing role in linalool conversion belongs to acid factor, especially the numbr of weak acid sites.

This is also indicated by the character of the change in selectivity (Tables 2 and 3, Fig. 7).

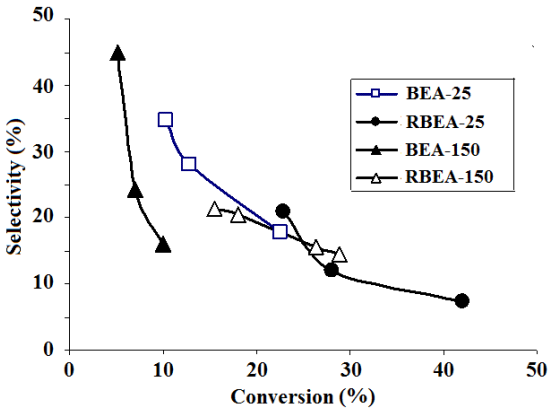

Fig. 7. Dependence of selectivity of linalool isomerization into geraniol and nerol on the conversion of linalool on micro and micro-mesoporous zeolites.

C. Catalytic conversion of geraniol

The detailed description of geraniol conversion is given in work [2], the main conversion products of geraniol on microporous BEA and micro-mesoporous RBEA catalysts over 60°C are the following compounds:

Isomerization products $C_{10}H_{18}O$ (mainly the products of the double bond transfer in geraniol and, to a lesser extent, cis-trans isomerization): β-Linalool and Nerol, also a very small amount (up to 0.6%) of cis-Isogeraniol ((3Z)-3,7-Dimethyl-3,6-octadien-1-ol) and cyclic product α-Terpineol (up to 1.2%); the selectivity of isomerization products decreases with increasing geraniol conversion.

Dehydration products $C_{10}H_{16}$: terpenic hydrocarbons α-Myrcene, β-Myrcene, α-Terpinolene, D-Limonene, trans-β-Ocimene, β-Ocimene, γ-Terpinene, 1,1,2-Trimethyl-3-(2-methyl-1-propen-1-ylidene) cyclopropane, α-Terpinene, (4E,6Z)-2,6-Dimethylocta-2,4,6-triene (allo-Ocimene); the selectivity of dehydration products increases with increasing geraniol conversion.

Carbon-chain-extending products C_{14} and C_{15} (sesquiterpene alcohols), selectivity of such products has an extreme dependence on the conversion of geraniol. Over the 40°C **diterpene alcohols** $C_{20}H_{34}O$ are formed up to 2-3%, only on the RBEA-25 and BEA-25 catalysts at 100-150°C the formation of up to1.0-1.5% of **monocyclic diterpene alcohols** (thunbergol) and up to 0.3-0.6% of **monocyclic terpene** (cembrene) is observed.

The first three ways of transformation of geraniol are shown in the Figure 8 where structures of isomerization, dehydration, and cyclization products are given.

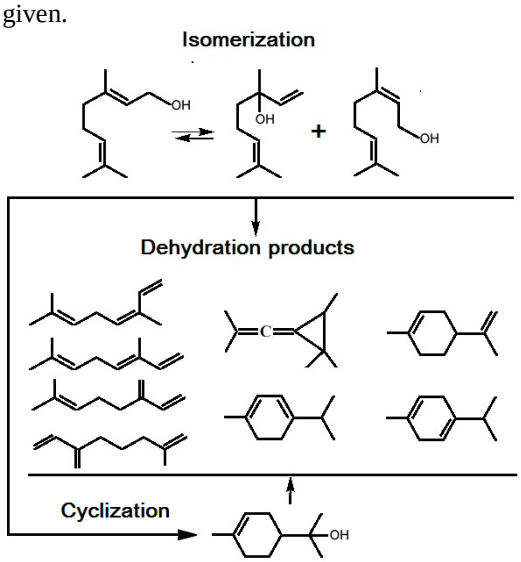

Fig. 8. Isomerization, dehydration, and cyclization of geraniol.

On all the catalysts investigated, the selectivity of the isomerization products ($C_{10}H_{18}O$-linalool, nerol, and slightly formed cis-isogeraniol and α-terpineol) decreases with growing geraniol conversion, but the selectivity for the dehydration products – the terpene hydrocarbons $C_{10}H_{16}$ increases and an extreme dependence of selectivities of trans, trans-farnesol and $C_{14}H_{24}O$ on the conversion of geraniol is observed (see the Fig. 9 using RBEA-25 as an example).

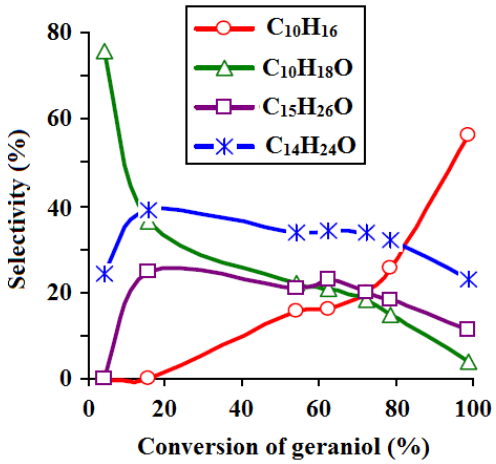

Fig. 9. Selectivity in the geraniol conversion, catalysed by RBEA-25, run time – 1 hour, nitrogen atmosphere, mass of catalysts– 0.05 g, ratio of geraniol/catalyst – 0.17 mol/g.

Similar selectivity versus conversion dependences are observed in the case of complex parallel-consequent reactions [19].

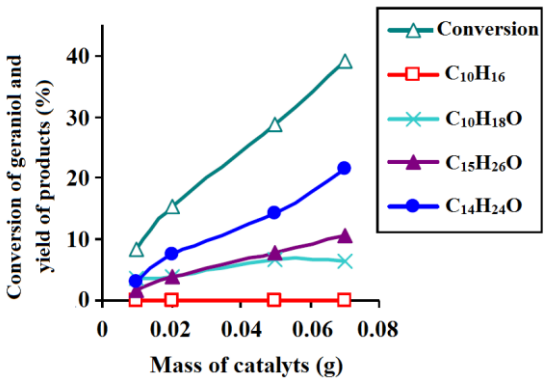

Fig. 10. The effect of mass of catalyst BEA-150 on conversion of geraniol and yield of products. Reaction conditions: geraniol - 0.0086 mol/h (1.5 mL/h), 100 ˚C, medium – N_2, the product $C_{10}H_{18}O$ includes linalool, nerol, cis-isogeraniol, and α-terpineol.

According to the results (Fig. 10), the conversion of geraniol and the yields of diterpene alcohols $C_{14}H_{24}O$ and $C_{15}H_{26}O$ are increasing with the growth of catalyst mass in the range 0.01- 0.07 g; under BEA-150 at a catalyst mass of 0.07 g and 40% conversion of geraniol, the selectivity for these diterpene alcohols

is 55% and 27%, respectively. It is belived that stereospecific syntheses of diterpene alcohols are multistage processes [20], but one-stage synthesis of these alcohols with greater yield can be successful on the investigated micro- and micromesoporous zeolites of the BEA type by selecting appropriate conditions.

It was shown that under the conditions studied in the atmosphere of nitrogen or argon the character of the transformation of geraniol is the identical.

For the temperature region above 80 °C, probably less complicated by external diffusion, a comparison of the activities of catalysts by the conversion of geraniol at the same temperature and same load of catalysts shows the following relative series of their catalytic activity: RBEA-25≥ BEA-25 > RBEA-150> BEA-150 (Fig. 11); this sequence correlates with the values of their total acidity ($a_0(NH_3)$, Table 1); the conversion of geraniol is greater on BEA-25 and RBEA-25 samples with higher acidity.

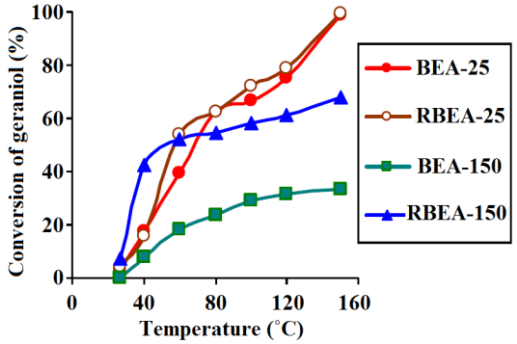

Fig. 11. Effect of reaction temperature on the conversion of geraniol; ratio of geraniol/catalyst – 0.17 mol/g, mass of the catalyst – 0.05 g.

With the introduction of mesopores into the microporous zeolite and the increase of acidity of the catalyst, the conversion of geraniol increases from 33.6 and 67.7% for the BEA-150 and RBEA-150, and up to 99% for the RBEA-25 and BEA-25.

The selectivity of formation of terpenic hydrocarbons $C_{10}H_{16}$ (Fig. 12) correlates with the acidity of the catalysts.

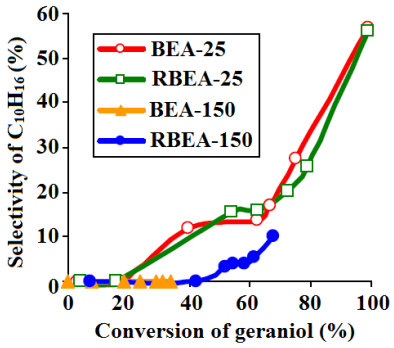

Fig. 12. Dependence of the selectivity of $C_{10}H_{16}$ from conversion of geraniol over catalysts; ratio of geraniol/catalyst – 0.17 mol/g, N_2 atmosphere, mass of the catalyst – 0.05 g.

On the catalyst with the lowest acidity (BEA-150) formation of $C_{10}H_{16}$ hydrocarbons is not observed. On BEA-25 and RBEA-25 samples with the highest acidity (1200 μmol/g) the selectivity of $C_{10}H_{16}$ formation reaches 57%.

At low degrees of geraniol conversion there are the following series of selectivity for linalool and nerol: BEA-25> RBEA-25> RBEA-150> BEA-150; this series shows that the effects of the acid factor and pore characteristics on the selectivity are intertwined; in particular, with the same acidity spectrum of the BEA-25 and RBEA-25 samples, it is likely that a large proportion of micropores in BEA-25 is responsible for its greater selectivity for linalool and nerol.

In the RBEA-150 and BEA-150 pairs, the high selectivity of the former is apparently associated with a large number of strong acid sites (138 μmol/ g) in it. Comparing the selectivity of the micro-mesoporous RBEA-25 and RBEA-150 with the same characteristics of micro- and mesopores it can be seen that the high selectivity for RBEA-25 correlates with a large number of acid sites in RBEA-25 (1179 μmol/g) than in RBEA-150 (233 μmol/g).

D. Carbon-chain extension

Geraniol has four rotatable C – C bonds and energetically the most favorable conformation is "extended" when the molecule has the maximum length and the minimum "diameter" of approx. 3.8 Å [15]. The same concerns isomers of geraniol and acyclic products, but even for compounds with six-membered cycles their effective diameter generally is defined not by the size of a ring, but of the gem-dimethyl group, so all these products can be formed in channels of the catalyst and move freely in them. It isn't so obvious to long-chain compounds and, in particular, for macrocycles, and demands special consideration.

According to obtained experimental data, catalytic redistribution and extension of the carbon chain results in formation of (2E,6E)-6,11-Dimethyl-2,6,10-dodecatrien-1-ol, $C_{14}H_{24}O$, and sesquiterpene alcohol (2E,6E)-3,7,11-Trimethyl-2,6,10-dodecatrien-1-ol, trans,trans-Farnesol, $C_{15}H_{26}O$, from monoterpene alcohol geraniol, which has a "head" at the methyl group and a "tail" at the gem-dimethyl group [21] and is freely moving in zeolite BEA channels.

At geraniol conversion up to about 20% the selectivity for linalool and nerol are sharply reduced and then approach zero; at the same time, competitive reactions of formation of terpene hydrocarbons $C_{10}H_{16}$ and $C_{14}H_{24}O$ and $C_{15}H_{26}O$ terpene alcohols are enhanced. With decrease of the selectivity of linalool and nerol the selectivity ratio of linalool/nerol increases, for example, from 0.6 to 20-25 and more for BEA-25 and RBEA-25. Thus the regioselectivity is achieved by linalool, i.e. in the migration of the

double bond in the geraniol molecule, especially in the case of BEA-25 and RBEA-25; however, on these catalytic systems, the yields of linalool and nerol are low (3-12%).

Formation of sesquiterpene from monoterpene can be presented if to assume that a cracking of monoterpenes takes place on the used BEA-type zeolite catalysts with formation of the isoprene units C_5H_8 joining to other monoterpene molecules according to Ruzicka's "isoprene rule".

It is much more difficult to understand formation of $C_{14}H_{24}O$, but this compound, most likely, doesn't take part in further transformations, and from this point of view it is a little interesting. On the contrary, the trans,trans-Farnesol can be involved in further transformations as it happens to this substance in the nature.

In biochemistry the trans,trans-Farnesol is considered as the biogenetic predecessor of mono-, bi-, and tricyclic sesquiterpenes, but such compounds aren't found among geraniol conversion products, but diterpenic alcohols $C_{20}H_{34}O$ – trans,trans,trans-Geranyl-geraniol, p-Camphorene and unidentified isomer of trans-Geranylgeraniol are present in reaction mixture. The possibility of obtaining of geranylgeranirol from farnesol by allylic rearrangement under $O=W(OR)_4$·Ligand catalysts was shown in study [6].

The molecule of trans,trans,trans-Geranylgeraniol has ten rotatable C – C bonds and variety of conformations including the "extended" one with an effective "diameter" of approx. 4 Å.

In this case the diterpenic alcohols formed in channels of the catalyst can freely pass through the 12-rings and diffuse not only in wide, but in narrow zeolite channels, like their predecessor trans,trans-Farnesol having seven rotatable C – C bonds.

However, staying in energetically most probable conformations, this molecules can move only in a wide channels, as shown in the Fig. 13.

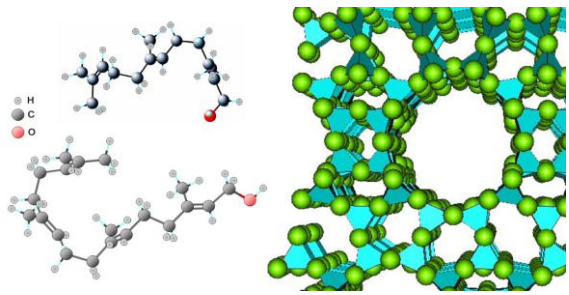

Fig. 13. Produced long-chain molecules and zeolite 12-rings.

Compared with other zeolites, BEA has a high density of stacking defects, which arise from the successive interconnection of layers in the [001] planes, where they link either in a left- or right-handed fashion. When a tertiary building unit in a layer rotates over 90° around the [001] direction with respect to the next building unit, defects, which contain partially coordinated aluminum, are created [22]. These stacking faults do not affect the micropore volume, but do influence the tortuosity of the channel along [001].

Open channels of the BEA-type zeolite have rather big diameter for diffusion of comparatively large molecules. Besides, the low content of aluminum in the crystal structure leads to the fact that the number of the compensating positively charged ions located in channels is also small, and cation don't interfere with penetration of organic molecules into channels.

In the transformation products of geraniol the content of stereoisomers of sesquiterpene alcohols: $C_{14}H_{24}O$ ((2E,6E)-6,11-dimethyl- 2,6,10-dodecatrien-1-ol**)** and $C_{15}H_{26}O$, trans,trans-Farnesol, ((2E,6E)-3,7,11-Trimethyl-2,6,10-dodecatrien-1-ol), is probably due to the presence of the chiral pore intersections in the structure of zeolite.

With the approximately identical geraniol conversion on samples of RBEA-25 and BEA-25 with the highest acidity (1179 and 1200 μmol/g, respectively), the selectivity to $C_{15}H_{26}O$ and to $C_{14}H_{24}O$ on the micro-mesoporous RBEA-25 is more due to its larger surface area (Fig. 14).

Formation of trans,trans-isomers of sesquiterpene alcohols $C_{14}H_{24}O$ and $C_{15}H_{26}O$ from geraniol takes place on BEA-150 and RBEA-150 samples with selectivity of about 50 and 30%, respectively.

This catalysts are characterized by low total acidity (180 and 233 μmol/g, respectively) and have large fraction of mesopores (0.82 and 0.74, respectively), the BEA-25 and RBEA-25 samples with higher acidity (1200 and 1179 μmol/g, respectively) demonstrate lower selectivity for $C_{14}H_{24}O$ and $C_{15}H_{26}O$ (Fig. 15).

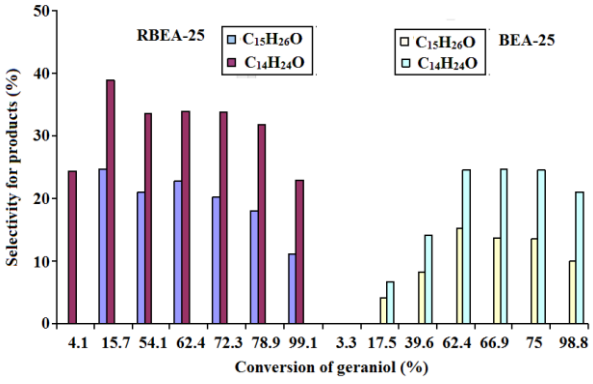

Fig. 14. The selectivity for $C_{15}H_{26}O$ and $C_{14}H_{24}O$ versus the conversion of geraniol on BEA-25 and RBEA-25 catalysts; ratio of geraniol/catalyst – 0.17 mol/g, N_2 atmosphere, mass of catalyst – 0.05 g.

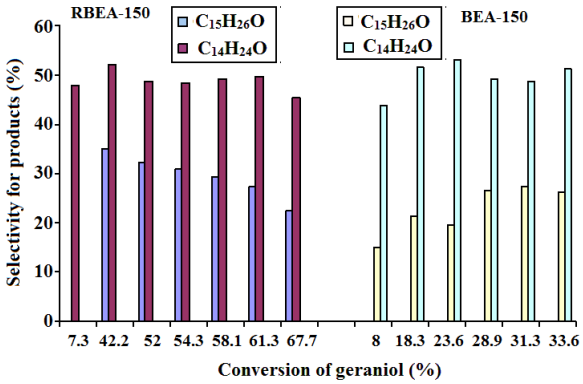

Fig. 15. The selectivity for $C_{15}H_{26}O$ and $C_{14}H_{24}O$ versus the conversion of geraniol on BEA-150 and RBEA-150 catalysts; ratio of geraniol/catalyst – 0.17 mol/g, nitrogen atmosphere, mass of catalyst – 0.05 g.

These facts agree with the lowest dehydrating ability of the RBEA-150 и BEA-150 samples, having lowest selectivity of $C_{10}H_{16}$ formation (see Fig. 12).

E. Macrocyclic compounds

Among products of conversion of geraniol there are monocyclic compounds having the sizes (averaged "diameter" of the C_{14}-ring 6.8 Å) comparable to the sizes of the $(SiO)_{12}$-ring of catalyst (see Fig. 16).

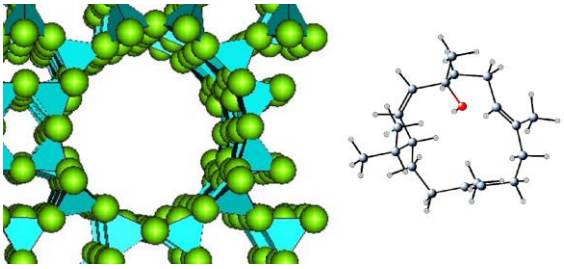

Fig. 16. Zeolite 12-ring and the thunbergol macrocycle.

Formation of thunbergol and its isomer isocembrol (1R,2E,4S,7E,11E)-4-Isopropyl-1,7,11-trimethyl-cyclotetradeca-2,7,11-trienol, $C_{20}H_{34}O$, in zeolite channels is possible by transformation of trans,trans,trans-Geranylgeraniol arranging bond between the C1 and C14 carbon atoms, as it was been shown earlier in [23].

Most likely, formation of diterpenic alcohols is followed by dehydration into cembrene (thunbergene, (1E,3Z,6E,10E)-3,7,11-trimethyl-14-(propan-2-yl)cyclotetradeca-1,3,6,10-tetraene, $C_{20}H_{32}$).

The scheme of formation of long-chain and macrocyclic molecules is submitted in the Figure 17.

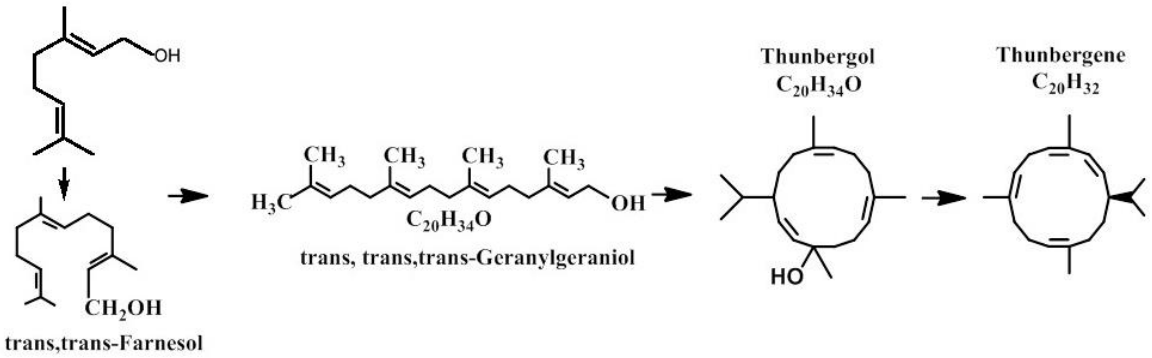

Fig. 17. Ways of geraniol transformation through farnesol into long-chain and macrocyclic molecules.

CONCLUSION

The catalytic conversion of terpene alcohols has been studied on samples of the BEA type microporous zeolites and on their modified micro-mesoporous forms having transport mesopores with pore diameters 3.5 and 3.8 nm, respectively. Micro-mesoporous catalysts have nearly identical porous structure, but they differ by nature and strength of acid sites: low-silicon catalysts have a high acidity, mainly due to weak acid sites, while high-silicon catalysts have a relatively low acidity and approximately equal number of weak and strong acid sites. Creation of the mesoporosity does not cause a noticeable change in the acidity.

Linalool transformation in inert atmosphere at 60-170°C proceeds many ways; reactions of dehydratation, cyclisation, condensation and isomerization take place resulting in several products with rather low yield, including target geraniol and nerol (2-5%); linalool conversion is not high (4-40%).

Comparison of values of conversion and selectivity with textural and acidic properties of catalysts allows us to make conclusion that the creation of mesoporosity in Beta-type catalyst leads to significant increase in the conversion of linalool and to slight increase in selectivity. High share of weak acid sites in the low-silicon microporous sample contributes to enhancement of selectivity in geranol and nerol isomerization.

The catalytic conversion of geraniol mainly results in isomerization products (linalool and nerol) and in terpene hydrocarbons $C_{10}H_{18}$, the conversion of geraniol increases with increasing acidity of the catalysts. The highest selectivity of nerol formation is 46 and 64% on the low-silicon and its mesoporous modification, respectively, at low geraniol conversion (4-8%) and low temperature (27-40 °C). The selectivity for terpene hydrocarbons correlates with the total acidity of the catalysts, the selectivity of $C_{10}H_{16}$ formation reaches 57% at 150˚C on samples with the highest acidity.

On the contrary, high-silicon catalysts with low acidity produce such long-chain molecules as trans, trans isomers of sesquiterpene alcohols $C_{14}H_{24}O$ and $C_{15}H_{26}O$ with selectivity of about 52 and 33% at conversions 18-34 and 42-61% on the high-silicon and its mesoporous modification, respectively.

Moreover, produced by one-pot method in "zeolitic reactor" trans,trans-farnesol attaches one more isoprene unit to form the long-chain molecule of trans,trans,trans-geranylgeraniol which can form a macrocycle of thunbergol $C_{20}H_{34}O$, which is dehydrated into diterpene thunbergene $C_{20}H_{32}$.

ACKNOWLEDGEMENT

This work was carried out under the Project #217868 "The new approaches in synthesis of geraniol, nerol, and citral" supported by the Shota Rustaveli National Science Foundation of Georgia. The authors thank all colleagues who participated in this study and were co-authors of previous publications.

REFERENCES

[1] Corma A., Iborra S., Velty A. "Chemical routes for the transformation of biomass into chemicals". *Chem. Rev*., 2007, vol.107, no 6, pp. 2411-2502.

[2] Kirk R.E, Othmer D.F. "Terpenoids" in *Encyclopedia of Chemical Technology*, 4th ed., Wiley: New York, 2000, vol. 23, pp. 423.

[3] Foß S., Harder J. "Microbial transformation of a tertiary allylalcohol: regioselective isomerization of linalool to geraniol without nerol formation". *FEMS Microbiology Letters*., 1997, vol. 149, no 1, pp. 71-75.

[4] Chabardes P., Kuntz S.J., Varagnat J. "Use of oxo-metallic derivatives in isomerization: Reactions of unsaturated alcohols". *Tetrahedron*. 1977, vol. 33**,** no 14-H, pp. 1775-1783.

[5] Semikolenov V.A., Ilina I.I., Maksimovskaya R.I. "Linalool to geraniol/nerol isomerization catalyzed by (RO)3VO complexes: studies of kinetics and mechanism". *J. Mol. Catal. A: Chemical*., 2003, vol. 204-205**, pp.** 201-210.

[6] Hosogai T., FujitaY., Ninagawa Y., Nishida T. "Selective allylic rearrangement with tungsten catalyst". *Chem Lett*., 1982, vol. 11, no 3, pp. 357-360.

[7] Baerlocher Ch., McCucker L.B., Olson D.H. Atlas of Zeolite Framework Types. Sixth revised Edition, Elsevier: Amsterdam, 2007, pp. 142-143.

[8] Newsam J.M., Treacy M.M.J., Koetsier W.T., de Gruyter C.B. "Structural characterization of zeolite beta". *Proc. Royal Society A*, 1988, vol. 420, no 1859, pp. 375-405.

[9] Ramishvili Ts.M., Yushchenko V.V., Charkviani M.K**.** "Catalytic conversions of linalool and linalyl acetate over wide-pore zeolites and mesoporous MCM-41". *Moscow Univ. Chem. Bull*., 2007, vol. 62, no 4, pp. 180-186.

[10] Beers A.E.W., van Bokhoven J.A., de Lathouder K.M., Kapteijn F. "Optimization of zeolite Beta by steaming and acid leaching for the acylation of anisole with octanoic acid: a structure–activity relation". *J. Catal*., 2003, vol. 218, no 2, pp. 239-248.

[11] Maier S. M., Jentys A., Lercher J.A. "Steaming of zeolite BEA and its effect on acidity: a comparative NMR and IR spectroscopic study". *J. Phys. Chem. C*., 2011, vol. 115, no 16, pp. 8005-8013.

[12] Ivanova I.I., Kuznetsov A.S**,** Yushchenko V.V., Knyazeva E.E. **"**Design of composite micro/mesoporous molecular sieve catalysts". *Pure Appl. Chem*., 2004, vol. 76, no 9, pp. 1647-1658.

[13] Tsitsishvili V., Ivanova I., Ramishvili Ts., Kokiashvili N., Bukia T., Dobryakova I., Kurtsikidze G.. "Catalytic conversion of linalool on micro-mesoporous BEA-type zeolite". *Bull. Georgian Nat. Acad. Sci*., 2017, vol. 11, no 3, pp. 79-87. http://science.org.ge/bnas/t11-n3/10_Tsitsishvili.pdf.

[14] Ramishvili Ts.M., Tsitsishvili V.G., Ivanova I.I., Bukia T.J., Kurtsikidze G.O., Kokiashvili N.G. "Catalytic conversion of geraniol on micro- and micro-mesoporous beta-type zeolite". *Int. J. Recent Sci. Res.*, 2018, vol. 9, is. 3, pp. 25454-25460. http://dx.doi.org/10.24327/ijrsr.2018.0903.1861

[15] Tsitsishvili V., Ramishvili Ts., Ivanova I., Dobryakova I., Bukia T., Kokiashvili N.. "Formation of long-chain and macrocyclic compounds during catalytic conversion of geraniol on micro- and micro-mesoporous BEA-type zeolite". *Bull. Georgian Nat. Acad, Sci.*, 2018, vol. 12, no.3, pp. 62-68. http://science.org.ge/bnas/t12-n3/10_Tsitsishvili.pdf.

[16] Ramishvili Ts., Tsitsishvili V., Ivanova I., Kokiashvili N., Bukia T., Kurtsikidze G.. "Synergic actions of beta-type zeolites and ultrasonic irradiation in the conversion of geraniol". *Asian J. Chem.*, 2019, vol. 31, no 2, pp. 438-444. https://doi.org/10.14233/ajchem.2019.21670

[17] Ivanova I.I., Knyazeva E.E. "Sposob poluchenia materiala s mikro-mezoporistoi structuroi", Russia Patent No 2282587, 2006 (in Russian).

[18] Ivanova I., Ponomareva O., Knyazeva E., Yushchenko V., Timoshin E., Asachenko E. "Sposob konversii uglevodoro-dov, katalizator dlia ego osushchestvlenia s mikro-mezo-poristoi strukturoi i sposob prigotovleniia katalizatora", Russia Patent No 2288034, 2006 (in Russian).

[19] Bochkarev V.V., Optimization of Technological Processes of Organic Synthesis. Tomsk Polytechnic University: Tomsk, 2010, 185 p.

[20] Bauer K., Garbe D., Surburg, H. Common Fragrance and Flavor Materials: Preparation, Properties and Uses. John Wiley & Sons, Science: Weinheim, 2008, 290 p.

[21] Ruzicka L. "The isoprene rule and the biogenesis of terpenic compounds". *Experimentia*, 1953, vol. 9, pp. 357-396.

[22] Treacy M.M.J., Newsam J.M. "Two new three-dimensional twelve-ring zeolite frameworks of which zeolite beta is a disordered intergrowth". *Nature*, 1988, vol. 332, pp. 249-251.

[23] Dauben W.G., Thiessen W.E., Resnick P.R. "Cembrene, a 14-membered ring diterpene hydrocarbon". *J. Am. Chem. Soc.*, 1962, vol. 84, no 10, pp. 2015-2016.

ლინალოოლის და გერანიოლის გარდაქმნა მიკრო-მეზოფოროვან BEA ტიპის ცეოლითებზე

ციური რამიშვილი[1]*, ვლადიმერ ციციშვილი[1], ირინა ივანოვა[2], ირინა დობრიაკოვა[2]

[1] *თსუ პეტრე მელიქიშვილის სახ. ფიზიკური და ორგანული ქიმიის ინსტიტუტი, ა.პოლიტკოვსკაიას ქ. 31, თბილისი 0186*

[2] *მ.ვ.ლომონოსოვის სახ. მოსკოვის სახელმწიფო უნივერსიტეტი, ქიმიის ფაკულტეტი, კინეტიკის და კატალიზის ლაბორატორია, მოსკოვი, რუსეთის ფედერაცია*

***v.tsitsishvili@gmail.com +995 599 988198*

რეზიუმე. შესწავლილია ტერპენული მესამეული სპირტების – ლინალოოლისა და გერანიოლის კატალიზური გარდაქმნები მიკროფოროვან BEA ტიპის ცეოლითებსა და მათ მოდიფიცირებულ მიკრო–მეზოფოროვან ფორმებზე. ამ კატალიზატორებზე ინერტულ გარემოსა და 60-170 °C ტემპერატურებზე ლინალოოლი მრავალი მიმართულებით გარდაიქმნება; ხდება მისი დეჰიდრატაციის, ციკლიზაციის, კონდენსაციის და იზომერიზაციის რეაქციები; ამ დროს ლინალოოლის გარდაქმნის ხარისხი მცირეა (4-40%), წარმოიქმნება მრავალი ნივთიერება, მათ შორის სამიზნე პროდუქტები გერანიოლი და ნეროლი ¬ მცირე გამოსავლიანობით (2 - 5%). მეზოფორების შეყვანით BEA ტიპის ცეოლითებში შესამჩნევად იზრდება ლინალოოლის გარდაქმნის ხარისხი და უმნიშვნელოდ, სელექტურობა გერანიოლის და ნეროლის მიმართ; ეს უკანასკნელი მიკროფოროვან BEA ტიპის ცეოლითების შემთხვევაში მით მეტია, რაც უფრო დიდია მათში სუსტი მჟავური ცენტრების რაოდენობა. ტრანს-გერანიოლის გარდაქმნისას აღმოჩენილია მისი დეჰიდრატაციის პროდუქტები – ტერპენული ნახშირწყალბადები $C_{10}H_{16}$, გერანიოლში ორმაგი ბმის გადანაცვლებისა და ცის-ტრანს-იზომერიზაციის და აგრეთვე ციკლიზაციის პროდუქტები (β-ლინალოოლი, ცის-გერანიოლი ანუ ნეროლი და α-ტერპინეოლი); ნახშირბადოვანი ჯაჭვის დაგრძელების პროდუქტები – სესკვიტერპენული სპირტები $C_{15}H_{26}O$ და $C_{14}H_{24}O$ (შესაბამისად, ტრანს, ტრანს-ფარნეზოლი ანუ (2E,6E)-3,7,11-ტრიმეთილ-2,6,10-დოდეკატრიენ-1-ოლი და (2E,6E)-6,11-დიმეთილ-2,6,10-დოდეკატრიენ-1-ოლი); მცირე რაოდენობით – გრძელჯაჭვიანი დიტერპენული სპირტის $C_{20}H_{34}O$ გეომეტრული იზომერები (ტრანს,ტრანს,ტრანს-გერანილგერანიოლი და ტრანს,ტრანს- გერანილლინალოოლი), ციკლური დიტერპენის დიმირცენის ($C_{20}H_{32}$) პარა- და მეტა-იზომერები. კატალიზატორებზე RBEA-25 და BEA-25 100-150˚C ხდება აგრეთვე მონოციკლური დიტერპენული სპირტის $C_{20}H_{34}O$, თუნბერგოლის (იზო-ცემბროლის, (1R,2E,4S,7E,11E)-4-იზოპროპილ-1,7,11-ტრიმეთილ-ციკლოტეტრადეკა-2,7,11-ტრიენოლის) და მონოციკლური ტერპენის $C_{20}H_{32}$, ცემბრენის (1E,3Z,6E,10E)-3,7,11-ტრიმეთილ-14-(პროპან-2-ილ)ციკლოტეტრადეკა-1,3,6,10-ტეტრაენი) წარმოქმნა.

Hydrothermal and ion-exchange transformation of Georgian natural zeolites

Vladimer Tsitsishvili*, Nanuli Dolaberidze, Nato Mirdzveli, Manana Nijaradze, Manan Burjanadze, Giorgi Tsintskaladze, Zurab Amiridze, Vakhtang Gabunia

Petre Melikishvili Institute of Physical and Organic Chemistry at Ivane Javakhishvili Tbilisi State University, 31 A.Politkovskaia str., Tbilisi 0186, Georgia
**v.tsitsishvili@gmail.com +995 599 988198*

Abstract. The present paper summarizes studies of hydrothermal transformation of natural zeolites analcime and phillipsite, widespread in Georgia, in order to obtain valuable products. It is found that phase-pure zeolite NaA with Si/Al~1 can be prepared in the form of cubic/rhombus crystallites with uniform micrometric (3-5 μm) dimensions by hydrothermal crystallization of aged at room temperature gel ($4.5Na_2O$: $0.45Al_2O_3$: $1SiO_2$: $178H_2O$) obtained from natural analcime, treated with hydrochloric acid before suspending in water and mixing with sodium hydroxide. Phase-pure zeolite NaX with Si/Al~1.5 can be prepared in the form of octahedral crystallites with uniform micrometric (2-7 μm) dimensions by hydrothermal crystallization of aged at room temperature gel ($2.9Na_2O$: $0.26Al_2O_3$: $1SiO_2$: $150H_2O$) obtained from water suspension of natural phillipsite, treated with hydrochloric acid and mixed with sodium hydroxide. Crystal structure of both zeolites is testified by X-ray diffraction patterns and infra-red spectra. Synthesized zeolite NaX is characterized by specific surface area of 589 m^2/g and total pore volume of 0.578 cm^3/g calculated by the Brunauer-Emmett-Teller method from the low-temperature nitrogen adsorption-desorption isotherms. Along with ordered homogeneous micropores, the obtained zeolite NaX has a developed system of cylindrical channels with an average diameter of 55 nm (calculated by the Barrett-Joyner-Halenda method), which opens up the prospect of its use in catalytic processes. Silver-, copper-, and zinc-containing micro-mesoporous materials have been prepared on the basis of Georgian phillipsite using ion-exchange reactions between zeolite and a salt of a transition metal in the solid phase followed by washing. Synthesized adsorbent-ion-exchangers are characterized by chemical analysis and sorption data, XRD patterns, FTIR spectra, SEM images; they remain the crystal structure and general properties of phillipsite, contain up to 230 mg/g of silver, 66 mg/g of copper, and 86 mg/g of zinc, and show bactericidal activity towards *Escherichia coli*..

Keywords: analcime, phillipsite**,** zeolite A, zeolite X , silver-, copper-, and zinc-containing zeolites.

INTRODUCTION

Zeolites ($M^{n+}_{x/n}[(SiO_2)(AlO_2)_x]\cdot wH_2O$, were M=Na, K, Ca, Mg, etc.) are porous crystalline aluminosilicates with open framework uniform structures formed from alternating SiO_4 and AlO_4^- tetrahedrons. Application of zeolites is based on the complex of their molecular sieve, sorption, ion exchange and catalytic properties. Synthetic zeolites characterized by uniform and precise nano-scale porosity, molecular shape selectivity, ion-exchange capacity, strong Brønsted acidity and other beneficial properties, find the greatest practical application [1,2], and the hydrothermal zeolite synthesis through transformation of natural silicates and industrial wastes has been used due to the search for cheap alumina and silica sources [3].

Among the zeolites known on the territory of Georgia the sedimentary and volcanic-sedimentary analcime is rather widespread, phillipsite-containing Eocene rocks were discovered firstly at the northern fringe of the Akhaltsikhe depression, along with other zeolites, and then in the Gurian range [4], zeolite phase content in rocks differs in a range of 60-80% [5].

Analcime belongs to minerals of tectosilicate group with zeolitic structure (crystal chemical data $|Na_{16}(H_2O)_{16}|$ $[Al_{16}Si_{32}O_{96}]$-**ANA**, cubic, *Ia*3*d*, a=13.73 Å [1]) with high framework density of 18.5T/1000 $Å^3$ (T = Si or Al). The analcime framework (Figure 1) consists of singly-connected 4-rings, arranged in chains coiled around tetrad screw axes.

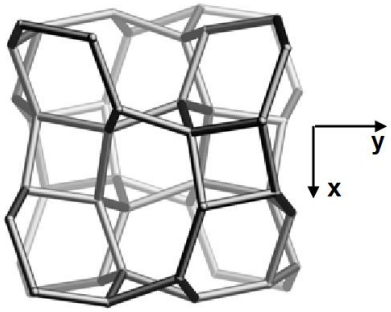

Fig. 1. Analcime framework viewed along [001].

Every 4-ring is a part of three mutually perpendicular chains, each parallel to a crystallographic axis. Cages, which contain the Na-cations and water molecules, occur near where chains interconnect, and each T-site is part of three cages. Irregular channels are formed by highly distorted eight-membered rings (8mR, Figure 2) and have small entrance windows of approx. 2.6 Å, and regular channels are formed by six-membered rings (6mR) along the [111] direction of the cubic lattice. These narrow channels affect both the cation exchange and dehydration/hydration behavior of analcime.

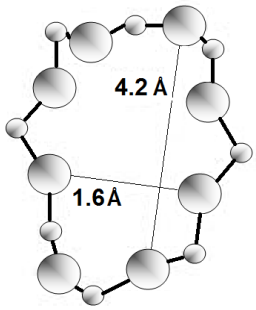

Fig. 2. Distorted 8mR viewed along [110].

The compact structure of analcime prevents the adsorption and diffusion of molecules in the cages and channels, therefore its use as an adsorbent or molecular sieve is limited, analcime-rich tuffs are known to be employed in construction as dimension stone or as pozzolanic addition to cement and concrete. At the same time, the analcime structure contains 4- and 6-member ring secondary building units [6] and may be suitable for the preparation of zeolite A (the crystal chemical formula $|Na_{12}(H_2O)_{27}|_8$ $[Al_{12}Si_{12}O_{48}]_8$-**LTA**) widely used in detergents as a water-softening builder [7] and in ion exchange separation [8].

Zeolite phillipsite has crystal chemical formula $|K_2(Ca,Na_2)_2(H_2O)_{12}|$ $[Al_6Si_{10}O_{32}]$-**PHI** and is structurally built up by layers of four- and eight-member rings (Figure 3) forming double crankshaft chains, the framework contains three systems of channels parallel to a, b and c : [100] **8** 3.8 x 3.8* ↔ [010] **8** 3.0 x 4.3* ↔ [001] **8** 3.2 x 3.3*.

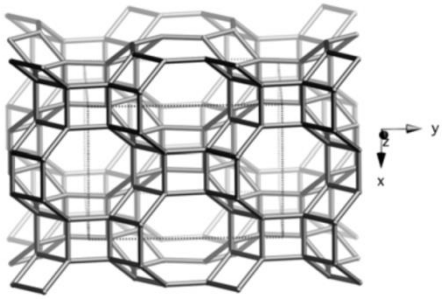

Fig. 3. Phillipsite framework viewed along [001].

Compared with clinoptilolite, analcime and phillipsite are not widely used, there are only some considerations about their use for water and wastewater treatment [9], pollution control [10] and other environmental applications [11].

Phillipsite is structurally built up by layers of 4- and 8-member rings forming double crankshaft chains [6], it may be applied to obtain zeolite X ($|(Ca,Mg,Na_2)_{29}(H_2O)_{240}|$ $[Al_{58}Si_{134}O_{384}]$-**FAU**), having a very widespread use in catalysis [12]

In our early research [13], it was shown that unprocessed natural phillipsite from Shukhuti is inert to *E. coli* and *Staphylococcus aureus*, while acid-treated samples show high bactericidal activity, recently we prepared silver-, copper-, and zinc-containing bactericidal phillipsites. Pylev et al. [14] reported on the carcinogenicity of phillipsite, but the International Agency for Research on Cancer (IARC) evaluated their study as inadequate [15].

EXPERIMENTAL

Raw materials. Preparation of synthetic zeolite materials was carried out using sodium analcime from Chachubeti with Si/Al~2 and phillipsite from the Akhaltsikhe field with Si/Al~2 described and characterized previously [16].

Processing of raw in target material. Zeolite-containing rocks were crushed in the planetary micro mill Pulverisette 7 (Fritsch Laboratory Instruments, Idar-Oberstein, Germany) to a size less than 0.063 mm (250 BSS mesh). Analcime powder was treated at room temperature by HCl water solution (12%) under stirring, washed by water before the complete disappearance of Cl^- ions, and dried in thermostat oven at 100-105^{o}C; water suspension (the solid to liquid ratio of 1 : 3) of homogeneous amorphous (XRD tested) material was prepared in Teflon flack; suspension was treated at room temperature by NaOH water solution (20%) under stirring. Phillipsite powder was suspended in Teflon flack placed in shaking water bath OLS 26 Aqua Pro (Grant Instruments, Cambridge, UK) controlling temperature at 90-95^{o}C; suspension was processed with a 12% hydrochloric acid solution at the rate of 5 mL per gram of the solid raw material; activated suspension was diluted with water and treated by adding of a 25% sodium hydroxide solution, followed by the formation of a homogeneous gel. The molar ratios SiO_2/Al_2O_3, Na_2O/Al_2O_3, and H_2O/Na_2O, optimal for obtaining zeolite A from analcime and zeolite X from phillipsite, are given in the Table 1, as well as duration of the gel aging at room temperature and crystallization in temperature-controlled water bath adjusted to prepare micrometric single crystals. Beginning of crystallization was detected by sampling and X-ray diffraction analyses. Separation

of produced crystalline material was carried out by filtration of mother solution, solid material was cleaned by distilled water until pH 8.0-8.5, and dried at 90-100°C.

Table 1. Optimal chemical composition of the gel, duration of its aging and crystallization.

Raw material	Chachubeti analcime	Akhaltsikhe phillipsite
Target product structure	LTA	FAU
Molar ratio SiO_2/Al_2O_3	2.2	3.8
Molar ratio Na_2O/Al_2O_3	9.8	12
Molar ratio H_2O/Na_2O	40	55
Gel aging duration, hr	72	96
Beginning of zeolitization, hr after start	30	16
Total crystallization time, hr	up to 120	up to 55

Preparation of MZs (bioactive-**M**etal-containing **Z**eolites) by "ion exchange synthesis" was carried out using Georgian natural phillipsite-containing tuff rock from Shukhuti (Western Georgia) also described in [16].

The conventional mechanical grinding of tuff to obtain <63 μm (240 mesh) fraction leads to the formation of a multitude of micrometric crystallites (Figure 4a). It is easy to obtain a highly dispersed fraction, since large crystallites (with dimensions of about 50 μm) consist of smaller (about 5 μm) bound together by clay minerals (Figure 4b).

Crushed and sieved rock was washed by diluted HCl solution (0.025 N) to remove clay impurities, and named as NPSH (natural phillipsite from Shukhuti).

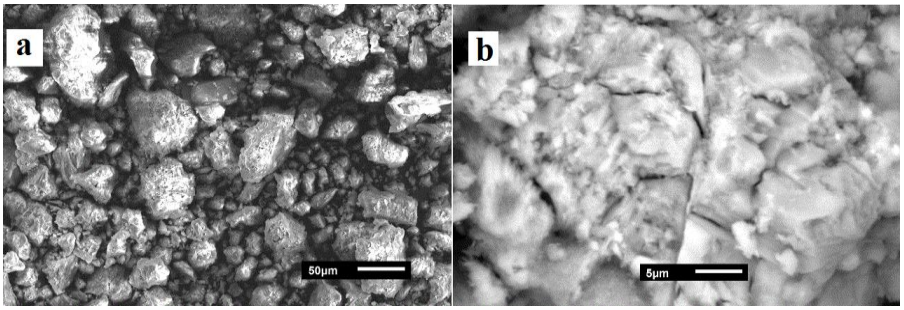

Fig. 4. SEM images with magnification 270 (a) and 2700 (b) of tuff from Shukhuti.

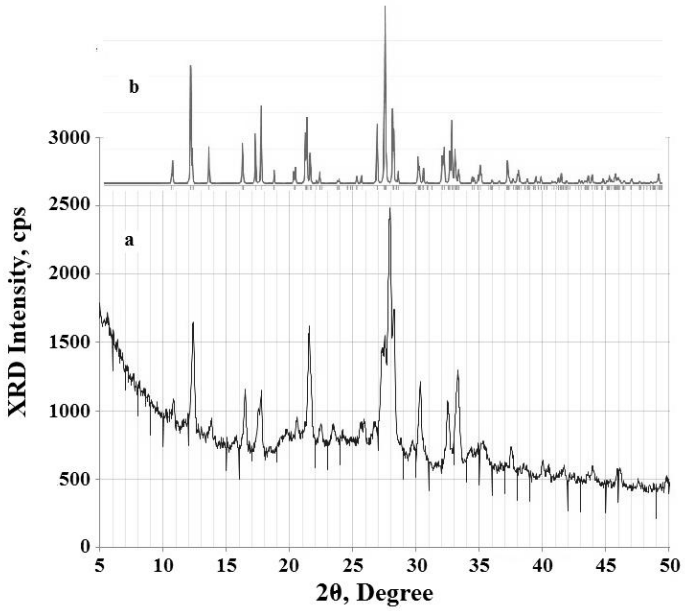

Fig. 5. Powder XRD pattern of NPSH (a) in comparison with calculated pattern (b).

The affiliation of the zeolite phase crystal structure to the PHI type for NPSH was confirmed by comparing the experimental powder X-ray diffraction pattern (Figure 5) with the calculated one from the Database of Zeolite Structures of the International Zeolite Association (http://www.iza-structure.org).

Chemical composition of NPSH corresponds to formula $(Na_{1.30}K_{2.0}Ca_{0.30}Mg_{0.25})Me_{0.10}[Al_{4.50}Si_{11.80}O_{32}]\cdot 11.4H_2O$, Me= $^1/_3Fe^{3+}$, $½Cu^{2+}$, $½Mn^{2+}$, etc. The Si/Al ratio value (2.6) and relatively high sodium content indicate the sedimentary origin of the rock; water content is in a good accordance with accepted crystal chemical formula [6].

Analytical grade silver nitrate $AgNO_3$, copper chloride $CuCl_2$, and zinc chloride $ZnCl_2$ were purchased from Merck KGaA (Darmstadt, Germany) and used without any further purification.

Ion exchange was carried out as follows: powder of zeolite NPSH and the corresponding salt were mixed in different weight ratios (from 1:1 to 1:6) and thoroughly grinded in an agate mortar for 5-10 minutes, depending on the cationic form and weight ratio. The solid mixture was then transferred to a filter and washed with distilled water until the absence of nitrate or chlorine anions, after which the modified samples were first dried in air and then at 100-105^{o}C in a thermostat; samples with a maximum silver content are labeled as AgPSH (silver-containing phillipsite), with a maximum copper and zinc content called CuPSH (copper-containing phillipsite) and ZnPSH (zinc-containing phillipsite), respectively.

Characterization. Chemical composition of samples was determined by elemental and energy dispersive X-ray (EDS) analysis. The crystalline phase was identified by powder X-ray diffraction (XRD) patterns obtained from a Dron-4 X-ray diffractometer (Russia) employing the Cu-K_α line (λ = 0.154056 nm), scanning in the 2Θ range of 5^o to 50^o with a speed of 1^o/min. Fourier transform infrared spectra (FTIR) were collected by a 10.4.2 FTIR spectrometer (Perkin-Elmer, UK) over the range of 400–4000 cm^{-1} with a resolution of 2 cm^{-1} using the KBr pellet technique for sample preparation. The morphology was observed by scanning electron microscope JSM6510LV (Jeol, Japan) equipped with X-Max 20 analyzer (Oxford Instruments, UK) for EDS. Nitrogen adsorption-desorption isotherms were measured at 77 K using an ASAP 2020 Plus analyzer (Micromeritics, Norcross, GA, USA), after evacuation of the samples at 350^{o}C during 2 hours; water adsorption capacity was measured under static conditions.

Metal release and antibacterial activity. The determination of the amount of metals released from MZs in normal salina solution (9 g of NaCl in 1 L of deionized water) was carried out under static conditions in a thermostatic bath (Grant Instruments OLS26 Aqua Pro) at a temperature of 37 ± 0.1 °C, without stirring or shaking. Sampling for analysis was carried out after 1, 3, 6 and 24 hours after loading 0.1 gram of zeolite in 100 ml of salina.

The antibacterial activity of NPSH and MZs was tested against Gram-negative bacteria *Escherichia coli*. Before testing the antibacterial activity, all dry zeolite products were sterilized at 70°C for 2 hours in a dry sterilizer. No microbial contamination of the prepared samples was found.

Luria Bertani (LB) medium sterilized by autoclaving (121^{o}C, 15 min) prior to the antibacterial activity tests was used as a growing medium, bacteria were grown aerobically in LB broth at 37°C for 12 hours, the culture was centrifuged twice (10,000 rpm), and the cells were washed and suspended in distilled water. 1 cm^3 of the prepared biomass suspension of approximately 10^7 colony-forming units (CFU) per cm^3 was inoculated into the Schott's bottles with 100 cm^3 of autoclaved saline, and zeolite samples in a concentration of 0.1 g/100 cm^3 were added. The bottles were incubated in a thermostatic water bath with shaking at 105 rpm for 24 hours at 37±0.1°C. The number of viable cells was determined taking 0.1 mL of water + bacteria + zeolite mixture at the beginning of the experiment, after 1 hour (the lag phase of bacterial growth), and after 3, 6, and 24 hours (the stationary phase). The aliquots were diluted in distilled water, spread on LB agar plates and incubated at 37°C for 24 hours. Bacterial colonies were counted using microscope.

Bacteriostatic properties of natural and modified zeolite samples were determined by the disk diffusion (Kirby-Bauer) method in standard conditions using the culture of *E.coli* grown on Mueller–Hinton agar medium at 37^{o}C for overnight and placed (10^9 CFU/ cm^3) on Mueller–Hinton agar (3 mm deep) poured into 100 mm Petri dishes. 0.2 g of zeolite in the form of pellets with 8 mm in diameter was placed into the plates. The plates were incubated at 37^{o}C over 5% CO_2 medium and, finally, the width of inhibition zone of each sample in the plates was measured at the end of the first day.

All experiments on antibacterial activity of NPSH and MZs were done in triplicate. The values obtained were averaged to give the final data with standard deviations.

RESULTS & DISCUSSION

Chemical composition and XRD of synthetic zeolites. The chemical composition of material, obtained from analcime, is described by the empirical formula $Na_{11.25(25)}(K,½Ca,½Mg)_{0.7(1)}$ $(Al_{11.95(25)}Si_{12.3(3)}O_{48})\cdot 18H_2O$, and is in a good accordance with crystal chemical formula of the LTA structure. There is only a small "lack" of the Al atoms (Si/Al=1.03±0.025), samples of zeolite A obtained from kaolin usually have Si/Al values from 1.15 [17,18] to 1.3 [19]. According to the data of the elemental and EDS analysis, counted on 384 oxygen atoms and 192 T-atoms in the unit cell, the empirical formula of the phillipsite recrystallization product can be represented as $|Na_{66(3)}$ $[Me]_{12(1)}$ $(H_2O)_{248(10)}|$

($Al_{78(3)}Si_{114(4)}O_{384}$) (Me = K, ½Ca, ½Mg, ½Cu and ½Zn, the latter is unevenly distributed). Compared to the crystal chemical formula of FAU [6] with ($Al_{58}Si_{134}O_{384}$) and $(H_2O)_{240}$, the resulting compound has elevated aluminum content with about the same number of crystallization water molecules.

Unambiguous assignment of peaks in the XRD patterns of compounds obtained from analcime (Figure 6) and from phillipsite (Figure 7), confirms the receipt of the target products, zeolites NaA and NaX, respectively.

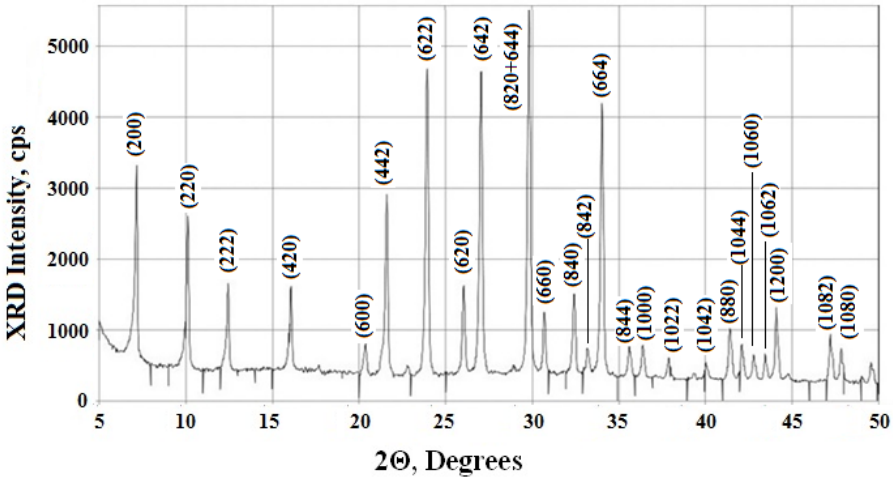

Fig. 6. Assignment of powder XRD pattern of the analcime recrystallization product to the LTA structure and corresponding Miller indices (hkl)

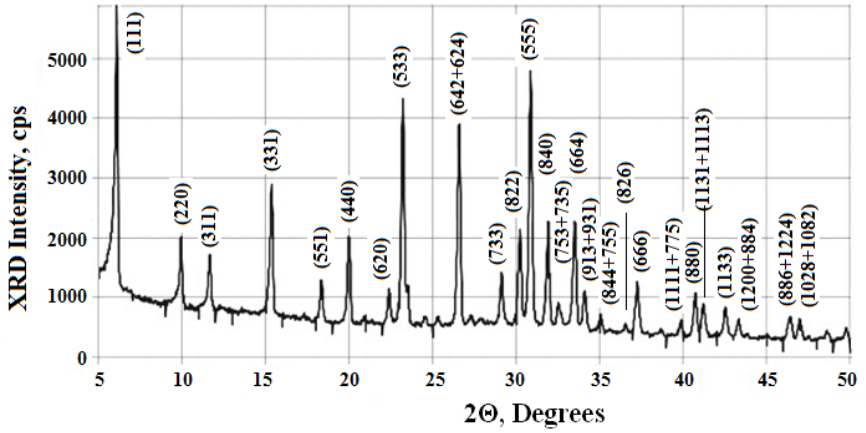

Fig. 7. Assignment of powder XRD pattern of the phillipsite recrystallization product to the FAU structure and corresponding Miller indices (hkl)

FTIR characterization of synthetic zeolites. The mid infra red peak patterns in FTIR spectra (Figure 8) testify formation of zeolite structure in both cases. The band of the internal deformation vibration modes of T-O-T bridges and the band of the internal vibration of T-O symmetric stretching have little influence from the Si/Al ratio: absorption peaks are at 465 and 663 cm^{-1} for zeolite NaA, and at 461 and 668 cm^{-1} for zeolite NaX, respectively. The band associated with the asymmetric external vibration of double 4-rings is more sensitive to the Si/Al ratio: 552 cm^{-1} for zeolite NaA, and 562 cm^{-1} for zeolite NaX.

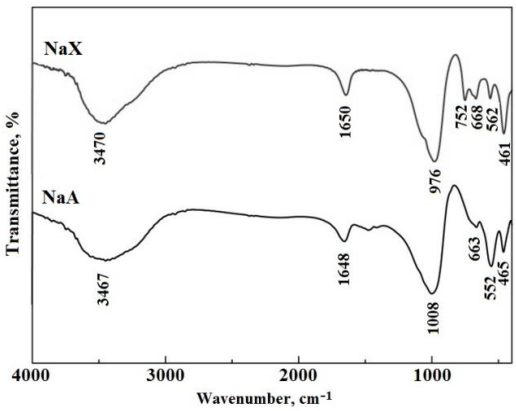

Fig. 3. FTIR spectra of obtained zeolites NaA and NaX.

The band of valence T–O–T vibrations gives resolved peak at 752 cm^{-1} only for zeolite NaX. The internal vibration of T-O asymmetric stretching gives peak at 1008 cm^{-1} for the NaA sample, for zeolite NaX it is shifted to the lower wavenumbers (976 cm^{-1}) due to higher silicon content [23]. In both spectra, bands are observed at ~1650 and ~3470 cm^{-1} corresponding to the presence of H_2O and hydroxyls, respectively. The observed FTIR bands are in good agreement with those reported for both zeolites [21], further proving the successful synthesis of zeolite NaA from analcime and NaX from phillipsite.

***Optimal conditions and parameters of transformation*.** Obtaining of zeolite NaX from a gel with molar ratio SiO_2/Al_2O_3 = 3.8 corresponds to preparation of a single phase NaX zeolite from sodium silicate and sodium aluminate with the SiO_2/Al_2O_3 molar ratio of 1.5–4.0 [22]. The use of pure chemicals leads to development of the NaA at SiO_2/Al_2O_3 = 1.0 in addition to the NaX, and generation of a single phase NaA at SiO_2/Al_2O_3 = 0.5. However, the use of natural precursors leads to other results, the synthesis of zeolite X from coal fly ash was carried out at SiO_2/Al_2O_3 = 5, and zeolite A at SiO_2/Al_2O_3 = 1.67 [21], so that the preparation of zeolite NaA by recrystallization of analcime at SiO_2/Al_2O_3 = 2.2 and large molar ratio Na_2O/Al_2O_3 is understandable. The optimal conditions for the recrystallization of the phillipsite in zeolite Na-X are $2.9Na_2O/SiO_2$ and $\sim 50H_2O/Na_2O$. The same zeolite was synthesized from the coal fly ash at lower sodium content, $2.2Na_2O/SiO_2$, compensated by comparatively low dilution, $\sim 40H_2O/Na_2O$ [21], synthesis of zeolite X from diatomite was carried out in conditions of slightly higher sodium content ($3.0Na_2O/SiO_2$) and lower dilution factor, $40H_2O/Na_2O$ [20]. As can be seen, the crystal structure of phillipsite PHI [6] has a rather low framework density (15.8T/1000$Å^3$), and high alkalinity is not needed for its transformation.

Aging also plays an important role in the nucleation of amorphous gel. In the study, out of considerations of energy saving, the room temperature was chosen for aging the gel and the optimum crystallization temperature was selected below the boiling point of water, eliminating the need for an autoclave and conducting the process of hydrothermal crystallization in a water bath. Of course, this led to a significant increase in the duration of aging, from about six to ten hours to several days, but this saves more than 100 Joules per gram of the reaction mixture.

Sorption properties. The N_2 adsorption-desorption plot at 77 K for the prepared zeolite NaX (Figure 9) up to relative pressure p/p_o~0.92 corresponds to typical Langmuir isotherm attributed to the filling of micropores. The specific surface area calculated by the Brunauer-Emmett-Teller (BET) method is 589 m^2/g, the total pore volume is 0.578 cm^3/g, the volume of micropores with a diameter of less than 8 Å is 0.301 cm^3/g.

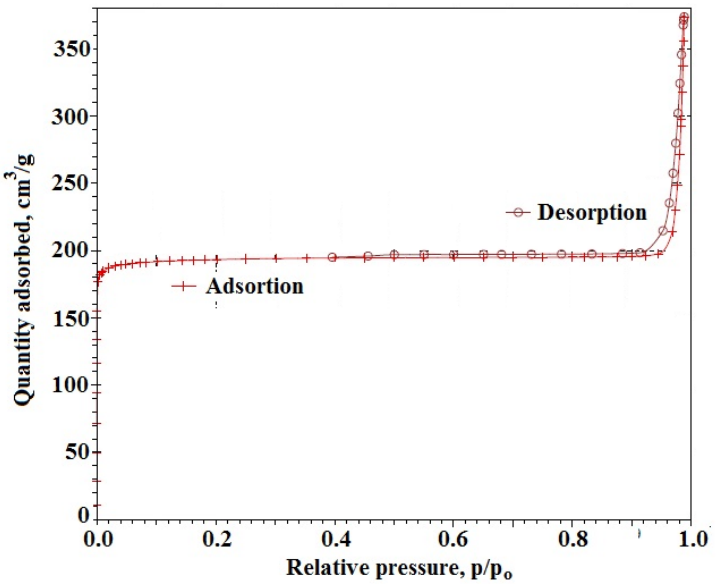

Fig. 9. N_2 adsorption-desorption isotherms on NaX

Type H_1 narrow hysteresis loop, corresponding to the filling of well defined cylindrical channels [24], is observed at high relative pressures (from 0.925 to 0.999). Average channel diameter calculated by the

Barrett-Joyner-Halenda (BJH) method is 55 nm, and a specific volume of channels is 0.277 cm^3/g, constituting ~48% of the total adsorption capacity of the zeolite.

The LTA structure has small pores (0.41 nm) comparable with the kinetic diameter of N_2 (0.364 nm), therefore, the BET surface area of the synthesized NaA sample was not measured; water adsorption capacity of micropores (p/p_0=0.40) is up to 0.24 cm^3/g and is consistent with most of the reports on phase-pure zeolite NaA.

Morphology of synthetic zeolites. In general, more than 92% of NaA crystallites have uniform size of 3 – 5 μm and cubic or rhombus morphology (Figire 10, left), and more than 95% of NaX crystallites have octahedral habit and uniform size of 2 – 7 μm (Figire 10, right). In the process of crystallization, a small amount (<2-3wt.%) of spherical or ellipsoidal nano (0.1 – 0.25 μm) crystallites is also formed, long crystallization results in micrometric crystals combined into honeycomb-like structure through nanocrystal bridges.

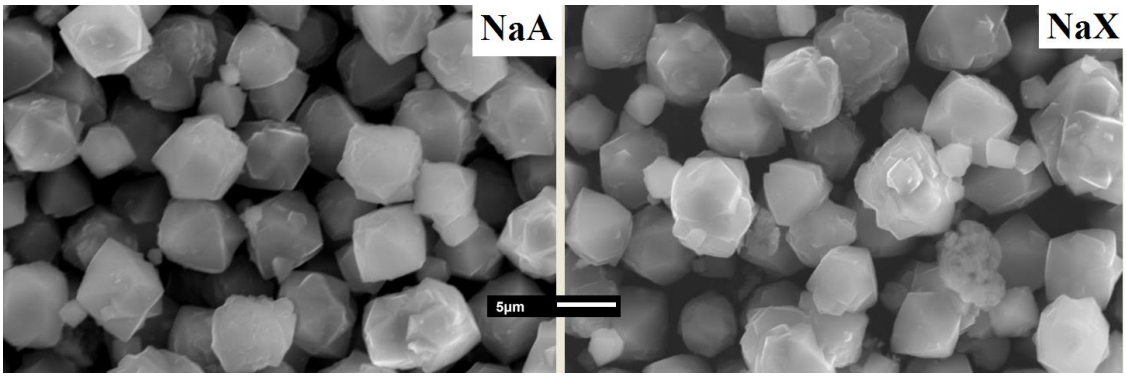

Fig. 10. SEM images (x2,700) of zeolite NaA (left) and zeolite NaX (right)

Metal-containing zeolites (MZs) are promising for environmental protection and medical application. Different studies have demonstrated effectiveness of zeolites for removal of heavy metals from aqueous waste [25, 26]. Besides, started at the beginning of the 21st century and continuing to this day, studies showed that natural and synthetic zeolites exchanged by ions of silver, copper, zinc, or some other transition metals exhibit antimicrobial activity toward a broad range of microorganisms [27-36], and silver-containing zeolites are characterized by the most powerful antibacterial activity [36-39]. In general, silver is considered as antibacterial agent with well-known mode of action, bacterial resistance against silver is well described [40], similarities and differences between silver ions and silver in nanoforms as antibacterial agents were discussed recently [41].

Along with medical use, application of MZs is helpful in the remediation of hazardous heavy metal-polluted soils [42] or in the purification of industrial wastewater [43], in such cases it is necessary to provide the sorption material with bactericidal properties in order to prevent the growth of microorganisms on its surface. It is believed that the porous zeolite structure enables metal cations to move freely from the lattice to the environment, and this seems to be responsible for their activity toward microorganisms [44], and zeolites not containing transition metals (silver, copper, zinc, mercury, cadmium, chromium, and lead) are not active [31, 45], but it has recently been established that in some cases the antibacterial activity could be attributed to the MZ itself [36, 46]. In the preparation of MZs by ion exchange, synthetic zeolites A, X, and Y, as well as cheap natural clinoptilolite of different origin have been used, a list of these works is given in our recent publication [36].

The purpose of the study to develop a fast, eco-friendly method for producing silver-, copper-, and zinc-containing MZs from natural phillipsite characterized by relatively high ion exchange capacity.

Chemical composition of natural phillipsite and its modified forms with a maximum silver, copper or zinc content are listed in the Table 2 in terms of the empirical formulas

$$x(M_aNa_bK_cCa_dMg_eMe_f)[Al_xSi_yO_{32}]\cdot nH_2O,$$

where Me^+ ion corresponds to the impurity metals, M= Ag^+, ½Cu^{2+}, or ½Zn^{2+}, and deviations are given in parentheses.

Table 2. Chemical composition of phillipsites.

Sample	NP	AgP	CuP	ZnP
a (½a for Cu and Zn)	0	0.76(4)	0.400(16)	0.41(15)
b	0.289(14)	0.0022(1)	0.0484(9)	0.0023(1)
c	0.444(24)	0.018(2)	0.0386(8)	0.077(5)
d	0.067(3)	0.056(3)	0.028(3)	0.017(2)
e	0.056(3)	0.045(3)	0.026(4)	0.028(4)
f	0.044(3)	0.013(1)	0.033(2)	0.011(1)
y/x=Si/Al	2.62(16)	2.52(15)	2.60(16)	2.64(16)
n	11.4(6)	14.2(8)	14.3(8)	15.6(9)
a+b+c+2d+2e+f	1.02(6)	1.01(6)	1.03(7)	1.02(6)

Table 3. Content of transition metals in different zeolites after ion exchange

Zeolite / Metal	Ag (mmol/g)	Cu (mmol/g)	Zn (mmol/g)
Shukhuti phillipsite	2.14	1.04	1.30
Calculated [37]	1.85	1.21	1.03
Natural clinoptilolite [33]	0.82		
Zlatokop clinoptilolite [31]		0.410	0.225
Semnan zeolitic tuff [35]	0.24	0.28	0.24
Synthetic Linde 4A [35]	0.27	0.27	0.28
Synthetic faujasite [47]	0.14		

According to the elemental analysis data, when silver, copper, and zinc ions are introduced into the phillipsite crystal lattice, monovalent potassium and sodium ions are mainly displaced. Degree of replacement is quite high, the obtained modified forms contain a large amount of transition metals – up to 230 mg/g (2.14 mmol per 1 g of zeolite) of silver in the AgPSH sample, up to 66 mg/g (~1 mmol per 1 g of zeolite) of copper in the CuPSH sample, and up to 86 mg/g (~1.3 mmol per 1 g of zeolite) of zinc in the ZnPSH sample. In Table 3, obtained results are compared with the maximum possible content of silver, copper, and zinc calculated from ion-exchange isotherms measured on natural clinoptilolite from Gördes, Turkey [37], and with the literature data for clinoptilolites and synthetic zeolites.

It is obvious that phillipsite is a more promising carrier of silver and zinc than natural clinoptilolite. The low content of transition metals in synthetic zeolites is not surprising. Zeolite Linde 4A (crystal chemical formula $|Na_{12}(H_2O)_{27}|_8\,[Al_{12}Si_{12}O_{48}]_8$-**LTA**) was designed for water softening, it is characterized by high aluminum content and is considered as an ideal ion exchanger, but this is true only for reactions with participation of the alkali and alkali earth metals $2Na^+ \leftrightarrow Ca^{2+}(Mg^{2+})$, the exchange of monovalent sodium, potassium and silver ions with cumulating of Ag^+ in crystal lattice is unlikely, as is the exchange of sodium or potassium with a strongly hydrated copper or zinc ion. Faujasite (crystal chemical formula $|(Ca,MgNa_2)_{29}\,(H_2O)_{240}|\,[Al_{58}Si_{134}O_{384}]$- **FAU**) is a weak ion-exchanger; besides, faujasite usually contains a lot of calcium and magnesium, which hardly enter into an exchange with ions in solution.

Silver ions Ag^+ quite easily enter the microporous structure of phillipsite, the introduction of copper Cu^{2+} and zinc Zn^{2+} ions requires an increased amount of salt and a longer contact with the surface of the zeolite. This can probably be explained by a slight difference in the hydration character of the ions entering the pores of the zeolite. So, an "isolated" silver ion Ag^+ (radius 0.115 nm) is larger than Cu^{2+} and Zn^{2+} ions (radii 0.073 and 0.074 nm, respectively), but the hydrated silver(I) ion contains four water molecules ($Ag(H_2O)_4^+$) in a linearly distorted tetrahedron configuration, whereas the hydrated copper(II) and zinc(II) ions contain six water molecules ($M(H_2O)_6^{2+}$) and have regular octahedral configuration [48].

Crystal structure of MZs. Ion exchange reactions do not change the crystal structure of the zeolite, this is confirmed both by the powder X-ray diffraction patterns and IR spectra of the modified samples: characteristic peaks remain in XRD patterns, only their intensities change, as shown in the Table 4, and no notable changes were observed in the IR spectra of the modified phillipsites as compared with the vibration bands of raw zeolitic mineral (Table 5), only the intensity of the broad band at 3200 – 3700 cm^{-1} corresponding to the asymmetric stretching of OH group is increased due to the larger number of water molecules in the samples containing silver, copper, and zinc.

The ratio of the absorbance of asymmetric stretching vibration of the external tetrahedron with frequency ν_{asym} to the absorbance of internal bending vibration with frequency δ was used for the evaluation of the IR spectra data for natural and modified Mexican zeolite [28]; for a mixture of

clinoptilolite-heulandite and corresponding MZs, this ratio varies from 1.34 to 1.64, but for phillipsite NP and its modifications, this ratio varies only slightly from 1.75 to 1.82. A narrow absorption band at 1385 cm^{-1} typical for NO stretching vibrations in nitro compounds was observed in IR spectra of insufficiently washed silver-enriched phillipsite, this effect can be used to monitor the purity of silver-containing samples.

Table 4. Miller indices (hkl), 2Θ angles and relative intensities in powder XRD patterns of natural and modified phillipsites.

Hkl	2Θ (°)	NPSH	AgPSH	CuPSH	ZnPSH
–101	10.9	<10	<10	12	<10
001	12.3	56	<15	43	73
011	13.8	23	35	30	18
120	16.5	<10	<10	23	45
021	17.5	36	24	18	28
–201	18.0			38	35
–211	19.0	<10.	<10.	15	<10
111	21.5	15	36	28	24
–112	21.6		59		61
–221	21.8	<10	<10	14	<10
140	27.2	35	33	37	40
022+041	27.9	100	100	100	100
–311	28.5	53	42	40	37
–321	30.5	<10	32	30	28
102	32.4	46	40	35	<15
112+150	33.0	48	36	27	23
–223	33.4	16	<10	<10	16

Table 5. The IR vibration bands (cm^{-1}) in FTIR spectra of phillipsites

Type of vibration / Sample	NPSH	AgPSH	CuPSH	ZnPSH
Asymmetric stretching of OH group	3436*	3530*	3440*	3570*
Bending vibration of H–OH	1647	1652	1636	1651
Bending vibration of bridging –OH-O–	1520*	1495*	1448	1463*
Internal asymmetric stretching	1200**	1100**		1100**
External asymmetric stretching (ν_{asym})	1030	1031	1033	1034
External symmetric stretching	760**	825	785	790**
Internal symmetric stretching	694	698	689	696
External tetrahedrons double ring vibration	606; 536	608; 536	592; 524	594; 532
Internal tetrahedrons bending vibration (δ)	444	440	444	442
Absorbance (ν_{asym})/ absorbance (δ)	1.82	1.80	1.78	1.75

* – maximum of broad peak; ** – shoulder at broad peak

Sorption properties of MXs. The nitrogen adsorption-desorption isotherms on natural phillipsite (Figure 11) and MZs demonstrate a hysteresis loop with a jump at p/p_0= 0.4-0.5 indicating the presence of mesopores including slit-shaped pores in non-rigid aggregates of particles (H_3 type hysteresis loop) and possibly well defined cylindrical pore channels (H_1 type hysteresis). Average pore diameter of mesopores, calculated by the Barrett-Joyner-Halenda metod using adsorption and desorption isotherm, is 22.0 and 54.4 nm, respectively.

Some changes are observed for adsorption isotherms of MZs at low relative pressures ($0.05<p/p_0<0.25$), under conditions of filling micropores. However, the pore sizes in phillipsite crystal structure are close to the kinetic diameter of N_2 (3.64 Å), and the Brunauer-Emmett-Teller method cannot be used to estimate the surface area and volume of micropores: despite the formal suitability of this method up to $p/p_0<0.2$, it gives an average pore diameter over 15 nm, typical for mesopores and not for micropores.

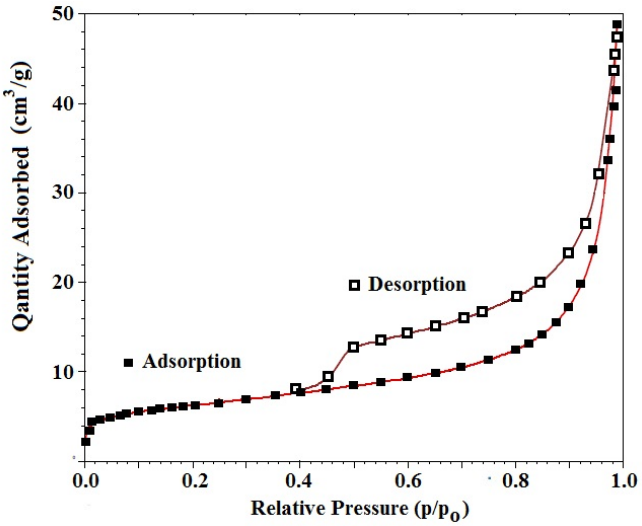

Fig. 11. N_2 adsorption-desorption isotherms on NPSH.

Table 6. The water adsorption capacity of phillipsites.

Water adsorption (mm^3/g)	**NP**	**AgP**	**CuP**	**ZnP**
In micropores (p/p_0=0.4)	130±6	100±5	120±8	118±6
Total (p/p_0=1.0)	285±15	282±12	286±18	290±15

Room temperature water adsorption capacity (Table 6) at the "plateau" pressure (p/p_0=0.40) is 7.25 mmol/g or 0.130 cm^3/g, and is 46% of the total water adsorption capacity 0.285 cm^3/g, which is close to the total pore volume 0.278 cm^3/g, determined from the low-temperature N_2 adsorption- desorption isotherms.

The total pore volume within the experimental error is preserved; the volume of micropores in the MZs available for the adsorption of water molecules decreases, especially for the silver-containing sample AgP. Apparently, transition metal ions, when introduced into the zeolite structure, at least partially retain their hydration shell, effectively reducing the free micropore volume.

Morphology of MXs. In general, the procedure of ion-exchange synthesis leads to a significant increase in the dispersion of the material, the size of the largest crystallites does not exceed 20 μm for AgPSH (Figure 12a) and 30 μm for ZnPSH (Figure 13a) and CuPSH. Compared with the natural phillipsite, the proportion of crystallites smaller than 2 μm is increased, especially for the AgPSH sample (Figure 12b). The silver- and copper- containing crystals are sufficiently isolated, whereas the aggregation of zinc-containing crystallites (Figure 13b) is preserved to a greater degree, like in the natural phillipsite.

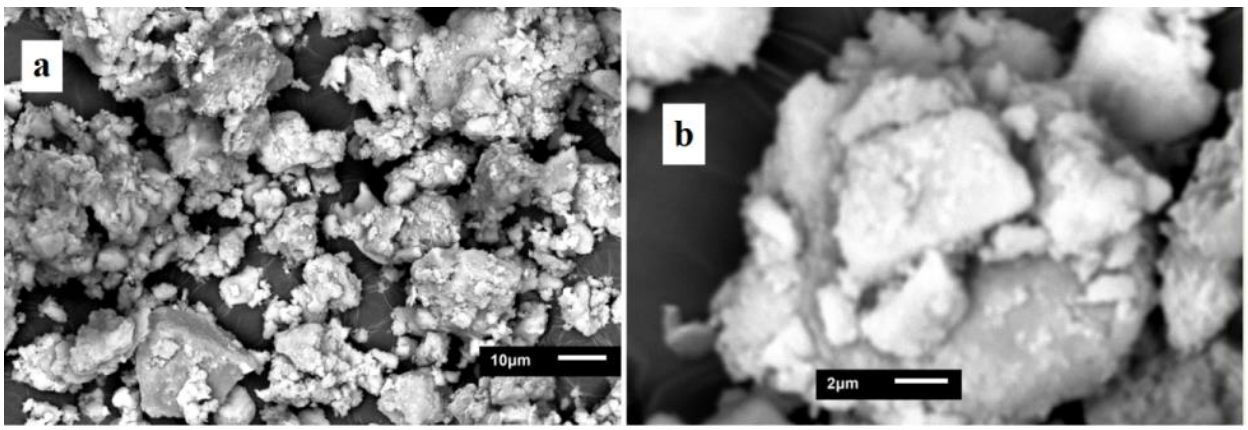

Figure 12. SEM images with magnification 1000 (a) and 5500 (b) of AgP

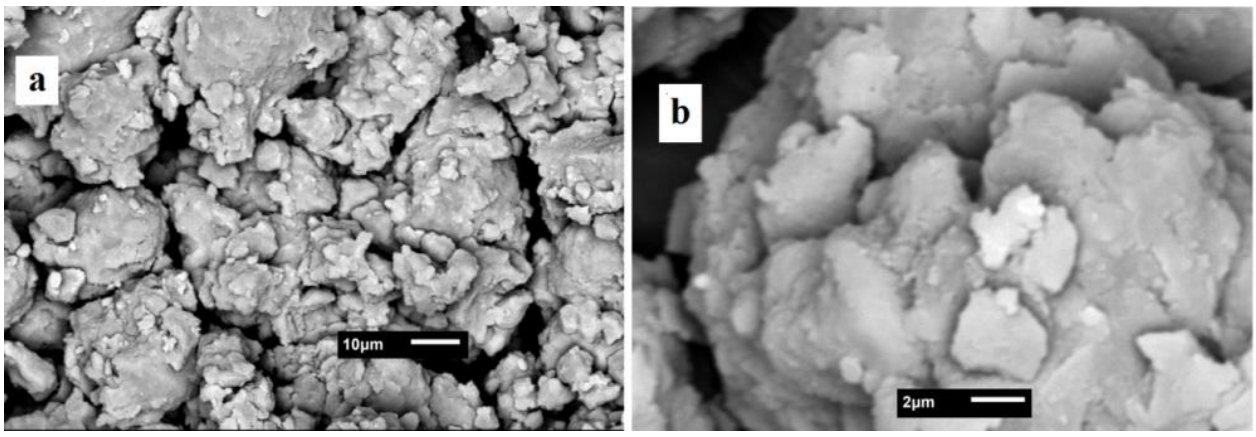

Fig. 13. SEM images with magnification 1000 (a) and 5500 (b) of ZnP

Release of metal ions from MXs. The amount of silver ions released after 6 hours (Table 7) corresponds to concentration of 0.067 mM, which is higher than the minimal inhibitory concentration (MIC) value for silver ions toward *E. coli*, 3.996 mg Ag in dm^3 [49] or 0.037 mM. On the contrary, the amount of copper and zinc ions released after 24 hours corresponds to concentration of 0.45 and 0.5 mM, respectively, lower than MIC value for copper and zinc ions toward *E. coli*, 1 mM [50].

Table 7. The leaching of metals (mg/L) from modified phillipsites

Ions	Ag^+ from AgP	Cu^{2+} from CuP	Zn^{2+} from ZnP
In 1 hour	<5	<5	5.2±1.2
In 3 hours	<5	8.5±2.5	12.7±2.5
In 6 hours	7.2±1.5	16.2±3.2	23.0±5.5
In 24 hours	20.6±4.5	28.7±4.5	32.4±6.6

Table 8. The change in the relative number of viable cells of *E. coli* in time

Sample	NP	AgP	CuP	ZnP
At the beginning	100	100	100	100
After 1 hr	102.5±4.2	72.0±4.1	85.0±5.0	93.2±6.5
After 3 hr	98.3±3.5	23.6±2.8	42.0±2.5	51.6±4.7
After 6 hr	99.6±4.5	0	12.0±2.0	30.4±2.2
After 24 hr	100.5±4.8	0	0	0

Table 9. Bacteriostatic properties of NP and MZs against *E. coli*

Sample	Diameter of inhibition zone (mm)
Petri dish with *E. coli* only (check)	0 – confluent growth
Petri dish with *E. coli* and NP	0 – confluent growth
Petri dish with *E. coli* and AgP	18.6±0.7
Petri dish with *E. coli* and CugP	15.7±1.0
Petri dish with *E. coli* and ZnP	16.3±0.9

Bactericidal activity of MZs. Table 8 shows the relative number of viable cells of *E. coli* suspended in water after their contact with natural and modified phillipsites in relation to the number of cells at the beginning of the experiment.

Taking into account the leaching of bioactive metals and their comparison with the values of the minimal inhibitory concentrations, we can conclude that the antibacterial activity of CuPSH and ZnPSH could be ascribed to the metal- containing zeolite M-Z itself and not to the leached metal ions. The silver-containing zeolite AgPSH also exhibits a certain antibacterial activity even before the concentration of ions in the solution reaches the MIC value, and its bactericidal effect could be ascribed not only to released Ag^+ ions but also to AgPSH itself.

The total number of bacteria in bottles with NPSH was not significantly different than in the corresponding controls, showing that natural and modified phillipsite had no antibacterial activity itself.

Bacteriostatic activity of MZs. Results of the Kirby-Bauer test are given in the Table 9. No antibacterial action was observed for the original

phillipsite. The width of the inhibition zones of the antibacterial metal-exchanged forms AgPSH, CuPSH, and ZnPSH is of the same order of magnitude as for silver-, copper, and zinc-containing clinoptilolite-rich mineral from Gördes, Turkey, Western Anatolia [37], and exceed diameter of inhibition zones reported for copper-containing clinoptilolite from the "Holinskoe" mineral deposit, Russia, Republic of Buryatia [43].

Environmental Aspect. Modern production of drugs must comply with environmental standards and principles. The use of synthetic and natural zeolites for the production of carriers of medicinal metals meets the conditions of wasteless production in relation to the main raw materials and reagents, but the consumption of associated materials is rather high. The Sheldon's factor E, the ratio of the mass of waste per mass of product [51], is an important environmental and green chemistry metrics, and its reduction is an urgent task. Table 10 presents data on the consumption of liquid materials for various methods of ion-exchange production of MZs. Information about the required quantities of zeolites, reagents and solutions have been obtained from recent publications [31], [33], [35], and [47].

Table 10. Waste generated in the production of one gram of MZs and Sheldon's factor E

Ion exchange method	Liquid waste (mL)		E
	Salt solution	Water	
Solid state on phillipsite	–	500	500
In solution on synthetic zeolite	>400	300	>700
One-step in solution on clinoptilolite	>500	300	>800
Two-step in solution on clinoptilolite	>1000	600	>1600

Data on the amount spent on washing the target products by distilled water, as a rule, are not given in publications. In accordance with our experience [52], washing of one gram of product filtered from a solution needs at least 300 mL of water, and washing after a "dry" ion exchange requires at least 500 mL. Solid waste such as zeolites, reagents, packaging and other consumables were not taken into account. The findings suggest that the solid-state "dry" method is preferable to the "wet" method of the ion exchange in solution.

CONCLUSIONS

Thus, it is found that phase-pure zeolite NaA with chemical composition ($Na_{11.25(25)}$ $(K,½Ca,½Mg)_{0.7(1)}$ $(Al_{11.95(25)}Si_{12.3(3)}O_{48}).18H_2O$) can be prepared in the form of cubic/rhombus crystallites with uniform micrometric (3-5 μm) dimensions by hydrothermal crystallization (95°C) of aged (72 hr) at room temperature gel ($4.5Na_2O$: $0.45Al_2O_3$: $1SiO_2$: $178H_2O$) obtained from natural analcime, treated with hydrochloric acid before suspending in water and mixing with sodium hydroxide. Phase-pure zeolite NaX ($|Na_{66(3)}$ $[K,½Ca,½Mg,½Cu,½Zn]_{12(1)}$ $(H_2O)_{248(10)}|$ $(Al_{78(3)}Si_{114(4)}O_{384})$) with specific surface area of 589 m_2/g and total pore volume of 0.578 cm_3/g can be prepared in the form of octahedral crystallites with uniform micrometric (2-7 μm) dimensions by hydrothermal crystallization (95°C) of aged (96 hr) at room temperature gel ($2.9Na_2O$: $0.26Al_2O_3$: $1SiO_2$: $150H_2O$) obtained from water suspension of natural phillipsite, treated with hydrochloric acid and mixed with sodium hydroxide. Zeolite NaX is characterized by high specific surface area (589 m^2/g) and volume of pores (0.578 cm^3/g) including uniform zeolitic micropores and cylindrical channels with an average diameter of 55 nm.

The resulting zeolites NaA and NaX in their characteristics are competitive with commercially available materials..

As a result of the conducted research on the ion-exchange synthesis, it was established that solid-state ion-exchange reactions between Georgian natural phillipsite and salt of corresponding transition metal followed by washing results in zeolite materials with a significantly higher content of silver (up to 230 mg/g), copper (up to 66 mg/g), and zinc (up to 86 mg/g), rather than obtained by ion exchange in solutions on synthetic zeolites and natural clinoptilolite.

Ion exchange reactions do not change the microporous crystal structure of the zeolite, this is confirmed by the powder X-ray diffraction patterns and FTIR spectra of the modified samples. Isotherms of nitrogen adsorption-desorption and water adsorption capacity indicate preservation of total pore volume and system of mesopores including cylindrical pore channels with average diameter of 22 nm and slit-shaped pores in non-rigid aggregates of particles (over 50 nm); SEM images show that the procedure of dry ion- exchange synthesis leads to an increase in the dispersion of the material. The introduction of hydrated silver, copper, and zinc ions into the channels and pores of the zeolite is facilitated by the developed system of macro- and mesopores in the used natural phillipsite.

Synthesized adsorbent-ion-exchangers show bactericidal activity towards *Escherichia coli*. According to the changes in the relative number of viable cells of bacteria contacting with zeolites and the data on leaching of metals from modified zeolites compared to the minimal inhibitory concentration (MIC) values for corresponding ions toward *E. coli*, the silver-containing zeolite exhibits a certain antibacterial activity even before the concentration of ions in the solution reaches the MIC value, and its bactericidal effect could be ascribed not only to released Ag^+ ions but also to Ag-phillipsite itself; the copper- and zinc-containing zeolites emit a small amount of ions (up to 0.5MIC) and their activity is entirely attributed to Cu-phillipsite and Zn-phillipsite themselves. Strong bacteriostatic activity of modified zeolites was established by the Kirby-Bauer test.

The resulting MZs have sorption and bactericidal properties, sufficient for their use in the purification and disinfection of water. The bactericidal activity of the modified materials themselves requires further detailed study of their surface properties.

AKNOWLEDGMENT

Investigation of zeolite hydrothermal transformations was carried out under the Projects FR-17_187 "Study of process of fine-dispersed zeolite crystal formation and scientific substantiation of possibility of creation of new materials" and FR-18-2600 "Scientific feasibility of creating nanocrystalline bactericidal sorbents on the basis of Georgian natural zeolites and the study of corresponding mechanisms" supported by the Shota Rustaveli National Science Foundation of Georgia.

REFERENCES

[1] Li Y., Li L., Yu J. "Applications of zeolites in sustainable chemistry". *Chem*, 2017, vol. 3, pp. 928-949.

[2] Bacakova L., Vandrovcova M., Kopova I., Jirka I. "Applications of zeolites in biotechnology and medicine – a review". *Biomaterials Sci.*, 2018, vol. 6, pp. 974-989.

[3] Abdullahi T., Harun Z., Othman, M.H.D. "A review on sustainable synthesis of zeolite from kaolinite resources via hydrothermal process". *Advanced Powder Technology*, 2017, vol. 28, pp. 1827-1840.

[4] Skhirtladze N. Genetic groups of Georgian zeolites, their main deposits and manifestations. Tbilisi University Press, Tbilisi, 1997, 27 p

[5] Tsitsishvili G.V., Skhirtladze N.S., Andronikashvili T.G., Tsitsishvili V.G., Dolidze A.V. "Natural zeolites of Georgia: Occurrences, properties, and application". *Stud. Surf. Sci. Catal*., 1999, vol. 125, pp. 715-722.

[6] Baerlocher Ch., McCucker L.B., Olson D.H. Atlas of zeolite framework types. Sixth revised edition. 2007, Elsevier, Amsterdam, 398 p.

[7] Hui K.S., Chao C.Y.H. "Pure, single phase, high crystalline, chamfered-edge zeolite 4A synthesized from coal fly ash for use as a builder in detergents". *Journal of Hazardous Materials*, 2006, vol. 137, no 1, pp. 401-409.

[8] Izidoro J.D.C., Fungaro D.A., Abbott, J.E., Wang, S. "Synthesis of zeolites X and A from fly ashes for cadmium and zinc removal from aqueous solutions in single and binary ion systems". *Fuel*, 2013, vol. 103, pp. 827-834.

[9] Kallo D. "Applications of natural zeolites in water and wastewater treatment". *Reviews in Mineralogy and Geochemistry*, 2001, vol. 45, pp. 519-550.

[10] Bhatnagar A. Application of adsorbents for water pollution control. Bentham Science Publishers, Sharjah, Oak Park, Bussum, 2012, p. 363-381.

[11] Rawajfih Z., Al Mohammad H., Nsour N., Ibrahim K. "Study of equilibrium and thermodynamic adsorption of α-picoline, β-picoline, and γ-picoline by Jordanian zeolites: Phillipsite and faujasite". *Microporous and Mesoporous Materials*, 2010, vol. 132, pp. 401-408.

[12] Gallego E.M., Teresa Portilla M., Paris C., León-Escamilla A., Boronat M., Moliner M., Corma A. ""Ab initio" synthesis of zeolites for preestablished catalytic reactions". *Science*, 2017, vol. 355, no 6329, pp. 1051-1054.

[13] Tsitsishvili V., Tsitsishvili G., Dolaberidze N., Alelishvili M., Chipashvili D., Tsintskaladze G., Sturua G., Nijaradze M., Gigolashvili N., Mirdzveli N. "Characterization of Georgian natural zeolites". In: *Chemistry of Advanced Compounds and Materials*, New-York: Nova Science Publishers, 2008, pp. 123-131.

[14] Pylev L.N., Kulagina T.F., Grankina E.P., Chelishchev N.F., Berenstein B.G. "Carcinogenicity of zeolite phillipsite". *Gigiena i Sanitaria*, 1989, vol. 8, pp. 7-10 (in Russian).

[15] Zeolites other than erionite (Group 3). IARC Monographs, 1997, vol. 68, pp. 307-333.

[16] Tsitsishvili V., Dolaberidze N., Alelishvili M., Tsintskaladze G., Sturua G., Chipashvili D., Nijaradze M., Khazaradze N. "Adsorption and thermal properties of zeolitic rocks from newly investigated deposit plots in Georgia". *Georgian Engineering News*, 1998, vol. **2**(6), pp. 61-65.

[17] Alkan M., Hopa Ç., Yilmaz Z., Güler H. "The effect of alkali concentration and solid/liquid ratio on the hydrothermal synthesis of zeolite NaA from natural kaolinite". *Microporous Mesoporous Mater*., 2005, vol. 86, pp. 176-184.

[18] Ríos Reyes C.A., Williams C.D., Castellanos Alarcón O.M. "Synthesis of zeolite LTA from thermally treated kaolinite". *Revista Facultad de Ingenieria Universidad de Antioquia*, 2010, vol. 2010, pp. 30-41.

[19] Ugal J.R., Hassan K.H., Ali I.H. "Preparation of type 4A zeolite from Iraqi kaolin: characterization and properties measurements". *Journal of the Association of Arab Universities for Basic Applied Sciences*, 2010, vol. **9**:, pp.2-5.

[20] Mozgawa W., Sitarz M., Rokita, M. "Spectroscopic studies of different aluminosilicate structures". *Journal of Molecular Structure*, 1999, vol. 511-512, pp. 251-257.

[21] Hu T., Gao W., Liu X., Zhang Y., Meng C. "Synthesis of zeolites Na-A and Na-X from tablet compressed and calcinated coal fly ash". *Royal Society Open Science*, 2017, vol. 4, no. 10, pp. 170921-170934.

[22] Zhang X., Tang D., Zhang M., Yang R. "Synthesis of NaX zeolite: Influence of crystallization time, temperature and batch molar ratio SiO_2/Al_2O_3 on the particulate properties of zeolite crystals". *Powder Technology*, 2013, vol. 235, pp. 322-328.

[23] Yao G., Lei J., Zhang X., Sun Z., Zheng S. "One-step hydrothermal synthesis of zeolite X powder from natural low-grade diatomite". *Materials*, 2018, vol. 11, pp. 906-920.

[24] Sing K.S.W., Everett D.H., Haul R.A.W., Moscou L., Pierotti R.A., Rouquérol J., Siemieniewska T. "Reporting physisorption data for gas/solid systems with special reference to the determination of surface area and porosity". *Pure & Applied Chemistry*, 1985, vol. 57, pp. 603-612.

[25] Fu F., Wang Q. "Removal of heavy metal ions from wastewaters: a review". *Journal of Environmental Management*, 2011, vol. 92, pp. 407-418.

[26] Steffin J.E., Dilson B.S., Manikandan P. M. "An overview on activated carbon and zeolites in water treatment," *Imperial Journal of Interdisciplinary Research*, 2016, vol. 2, pp. 6-11.

[27] Kawahara K., Tsuruda K., Morishita M., Uchida M. "Antibacterial effect of silver-zeolite on oral bacteria under anaerobic conditions". *Dental Materials Journal*, 2000, vol. 16, no 6, pp. 452-455.

[28] Rivera-Garza M., Olguin M.T., Garcia-Sosa I., Alcantara D., Rodriguez-Fuentes G. "Silver supported on natural Mexican zeolite as an antibacterial material". *Microporous and Mesoporous Materials*, 2000, vol. 39, pp. 431-444.

[29] De la Rosa-Gomez I., Olguin M.T., Alcantara D. "Bactericides of coliform microorganisms from wastewater using silver-clinoptilolite rich tuffs". *Applied Clay Science*, 2008, vol. 40, no 1-4, pp. 45-53.

[30] Ferreira L., Fonseca A.M., Botelho G., Almeida-Aguiar C., Neves I.C. "Antimicrobial activity of faujasite zeolites doped with silver". *Microporous and Mesoporous Materials*, 2012, vol. 160, pp. 126-132.

[31] Hrenovic J., Milenkovic J., Ivankovic T., Rajic N. "Antibacterial activity of heavy metal-loaded natural zeolite". *Journal of Hazardous Materials*, 2012, vol. 201-202, pp. 260-264.

[32] Guerra R., Lima E., Viniegra M., Guzman A., Lara V. "Growth of Escherichia coli and Salmonella typhi inhibited by fractal silver nanoparticles supported on zeolite". *Microporous and Mesoporous Materials*, 2012, vol. 147, no 1, pp. 267-273.

[33] Akhigbe L., Ouki S., Saroj D., Min Lim X. "Silver-modified clinoptilolite for the removal of Escherichia coli and heavy metals from aqueous solutions". *Environmental Science and Pollution Research*, 2014, vol. 21, no 18, pp. 10940-10948.

[34] Rossainz-Castro L.G., De la Rosa-Gomez I., Olguín M.T., Alcantara-Díaz D. "Comparison between silver- and copper-modified zeolite rich tuffs as microbicidal agents for Escherichia coli and Candida albicans". *Journal of Environmental Management*, 2016, vol. 183, no 3, pp. 763-770.

[35] Milenkovic J., Hrenovic J., Matijasevic D., Niksic M., Rajic N. "Bactericidal activity of Cu-, Zn-, and Ag-containing zeolites toward *Escherichia coli* isolates". *Environmental Science and Pollution Research*, 2017, vol. 24, pp. 20273–20281.

[36] Dolaberidze N.M., Tsitsishvili V.G., Khutsishvili B.T., Mirdzveli N.A., Nijaradze M.O., Amiridze Z.G., Burlanadze M.N. "Silver- and zinc-containing bactericidal phillipsites". *New Materials, Compounds and Applications*, 2018, vol. 2, no 3, pp. 247-260.

[37] Top A., Ülkü S. "Silver, zinc, and copper exchange in Na-clinoptilolite and resulting effect on antibacterial activity". *Applied Clay Science*, 2004, vol. 27, no 1-2, pp. 13-19.

[38] Hrenovic J., Milenkovic J., Goic-Barisic I., Rajic N. "Antibacterial activity of modified natural zeolite against clinical isolates of

Acinetobacter baumannii". *Microporous and Mesoporous Materials*, 2013, vol. 169, pp. 148-152.

[39] Demirci S., Ustaoğlu Z., Yılmazer G.A., Sahin F., Baç N. "Antimicrobial properties of zeolite-X and zeolite-A ion-exchanged with silver, copper, and zinc against a broad range of microorganisms". *Applied Biochemistry and Biotechnology*, 2014, vol. 172, no 3, pp. 1652-1662.

[40] Klasen H.J. "Historical review of the use of silver in the treatment of burns. I. Early uses. II. Renewed interest for silver". *Burns: journal of International Society for Burn Injuries*, 2000, vol. 26, no 2, pp. 117-138.

[41] Kędziora A., Speruda M., Krzyżewska E., Rybka J., Łukowiak A., Bugla-Płoskońska G. "Similarities and differences between silver ions and silver in nanoforms as antibacterial agents". *International Journal of Molecular Sciences*, 2018, vol. 19, no 2, pp. 444-461.

[42] Shi W.Y., Shao H.B., Li H., Shao M.A., Du S. "Progress in the remediation of hazardous heavy metal-polluted soils by natural zeolite". *Journal of Hazardous Materials*, 2009, vol. 170, no 1, pp. 1-6.

[43] Martemianova I., Nadeina L., Plotnikov E., Martemianov D. "Modification of natural sorbent for providing it with bactericidal and bacteriostatic properties". *MATEC Web of Conferences*, 2016, vol. 85, p. 01030.

[44] Kwakye-Awuah B., Williams C., Kenward M.A., Radecka I. "Antimicrobial action and efficiency of silver-loaded zeolite X". *Journal of Applied Microbiology*, 2008, vol. 104, pp. 1516-15248.

[45] Jiraroj D., Tungasmita S., Tungasmita D.N. "Silver ions and silver nanoparticles in zeolite A composites for antibacterial activity". *Powder Technology*, 2014, vol. 264, pp. 418-422.

[46] Milenkovic J., Hrenovic J., Matijasevic D., Niksic M., Rajic N. "Bactericidal activity of Cu-, Zn-, and Ag-containing zeolites toward *Escherichia coli* isolates". *Environmental Science and Pollution Research*, 2017, vol. 24, pp. 20273–20281.

[47] Jędrzejczyk R.J., Turnau K., Jodłowski P.L., Chlebda D. K., Łojewski T., Łojewska J. "Antimicrobial properties of silver cations substituted to faujasite mineral," *Nanomaterials (Basel)*, 2017, vol. 7, no. 9, pp. 240-251.

[48] Persson I. "Hydrated metal ions in aqueous solution: How regular are their structures?," *Pure and Applied Chemistry*, 2010, vol. 82, no. 10, pp. 1901-1917.

[49] Mulley G., Jenkins A.T.A., Waterfield N.R. "Inactivation of the antibacterial and cytotoxic properties of silver ions by biologically relevant compounds". PLoS ONE, [Online], 2014, vol. 9, no 4, pp. e94409 (Available: https://doi.org/10.1371/journal.pone.0094409).

[50] Navarro C.A., von Bernath D., Jerez C.A. "Heavy metal resistance strategies of acidophilic bacteria and their acquisition: Importance for biomining and bioremediation". *Biological Research*, 2017, vol. 46, no 4, pp. 363-371.

[51] Sheldon R.A. "The E factor: fifteen years on," *Green Chemistry*, 2007, vol. 9, no. 12, pp. 1273-1283.

[52] Tsitsishvili V., Dolaberidze N., Urotadze S., Alelishvili M., Mirdzveli N., Nijaradze M. "Ion exchange properties of Georgian natural zeolites," *Chemistry Journal of Moldova*, 2017, vol. 12, no. 1, pp. 95-101.

საქართველოს ბუნებრივი ცეოლითების ჰიდროთერმული და იონმიმოცვლითი გარდაქმნები

ვლადიმერ ციციშვილი*, ნანული დოლაბერიძე, ნატო მირძველი, მანანა ნიჟარაძე, მანანა ბურჯანაძე, გიორგი წინწკალაძე,ზურაბ ამირიძე, ვახტანგ გაბუნია

თსუ პეტრე მელიქიშვილის სახ. ფიზიკური და ორგანული ქიმიის ინსტიტუტი, ა.პოლიტკოვსკაიას ქ. 31, თბილისი 0186
**v.tsitsishvili@gmail.com +995 599 988198*

რეზიუმე. წარმოდგენილ ნაშრომში შეჯამებულია საქართველოში ფართოდ გავრცელებული ბუნებრივი ცეოლითების (ანალციმისა და ფილიპსიტის) ჰიდროთერმული და იონმიმოცვლითი გარდაქმნების კვლევები ადგილიბრივი ნედლეულის საფუძველზე ღირებული პროდუქტების მიღების მიზნით.
აღმოჩენილია, რომ ფაზურად სუფთა NaA ტიპის ცეოლითი, სილიკატური მოდულით Si/Al~1, ერთგვაროვანი მიკრომეტრული (3-5 მკმ) კუბური და რომბული კრისტალიტების სახით, მიიღება მარილმჟავის წყალხსნარში წინასწარ დამუშავებული ბუნებრივი ანალციმისაგან, მისი სუსპენდირებით, ნატრიუმის ჰიდროქსიდთან შერევით, ჰომოგენიზაციის შედეგად მიღებული ალუმინ-სილიკატური გელის ($4.5Na_2O$: $0.45Al_2O_3$: $1SiO_2$: $178H_2O$) ოთახის ტემპერატურაზე ხანგრძლივი დაბერებით და შემდგომი ჰიდროთერმული კრისტალიზაციის გზით. ფაზურად სუფთა NaX ტიპის ცეოლითი, სილიკატური მოდულით Si/Al~1.5, ერთგვაროვანი მიკრომეტრული (2-7 მკმ) ოქტაედრული კრისტალიტების სახით, მიიღება ბუნებრივი ფილიპსიტის წყლიანი სუსპენზიისაგან, მისი მჟავური დამუშავებით, ტუტესთან შერევის შედეგად მიღებული და დაბერებული გელის ($2.9Na_2O$:$0,26Al_2O_3$: $1SiO_2$:$150H_2O$) ჰიდროთერმული კრისტალიზაციის გზით. ორივე ტიპის ცეოლითის კრისტალური სტრუქტურა დადასტურებულია რენტგენოგრამებით და ინფრაწითელი სპექტრებით. მიღებული NaX ტიპის ცეოლითი ხასიათდება მაღალი ხვედრითი ზედაპირის ფართობით (589 $მ^2$/გ, გამოანგარიშებულია ბრუნაუერ-ემეტ-ტელერის მეთოდით აზოტის ადსორბცია-დესორბციის დაბალტემპერატურული იზოთერმების გამოყენებით) და ფორების მოცულობით (0,578 $სმ^3$/გ); ერთგვაროვან, მოწესრიგებულ ცეოლითურ ფორებთან ერთად NaX ტიპის ცეოლითში არის ცილინდრული არხების (საშუალო დიამეტრი 55 ნმ, გამოთვლილია ბარეტ-ჯოინერ-ჰალენდას მეთოდით) განვითარებული სისტემა. ამ მხრივ, მისი გამოყენება მეტად პერსპექტიულია კატალიზურ პროცესებში.
ვერცხლის, სპილენძისა და თუთიის შემცველი ცეოლითური მასალები მიღებულია საქართველოს ბუნებრივი ფილიპსიტებიდან მყარ ფაზაში მიმდინარე იონმიმოცვლითი რეაქციების გზით. მიღებული მასალები დახასიათებულია ქიმიური ანალიზისა და სორბციული გაზომვების შედეგებით, აგრეთვე რენტგენული დიფრაქტოგრამებით, ინფრაწითელი სპექტრებითა და ელექტრონულ-მიკროსკოპული სურათებით. დადგენილია, რომ მიღებული მასალები ინარჩუნებენ ცეოლითურ კრისტალურ სტრუქტურას, შეიცავენ 230 მგ/გ-მდე ვერცხლს, 66 მგ/გ-მდე სპილენძს და 86 მგ/გ-მდე თუთიას, და ამჟღავნებენ ბაქტერიციდულ და ბაქტერისტატიკულ მოქმედებას ნაწლავის ჩხირის მიმართ.

Adsorption properties of ion-exchanged forms of type X zeolite

Leonid Kwitkowsky[1], Liubov Katrenko[1], Luba Eprikashvili[2]*, Maia Dzagania[2], Nino Pirtskhalava[2]

[1]*National University "Lviv Polytechnic",st. Stepan Bandery 12, Lviv, 79013, Ukraine, E-mail: kwitkowskyj@gmail.com ; lubowkatrenkoma@gmail.com*
[2]*Iv.Javakhishvili Tbilisi State University, P.Melikishvili Institute of Physical and Organic Chemistry, 31 Politkovskaya str., 0186, Tbilisi, Georgia, E-mail: leprikashvili@hotmail.com; +995599565612*

Abstract. The ion exchange for NaX zeolite was studied and the degree of substitution of the Na ion for one and two-valency cations was determined. The substitution of the Na ion in the starting NaX zeolite on the monovalent cation is within the range of 55-81 mass. %, and a two-valency in the range of 62-94 mass. %. In zeolite there are about 60 mol. % of the excess cation needed to compensate for the negative charge of the tetrahedron. The cube-octahedron can change its spatial geometry depending on the ion exchange cation and form an elementary lattice. The adsorption properties of ion exchange forms of zeolites on the example of hydrocarbons C_6 - C_8 have been studied. It was shown that xylene isomers adsorbed differently depending on the ion exchange cation. The ion exchange cation affects the adsorption volume and changes the energy field.

Keywords: synthetic zeolites, silicate module, adsorption, cube octahedron, ion exchange, thermographic analysis.

Introduction

A group of aluminosilicate minerals of the crystalline form of a frame structure - zeolites have been known for a long time, but when in 1948 Barrer RM [1] published a method for their synthesis, and in 1959, Linde's researchers developed a technology for the industrial production of zeolites of type A and X, an interest in them in the scientific environment has grown dramatically. At the same time, in Kiev at the Institute of Physical Chemistry of the Academy of Sciences of the USSR in the laboratory of Neimark I. E., a technologically simpler way of obtaining synthetic zeolites of type A, X, Y, L was developed. Within a short period of time, many articles about the structure, properties and technological use of zeolites appeared in the scientific literature [2,3]. Dubinin M. M, having analyzed the available at that time work on the chemical composition of zeolites of type A and X, and the data of X-ray diffraction analysis, came to the same conclusion as other authors, namely that zeolites of type A, X, Y, L are constructed from structural elements - cube octahedrons, formed of 24 elemental structural units of aluminum oxide AlO_2 and silicon dioxide SiO_2 tetrahedron [4]. The negative oxygen valence is compensated by the ion exchange cation. All this system is thermodynamic equilibrium, but the rate of equilibrium is very small and practically no equilibrium occurs in the synthesis process. As a result, the compound and structure of zeolites depends on many factors. The crystalline structure of zeolites is described in the monograph [5] and is based on the laws of crystallography.

In particular, the structure of synthetic zeolites of type A, X, Y, L. was studied in detail. Depending on the association between cube octahedrons, different types of zeolites are formed. However, the position of the ion exchange cation in the zeolite is not clearly identified, various publications indicate different locations where it can be found. However, when the zeolite is dehydrated, it is not possible to determine the location of the cation.

The purpose of this work was to study the effect of the size of the ion exchange cation on the structure of the X-type zeolite, depending on its adsorption properties.

Experimental

For the study, an industrial sample of crystalline zeolite NaX-296 was taken. Ion exchange was carried out by repeated treatment (5-7 times) of crystalline zeolite NaX 1N solution of chloride or nitrate of a replacement cation at pH 8-10. For each treatment of zeolite, the volume of solution was taken, which includes 5 times more ion-exchange cation than in the sample of NaX zeolite. Treatment of zeolite was carried out at room temperature for 5-8 hours using vibration mixing. After that, the sample was washed with distilled water in the absence of chlorine ions, dried in a drying cabinet at 383 K, burned in a muffle cabinet at 673 K for three hours and stored in a sealed container.

For each ion-exchange form of zeolite, the chemical composition and degree of substitution of

the Na ion for other cations were determined. The degree of substitution is within the range of 55 - 95%. (Table 1a). In Table 1a and Table 1b, the sample numbers were taken so that the serial number was simultaneously the number of the sample of the ion-exchange form of the zeolite of type X. This series begins with the initial sample of zeolite NaX-296, and further sequential numbers 2 and 3 are given to ion-exchange forms with monovalent cations, and starting from 4 numbers - samples with bivalent cations from Be to Ba with increasing radius of ion exchange cation from 0,0314 to 0,1395 nm.

Table 1a. Characteristics of synthetic zeolites such as fagasite.

S. No	Zeolite	Degree of Substitution	Chemical composition, % mass.				ψ
			Na_2O	MeO	SiO_2	Al_2O_3	
1	NaX-296		19,80		47,7	32,50	1,00
2	LiX	55,0	8,36	6,18	50,80	34,66	0,94
3	KX	80,7	4,12	21,60	44,20	30,08	1,08
4	BeX	62,4	6,85	5,95	52,0	35,2	0,92
5	ZnX	78,0	4,58	18,80	45,50	31,12	1,05
6	CoX	67,4	6,63	15,35	46,40	31,62	1,03
7	MgX	57,2	8,11	8,11	49,80	33,98	0,96
8	FeX	69,6	6,05	15,40	46,50	32,05	1,01
9	Cd_1X	79,7	4,64	26,80	41,40	27,16	1,16
10	Cd_2X	82,2	4,10	27,00	41,10	27,80	1,17
11	CaX	75,6	4,77	13,80	48,30	31,13	0,99
12	SrX	94,8	1,16	27,50	42,40	28,94	1,12
13	Ba_1X	79,6	5,03	28,10	39,50	27,37	1,24
14	Ba_2X	85,2	3,67	30,90	38,80	26,53	1,25

The coefficient ψ (Table 1a) is the conversion factor of mass of ion exchange forms of zeolite in order to maintain a constant amount of elementary lattices that were in the initial sample of zeolite NaX.

The crystallinity of samples of ion-exchange forms of type X zeolite was checked by powder X-ray diffraction method. All samples retain a crystalline form, except for the ion-exchange form of FeX, where a partial destruction of the crystalline structure takes place.

A thermographic analysis was performed for all samples of ion-exchange forms of type X zeolite, and it was observed that ion-exchange forms with monovalent cations have two exothermics within 1073-1173 K and 1173-1273 K, and for samples with bivalent cations, the first exothermic practically disappears.

RESULTS

In the work of Smith J.V. [5] has been demonstrated that, in the process of ion exchange in zeolite there is a reorganization of the main block (cube octahedron) and the bonds between them, which leads to some changes in the adsorption volume of the elementary lattice. In the process of ion exchange, the whole system can become labile before changing the silicate module (SiO_2/Al_2O_3) (Table 1b). In general, zeolites in the ion exchange process keep a silicate module. According to the established model of cube octahedron, the silicate modulus is a discrete quantity (Table 2).

Table 1b. Characteristics of synthetic zeolites such as fagasite.

S. No	*Al*, %		ΣMO+ Na_2O/ Al_2O_3 mol/ mol	Excess ion exchange cation % mol	MO/ Al_2O_3 mol/ mol	Unutilized ion exchange cation % mol	SiO_2/ Al_2O_3 mol/ mol
	7	8					
1	26	74	1,00	64,9			2,49
2	26	74	0,99	64,1	0,60	0,99	2,49
3	27	73	1,00	64,9	0,78	27,8	2,49
4	30	70	0,98	62,0	0,69	13,0	2,50
5	24	76	0,99	64,3	0,76	24,5	2,48
6	26	74	1,08	64,5	0,76	25,5	2,49
7	26	74	0,99	63,9	0,60	0,99	2,49
8	21	79	0,99	63,2	0,68	12,1	2,46
9	45	55	1,06	74,8	0,78	28,9	2,59
10	30	70	1,01	66,8	0,77	26,9	2,51
11	55	45	1,05	74,0	0,81	32,5	2,63
12	25	75	1,00	64,6	0,93	53,6	2,49
13	18	82	0,98	62,1	0,68	12,3	2,45
14	23	77	0,99	64,2	0,77	26,9	2,47

Table 2. The magnitude of the silicate module SiO_2/Al_2O_3 of the adopted cube octahedron model

S No	Number of atoms		SiO_2/Al_2O_3 mol/mol
	Si	Al	
1	8	16	0,5894
2	10	14	0,8420
3	12	12	1,1788
4	13	11	1,3931
5	14	10	1,6503
6	15	9	1,9646
7	16	8	2,3576
8	17	7	2,8628
9	18	6	3,5360
10	19	5	4,4800
11	20	4	5,8940
12	21	3	8,2520
13	22	2	12,9660
14	23	1	27,1128

For for the initial sample of NaX zeolite, according to the chemical composition, the silicate module is 2.49, while it should be equal to 2.36 or 2.86. This is explained by the fact that the part of aluminate or silicate can be found in pores of zeolite [4]. Since the process is equilibrium, some aluminates and silicates have not been used, remain outside the structure of the cube octahedron and are removed at washing (Table 1b). This system is similar to systems that follow normal (Gaussian) distribution. In elementary lattices of the crystalline structure of zeolite, there will be cube octahedrons with different Si/Al ratios, as well as a certain number of cube octahedrons, in

which this ratio will be varied. For the adopted model, the distribution is based on two closest indicators of SiO_2/Al_2O_3 and the predominant number of cube octahedrons is determined by the ratio of atoms of Al to Si in percent (Table 1b). In the initial sample of zeolite, NaX-296 predominately include cube octahedrons (74%), which have 8 Al atoms and 16 Si atoms, and cube octahedrons (26%), which have 7 Al atoms and 17 Si atoms (Table 1b), calculated on two values of the ratio SiO_2/Al_2O_3 (Table 1b). Usually, such sample includes a whole spectrum of cube octahedrons, which correspond to different ratios of Al atoms to Si atoms. According to the crystallochemical study and the accepted model of the crystalline lattice of type X zeolite, the ratio of SiO_2/Al_2O_3 should not change with ion exchange, as evidenced by experimental data (Table 1b).

Significant impact on the crystalline structure of zeolite has the geometric shape of the cube octahedron, which in turn depends on the nature of the ion exchange cation, as also mentioned in [6]. To compensate for a negative charge in an aluminum oxide tetrahedron, one monovalent cation is required. In the initial sample of NaX zeolite, such a cation is Na^+ and therefore the molar ratio of Na_2O/Al_2O_3 will be 0.608. By chemical composition (Table 1b), the molar ratio Na_2O/Al_2O_3 is approximately equal to one that exceeds the Na_2O content by 64-65 mol. %. This state shows that at each cube octahedron there must be a certain amount of ion exchange cation in the aqueous solution and it is practically the same for each ion-exchange form of zeolite. In the process of ion exchange in the solution there was a significant surplus of cation, which replaces Na^+. After washing in zeolite there was partially a cation that replaced Na^+, but the value of this residue depends on the nature of the cation (Table 1b). The exceptions are cations Li and Mg, which are practically absent in a liquid that surrounds the cube octahedron. Such cations as Sr require 53.6 mol. % in the solution from that contained in the cube octahedron, Ca - 32.5 mol. %, and K - 27.8 mol. %. Their values are determined from the chemical composition of the ion exchange forms of zeolites by dividing the value of the molar ratio MO/Al_2O_3 for each sample (Table 1b) to the Na_2O/Al_2O_3 molar ratio in the NaX zeolite sample, which is equal to 0.608.

Modern methods allow to determine the location of ion exchange cations, but it is not known which ones those who compensate a negative charge in an aluminum oxide tetrahedr or those that are in an aqueous medium to maintain equilibrium. After dehydration, the cation that maintains the equilibrium must somewhere join the cube octahedron and additionally affect the volumetric shape of the cube octahedron and, as a result, the entire crystalline structure of the zeolite sample of this ion-exchange form. A certain explanation can give a definition of their adsorption properties: the adsorption volume and energy adsorption volume.

Adsorption properties of ion-exchange forms of zeolites of type X were studied with the maximum possible filling of adsorption volume of zeolites. This is the easiest way to carry out adsorption with isobars at atmospheric pressure. The processing was carried out with the help of the theory of volume filling of the micropore [7]. The adsorption isobars were determined by a dynamic method in the range of temperatures 423-623 K and atmospheric pressure with increasing temperature, and then at its decrease (Figure 1). All isobars of type X zeolite ion-exchange forms have similar appearance (Figure 1), with the exception of BeX for which the isobar form is close to the straight line. A special shape has isobar for the sample FeX, a curve similar to isobar obtained on silica gel (Figure 1). The values of the adsorption capacity of zeolites at certain temperatures are given in Table 3.

Table 3. Adsorption capacity of zeolites at atmospheric pressure in $kg \cdot 10^{-6} / kg \cdot 10^{-3}$ of dehydrated sample

S. No	T= 423 K	T =473K					T= 523 K
	Benzene.	Toluene	Mesitylene	n-Hexan	n-Heptan	n-Nonan	Benzene
1	178	176	187	123		143	152
2	129	129	134	92,5		103	111
3	129	127	131	89,5		102	109
4	66,8	53,2	97,6	38,6	41,2	65,5	36,2
5	125	119	136	78,1	90,7	106	102
6	94,0	90,6	94,6	59,2	73,9	72,6	72,1
7	138	133	146	87,7	95,3	105	114
8	32,7	29,2	46,0	17,7	19,2		17,5
9	96,5	97,8	94,4	67,4		77,8	78,6
10	106	100	110	75,0		90,0	90,1
11	183	165	199	114	120	134	156
12	138	121	132	81,9	91,8	102	118
13	130	123	125	83,2		99,1	109
14	62,1	57,1	62,9	43,5	44,7	50,8	53,5

.

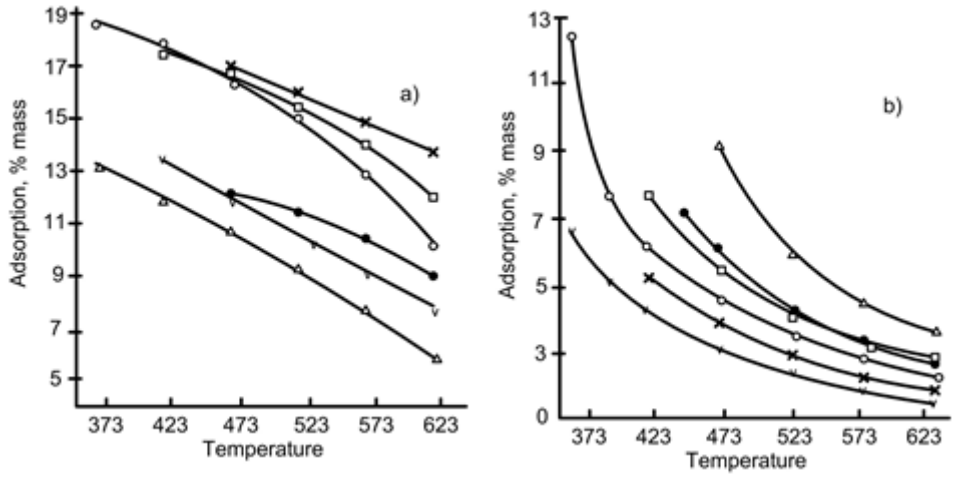

Fig.1 Isobar adsorption on
a). NaX **, b).** FeX
o - benzene, □ - toluene, △ - mesitylene, ∨ - n-hexane, × - n-heptane, ● - n-nonane

The analysis of the data presented in Table 3 shows that the value of adsorption of aromatic hydrocarbon exceeds the value of adsorption of n-paraffin hydrocarbon and is in the range of 30 to 60%. This is due to the significant component of the polar interaction between the polarity of the adsorption space of zeolite and the ability to polarize aromatic hydrocarbons. Ion-exchange forms of zeolite of type X differ in this constituent and, unfortunately, do not have a clear dependence on the size of the ion exchange cation. Such a lack of a clear dependence indicates that the ion exchange cation has an effect on the shape of the cubo octahedron, which forms the crystalline structure of the zeolite.

For processing of experimental data one of the modifications of the thermal adsorption equation has been used:

$$a = \frac{W_0}{V^x} \cdot \exp\left[-\left(\frac{A}{\beta \cdot E_0} \right)^2 \right] \quad (1)$$

where: a – the amount of adsorption;
V^x - volume of 1 millimol of adsorbate;
β - coefficient of affinity;
A - structural coefficient;
E_0 - energy interaction determined by a number of factors.

In coordinates $\left(T \cdot \lg \frac{P_s}{P} \right)^2$ and $\lg\left(a \cdot V^x \right)$ a straight-line dependence is obtained, from which the boundary adsorption volume W_0 ($m \cdot 10^{-6} / kg \cdot 10^{-3}$) and the energy characteristic E ($4{,}18 \cdot J / mol$) are determined (Table 4). For ion-exchange forms CoX, CdX and CaX at adsorption of benzene in the temperature range 473 - 523 K, on the straight lines there is a marked fracture indicating changing the form of stacking the molecules, or breaking the structure of the crystalline system.

Additional information for an understanding of the structure of the adsorption volume W_0 in ion exchange forms of zeolite will give a study of the energy characteristics of E of adsorption volume through the adsorption of binary systems on an example of hydrocarbons.

Table 4. Parameters of microporous structure of zeolites

Zeo -lite	n-Hexan			Benzene		
	I W_0	E_I	I W_0	II W_0	E_I	E_{II}
NaX -296	0,24	4124	0,23	0,22	3071	3294
LiX	0,16	2470	0,19		3310	
KX	0,19	2771	0,15		3007	
ZnX	0,17	1500	0,16		2411	
CoX	0,12	2028	0,12	0,13	1695	3207
MgX	0,18	1983	0,13		2323	
CdX_1	0,15	1803	0,14	0,14	2067	2887
CdX_2	0,13	1998	0,12		2346	
CaX	0,23	3163	0,24	0,24	2641	2992
SrX	0,17	1551	0,18		2926	
BaX_1	0,17	1907	0,17		2566	
BaX_2	0,08	2623	0,08		2102	

To study the adsorption of binary systems, aromatic and n-paraffinic hydrocarbons with the same number of carbon atoms and close boiling points were taken: benzene-n-hexane, toluene-n-heptane and mesitylene-n-nonane. The determination was carried out by a dynamic method at different temperatures and atmospheric pressure. The obtained results are presented in the coordinates of x and y; x - the concentration of aromatic hydrocarbon in the equilibrium steam phase and y - the concentration of it in the adsorbed phase (Figure 2).

This dependence is described by the equation of equilibrium for the binary system:

$$\frac{y}{1-y} = k\frac{x}{1-x} \quad (2)$$

where $1-x$ and $1-y$ - the concentration of n-paraffin component.

If we take into account Dubinin's assumption [7], that the adsorbed layer has the same density as the liquid, and Mayer and Prausnitz that is obeys Raoult's law, then the equation will have the following form:

$$\frac{y}{1-y} = \frac{P_1^s \cdot j_1 \cdot x}{P_2^s \cdot j_2 \cdot (1-x)} \quad (3)$$

where P_1^s, P_2^s - elasticity of vapor at the experimental temperature;

j_1, j_2 - coefficients of activity in the adsorbed state.

Further transformations have shown that the initial equation of equilibrium can be written as follows:

$$\frac{y}{1-y} = k_1 \cdot k_2 \frac{x}{(1-x)} \quad (4)$$

where $k_1 = \frac{P_2^s}{P_1^s}$ (from the law of Raoul) , k_2 - the magnitude of the polar component.

As can be seen from Figure 2, the adsorption equilibrium curves are not symmetric, but steeply rise up at low concentrations of aromatic hydrocarbons in the equilibrium steam phase.

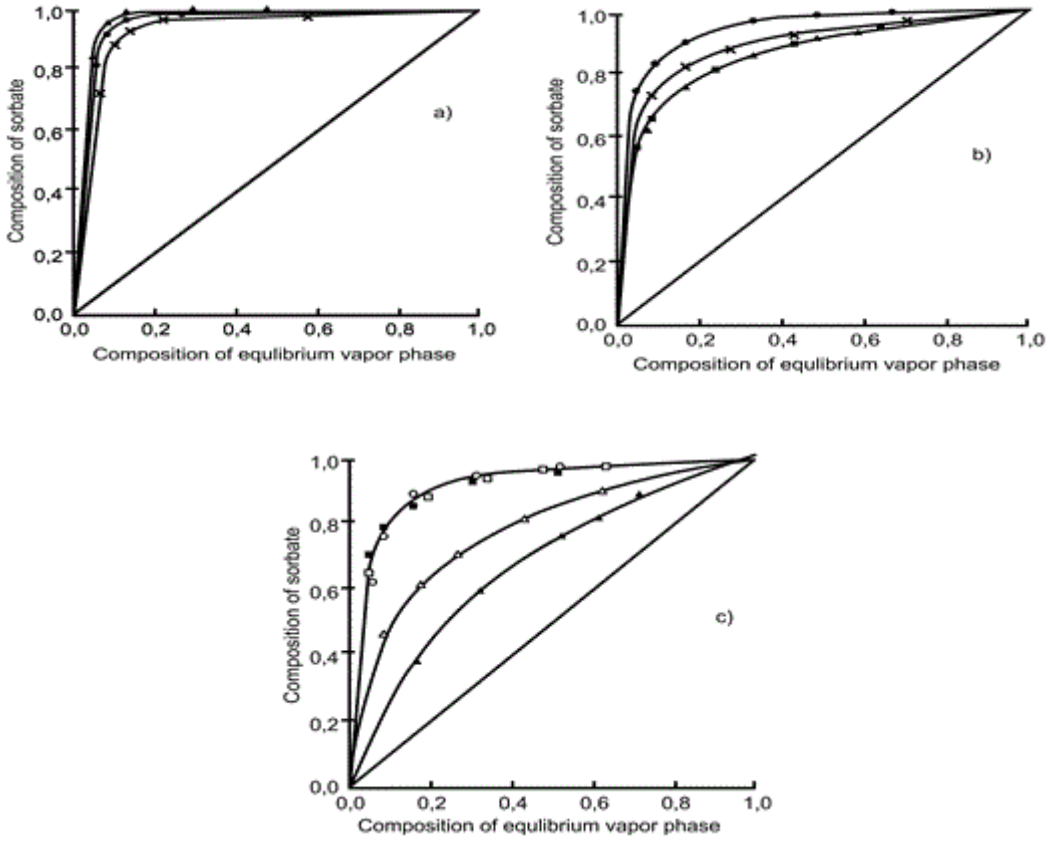

Fig.2. Adsorption equilibrium curves:
a). toluene-n-heptane on: o - NaX, △- LiX, ×-KX
b). benzene- n-hexane on: o - CaX, × - MgX, △ -CoX, □ - ZnX
c). benzene-n- hexane on: o - BaX, △ - BeX, □ -SrX
toluene-n-heptane on ▲ - BeX, ■ - SrX.

Table 5. The values of the absorption equilibrium coefficients of the binary system

S. No	Benzene-n-hexane				Toluene-n-heptane			
	0,05	0,10	0,20	0,40	0,05	0,10	0,20	0,40
1	160	150	145	138	150	140	130	122
2	230	220	215	220	220	200	195	198
3	135	130	119	120	125	120	119	108
4	10,4	8,3	7,0	6,0	3,5	3,4	3,2	3,2
5	22,3	17,5	14,6	15,2	32,4	25,0	20,2	19,3
6	20,6	16,7	14,6	11,6	29,7	25,6	20,2	21,6
7	35,3	26,3	20,3	18,5	37,8	28,5	22,5	21,6
8					1,8	1,8	1,9	1,9
9					17,0	16,5	15,0	14,1
10	26,0	25,0	24,5	22,0	23,0	22,9	22,3	19,2
11	80,2	65,6	66,0	38,5	92,9	86,5	85,0	48,4
12	38,6	31,9	32,4	28,5	45,5	38,4	35,5	28,6
13					60,2	50,0	52,1	49,1
14	23,2	41,0	46,0	28,5	45,0	38,0	32,1	31,0

This shows that in the adsorption volume of zeolite, a high energy field can induce a dipole moment in hydrocarbons having fixed C-C bonds: aromatic, unsaturated, and the like. Table 5 shows the values of adsorption equilibrium coefficients for various concentrations of aromatic hydrocarbons in the equilibrium steam phase.

Available data show that, with increasing concentration of aromatic hydrocarbon, the adsorption equilibrium coefficient in the binary system decreases. For ion-exchange forms of zeolite with monovalent ions, the adsorption equilibrium coefficient decreases within 0-20%, moreover it decreases with an increase in the radius of the ion. For samples of ion-exchange forms of zeolites with bivalent cations, the adsorption equilibrium coefficients also decrease with an increase in the concentration of aromatic hydrocarbons in the equilibrium steam phase. But the decrease is not the same and not commensurate with the ionic radius of the cation. Thus, a sample of BeX with the smallest radius of the ion (Be^{+2} = 0.0314 nm) has the form of isobar similar to zeolites, and the equilibrium coefficient in the binary system is similar to that of silica gel [8]. The form of isobars and the adsorption equilibrium coefficient of the iron-exchange like form are similar to those of silica gel, although the chemical composition corresponds to zeolite. Zeolite CaX, in which the adsorption equilibrium coefficient (k) is approximately two times smaller than the NaX sample, is sensitive to the concentration of aromatic hydrocarbons in the equilibrium binary steam phase (Table 5).

Of particular interest is the mutually competitive adsorption of two aromatic hydrocarbons: toluene-benzene and each of the aromatic hydrocarbons C_8 in pairs with toluene (Figure 3).

Quantitative evaluation of these systems is more convenient to display through the value of the coefficient of adsorption equilibrium for binary systems (k). Aromatic hydrocarbon with a higher molecular weight is adsorbed more strongly, but this advantage is negligible.

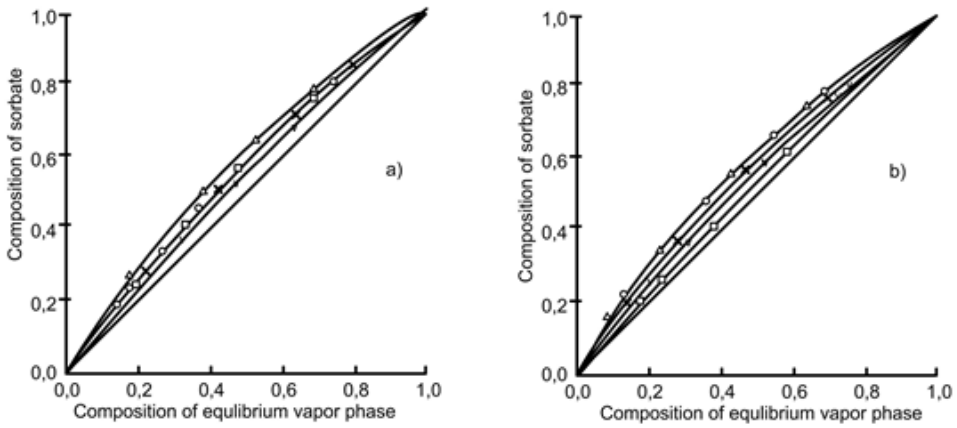

Fig.3. Curves of the adsorption equilibrium of binary systems on zeolites: a). NaX, b) – CaX.
o - toluene-benzene, × - ethylbenzene-toluene,
△- o-xylol-toluene, □ - m-xylol-toluene, ∨ - p-xylol-toluene

From the analysis of the adsorption properties of aromatic binary systems data on ion-exchange forms of zeolites of type X, zeolite samples with monovalent and bivalent cations give a slight advantage to an aromatic hydrocarbon with a higher molecular weight. But this advantage manifests itself differently: for samples with monovalent cations, it increases with an increase in the size of the ion, and

for samples with divalent cations, it does not have a clear dependence on the size of the ion.

This law should be considered from the standpoint of equilibrium equation (4), in which the equilibrium coefficient consists of two parts; k_1, which is determined by the molecular mass and the polar component k_2. If the adsorbate-adsorbent (k_2) is allocated from the total coefficient of equilibrium, then it can be noted that for the ethylbenzene-toluene system, this coefficient is less than unity and its value for different ion-exchange forms is different (Table 6).

Table 6. The polar component of the adsorbate-adsorbent interaction k_2 (formula 2)

S. No	Toluene -benzene	Ethyl benzene -toluene	p-Xylol -toluene	m-Xylol -toluene	o-Xylol -toluene
1	0,700	0,815	0,690	0,706	0,727
2	0,682	0,647	0,674	0,706	0,725
3	0,739	0,902	0,762	0,737	1,010
4	0,710				
5	0,630	0,654	0,795	0,990	0,810
6	0,393	0,382	0,551	0,871	0,320
7	0,653	0,625	0,762	0,893	0,669
8	0,710				
9/	0,653	0,654	0,939	0,737	1,135
10	0,805	0,659	0,674	1,375	1,620
11	0,588	0,474	0,900	1,375	1.245
12	0,474				
13	0,842				
14	0,653	0,578	0,762	0,737	0,669

Similar values were obtained for the system: p-xylol - toluene. While for m-xylol - toluene on adsorbents such as Cd_2X and CaX (samples No. 10, 11), the coefficient k_2 is greater than unity (Table 6). Something similar is also for the o-xylol-toluene system for samples KX, Cd_1X, Cd_2X, CaX (samples No. 3, 9-11). The polarization is influenced by the magnitude of the energy field, which contains an aromatic hydrocarbon, its molecular weight and a separately steric factor - entropy. These factors depend on the structure of the adsorption capacity W_0 of the elementary lattice, which changes its shape and even volume when ion exchange. The molecules of benzene and toluene of similar shape have a smaller critical size than xylene isomers.

CONCLUSION

Thus, the adsorption equilibrium of binary systems indicates that various ion-exchange forms have their energy field due to the structure of the adsorption space, which is quantitatively determined by the coefficient of the polar component (k_2). The ion exchange cation affects the form of adsorption volume and changes the energy field.

The cube octahedrons does not have a spherical shape and can change its spatial structure depending on the nature of the ion exchange cation.

REFERENCES

[1] Barrer R.M., "Synteses and reactions of mordenite", *Abbrev. Journal of the Chemical Society*, 1948, Issue 0, pp.2158-2163, **Doi:** 10.1039/JR9480002158.

[2] Smith J.V., "Structural classification of zeolites, Third general meeting structural classification of zeolites", *Abbrev. Mineralogical society of America.,* Chicago., USA, 1963, Special paper 1, pp.281-290.

[3] Breck D.W., "Structure of zeolites**, in Zeolite Molecular Sieves: Structure, Chemistry, and Use", Publisher:** (Union Carbide Corporation, Tarrytown, New York) John Wiley and Sons, New York, London, Sydney, and Toronto, 1974, pp.37-195.

[4] Dubinin M.M., "On the composition of cubooctahedral structural units of synthetic zeolites, Synthetic zeolites, preparation, study and application", Publisher: Ed. Academy of Sciences of the USSR: Moscow, 1962, pp.86-90.

[5] Smith J.V., "Structure of zeolites, in Zeolite chemistry and catalysis", Publisher: ACS Monograph 171, (Editor Rabo J.A.), American chemistry society: Washington. D.C., 1976, pp.11-103.

[6] Andronikashvili T.G, Tsitsishvili G.V. Sabelashvili Sh.D., Chumburidze T.A., "The Influence of Nature and the Degree of Substitution of some cations in type X zeolites on their Chromatographic Properties", *Zeolites, their Synthesis, Properties and Applications*. Moscow, Leningrad, pp.179-185, 1962 (in Russian).

[7] Dubinin M.M., "Features of adsorption of vapors of various substances on zeolites as on microporous adsorbents", *Zeolites, their synthesis, properties and priming.* Materials of the Second All-Union Meeting on Zeolites, Leningrad, USSR, p.5-12, 1965 (in Russian).

X ტიპის ცეოლითების იონმიმოცვლითი ფორმების ადსორბციული თვისებები

ლეონიდ კვიტკოვსკი[1], ლიუბოვ კატრენკო[1], ლუბა ეპრიკაშვილი[2], მაია ძაგანია[2], ნინო ფირცხალავა[2]

[1]*ეროვნული უნივერსიტეტი „ლვოვი პოლიტექნიკური“, სტეფან ბანდერას ქ.12, 79013, ლვოვი, უკრაინა*
E-mail: kwitkowskyj@gmail.com ; lubowkatrenkoma@gmail.com
[2]*ივ.ჯავახიშვილის თბილისის სახელმწიფო უნივერსიტეტი; პ.მელიქიშვილის ფიზიკური და ორგანული ქიმიის ინსტიტუტი, ა.პოლიტკოვსკაიას ქ.31, 0186, თბილისი, საქართველო*
E-mail: leprikashvili@hotmail.com; +99559565612

რეზიუმე. შესწავლილ იქნა NaX-ის მიმოცვლა და განისაზღვრა Na-ის იონის ჩანაცვლება რაიმე ორვალენტიანი კატიონით. Na-ის იონის ჩანაცვლება NaX საწყის ცეოლითში ერთვალენტიანი კატიონით არის 55-81 მასური %-ის ზღვრებში და ორვალენტიანის 62-94-ის მასური %-ის ზღვრებში. ცეოლითში არის დაახლოებით 60 მოლ % ჭარბი კატიონი, რომელიც საჭიროა ტეტრაჰედრონის უარყოფითი მუხტის კონპენსაციისათვის. კუბურმა ოქტაჰედრონმა შეიძლება შეიცვალოს სპეციალური გეომეტრია იონ-მიმოცვლით კატიონზე დამოკიდებულებით და შექმნას ელემენტარული კარკასი. შესწავლილ იქნა ცეოლითის იონ-მიმოცვლითი ფორმების ადსორბციული თვისებები C_6-C_8 ნახშირწყალბადების მაგალითზე. ნაჩვენებია, რომ ქსილოლის იზომერები სხვადასხვაგვარად ადსორბირდება იონ-მიმომცვლელ კატიონზე დამოკიდებულებით. იონ-მიმოცვლითი კატიონი ზეგავლენას ახდენს ადსორბციის მოცულობაზე და ენერგიის ველის ცვლილებაზე.

Actions of factors caused by lightning on historical and cultural monuments and the possibilities of their prevention on the example of Abuli fortress

Giorgi Tsintskaladze[1]*, Teimuraz Kordzakhia[1], Thinathin Sharashenidze[1], Vakhtang Gabunia[1], Marine Zautashvili[1], Manana Burjanadze[1]

[1] *Ivane Javakhishvili Tbilisi State University, Petre Melikishvili Institute of Physical and Organic Chemistry, 31 Politkovskaya str., 0186, Tbilisi, Georgia,*
**E-mail: giorgi.tsintskaladze@tsu.ge; +995599320592*

Abstract. Among the natural and anthropogenic factors affecting historical and cultural monuments of particular interest are the damages caused by lightning, which are still not well studied. Due to the fact that lightings are very common for the region, it is very important to study the historical and cultural monuments located here.
As a subject of research, we propose the Abuli megalithic fortress and the place of a former settlement located in the south of Georgian highland. The climatic conditions of this region, as well as the structure and composition of construction materials were studied (using physical-chemical methods of research). Damage to the fortress caused by lightings has been established and procedures have been proposed to prevent it. Such approach can be used in any region of the world, where there is a danger of damage from lightings in order to protect cultural heritage sites.

Keywords: Abuli fortress, lightning, ecology, megalithic monument, the south of Georgian highland, lighting conductor.

INTRODUCTION

Historical and cultural monuments are an essential part of world civilization, so the care, protection and preservation of these monuments for future generations are an important and responsible task. Damage to monuments is mainly due to natural and anthropogenic factors [1]. In general, these factors equally affect the monuments in every part of the world, although the location of the monument is of great importance.

Lightning is a frequent event in Georgia. Therefore, damages caused by lightning is very important for some regions of Georgia. The study of lightning processes has always been relevant in our country. The period of regular meteorological observations of atmospheric conditions in Georgia is counting 100 years.

Lightning is a dangerous phenomenon of nature. It negatively affects human life and wildlife. As a result of a lightning strike, people are dying, agricultural objects, cultural and historical monuments, airplanes, oil and gas pipelines are being destroyed, radio communications and electricity supply are interrupted, forests are burnt by fire etc. On average, a lightning strike on earth occurs 8 million times a day. The corresponding area varies from $40 \cdot 10^4$ km^2 (at 4 am) to $110 \cdot 10^4$ km^2 (at 14-20 am) [2]. Changes in lightning strikes are associated with global climate changes. In particular, according to NASA (National Aeronautics and Space Research), the number of lightning on earth has increased 100 times in the last decade [2].

The southern part of the highland of south Georgia, covering an area of 5,700 km^2, is the most dangerous in terms of lightnings in Georgia. In some years the number of days with lightning was 95-96.

Mountain slopes oriented towards humid air masses is characterized by the largest number of days with lightning. At this time, dynamic turbulence increases and the upward flow on the mountainside forms an additional impulse powerful convection processes that enhance lightning [2,3].

An increase in the number of days with lightning is observed up to 2400-2600 m height. Above this height, the effect of lightning decreases, which is associated with a decrease in air temperature. There are two periods with maximum lightning days in Georgia: one in June-July and the second in August. The minimum daily lightning hours throughout Georgia is 6-12 hours. The maximum duration occurs in the second half of the day. The maximum duration of lightning is 140-1250 hours. This value is observed in the mountainous region of southern Georgia [4].

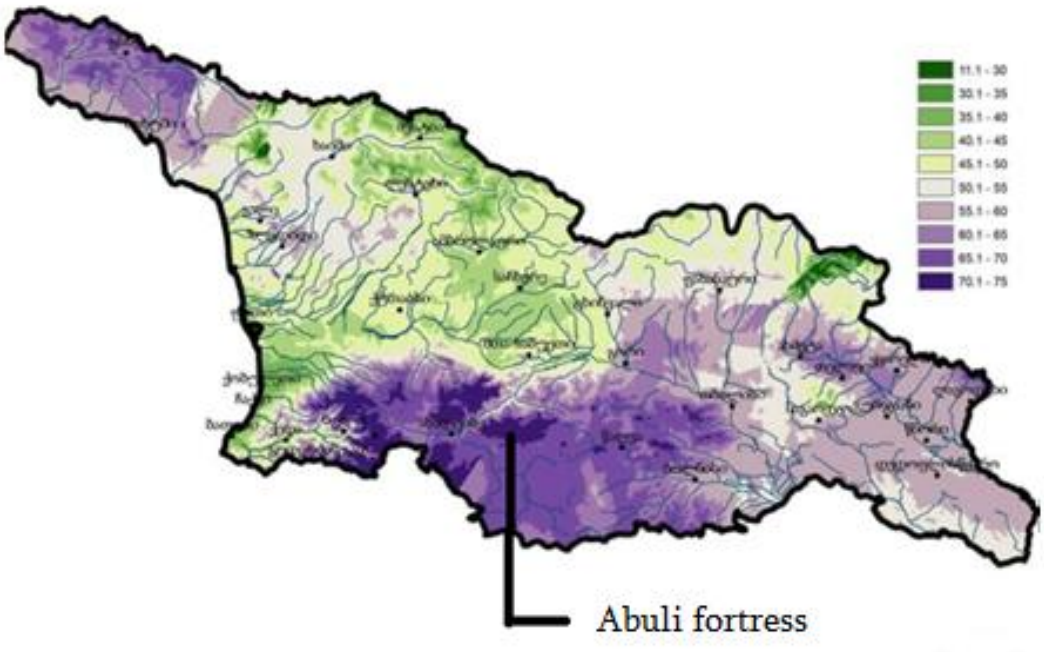

Fig. 1. The annual distribution of lightning on the territory of Georgia [8].

Lightning is especially dangerous in the mountains. A lightning strike is associated with a landscape. It is known that the edges and peaks of the mountains attract and accumulate a charge of lightning. Any bulge on the mountainside is most likely a place for a lightning strike. It should be noted that the lightning current is very dangerous and not well studied. When the lightning strikes the top of a mountain, the forming current looks for a path with minimal resistance and goes to the surface of the rocks, penetrates into cracks.

Therefore, all these places during a lightning are dangerous to humans [6].

To determine the probability of lightning processes on the southern slopes of this region, observations of 7 meteorological stations for 60 years were analyzed. It turned out that compared with other areas of this region the probability of lightning is very high. The probability of days with lightning varied from 0.27 to 0.61, and in the case of the maximum number of days with lightning - from 0.37 to 0.75. Thus, there are favorable conditions for the formation of lightning processes, and therefore from this point of view the above mentioned region appears to be especially dangerous.

Megalithic cultures are the common name of archaeological cultures, which covers the Eneolithic and Bronze Age (in some cases, the Neolithic period, too). They are found in almost every region of the world (except Australia). Characteristic monuments of these cultures are: Dolmen, Mengir, Krommhel, Kvakuti (The tomb is made of stone tiles) and stone-covered corridors [7].

EXPERIMENTAL

Megalithic monuments in Georgia are distinguished by their scale, monumentality and versatile purpose. They had both residential and defensive, as well as religious functions [8]. Due to their uniqueness, these monuments have acquired international significance from both historical and scientific points of view. In addition, monuments are of great importance for the development of tourism in our country.

Subject of our interest - megalithic monument - cyclopean fortress of Abuli located in the southern mountainous region of Georgia - historical province Javakheti, on the southern slopes of small Abuli mountain, at an altitude of 1670 m above sea level.

The monument is large and quite well preserved. It consists of a fence, an inner fortress and dwellings built to its walls from inside. The height of the dry ground walls in some places reaches 5 m, the width is 3 m. The “Inner castle” occupies an area of about 40x60 m. The inner fortress from outside is surrounded by rooms and caches in the form of terraces, which had a stone roofing [9,10].

RESULTS

As mentioned above, the monument is located on the southern slopes of the South Caucasus Mountains. These places are characterized by frequent lightning strikes, which damages the monument. During lightning strikes, stone tiles are crumbling - they are broken. Therefore, most of the monument is a cluster of broken stones. A lightning strike is also dangerous for visitors - tourists and interested people. Therefore, creating a relatively safe environment for people is important.

The southern slopes of the small Abuli, where the fortress is located, are covered with moraines of volcanic origin. Builders used these stones during construction. The construction material looks homogenous, although dark pink, light pink and gray tones stand out. A petrographic study of stones has shown that construction material is andesite and in some cases pyroxene. The main material is the mineral plagioclase, rarely monoclinic pyroxene and amphibole. Secondary mineral is chlorite and carbonate.

Mineral structure is porphyrial, with the main mass of microlite. Texture is fluidal.

Rock is mainly represented by volcanic glass, middle plagioclase, chlorite and ore mineral. Percentage of pyroxene and amphibole is small and in total - less than 5%.

The plagioclase is found in the form of thin and elongated idiomorphic and sometimes - xenomorphic grains. Rarely it is represented in the form of porphyrial buildups. Its size varies from 0.01 mm to 0.8 mm.

Pyroxene and amphibole are found in the form of xenomorphic grains ranging in size from 0.08 mm to 1 mm. Pyroxene is mainly in the form of rounded buildups. Amphibole is in the form of individual rounded and opacities grains.

Chlorite is formed on the basis of volcanic glass pyroxene and amphibole. It occupies the vacant space between the grains. The mineral of the ore is probably represented by pyrite-pyrotin.

The study of construction stones (gray, dark pink and light pink samples) of Abuli fortress using X-ray diffractometer and infrared spectroscopy methods showed that the structure of the main minerals is identical. It consists of the mineral anorthite, but there is the existence of other minerals (pyroxene, amphibole, chlorite, pyrite, pyrocin, etc.). The various contents in these minerals of iron, magnesium and aluminum determine minor structural changes. This causes the visual difference between the stones and the different intensity or complete absence of some frequency lines in the IR spectra. For example, in all three spectra, the bands at 543, 584 cm^{-1}, corresponding to Al, Mg, Fe – O bonds have different intensities, and the spectrum band at 384 cm^{-1}, which is fixed in a dark pink sample, corresponds to the bond of the compound of iron and sulfur [11,12].

Examination of samples by X-ray diffraction analysis confirmed the results of IR spectroscopy. X-ray diffractogram of all three samples with $Cu_{k\alpha}$ emission were taken. X-ray fluorescence spectrum were taken using the Soler method with an anode of the BSM-19 tube receiver. Monochromator: graphite monocrystal with (002) plane.

The different intensity and shape of the x-ray diffractogram peaks in the range (29-45)Å indicate a change in the concentration of cations in the anorthite mineral from C to K and vice versa. In addition, the X-ray fluorescence spectrum showed a certain amount of iron in the mineral composition. It is interesting to note that the mineral also contains strontium.

CONCLUSION

Thus, the damage of Abuli megalithic fortress caused by lightning processes is caused not only by the location of the fortress, but also by the composition of construction materials. In order to avoid damage to the fortress caused by lightning processes and to protect tourists and scientists visiting the monument, it is necessary to install lightning arresters on the monument, as it is done around the world.

REFERENCES

[1] Tsintskaladze G., Kordzakhia T., Gvakharia V., Tsintskaladze P., Zautashvili M., Burkiashvili N., "Ecological factors affecting sandstone and zeolites used in Georgian architecture", *Transactions of Petre Melikishvili Institute of Physical and Organic Chemistry*, 2015, p.152-155 (in Georgian).

[2] Muranov A.P., "In the world of unusual and lightning phenomena of nature", Publisher: Procveshenie, 1977, 176 pp. (in Russian).

[3] Amiranashvili A.G., Varazashvili O.Sh., Nodia A.G., Tsereteli N.C., Mkurnalidze I.P., "Characteristics of lightning activity in Georgia", *Proceedings of the Institute of Hydrometeorology of Georgia*, 2008, №115, pp.10-18 (in Georgian).

[4] Amiranashvili A.G., Varazashvili O.Sh., Nodia A.G., Tsereteli N.C., "Statistical characteristics of the number of days with hail per year in Georgia", *Proceedings of the Institute of Hydrometeorology of Georgia*, 2008, №115, pp. 27-39 (in Georgian).

[5] Georgian Lightning Cadastre - Ministry of Nature Protection of Georgia, Department of Hydrometeorology of Georgia, National Agency for Environmental Protection. Tbilisi, 2010., https://napr.gov.ge/p/614 Developed by Atami Group 20.02.20

[6] Tatishvili M., "Hazardous hydrometeorological phenomena over Georgian territory against the global climate change background", *Journal of Environmental Studies*, 2015, vol. 4, pp.214-220.

[7] Rodger G. Barry, "Mountain Weather & Climate", Routledge: London, 1992, 231 p.

[8] Berdzenishvili D., Articles from the Historical Geography of Georgia: Zemo Kartli-Tori, Javakheti, Mecniereba: Tbilisi, 1985, 159 p. (in Georgian).
[9] Melkised-Beg L., Megalithic Culture in Georgia, Publisher: Tbilisi, 1983, pp. 67-70 (in Georgian).
[10] Berdzenishvili D., "Old fortresses of Javakheti, history and contemporaneity", Publisher: Akhaltsixe, 2002, pp.181-203 (in Georgian).
[11] Plusnina I.I., IR-Spectra of Minerals, Moscow State University: Moscow, 1977, 173 p. (in Russian).
[12] Plusnina I.I., IR-Spectra of Silicates, Moscow State University: Moscow, 1967, 183 p. (in Rusian).

ისტორიული და კულტურის ძეგლებზე ელჭექით გამოწვეული ფაქტორები და მისი პრევენციის შესაძლებლობა აბულის ციხე-ნამოსახლარის მაგალითზე

გიორგი წინწკალაძე[1]*, თეიმურაზ კორძახია[1], თინათინ შარაშენიძე[1], ვახტანგ გაბუნია[1], მარინე ზაუტაშვილი[1], მანანა ბურჯანაძე[1]

[1] *ივ.ჯავახიშვილის თბილისის სახელმწიფო უნივერსიტეტი; პ.მელიქიშვილის ფიზიკური და ორგანული ქიმიის ინსტიტუტი (ა.პოლიტკოვსკაიას ქ.31, 0186, თბილისი, საქართველო)*
**E-mail: giorgi.tsintskaladze@tsu.ge; +995599320592*

რეზიუმე. კულტურისა და ისტორიულ ძეგლებზე მოქმედი ბუნებრივი და ანთროპოგენური ფაქტორებიდან განსაკუთრებით საინტერესო, მნიშვნელოვანი და ჯერ კიდევ შეუსწავლელია ელჭექით გამოწვეული დაზიანებები. რადგან საქართველო წარმოადგენს ელჭექსაშიშ რეგიონს, ამიტომ მნიშვნელოვანია დაკვირვება და შესწავლა კულტურისა და ისტორიის იმ ძეგლებისა, რომლებიც საქართველოს ამ რეგიონებში მდებარეობენ. საკვლევ ობიექტად შემოთავაზებულია საქართველოს სამხრეთ მთიანეთში მდებარე მეგალითური ციხე-ნამოსახლარი ე.წ. აბულის ციხე. შესწავლილია რეგიონის კლიმატური მდგომარეობა, ასევე კვლევის ფიზიკურ-ქიმიური მეთოდებით ციხე-ნამოსახლარის სამშენებლო მასალების სტრუქტურა და შემადგენლობა. დადგენილია ძეგლის ჭექა-ქუხილის ფაქტორით გამოწვეული დაზიანებები და შემოთავაზებულია მისი თავიდან აცილების ღონისძიებები. ასეთი მიდგომა შეიძლება გამოყენებული იყოს მსოფლიოში ნებისმიერ ელჭექ-საშიშ რეგიონში არსებული კულტურული მემკვიდრეობის ძეგლების დაცვის მიზნით.

Influence of composites from zeolitic tuffs and coal industry wastes on soil bio-productivity

Luba Eprikashvili[1]*, Marine Zautashvili[1], Teimuraz Kordzakhia[1], Maia Dzagania[1], Nino Pirtskhalava[1], Giorgi Antia[1]

[1] *Iv.Javakhishvili Tbilisi State University; P.Melikishvili Institute of Physical and Organic Chemistry, (31 A.Politkovskaya str., 0186, Tbilisi, Georgia)*
**E-mail luba.eprikashvili@tsu.ge and phone number +995599565612*

Abstract. The paper presents materials on the study of the effect of the complex fertilizer zeolite + brown coal on the development of a test plant (barley). The aim of the work was to study the possibility of improving the agrochemical and biological properties of the soil under the influence of complex fertilizer, the assessment of expediency and its long-term operation. Brown coal (Akhaltsikhe deposit, Georgia) and natural zeolite - clinoptilolite of sedimentary origin (Tedzami deposit, Handaki, Georgia) modified with potassium and ammonium ions were used as a source of organic matter for complex fertilizer.

The experiment was carried out on meadow-brown soil type, with a weakly alkaline reaction of an aqueous solution (pH = 7.3-7.9), in vegetation vessels, in five variants, each in three replications.

The assessment of the feasibility of using the developed substrate in plant growing and the possibility of its long-term operation was determined by the ratio of dry biomass of plants grown in the first crop to the biomass of plants grown in subsequent crops (respectively, second, third, etc.). An increase in this indicator (index) indicates a depletion of soil fertility, in our case, a substrate during its operation, and a decrease indicates, on the contrary, an increase in fertility. The following biometric indicators were also determined: germination energy (GE), relative germination energy (RGE), germination (GC), relative seed germination (RSGS). The greatest increase in germination and germination energy occurs when using zeolites modified with potassium and ammonium cations and brown coal during the third sowing.

Among the promising techniques that increase yields and quality of crop production are the composites proposed in the work (zeolite + brown coal) that can stimulate physiological and biological processes during the germination of grain crops, which increases the resistance of emerging plants to environmental stress factors and directly affects on economically useful traits and productivity of cultivated crops.

Keywords: zeolite, brown coal, humic substances, germination energy, germination capacity, modification of the zeolite with ammonium and potassium cations.

INTRODUCTION

To solve the problem of providing the population with food, one of the most important points is to increase the yield of ecologically safe agricultural products and to develop new alternative methods for improving soil fertility [1,2]. The preservation and improvement of soil fertility, the improvement of the supply of plants with mineral nutrition elements, which are the basis for obtaining high stable yields, are associated with scientifically based systems for the use of mineral and organic fertilizers. The growth and development of the plant is subject to the laws of Shelford Laws of Tolerance. According to the first law, the plant grows and develops until the deficient factor is sufficient. According to the second law, the excess of any factor can adversely affect the plant or the soil. The results of studies of increasing the yield of agricultural products by introducing organo-zeolite fertilizers into the soil [3] are known. Among organic fertilizers, a group of organic substances of natural origin, known as humic fertilizers, stands out [4]. The content of humus in the soil is important not only for its fertility [5].

Humus contains up to 99% of soil nitrogen, 60% of phosphorus, up to 80% of sulfur and other trace elements. But these nutrients are inaccessible to plants and they become food for them only after decomposition, when carbon dioxide, which is the source of their air supply, is released. Humic substances affect the plant directly or indirectly. Under the influence of humic substances, the permeability of cell membranes changes, the activity of many enzymes, respiration, synthesis of proteins and carbohydrates increase. They have a positive effect on the mineral nutrition of plants, water exchange, increasing the content of chlorophyll, the productivity of photosynthesis and transpiration. All this ultimately leads to increased growth, increased yield, accelerated ripening and improved product quality. The indirect effect is associated with the improvement of the water-physical properties of the soil, the activation of microflora, the effect on the

migration of nutrients, the increase in the utilization rate of mineral fertilizers, the binding of toxic agents (pesticides, herbicides, heavy metals, etc.). Along with this, humic substances have a direct deep and diverse effect on plant growth processes, i.e. regulate them [6].

The practice of using humic preparations obtained from brown coal in plant cultivation, and numerous comparative studies [7] indicate that humic substances from brown coal are similar in their properties to soil humic acids, at least in terms of participation in the soil-forming process and in a stimulating effect on plant growth and development. Humic substances have the property of binding toxic substances, such as heavy metal salts, radionuclides, aromatic hydrocarbons and other compounds that appear in the process of industrial and other human activities, which is their main protective or environmental property. The ecology polluters connected in this way are "preserved" and do not enter the organisms of living beings and humans [8]. The highest content of humic substances is in brown coal, peat and sapropel.

Coal deposits are an almost unlimited source of humic substances, which is a unique product that plays a key role in the formation and functioning of the soil and can be used to solve many agricultural and environmental problems.

Zeolites are an extensive group of minerals, which is the sixth in the stratosphere in terms of prevalence and mass, after feldspars, quartz, mica, clay minerals and carbonates. Out of all (more than 30) the mineral zeolites known in nature, only a few meet the requirements for practical use, in particular, they form large, almost monomineral concentrations and at the same time, have corresponding useful properties: high adsorption capacity, cationic capacity and acid- and heat resistance [9]. Zeolites are nanoporous crystalline solids and have a frame structure with alumina-silicon-oxygen base. Zeolites that are currently of practical importance include clinoptilolite, mordenite, and shabazit.

Clinoptilolite tuffs have an exchange capacity of about 2 $mgmol^{-1}/g$ and a zeolite water content of about 15%. Due to the secondary porosity of rocks, total moisture capacity reaches 45%. Therefore, the introduction of clinoptilolite into the soil significantly increases its moisture and ion-exchange capacity. A distinctive feature of ion exchange on clinoptilolite is a highly expressed selectivity towards such massive cations such as K^+ and NH_4^+, which are the main active elements of mineral fertilizers. This determines their constant transition to the soil, delays the removal of ground waters and rainwaters and increases the efficiency of the fertilizer [10,11]. The use of prolonged action fertilizers with the gradual release of nutrients is a promising direction in technology of agricultural crops, as it has a number of significant advantages compared with the use of traditional mineral fertilizers [12].

High exchange capacity, selectivity to potassium and ammonium ions, as well as high rates of exchange reactions allow clinoptilolite to be considered as a soil sorption-type soil improver. When using zeolite tuffs as artificial soil, it is necessary to pre-saturate clinoptilolite with nutrient components. In particular, potassium-ammonium form of clinoptilolite can be used for these purposes. The experimentally established high biological activity of the ammonium form, expressed in a significant increase in yield and protein content in the grain, makes it possible to consider the clinoptilolite in the ammonium or potassium-ammonium form as a very effective long-acting fertilizer [10,13,14]. Clinoptilolite has a significant effect on the distribution of microelements in the soil-plant system, drastically reducing the content of toxic metals in the green mass and grain. The duration of the protective action of clinoptilolite is associated with the process of self-cleaning, due to the periodic entry of contamination. This property of clinoptilolite acquires particular importance when used in crop production of composts, irrigation water and fertilizers containing toxic substances [15-18].

The aim of the work was to study the possibility of improving the agrochemical and biological properties of the soil under the influence of complex fertilizer: modified zeolite + brown coal, its influence on some biometric indexes of test cultures.

EXPERIMENTAL OR MATERIALS & METHODS

In this work, Brown coal (from the Akhaltsikhe deposit of Georgia) and natural zeolite –clinoptilolite of sedimentation origin (from the Tedzami deposit, the Khandaki district of Georgia) modified with potassium and ammonium ions were used as a source of organic matter to obtain complex fertilizer.

X-ray fluorescence spectroscopic analysis of brown coal showed that the content of toxic elements does not exceed the maximum permissible norms (MPN).

Modification of the zeolite with ammonium and potassium cations was carried out by treating the initial natural clinoptilolite with 0.1N solutions of NH_4Cl and KCl, respectively. Untreated brown coal was used as the second component of the fertilizer [19].

The experiment was carried out on meadow-brown soil type, with a weak alkaline reaction of an aqueous solution (pH=7.3-7.9). The soil is characterized by a low content of humus from 1.93 to 2.90%, and its granulometric composition is classified as heavy loamy soil.

The experiment was carried out in vegetation vessels, in five variants, each in three replications.

Barley of "Alaverdi-1"variety was used as a test plant to test the fertility of substrates. Sowing of this culture in substrates was carried out repeatedly (5 sowing), in permanent circulation, i.e. in the variant of monoculture, which most aggressively affects the fertility of the soil, causing the so-called "soil fatigue" [20].

In the first case, the soil was used as a reference (comparison object). In the second case, the substrate was prepared by mixing finely ground natural, unmodified zeolite+soil. The third version is soil + zeolite modified with potassium and ammonium cations. The fourth version of substrate was made by using raw brown coal and natural zeolite (without soil), fifth - brown coal + zeolite modified with potassium and ammonium cations (without soil).

Before the experiment began, the sowing qualities of barley seeds, germination capacity (91%) and germination energy (85%) were determined. Germination energy was determined in Petri dishes on damp filter paper placed in a thermostat (at 20°C) after three days and germination capacity – on the seventh day. The number of normally germinated seeds under optimal conditions established by the standard for each culture, shown in percentage is considered under the germination capacity of seeds. Germination energy was also determined. The germination energy, characterizing the intergrowth in unison of seed germination, is the number of normally germinated seeds for a certain period established for each crop, shown in percentage.

Germination capacity and seed germination energy are the most important indexes of their sowing qualities. Seeds with good germination capacity and high germination energy with normal agricultural technology always give friendly and full-fledged seedlings.

Seeds of barley in the amount of 50 pieces were sown on each substrate (vessel). After 30 days from sowing, the sprouts together with the roots were carefully removed from the substrate, washed with distilled water, dried at 75°C until a constant weight was reached. Dry plant biomass per one vessel was determined by weighing, taking into account both the whole plant (total underground and surface part) and the root system only.

In total, five sowing were carried out consequently with appropriate processing of the obtained results. The assessment of the expediency of using the developed substrate in plant growing and the possibility of its long-term operation was determined by the method proposed by Bulgarian scientists: the ratio of dry biomass of a plant grown in the first crop to the biomass of plants grown in subsequent crops (respectively, second, third, etc.) [21]. An increase in this index indicates an exhaustion of the soil fertility (in our case a substrate during its exploitation) whereas a decrease indicates an increase in fertility.

RESULTS

The following biometric indexes were determined: germination energy (GE), relative germination energy (RGE), germination capacity (GC), relative seed germination capacity (RSGC). Table 1 shows the arithmetic mean data determined from three replications of each option.

Table 1. The impact of the substrate on the biometric indexes of barley.

Biometric indexes	Sowing	substrate				
		Soil (comparison object)	Soil+zeolite	Soil+modified zeolite	Brown coal+zeolite	Brown coal+modified zeolite
GE	I	70	30	34	36	40
	II	66	50	55	58	63
	III	40	82	90	84	95
	IV	34	71	88	76	90
	V	20	52	60	55	83
RGE	I	-	-0.57	-0.52	-0.48	-0.43
	II	-	-0.24	-0.17	-0.12	-0.04
	III	-	1.05	1.25	1.10	1.37
	IV	-	1.08	1.59	1.24	1.65
	V	-	1.60	2.00	1.75	3.15
GC	I	76	38	42	52	55
	II	78	60	64	76	84
	III	46	86	94	92	99
	IV	40	83	90	87	97
	V	36	76	85	80	90
RSGS	I	-	-0.50	-0.44	-0.32	-0.27
	II	-	-0.23	-0.18	-0.02	0.07
	III	-	0.87	1.04	1.00	1.15
	IV	-	1.07	1.25	1.17	1.43
	V	-	1.12	1.36	1.23	1.50

Analysis of the data given in Table 1 indicates that the application of zeolites and brown coal has a positive effect on the germination and germination capacity of barley seeds. The biggest growth in germination capacity and germination energy occurs while using zeolites modified with potassium and ammonium cations and brown coal during the third sowing. The high bioproductivity of plants grown on a substrate consisted of modified zeolite and brown coal, as compared with bioproductivity on other variants, can presumably be explained as follows: In studies [22,23], it was shown that the cations that are part of zeolites, have the ability to get intoion exchange reaction not only in aqueous solutions, but also in the solid state. Although, the exchange reaction is more slow in this case. Therefore, the following mechanism of ion exchange is assumed in substrates: the NH_4^+ + and K^+ cations from zeolite get into exchange reactions with humic and fulvic acids, forming the corresponding salts, soluble in the aqueous medium. In such condition, these formed

organic substances can contribute to the humification of the substrate, as well as their digestibility by plants. On the other hand, the high bioproductivity of this substrate, presumably, can be associated with the formation of a favorable microbial landscape of the soil (biota), promoting plant growth and development, in the system – soil-zeolite-brown coal-plant [24,25].

As we can see from the table, germination energy and germination capacity gradually decrease on the soil (the object of comparison) from the first to the fifth sowing. This is probably due to the exhaustion of the soil. These indicators increase on substrates and on the third crop reach the highest index. An increase in fertility on substrates, containing modified zeolite and brown coal occurs due to these components.

The structure and flexibility of the root system play an important role in improving growth and increasing crop yields. The figure shows plants grown on different substrates.

Fig. 1. Plant germination on various substrates: a) soil (object of comparison); b) soil + zeolite; c) brown coal + zeolite; d) soil + modified zeolite; e) brown coal + modified zeolite.

As we can see from the Figure, the enrichment of the soil with substrates affects the growth of both, the over ground part and the root system of the plant. Al though, this indicator varies on different substrates. The root system develops more on the substrate: soil + zeolite and brown coal + zeolite; the over ground part – on the substrate: soil + modified zeolite. A big difference is shown in case of lignite + modified zeolite. Differences were also noted in the dry mass of plants, both the land part and the root system, which demonstrate an increase in the growth of plants grown on composites with substrates. These indicators are shown on the diagram, which is constructed according to the third sowing. Table 2 shows plant masses on various composites.

As we know, barley is characterized by an intensive growth of vegetative organs in a short time; In this time, it forms a sufficiently powerful root system and leaf surface. According to tables 1.2 and diagrams, in the third sowing period, seed germination capacity was 99% on the substrate – brown coal-modified zeolite.

Table 2. Plant masses on various composites (g).

Sowing	Mass (g)									
	Soil (comparison object)		Soil + zeolite		Soil + modified zeolite		brown coal + zeolite		brown coal + modified zeolite	
	Root	Land	Root	Land	Root	Land	Root	Land	Root	Land
I	1.5	1.3	1.8	1.5	1.2	1.0	2.9	2.3	2.3	1.3
II	0.8	1.1	2.3	1.9	1.3	1.2	4.3	2.5	4.5	2.8
III	0.7	0.7	4.5	2.8	4.0	6.0	5.5	5.0	6.5	8.5
IV	0.5	0.6	4.0	2.0	3.5	4.0	5.0	4.3	7.0	8.0
V	0.5	0.5	2.3	1.7	3.0	2.3	4.5	4.0	6.0	6.5

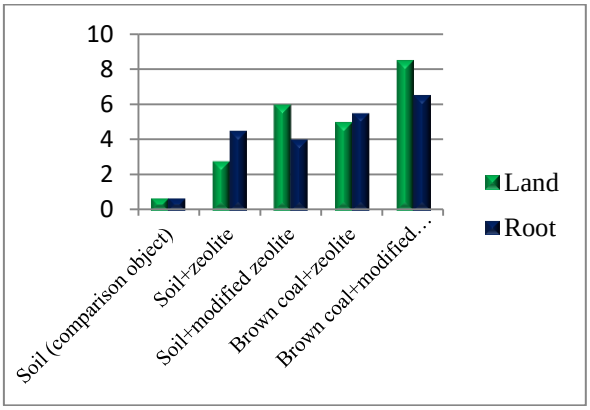

Diagram. Changes in the dry mass of plants on different composites during the third sowing

An increase in the mass of germinated plants was also noticed. Manipulation of the vegetative organism by enriching the soil with biologically active substances is currently very common.

CONCLUSION

Among the promising methods for increasing the yield and quality of crop production are the composites proposed in the work (zeolite, lignite). They are able to stimulate physiological and biological processes during the germination of crops, which increases the resistance of forming plants to environmental stress factors and directly affects the

economically useful traits and productivity of the crops grown. Further studies in this direction are highly relevant: from an environmental point of view, they promote the utilization of substandard coal industry wastes as an organic component of substrates that increase soil fertility.

REFERENCES

[1] Ivanov A.L., "Priorities and the main directions of agriculture development", *Zemledelie*, 2007, #3, pp.2-4 (in Russian).

[2] Kiryushin V.I., "Problems of minimization of the soil treatment: Prospects of the development and problems of the study", *Zemledelie*, 2013, #7, pp.3-6 (in Russian).

[3] Naumkin V.N., "Problem approach in the modern agriculture", *Agromir*, 2004, #5(12), (in Russian).

[4] Chen Y., Clapp C.E., Magen H., Cline V.W., "Simulation of Plant Growth by Humic Substances: Effect of iron Availability. Understanding Humic Substances", Advanced Methods, Properties and Applications EDS E. Ghabbour, G.Davies. Cambridge, 1990, 150 p.

[5] Levin B. V., Ozerov S. A., Garmash G. A., Latina N.B., Garmash H.U., "Raise of Agrochemical Efficiency of Complex Phosphoric Fertilizes at the expense of Humate Additives", *Plant Nutrition*, 2015, #2, pp.2-8.

[6] Paul I. Fixen, "The concept of increasing the productivity of agricultural crops and the efficiency of using elements of plant nutrition", *Plant nutrition: Bulletin of the International Institute of Plant Nutrition*, 2010, №1, pp.2-7.

[7] Usanbaev N., Namazov Sh., Beglov B., Rahmanjanov U., Eshimbetov A., "Obtainment of nitrogen-humic fertilizers based on urea, oxidized brown coal and their IR-spectroscopic study", *Universum: Technical science*, 2016, #9(30) (in Russian).

[8] Ul'yanova O.A., "Effect of new compound fertilizers prepared from bark and zeolite on the transformation of organic matter of soil", *Journal Fertility*, 2009, #2, pp.23-25 (in Russian)

[9] Razmakhnin K., Khatkov A., "Modification of the properties of zeolites for the purpose of expanding the areas of their application", *Scientific and Technical Journal: Mining Information and Analytical Bulletin*, 2011, pp. 246-252 (in Russian).

[10] Chelishchev N.F., Bernstein B.G., Volodin V.F., "Zeolites - a new type of mineral raw materials", Publisher: Moscow, Nedra, 1987, 176 p. (in Russian).

[11] Andronikashvili T.G., Urushadze T.F., Eprikashvili L.G., "Zeolite-containing substrates a new way from plant growing in plant production", *Annals of Agrarian Science*, 2009, #7, pp.14-45.

[12] Perminova V., Zhilin D.M. "Humic substances in contact of green chemistry", *Green chemistry in Russia*. Moscow, 2004, pp.146-162 (in Russian).

[13] Andronikashvili T.G., Urushadze T.F. "Application of zeolite-containing rocks in plant growing", *Agrochemistry*, 2008, #12, p.63-79 (in Russian).

[14] Buondonno A., Coppola E., de'Gennaro B., Leone A.P., Letizia A. and Colella C., "Morpho-structural and chemical-physical properties of soil ped aggregate models by interaction of phillipsite-chabazitic or clinoptilolitic tuffs with different organic matter", in *8th International Conference of the Occurrence, Properties, and Utilization of Natural Zeolites*, Sofia, Bulgaria, 2010, 10-18 July, pp.52-53.

[15] Leggo P.J., "The organo-zeolitic-soil system: A comprehensive fertilizer", *International Journal of Waste Resources*, 2014, v.4, issue 3, pp.4-17.

[16] Febles J.A., Núñez G.M.S., "Natural zeolite in the industry of fertilizers – agronomic results", in *8th International Conference of the Occurrence, Properties, and Utilization of Natural Zeolites*, Sofia, Bulgaria, 2010, 10-18 July, pp.86-87.

[17] Andronikashvili T.G., Zautashvili M.G., Eprikashvili L.G., Burkiashvili N.O., Pirtskhalava N.V., "Natural Zeolite – one of the Possibilities of transition from "Chemical" to Biological Agronomy", *Bulletin of the Georgian National Academy of Sciences*, 2012, v.6, #2, p.111-118.

[18] Eprikashvili L.G., Zautashvili M.G., Dzagania M.A., Pirtskhalava N.V., Burkiashvili N.O., "Influence of synthetic zeolite on wheat seed germination", *Proceedings of the Georgian National Academy of Sciences, Chemical series*, 2008, v.34, #1, p.103-106 (in Russian).

[19] Urushadze T.F., "The main soils of Georgia", Metsniereba: Tbilisi, 1997, 267 p. (in Georgian).

[20] De Gennaro M., Langella A., Colella C., Coppola E., Buandanno A., "Italian zeolitized tuffs as soil conditioners. Recent research advances", in *Natural Zeolites Sofia'95*, Sofia-Moscow, 1997, p.93-100.

[21] Name of the invention "Method for obtaining ion-exchange zeolites", Tsitsishvili G.V., Avaliani K.E., Adolashvili M.G., Certificate of Authorship SSR 223784, 1968 (in Russian).

[22] Andronikashvili T.G., Urushadze T.F., Eprikashvili L.G., Gamisonia M.K., Nakaidze E.A., "Towards the biological activity of the natural zeolite – clinoptilolite – containing tuff", *Bulletin of the Georgian National Academy of Sciences*, 2008, v.2, #3, p.99-108.

[23] Eprikashvili L.G., Tsitsishvili V.G., Zautashvili M.G., Kordzakhia T.N., Dzagania M.A., Pirtskhalava N.V., "Influence of the ground-free substrate on the biometric parameters of bean and barley germination", *Bulletin of the Georgian National Academy of Sciences*, 2015, v 9, # 1, p.139-144.

[24] Eprikashvili L.G., Zautashvili M.G., Kordzakhia T.N., Pirtshkalava N.V., Dzagania M.A., Rubashvili I.M., Tsitsishvili V.G., "Intensification of Bioproductivity of Agricultural Cultures by Adding Natural Zeolites and Brown Coals into the Soil", *Annals of Agrarian Science*, 2016, v.14, p.67-71.

[25] Eprikashvili L.G., Pirtskhalava N.V., Zautashvili M.G., Kordzakhia T.N., Dzagania M.A., Tsintskaladze G.P., "Use of Georgian non-traditional agricultural resources in agriculture", *International Journal of Advanced Research (IJAR)*, 2018, 6(1), p.1408-1415. **doi:** http://dx.doi.org/10.21474/IJAR01/6366

ცეოლითური ტუფისა და ნახშირის წარმოების ნარჩენებისაგან შემდგარი კომპოზიტების გავლენა ნიადაგის ბიოპროდუქტიულობაზე

ლუბა ეპრიკაშვილი[1]*, მარინე ზაუტაშვილი[1], თეიმურაზ კორძახია[1], მაია ძაგანია[1], ნინო ფირცხალავა[1], გიორგი ანთია[1]

[1] *ივ.ჯავახიშვილის თბილისის სახელმწიფო უნივერსიტეტი; პ.მელიქიშვილის ფიზიკური და ორგანული ქიმიის ინსტიტუტი (ა.პოლიტკოვსკაიას ქ.31, 0186, თბილისი, საქართველო)*
** E-mail: luba.eprikashvili@tsu.ge; +995599565612.*

რეზიუმე. სამუშაოში წარმოდგენილია მასალები ტესტური მცენარის (ქერის) განვითარებაზე კომპლექსური სასუქის - ცეოლითი+მურა ნახშირი გავლენის შესახებ. კვლევის მიზანი იყო კომპლექსური სასუქის გავლენით ნიადაგის აგროქიმიური და ბიოლოგიური თვისებების გაუმჯობესების შესაძლებლობა, მიზანშეწონილობის შეფასება და მისი ხანგრძლივი ექსპლუატაცია. კომპლექსური სასუქის მისაღებად ორგანული ნაერთის წყაროდ გამოყენებული იყო მურა ნახშირი (ახალციხის ადგილმდებარეობის, საქართველო) და სედიმენტაციური წარმოშობის ბუნებრივი ცეოლითი - კლინოპტილოლიტი (თეძამის ადგილმდებარეობის, ხანდაკის ნაკვეთი, საქართველო) მოდიფიცირებული კალიუმისა და ამონიუმის იონებით.
ექსპერიმენტი განხორციელდა მდელოს - ყავისფერი ნიადაგის ტიპზე, წყალხსნარის სუსტი ტუტე რეაქციით (pH = 7.3-7.9), სავეგეტაციო ჭურჭელში, ხუთი ვარიანტით, თითოეული სამი განმეორებადობით.
შემუშავებული სუბსტრატის მემცენარეობაში გამოყენების მიზანშეწონილობის შეფასება და მისი ხანგრძლივი ექსპლუატაციის შესაძლებლობა განისაზღვრა პირველი დათესვისას მცენარის მშრალი ბიომასის შესაბამისობით შემდგომი დათესვისას (მეორე, მესამე და ა.შ) აღმოცენებული მცენარის ბიომასებთან. ამ მაჩვენებლის (ინდექსის) ზრდა მიუთითებს ნიადაგის, ჩვენს შემთხვევაში კი ექსპლუატაციის დროს სუბსტრატის გამოფიტვაზე, ხოლო შემცირება კი პირიქით ნაყოფიერების ზრდაზე. ასევე განისაზღვრა შემდეგი ბიომეტრული მაჩვენებლები: აღმოცენების ენერგია (GE), აღმოცენების ენერგიის ფარდობითი სიდიდე (RGE), აღმოცენების უნარი (GC), თესლის აღმოცენების ფარდობითი სიდიდე (RSGS). აღმოცენების ენერგიისა და აღმოცენების უნარის შედარებით მაღალი მაჩვენებელი შეიმჩნევა კალიუმისა და ამონიუმის იონებით მოდიფიცირებული ცეოლითისა და მურა ნახშირის კომპოზიტზე მესამე დათესვისას.
პერსპექტიული მეთოდების რიცხვს, რომელიც მემცენარეობაში მოსავლიანობისა და პროდუქციის ხარისხის ზრდას განაპირობებს, შეიძლება მივაკუთვნოთ სამუშაოში შემოთავაზებული კომპოზიტები (ცეოლითი+მურა ნახშირი), რომლებსაც მარცვლოვანი კულტურების აღმოცენებისას ფიზიოლოგიური და ბიოლოგიური პროცესების სტიმულაცია შეუძლია. ეს კი ზრდის ფორმირებული მცენარის მდგრადობას სტრეს-ფაქტორებისადმი და უშუალო გავლენას ახდენს აღმოცენებული კულტურების პროდუქტიულობასა და სამეურნეო-სასრგებლო ნიშნებზე.

Mixed-ligand chelates containing premixes for nutrition of rabbits

Iamze Beshkenadze[1]*, Giorgi Chagelishvili[2], Nazibrola Klarjeishvili[1], Maia Gogaladze[1], Omar Lomtadze[1]

[1] *Petre Melikishvili Institute of Physical and Organic Chemistry, Ivane Javakhishvili Tbilisi State University, Tbilisi, Georgia, 31 A.Politkovskaia, 0186*
[2]*Agricultural University of Georgia, 240 David Aghmashenebeli Alley, 0131*
*E-mail: iamze.beshkenadze@tsu.ge (+995) 571188 525

Abstract. The premixes prepared according to the general formula $M{\cdot}gl{\cdot}L{\cdot}nH_2O$ (where M=Mn, Zn, Fe, Co, Cu; gl= Glutamine Acid; L = Citrate-ion) on the base of the synthesized mixed-ligand chelate compounds and their compositions and of the compositions of natural Zeolite – Clinoptilolite, have been tested in the combined nutrition of rabbits. The probation and the main experiments were conducted for three groups: I – the trial group where the food was balanced with 0,5% premix and 2% Clinoptilolite. II – the trial group where the food was balanced with 0,5% premix and III – Control group where the food was balanced with the factory-made premix. The study of the rabbits' productivity indicator has shown that all the data received in the trial groups, exceeded the ones of the control group. According to the hematological studies, concentration of the hemoglobin in the blood of the rabbits of all three groups were was satisfactory. The leukocytes is law in the I and II trial groups, while in the control group it is near to the norm (5-9%). The segment-nuclei is within the norm (33-39%) only in the blood of the control group rabbits and is slightly higher in both trial groups. As for the amount of eosinophiles (1-3% by the norm) it is slightly more in the I and in the control groups of rabbits. Calculation of the economic efficiency for 100 rabbits demostrated that the cost of the manufactured meat was the lowest in the I trial roup – 5.66GEL. Thus, a profit is the higher just in case of this I trial group. A profit for 100 rabbits in the I group made 406 GEL, in the II group – 350 GEL, and in the control group - 268 GEL.

Keywords: Mixed-ligand; Blood; Productivity; Hematological indicator; Economic efficiency.

INTRODUCTION

Deficit of microelements in the plants, soil, as well as in the organism of the agricultural animals and poultry is one of the main reasons that determines the low qualitative and quantitative indicators of the food products. The critical role in solving this problem is given to the provision of optimal amount and ration of the microelements of the living organism where they play their function in a form of the chelate compounds. Therefore, when filling the deficit by this way, a sharp increase of their biological activity is observed. This may be explained by the fact that the microelements in a form of the chelates, have a low toxicity, a high ability of assimilation, and an increased rate of efficiency when using in small doses, that, in its turn, predetermines an ecological safety of use of the microelements in this form. as to the inorganic salts, they are characterized by a high toxicity, low rate of assimilation and efficiency, that is conditioned by their poor solubility in the intestinal tract of animals and poultry and creation of the poorly assimilating compounds [1-5]. Therefore, importance of the additives containing the compounds of this type in the nutrition of animals and poultry, is substantiated both theoretically and practically [6-12]. The role of the chelate compounds containing the organic substances (vitamins, amino-acids, organic acids) and the microelements in the metabolic processes taking place in the organism of animals and poultry, is well known, but nevertheless, to define the conditions of synthesis of the oxi-acids, namely the lemon acid and the chelate compounds containing microelements (Zn,Co,Fe,Mn,Cu), physical-chemical research of the synthesized compounds and determination of efficiency of their use in feeding, still remains actual.

MATERIALS & METHODS

The following issues were studied in the course of the experiment:

- ✓ Alive mass of a rabbits at the beginning of the experiment – by their weighting (g)
- ✓ Alive mass of a rabbits at the end of the experiment – by their weighting (g)
- ✓ An absolute growth in the alive mass M(g) during

the experiment, was calculated by the following formula:

$$\mathbf{M = V_1 – V_2}$$

M – Absolute growth during the experiment (g)

V_1- Alive mass at the beginning of the experiment (g)

V_2- alive mass at the end of the experiment (g)

- ✓ A daily growth of the alive mass **M** (g) during the experiment, was calculated by the following formula:

$$\mathbf{M= (V_1 – V_2)/ t}$$

M – A daily growth iub the alive mass (g)

V_1 Alive mass at the beginning of the experiment (g)

V_2 - Alive mass at the end of the experiment (g)

t - Period of the experiment (days)

- ✓ Consumed food products during the period of the experiment – with daily accounting of the consumed food
- ✓ Preservation of rabbits during the period of the experiment – with accounting the fallen and unfit rabbits
- ✓ Some blood indicators at the end of upbringing – blood taken from 5-5 rabbits of all groups
- ✓ The economic efficiency was calculated based on the results of the experiment.

RESULTS

In the laboratory of the Agricultural Chemistry Problems, the researches are contibued in the direction of creation of new generation of the premixes and their experimental testing [13-19]. We have synthesized the mixed-ligand chelate compounds by the general formula $M{\cdot}gl{\cdot}L{\cdot}nH_2O$, where M=Mn,Zn,Fe,Co,Cu; gl=Glutamine Acid; L=Citrate-ion. The chelate compounds are studied through a number of the physical-chemical research methods [20, 21]. The premixes prepared on the basis of the synthesized mixed-ligand chelate compounds and their compositions and of the compositions of natural Zeolite – Clinoptilolite, have been tested in the combined nutrition of rabbits. At present, we are targeted at testing the premixes prepared on the basis of the synthesized chelate compounds and the compositions of their natural Zeolite – Clinoptilolite, in the nutrition of rabbits.

A task of the research was to study an effect of the premixes prepared on the base of the synthesized chelate compounds and of the composition of Clinoptilolite on the productivity of the meat rabbits, blood hematological indicators and economic efficiency.

We have chosen 30-day old age rabbits by the principle of analogs (all of them were males, born at one and the same day) and conducted the tests for three groups: I trial group, II trial group, and III control group (10-10 rabbits in each group: 5 gray big and 5 Californian breed).The tests lasted for three months. The first weighting conducted when they were 45-day old, 15 days after their completing, while the following weightings were conducted when they were 60, 90, and 120-day old.

At the beginning of the experiment, the alive mass was equalized and varied from 1,42 to 1,57 kg range. The technological parameters (temperature, humidity, lighting, etc.) during the period of upbringing were one and the same for all three groups. Only the food was different: In the I trial group the rabbits were given 0,5% premix, which contained the microelements in the chelate form and 2% Clinoptilolite. In the II trial group the rabbits were given the food with 5% premix, which contained the microelements in the chelate form, while the rabbits in the III control group were given the food which contained the factory-made 1% premix for rabbits. The impact of premixes prepared on the base of the synthesized mixed-ligand chelate compounds and their compositions and of the compositions of natural Zeolite – Clinoptilolite on the productivity of rabbits have been studied. The results are shown in Table 1.

Table 1. Indicators of productivity of rabbits for meat

Indicators	Unit Measure	Group		
		I Trial	II Trial	III Control
Number	piece	100	100	100
Period of experiment	day	90	90	90
Preservation during the experiment	%	99	99	97
Alive mass at the beginning of the experiment	g	1570	1540	1550
Alive mass at the end of the experiment	g	3310	3240	3150
Absolute Increment during the period of experiment	g	1740	1700	1600
Daily increment during the period of experiment	g	29,0	28,3	26,7
Food consumed during the period of experiment	kg	960	988	990
Food consumed by 1 rabbit during the period of experiment	kg	9,6	9,9	10,2
Food consumed for 1kg increment during the period of experiment	kg	5,50	5,80	6,38

Slaughter of rabbits took place in their 120-day old age,with preliminary taking the blood for studying some hematological indicators. Results of the analysis are given below, in Table 2.

Table 2. Some hematological indicators of the rabbits blood

Indicators	Groups		
	I Trial	II Trial	III Control
Hemoglobin HGB	110	112	118
Erythrocytes RBC	$4,6\cdot10^{12}$	$5,0\cdot10^{12}$	$4,7\cdot10^{12}$
Color Index	0,83	0,89	0,83
Thrombocytes PTL	120	245	250
Leukocytes WBC	$5,5\cdot10^{9}$	$5,0\cdot10^{9}$	$5,5\cdot10^{9}$
Neutrophils NEUT:			
Rod nuclear	4	2	6
Segmented nuclear	40	48	38
Eosinophils EOS	5	1	4
Monocytes MON	5	4	4
Lymphocytes LYM	44	46	46
Erythrocytes Sedimentation Rate ESR	2	2	2

Based on the results of the experiment, an economic efficiency is calculated for 100 rabbits.The results are given in Table 3.

Table 3. Calculation of the economic efficiency

Indicator	Unit Measure	Group		
		I Trial	II Trial	III Control
Rabbits number	Piece	100	100	100
Increase received during the experiment	Kg	174	170	160
Food consumed during the experiment	Kg	960	988	990
Cost of 1 kg food	GEL	0,85	0,85	0,85
Total cost of the consumed food	GEL	816	840	842
Other expenses	GEL	170	170	170
Total costs	GEL	986	1010	1012
Cost of 1 kg meat produced during the period of experiment	GEL	5,66	5,94	6.33
Sales price of 1 kg meat	GEL	8,0	8,0	8,0
A sum gained by sale of the meat during the period of experiment	GEL	1392	1360	1280
Profit calculated for 100 rabbits	GEL	406	350	268

DISCUSSION

As a result of study of impact of the premixes prepared according to the general formula $M\cdot gl\cdot L\cdot nH_2O$ (where M=Mn, Zn, Fe, Co, Cu; gl= Glutamine Acid; L=Citrate-ion) on the base of the synthesized mixed-ligand chelate compounds and their compositions and of the compositions of natural Zeolite – Clinoptilolite on the rabbits' productivity (Table 1), it is established that during the period of the experiment that lasted for 90 days, a preservation on the I trial group dame 99%, while in the control group – by 2% less (97%) As seen from the Table, alive mass of all rabbits in all three groups was almost one and the same – 1540-1570g. At the end of weight increase, in 120-sday old age, the highest alive mass was observed in the rabbits of the I trial group - 3310g, by 160g i.e. 4,8% higher than the rabbits of the control group and by 70g i.e. 2,1% higher than the rabbits of the II trial group. The rabbits of the II trial group were by 2.1%)less in weight than the rabbits of the I trial group, but by 90 g i.e. 2.8% higher in weight than the rabbits of the control group.

Naturally, during the period of the experiment, both the absolute increase and the daily increments were higher in the I and II trial groups, to compare with the control group. In the I trial group the absolute increment was by 8,75 higher than in the control group and by 2,35% higher than in the II trial group. While this indicator of the II trial group was by 6.25% higher to compare with the control group.

Consumption of food during the weight-increasing period made 9,6 kg in case of per rabbit of the I trial group, that was by 6.25% less than in the control group, while the food consumption by per rabbit in the II trial group was by 3,03% less to compare with the control group.

Consumption of food for 1 kg increment during the weight-increasing period in the I trial group made 5,5kg,that was almost by 13,78% less than in case of the control group. while in the control group this indicator as by 9,09% higher than in the II trial group.

The hemoglobin content in the blood shows intensive work of blood-forming organs, as well as the liver's condition, the level of nutrients, especially the full-scale proteins and microelements, the ongoing oxidation-restorative processes in the body and so on. In the given case the hemoglobin content in the blood of the rabbits of all three groups is satisfactory, since according to the norm, this indicator in the rabbits varies from 105 to 125 g/l (Table 2).

The erythrocytes number is satisfactory also. According to the norm, this indicator is from 4,5 to $7,5\cdot10^{12}$l ranges.

The leucocytes which perform the protective function in the organism and contribute to reproduction and restoration of tissues, like the erythrocytes number in the blood, indicate on the process of metabolism in the organism.

According to the norm, the leucocytes in the

rabbits blood should vary within 6,5-9,5·10^9 l ranges. Considering the results of our experiment, this indicator in the blood of the experimental rabbits is lower, and varies within 5,5·10^9 range in the I trial group, 5,0·10^9 range in the II trial group, and 5,5·10^9 range in the control group.

The rod-nuclear indicator is also lower in the I and II trial groups and is near the norm (5-9%) in the control group.

The segmented nuclear is within the norm (33-39%) in the control group only, and is slightly higher in the I and II trial groups.

As for the Eosinophils (Norm = 1-3%) it was slightly higher in the rabbits of the I trial group and III controlled group.

Monocytes are within the normal ranges (1-4%) in the II trial group an the control group but slightly higher ibn the I trial group.

As to the Erythrocytes Sedimentation Rate (N=1-3%) it is equal in the blood of the animals of all groups while, the indicator of lymphocytes is slightly less of the norm.

Based on the results of the experiment, calculation of the economic efficiency for 10 rabbits (Table.3) shows that a cost of the produced meat was the lowest in case of the I trial group – 5.66GEL, followed by II trial group – 5,94GEL and the control group – 6.33GEL.

The sales price was one and the same in all three groups – 8,0GEL. Cost of the meat produced during the testing period was the lowest in the I trial group, therefore, the profit is the highest just in this group.

As seen from the Tables, the proceeds gained from the I trial group during the testing period made 1392 GEL, in the II trial group – 1360 GEL, while in the control group – 1280 GEL.

The profit on initial 100 rabbits in the I group made 406 GEL, in the II group – 350 GDEL, while in the control group – 268 GEL.

Calculation of the economic efficiency for 100 rabbits, has shown that a cost of the produced meat is the lowest in the I trial group – 5,66GEL. Thus, the profit is the highest just in this I trial group.

CONCLUSION

As established by the analysis of the results of this experiment, in case of use of the microelements (Mn,Zn,Fe,Co,Cu) and the chelate compounds of the Glutamine acid and their compositions and of the compositions of natural Zeolite – Clinoptilolite in the composition of the combined food premixes for the rabbits, instead of the simple salts,] certain increase of the indicator of productivity and the economic efficiency of the rabbits and improvement of the blood biochemical indicators are observed in line with a number of another indicators [22,23] that is conditioned by a circumstance that in case of use of the chelate compounds of the microelements, a physiological state of the animals is improved, a pass of the food through the intestinal tract is slowed down (the effect of prolongation) and respectively, a rate of assimilation of food is increased, a toxicity is reduced, stability of the immune system is improved, while a loss of food is reduced. Considering all the above stated, we can say that our assumption that use of the chelate compounds of the microelements and their composites and the ones of the zeolites in the composition of premixes should ensure increase of their biological activity and the economic efficiency, turned to be approved by the industrial experiment and calculations of the economic efficiency.

Thus, based of the researches conducted, we may conclude that synthesis and studies of the chelate compounds are interesting both by the scientific and practical views. The compositions created on the basis of them and of the zeolites - Clinoptilolite may be successfully used in the composition of premixes and, on their ground, it may be created the additives of industrial importance for the combined feeding of the animals and poultry.

ACKNOWLEDGEMENT

We thank Science & Technology Center in Ukraine and Shota Rustaveli National Science Foundation for financial support. The work was implemented with the support of Science & Technology center in Ukraine project proposal #5461 and Shota Rustaveli National Science Foundation grant #30/06.

REFERENCES

[1] Loginov G. “Effect of Metal Chelates with Amino Acids and Protein Hydrolysates on the Productive Functions and Metabolic Processes in Animal Body.” Doctor’s thesis, Kazanj, 2005. 359.

[2] Kalashnikov A.P., Fisinin V.I., Shchuglov V.V., Kleimanov N.I., Pervov, N. G. “*Norms and Rations of Feeding of Agraricultural Animals.”* M., 2003. 456.

[3] Kochetkova N.A. “Influence of Metal Citrates on Biochemical Indices of Tissues and Organs of Chicken-Broilers and the Quality of the Products” Abstract of a Thesis. Specialty biochemistry. 2009. 03.04.” www.webpticeprom.ru.

[4] Hong S.J., Lim H.S., Paik I. K. “Effects of Cu and Zn Methionine Chelate Supplementation on the Performance of Broiler Chockens.” *J. Anim. Sci. Technol. Korea* 2002. 44: 399-406.

[5] Kochetkova N., Shaposhnikov A., Zateev S.“Citrates of Biometals in the Chicken-Broiler’s Diet. ”*J.Poultry Raising* 2010. www.webpticeprom.ru.

[6] Boiko I., and Miroshnichenko I. “Application of Manganese Citrate in Rearing Chicken-Broilers.” *J. Poultry Poultry Factory*, 2011. 11: 110-7.

[7] Lebedev S.V., Miroshnikov S.A., Sukhanova O.N., Rakhmatullin, Sh. G.“Method of Elevation of Productivity of

Broiler-Chicks." Patent for invention, # 2370095 A23K 1/00. 2009.
[8] Beshkenadze I.A., Urotadze S.L., Zhorzholiani N.B., Gogaladze M.A., Burkiashvili N.O., Gogua L.D. "Synthesis of the Chelates Containing Amino Acids and Citric Acid for Creation of New Generation Premixes." *Annals of Agrarian Science*, 2013. 11 (2): 84-6.
[9] Beshkenadze I.A., Gogaladze M.A., Urotadze S.L., Tsintsadze M.G., Tsintsadze T.G., Zhorzholiani, N.B., Kvernadze T.K. "Chemical Admix to Poultry Fooder." *Sakpatenti # P4917*. 2008.
[10] Beshkenadze I.A., Gogaladze M.A., Urotadze S.L., Tsintsadze M.G., Tsintsadze T.G., Zhorzholiani N.B., Osipova N. A."Chemical Admix to Poultry Fodder. " *Sakpatenti # P4918*. 2008
[11] Tsintsadze G.V., Beshkenadze I.A., Mestiashvili N.D., Zhorzholiani N.B. "Physical-Chemical Investigation of $M^{I}{\cdot}M^{II}{\cdot}L{\cdot}nH_2O$ Heteronuclear Citrates." *Proceedings of the Georgian Academy of Sciences, Chemical Series* 2006. 32 (3-4): 248-52.
[12] El-Said Asma I., Zidan Amna S.A., El-Meliqy Mahmoud, S., et al. "Synth, and Rect." *Inorg. and Metal-Org. Chem.* 2001. 31 (4): 633-48.
[13] Zhorzholiani N.B., Beshkenadze I.A., Gogaladze M.A., Begheluri G.T. "Synthesis and Study of Heteronuclear Citrates." *Journal of Chemistry and Chemical Engineering* 2014. 8 (4): 385-9.
[14] Beshkenadze I.A., Zhorzholiani N.B., Gogaladze M.A., Urotadze S.L., Tsitsishvili V.G. "Possibility of Obtaining The New Generation Premixes Containing Bio-Metals and Natural Zeolites." *Transactions of P.Melikishvili Institute of Physical and Organic Chemistry*, 2011. 94-7.
[15] Beshkenadze I.A., Tsitsishvili V.G., Urotadze S. L., Gogaladze M.A., Zhorzholiani, N.B. "Natural Zeolites and Biometal-Containing Composites." In *Materials of IV International Conference—Sorbents as Factors of Life and Health Quality*, Belgorod, 2012. 13-17.
[16] Beshkenadze I.A., Urotadze S.L., Zhorzholiani N. B., Begheluri G.T., Gogaladze M.A. "Study of Physiological Activity of Bio-Coordinated Substances and Their Premixes with Natural Zeolite-Containing Composites." *International Scientific Journal Intellectual* 2014. 26: 245-50.
[17] Beshkenadze I.A., Urotadze S.L., Zhorzholiani N. B., Gogaladze M.A., Begheluri G.T., Osipova N.A., Kvernadze T.K."Chelate-Containing Admixes to Poultry Fodder." Sakpatenti, *Tbilisi, #U1787*. 2014.
[18] Beshkenadze I.A., Urotadze S.L., Zhorzholiani N. B., Gogaladze M. A., Begheluri G.T., Osipova N.A., Kvernadze T.K."Chemical Admix for poulTry Nutrition." Sakpatenti, *Tbilisi, #U1800*. 2014.
[19] Beshkenadze I.A., Urotadze S.L., Zhorzholiani N.B., Gogaladze M. A., Chagelishvili A.A., Begheluri G.T., Heteronuclear Citrates containing Admix for Poultry Feeding." *Sakpatenti, Tbilisi, # U1887*. 2016.
[20] Beshkenadze I.A., Urotadze S.L., Zhorzholiani N.B., Gogaladze M.A., Gogua L.D., Lomtadze I.L."Synthesis and Study of Glutamine Acid Containing Citrates." *Journal of Chemistry and Chemical Engineering* 2015. 9 (1): 56-60.
[21] Beshkenadze I.A., Gogaladze M.A., Klarjeishvili N.A. Lomtadze O.G., Kozmanishvili G.A., Khurtsilava N.R. "Results of Physical-Chemical Study of Chelate-Type Compounds with Mixed Ligands." *Georgian National Academy of Sciensces Bulletin* 2017. 11 (2): 57-61.
[22] Beshkenadze I.A., Urotadze S.L., Chagelishvili A.A., Zhorzholiani N.B., Gogaladze M.A., Begheluri G.T., Klarjeishvili N.A.. "New Generation Premixes of Rabbit Nutrition." *Annals of Agrarian Science* 2016. 14: 288-91.
[23] Beshkenadze I.A., Chagelishvili A.A., Gogaladze M.A., Klarjeishvili N.A., Chagelishvili G.A."Study of Physiological Activity of Microelements- and Glutamine Acid-containing Chelate Citrates." *Annals of Agrarian Science* 2017. 15: 243-6.

შერეულლიგანდიანი ხელატების შემცველი პრემიქსები ბოცვრის კვებაში

იამზე ბეშკენაძე[1*], გიორგი ჩაგელიშვილი[2] , ნაზიბროლა კლარჯეიშვილი[1], მაია გოგალაძე[1], ომარ ლომთაძე[1]

[1] ივ.ჯავახიშვილისსახ.თბილისის სახელმწიფო უნივერსიტეტი,პეტრე მელიქიშვილის ფიზიკური და ორგანული ქიმიის ინსტიტუტი,საქართველო,თბილისი,ა.პოლიტკოვსკაიას 31, 0186
[2] საქართველოს აგრარული უნივერსიტეტი,თბილისი, დავით აღმაშენებლის ხეივანი #240, 0131
***iamze.beshkenadze@tsu.ge** (+995) 571188 525

რეზიუმე. ზოგადი ფორმულით $M{\cdot}gl{\cdot}L{\cdot}nH_2O$ (სადაც M=Mn,Zn,Fe,Co,Cu; gl=გლუტამინის მჟავა, L=ციტრატ-იონი) სინთეზირებული შერეულლიგანდიანი ხელატური ნაერთების, მათი და ბუნებრივი ცეოლითის - კლინოპტილოლითის კომპოზიციების საფუძველზე მომზადებული პრემიქსები გამოცდილია ბოცვრის კომბინირებულ საკვებში. მოსინჯვითი და ძირითადი ექსპერიმენტი ჩატარდა სამი ჯგუფისათვის: Iსაცდელი, რომლის საკვებიც ბალანსდებოდა 0.5% პრემიქსით და 2%კლინოპტილოლითით. IIსაცდელი, რომლის საკვებიც ბალანსდებოდა 0.5% პრემიქსით და III საკონტროლო, რომლის საკვებიც ბალანსდებოდა ფაბრიკაში არსებული პრემიქსით. ბოცვრის პროდუქტიულობის მაჩვენებელების შესწავლით დადგენილია, რომ საცდელი ჯგუფების ყველა მონაცემი ამ მიმართულებით აღემატება საკონტროლო ჯგუფისას. ჰემატოლოგიურმა კვლევებმა გვიჩვენა სამივე ჯგუფის ცხოველთა სისხლში ჰემოგლობინის (რომელიც

მიუთითებს სისხლმბადი ორგანოების ინტენსიურ მუშაობაზე, აგრეთვე ღვიძლის მდგომარეობაზე, საზრდო ნივთიერებებით უზრუნველყოფის დონეზე, ორგანიზმში მიმდინარე ჟანგვა-აღდგენით პროცესებზე) შემცველობა დამაკმაყოფილებელია. ლეიკოციტები (რომლებიც ორგანიზმში ასრულებენ დამცველობით ფუნქციას), ისევე როგორც ერითროციტების რიცხვი (რომლებიც სისხლში გვიჩვენებს ორგანიზმში მიმდინარე ნივთიერებათა ცვლის პროცესებს) ნორმის ფარგლებშია. დაბალია ჩხირბირთვას მაჩვენებლი I და II სააცდელ ჯგუფებში, ხოლო საკონტროლოში ნორმასთან (5-9%) ახლოსაა. ნორმის ფარგლებშია (33-39%) სეგმენტბირთვა მხოლოდ საკონტროლო ჯგუფის ცხოველთა სისხლში, ხოლო საცდელ ჯგუფებში ოდნავ მეტია. რაც შეეხება ეოზინოფილების ოდენობას (ნორმით 1-3%) ოდნავ მეტია I და საკონტროლო ჯგუფის ცხოველებში. ნორმის ფარგლებშია მონოციტებიც (1-4%) II საცდელ და საკონტროლო ჯგუფებში, ხოლო I საცდელში - ოდნავ მეტია. ერითროციტების დალექვის სიჩქარე (ნორმით 1-3%) ყველა ჯგუფის ცხოველთა სისხლში ერთნაირია, ხოლო ლიმფოციტების მაჩვენებლები ოდნავ ჩამორჩებიან ნორმას. 100 სულ ბოცვერზე ეკონომიკური ეფექტურობის გაანგარიშებამ გვიჩვენა, რომ წარმოებული ხორცის თვითღირებულება ყველაზე დაბალი I საცდელ ჯგუფში იყო -5.66ლარი. აქედან გამომდინარე მოგებაც ყველაზე მაღალი სწორედ I ჯგუფშია. 100 სულ ბოცვერზე მოგებამ I ჯგუფში -406 ლარი, II ჯგუფში -350 ლარი და საკონტროლოში - 268 ლარი შეადგინა.

OBTAINING OF GRAPHENE AND REDUCED GRAPHENE OXIDES FROM GRAPHITE FOIL WASTES

Natia Barbakadze[1]*, Vladimer Tsitsishvili[1], Tamar Korkia[1], Ketevan Sarajishvili[1], Lili Nadaraia[2]**, Roin Chedia[1]

[1] *Laboratory of Problems of Chemical Ecology, Petre Melikishvili Institute of Physical and Organic Chemistry at Ivane Javakhishvili Tbilisi State University, 31, Ana Politkovskaia str, Tbilisi 0186, Georgia*
**E-Mail: chemicalnatia@yahoo.de; phone: (+995 599) 76-53-15*

[2]*Republic Center for Structure Researches of Georgia, Georgian Technical University, 77, Kostavs str, Tbilisi 0171, Georgia*
***E-mail: likanad@gmail.com;* phone: *(995 593) 122035*

Abstract: In industry graphite foil is obtained by graphite intercalation with various substances, their further thermal shock treatment and calendering of the obtained expanded graphite. Powdered graphite foil wastes (pGFW) are obtained by grinding the wastes of various technological processes. The EDX analysis showed that the powder consists only of carbon and oxygen. The paper presents results oxidation of pGFW with Hummers method at low-temperature (~0°C; $KMnO_4$–$NaNO_3$–H_2SO_4) and relatively high-temperature (~50°C; $KMnO_4$–H_2SO_4) modes. The methods of synthesis of GO and its separation from the reaction mixture were partially corrected. In case of low-temperature mode oxidation of pGFW the C:O ratio (at.%) is 61:38. By the reduction of GO with ascorbic acid the C:O ratio decreases (C:O= 81:19). XRD analysis also confirmed that the peak of GO at 2Θ = 10.90° completely disappeared during the reduction process and appeared a broad diffraction maximum for rGO at 2Θ=23.80°. GO was reduced to the rGO with ascorbic acid, zinc powder and hydrazine. By the high-temperature treatment (1000-1500°C) of rGO graphene is obtained with a defective structure.

Keywords: Hummers method, graphite foil waste, graphene oxide, reduced graphene oxide, graphene.

INTRODUCTION

Compounds with carbon 2D and 3D structures are great importance and perspective. We can say that now they are widely used in any field of science and technology, which is reflected in the scientific and patent literature. In scientific research and technological processes, various methods of obtaining GO and RGO are used. Graphite oxide was first prepared in the nineteenth century [1-3] Chemical oxidation of graphite is based on methods of Brodie [2], Staudenmaier [3] and Hummers [4]. In all methods are used strong acids and oxidants (HNO_3, $HClO_4$, H_2SO_4, H_3PO_4, $KClO_3$, $NaNO_3$, $KMnO_4$ and etc.).

The graphite oxide and graphene oxide (GO) and reduced graphene oxide (rGO) are graphite single layer (graphene) oxidation products. Discussion about their structure in scientific literature continues (Fig. 1). A reviews are summarized by the data of various authors on the GO structure [5,6]. Obtaining of rGO from graphite will be displayed by the following scheme (Fig. 2):

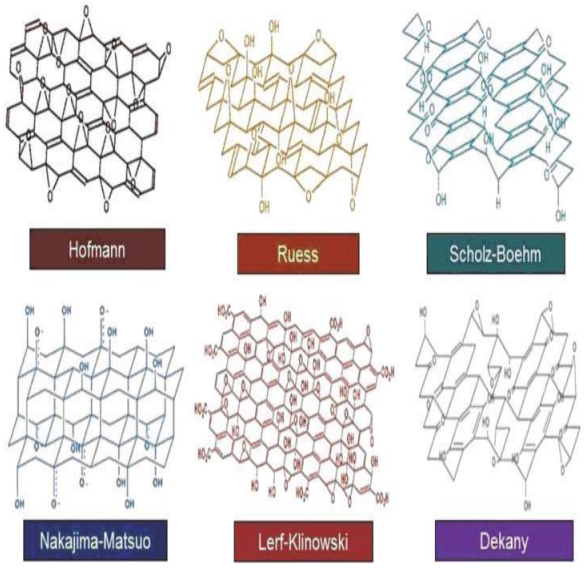

Fig. 1. Schemic structures of GO, suggested by various authors [5,6].

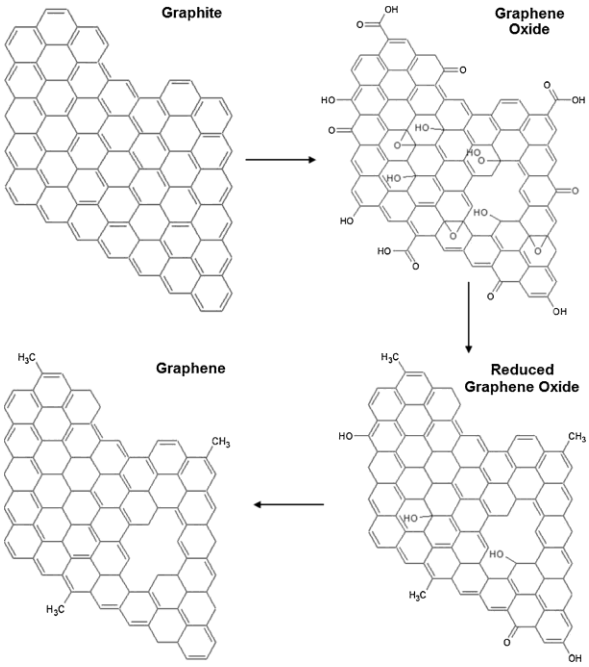

Fig. 2. Chemical structures of graphite, graphene oxide, reduced graphene oxide and graphene [7].

Accordingly, GO and rGO physical-mechanical properties or chemical composition changes within a wide range [8-15]. GO and rGO have organic functional groups (carboxylic, carbonyl, hydroxyl, epoxide). Their future functionalization or joining (immobilization) in organic or inorganic precursors may be performed. There are many organic–organic [16-20] and organic-inorganic [21-24] derivatives containing graphene structures and they have a wide area of application. Below we would like to discuss some methods of obtaining GO and RGO from different graphite precursors, which were used by us in the previous work [15]. Introduction of above mentioned early work is partially used in present work.

Currently, flake graphite is used for the obtaining of GO and rGO. Both, natural and synthetic graphite can be used to prepare these materials**.** The natural flake graphite powders with a particle size of less than 400 μm are mostly used in industry or laboratory practice. Purification of the natural graphite from impurities is carried out by separation or flotation, chemical processing. For example, by the enrichment of raw ore containing 68% C graphite is obtained after enrichment with 97.68% C graphite content, which can be used in the synthesis of GO and rGO [25]. Thorough cleaning of graphite is necessary, because the impurities in it could be found in targeted product [26].

The use of different precursors of graphite for GO synthesis is discussed in many scientific sources [27]. Dependence of oxidation degree, hydrophilicity and microstructure of GO prepared on nature of graphite precursors were studied with using flake, expendable and microcrystalline graphite precursors. It is estimated that the GO prepared on the basis of expandable graphite is characterized by a higher degree of oxidation than in case of microcrystalline graphite [28].

GO could be obtained by a modified Hummers method from synthetic graphite powders. The graphite powder SP-1 was washed with NaCl solution, then oxidized with $KMnO_4$–H_2SO_4 at low temperatures (<20°C) [29]. For the synthesis of GO it was successfully used expanded graphite. The process of synthesis was done below <20 °C in $KMnO_4$–H_2SO_4 system [29].

One of the interesting methods for GO synthesis is the improved Hummers method, where flake graphite oxidation is performed with $KMnO_4$–H_2SO_4–H_3PO_4 mixture at 50 °C and at a ratio of H_2SO_4/H_3PO_4= 9:1, and the optimized conditions led to GO in 3 h [11]. Above mentioned method is simplified in the work [31]. $KMnO_4$–H_2SO_4 are used as oxidizing systems, temperature mode of the process is being at 50°C.

GO and rGO could also be obtained from commercial expanded graphite with grain size D_{50} ~ 15 μm. GO was obtained by a new modified Hummers method. At the initial stage the powder of graphite and potassium permanganate is mixed, cooled and then sulfuric acid (98 %) is added [32]. The synthesis ends in a relatively short period of time since the particles of the graphite powder used were small.

Expanded graphite was also used in 10–30 μm size [33]. The synthesis was conducted using ultrasonic cleaner used after the reaction is terminated with water (90°C, 10 min). Thus, for obtaining of the GO and rGO, natural and synthetic graphites, graphite intercalated with different compounds and expanded graphite also can be used. It is established that the reduction of the GO obtained from the samples of the different types of graphite are formed graphenes, in which the number of layers was very different (1–10 layers or more) [34-38].

Flexible graphite foils in various thickness and width are used in modern technologies. The remaining graphite foil pieces (wastes) are expanded graphites, and their chemical oxidation to GO or to obtain graphene can be conducted using known methods with some adjustments [39]. The purpose of the present work is studying the usability of wastes of the graphite foils as the precursors for GO and rGO synthesis. Information on the properties and the fields of the application of the products and graphite foil manufacturer companies are available on web sites [40].

What is the graphite foil? It is obtained from graphite intercalated compounds (GIC). The GIC is received by inserting of various compounds between layers (gaseous compounds, HNO_3, H_2SO_4, CrO_3, $KMnO_4$, H_2O_2, $FeCl_3$, $AlCl_3$ and etc.). In the result of intercalation, expandeble graphite is obtained. By thermal shock treatment of GIC high pressure is created between the graphite layers and the crystalline structure of graphite collapses in layers that consist of 1–20 layers. By its further treatment with pressure, graphite products and materials are received, which are used in various fields of technology. Graphite foil is known under different names: Graflex, Grafoil, Perma-Foil, Carbonax and etc [40]. Production of graphene foil consists of the following steps:

graphite ⟶ intercalated graphite ⟶
hydrolisis ⟶ thermal shock ⟶
expanded graphite ⟶ calendering ⟶
graphite foil. Graphite foils are used in many fields: chemical and petrochemical industries, refineries, and the energy, engineering and automotive sectors, where hermetic and reliable connection of parts and equipment is necessary, also are used as an adsorbents, sealing products, antifriction materials and etc. By the mechanical exfoliation of graphite graphene was obtained [41].

MATERIALS AND METHODS

Flake graphite, $KMnO_4$, $NaNO_3$, H_2SO_4 (98 %), HCl (37 %), HI (57 %) and ascorbic acid were purchased from Sigma Aldrich. The morphology of the samples was studied by optical and scanning electron microscopes (Nikon ECLIPSE LV 150, LEITZ WETZLAR and JEOL JSM–6510 LV-SEM). Samples X-ray diffraction (XRD) patterns were obtained with a DRON–3M diffractometer (Cu–K_α, Ni filter, 2°/min). After purification, graphite foil powders were analyzed using EDS. Thermal treatment of GO and rGO (1000-1500°C) was implemented in high temeperature vacuum furnace (Kejia furnace). For the ultrasound treatment and homogenization of suspensions was used Ultrasonic cleaner (40 KHz) and JY92-IIDN Touch Screen Ultrasonic Homogenizer (20-25 KHz, 900 W). GO and rGO particle sizes were determined by Winner802 DLS Photon correlation nano particle sizer analyzer.

Obtaining of powdered graphite foil wastes (pGFW): The initial powders were obtained by grinding of flake wastes in water (blender). After drying the powder, that was still dry ground using a laboratory mill. Removal of impurities from the powders was carried out with chemical reagents and their subsequent sifting fractions with particles <140 μm were collected. From these powders, the graphene oxide was obtained with different oxidation systems ($KMnO_4$–$NaNO_3$–H_2SO_4 and $KMnO_4$–H_2SO_4) (Fig.3, 4).

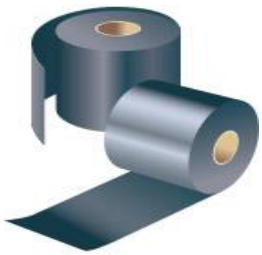

Fig. 3. Industrial graphite foil
http://www.toyotanso.com/Products/index.html

I II

Fig. 4. Graphite foil wastes (I) and pGFW (II).

Graphene oxide synthesis with Hummers method: In details, 0.75g $NaNO_3$ and 80 ml of 98% sulfuric acid were added to 1 g of pGFW. The reaction mixture was cooled up to -2 – +1°C and stirred for 30 min. Over the next 50 min, 6 g of $KMnO_4$ was added. The temperature was left to raise until room temperature (3 h) during stirring, and the mixture was further stirred for half an hour at 35–40 °C. The reaction mixture was diluted with 100 ml of cold water, keeping the temperature below 90°C, and then stirred at this temperature for 30 min. The mixture was diluted to 300 ml. Residual amount of potassium permanganate was removed by 3 % hydrogen peroxide solution. A yellowish suspension of graphite oxide was obtained, its color gradually changed to dark brown.

The resulting suspension was left to stand for 20 min, and then the precipitate was removed by decantation. This operation was repeated twice. For the rapid precipitation of graphene oxide from the suspension, a 5 % solution of hydrochloric acid (300 ml) was added. Decantation was repeated 3 times in 10 min intervals. An aqueous gel-like mass was obtained by centrifuging and washing the sediment, the pH was between 5 and 6. The sediment was washed with acetone 3 times and is dried in vacuum at 70 °C for 4 h.

The decanted solutions contained 12–17 wt.% of GO. Its reduction to the rGO was conducted with ascorbic acid, zinc powder and hydrazine. For example: the decanted solutions were mixed with 1 g of ascorbic acid and heated until 80 °C. The brown solution darkens rapidly due to the formation of reduced graphene oxide. rGO precipitation occurred when the reaction mixture was cooled (10 min). The precipitate was filtered, washed with sodium

bicarbonate solution, then with water until reaching pH = 6, acetone (x3) and dried in vacuum at 70 °C.

Oxidation of pGFWwith $KMnO_4$–H_2SO_4 system: For oxidation of pGFW, we used a simplified oxidation system of $KMnO_4$–H_2SO_4 [31]. In more details, 40 ml of 98 % sulfuric acid is added to 1 g pGFW (<140 μm) in a glass reactor. The mixture was stirred at 35–40 °C for half an hour and 3 g of potassium permanganate was added at 40–45 °C under 1 h (the temperature can reach 50°C). The mixture was stirred for 3 h. A gray viscous mass was obtained, which was cooled to 10°C and 100 ml of ice-water was added to the glass reactor. A sharp change in the temperature of the reaction mixture was not observed while adding the water. After adding 3–4 drops of hydrogen peroxide (30 %), the reaction mixture becomes sharp yellow. Isolation of graphene oxide from the suspension and receiving of rGO from decanted solutions was carried out using the way mentioned above. Synthesis scheme of GO, rGO and grapheme from graphite foil wastes are shown in fig.5.

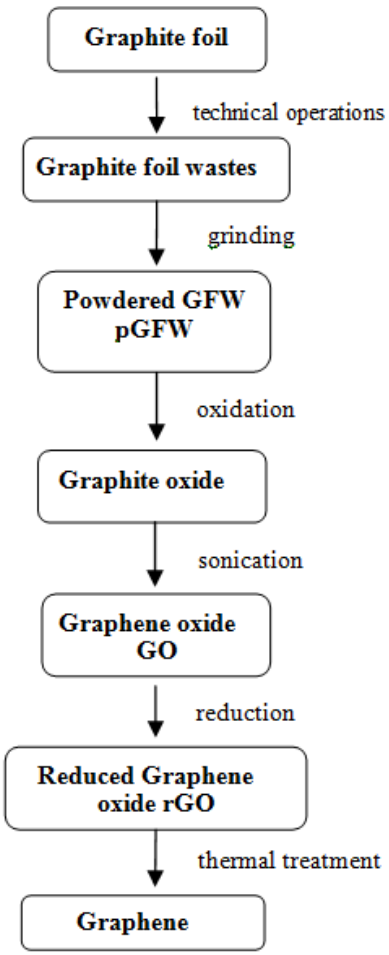

Fig. 5. Scheme of obtaining graphene oxide, reduced graphene oxide and graphene from graphite foil wastes

RESULTS AND DISCUSSION

Graphite foil wastes from various technological processes are contaminated with various types of organic and inorganic compounds which can be removed with various methods after grinding the waste. The graphite foil wastes used in our experiments contained about 6% oxygen and some other elements as well. After their wet grinding, a powder with a particle size of <1 mm was obtained, and the amount of fine fraction (<50 μm) does not exceed 6–8 %. In the case of dry grinding of these powders, a fraction with a particle size of <140 μm could be obtained, which was treated with various reagents to remove the impurities. As the EDX analysis showed, the powder produced consisted of carbon and oxygen.

The SEM image shows that each particle of the powder is composed of layers rolled on each other and had different forms. The thickness of the sheets was found to be ~0.5 μm (Fig. 6).

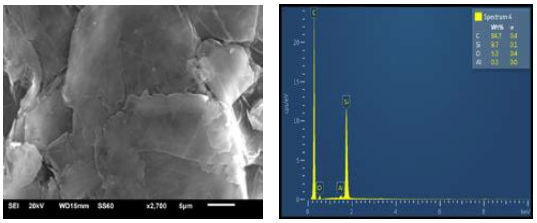

I II

Fig. 6. SEM image (I) and EDX spectrum (II) of pGFW.

Oxidizing reagents can easily penetrate the layers and intercalation or functionalization-oxidation processes can be occurred resulting in graphite oxide. Using of pGFW with a particle size of 200–500 μm to prepare of GO and the rGO may also possible.

The GO synthesis from pGFW was conducted using the same methods as in case of other types of graphite precursors. The $KMnO_4$–H_2SO_4 and $KMnO_4$–$NaNO_3$–H_2SO_4 systems were tested in the pGFW oxidation using low-temperature (~0°C; $KMnO_4$–$NaNO_3$–H_2SO_4) and relatively high-temperature (~50°C; $KMnO_4$–H_2SO_4) modes. The characteristic XRD peak of pGFW at 2Θ=26.45–26.50° completely disappears during the oxidation process (Fig.7) due to complete oxidation of pGFW into graphite oxide. XRD analysis also confirmed that both oxidation methods led to the GO-phases characterized with the peaks located at 2Θ = 10.90 and 10.60°, respectively (Fig. 7). The obtained results correspond to the available data of processes used flake graphite or expanded graphite as a precursor [28, 35, 36]. In case of low-temperature mode oxidation of

pGFW, the C/O ratio (at.%) was found to be 61:38. During its reduction with ascorbic acid, the C/O ratio was modified to be 81:19. The peak of GO at 2Θ = 10.90° completely disappeared during the reduction process and appeared a broad diffraction maximum for rGO at 2Θ=23.80°.

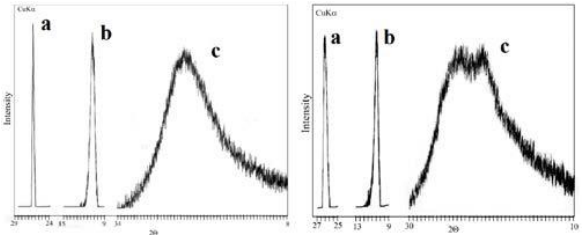

I II

Fig. 7. XRD patterns of graphite foil (Ia), GO (Ib), rGO (Ic), and pGFW (IIa), GO (IIb), rGO (IIc). GO was obtained by oxidation of pGFW with $KMnO_4$–$NaNO_3$–H_2SO_4 (Ib) and with $KMnO_4$–H_2SO_4 (IIb).

When the pGFW was oxidized in a high temperature mode (~50°C, $KMnO_4$–H_2SO_4), the C/O ratio (at.%) was found to be 64:35. In case of its reduction with ascorbic acid, rGO is obtained and the C/O ratio (at.%) was changed to 80:20. The diffraction peak at 2Θ = 10.6° disappeared and two peaks of rGO appeared at 2Θ = 21.2 and 23.7° (the sample was dried in vacuum at 150 °C in 2 h).

During the reduction of GO to rGO by the different methods, the diffraction peak maximums appeared at different values of 2Θ between 20.0 and 26.6° [28, 35, 36]. The location of the peaks depended on the rGO drying temperature and shifted to higher values with increasing that. Using the hydroiodic acid solution (57 %) to reduce GO obtained by us, this diffraction maximum could be detected at 2Θ=23.7°. pGFW oxidation requires 8–15 % more sulfuric acid than flake graphite because the viscosity of the reaction medium increases. Herewith it is confirmed that the powder oxidation process effectively passes using 93–95 % sulfuric acid as well, because it is cheaper and more available than the concentrated H_2SO_4 (98 %).

The method of synthesis of GO and its separation from the reaction mixture was partially corrected in a way that the experiments would finish after 8–10 h only. Sulfuric acid and metal ions (K^+, Na^+, and Mn^{+2}) were removed with decanting (2 times with H_2O, 3 times with 5% HCl solution). A 5 % solution of HCl precipitates GO-flakes in 7–10 min, thus, the process to remove the main impurities could be accelerated. Subsequent GO purification was carried out using traditional centrifuging and washing methods.

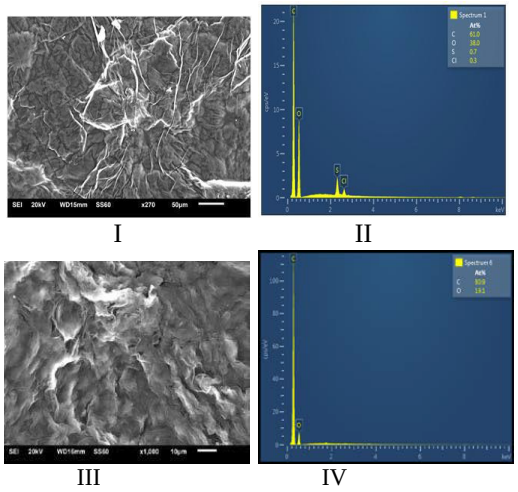

I II III IV

Fig. 8. SEM image (I and III) and EDX spectrum (II and IV) of GO platelets and rGO sheets, respectively.

It is confirmed that the received GO (Fig. 8) contains sulfur and chlorine as impurities, S:Cl atomic ratio (at.%) was found to be 0.7:0.3. A similar result was obtained using flake graphite (0.7–2.8):(0.6–0.8) [11, 31]. These impurities can be removed during the reduction process of GO. During the decantation of reaction medium thin fraction of GO moves into the filtrate. Using Photon correlation nano particle sizer analyzer it is confirmed, that their sizes varies in wide range and reaches 60-1000 nm (Fig. 9).

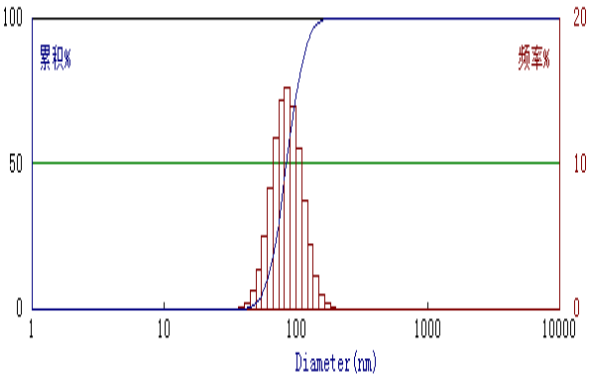

Fig. 9. Particle size distribution in GO decanted solution.

The decanted solutions contained 12–17 wt.% GO, but the large volume of the solutions complicated the separation. It is easier to remove the GO from these acidic solutions in its reduced form. In strong acidic solutions, GO can be reduced to rGO using various chemical reagents [34, 35]. We selected ascorbic acid to reduce GO in solutions to rGO (Fig. 8) at 80°C. The EDX analysis confirmed the completeness of reduction and elimination of the chlorine and sulfur-containing contaminants.

Using a high-temperature (1000–1500°C) thermal treatment, the reduced graphene oxide can be

transformed into graphene with a defect structure.

CONCLUSION

Grinding of waste industrial graphite foils resulted in graphite powders (pGFW) with a particle size of <140 μm, which oxidation to obtain GO was carried out with $KMnO_4$–$NaNO_3$–H_2SO_4 oxidation system (Hummers method). The C/O ratio in GO and its ascorbic acid reduced from (rGO) were found to be 61:38 and 81:19, respectively.It was confirmed that GO could also be obtained from pGFW using $KMnO_4$–H_2SO_4 system as well at 50 °C. Industrial wastes of graphite foils were found to be appropriate precursors for an eco-friendly synthesis of GO and rGO, which can be transformed into graphene by thermal treatment at high temperature

ACKNOWLEDGEMENT

We would like to thank Dr. Vakhtang Ugrekhelidze (National High Technology Center, Tbilisi, Georgia), who provided us with graphite foil samples.

Paper was presented at the 5th International Conference "Nanotechnologies", November 19–22, 2018, Tbilisi, Georgia (Nano–2018).

REFERENCES

[1] Schafheutl C. "Ueber die Verbindungen des Kohlenstoffes mit Silicium, Eisen und anderen Metallen, welche die verschiedenen Gallungen von Roheisen, Stahl und Schmiedeeisen bilden". *J. Prakt. Chem*., 1840, 21, pp. 129–157.

[2] Brodie B.C. "On the atomic weight of graphite". *Philos. Trans. R. Soc*., 1859, 14, pp. 249–259.

[3] Staudenmaier L. "Verfahren zur Darstellung der Graphitsaure". *Ber. Deut. Chem. Ges*., 1898, 31, pp. 1481-1487.

[4] Hummers, W.S., Offeman, R.E. "Preparation of graphitic oxide". *J. Am. Chem. Soc*., 1958, 80, p. 1339.

[5] Dreyer D.R.., Park S., Bielawski C.W., Ruoff R.S. "The chemistry of graphene oxide". *Chem. Soc. Rev.*, 2010, 39, pp. 228–240; DOI: 10.1039/b917103g.

[6] Khan Z.U., Kausar A., Ullah H., Badshah A.. Khan W.U. "A review of graphene oxide, graphene buckypaper, and polymer/graphene composites: Properties and fabrication techniques". *Journal of Plastic Film & Sheeting*, 2016, 32, pp. 336–379. DOI: 10.1177/8756087915614612.

[7] Mohan V.B., Jayaraman R.B.Kr., Bhattacharyya D. "Characterisation of reduced graphene oxide: Effects of reduction variables on electrical conductivity". *Materials Science and Engineering, B*, 2015, 193, pp. 49–60. http://dx.-doi.org/10.1016/j.mseb2014.11.002.

[8] Pei S., Cheng H.M. "The reduction of graphene oxide". *Carbon*, 2012, 50, pp. 3210-3228. https://doi.org/10.1016/j.carbon.2011.11.010.

[9] Ramakrishnan M.C., Thangavelu R.R. "Synthesis and characterization of reduced graphene oxide". *Advanced Materials Research*, 2013, 678, pp. 56-60. https://doi.org/10.4028/www.scientific.net/AMR.678.56 .

[10] Stobinski L., Lesiak B., Malolepszy A., Mazurkiewicz M., Mierzwa B., Zemek, J., Jiricek P., Bieloshapka I. "Graphene oxide and reduced graphene oxide studied by the XRD, TEM and electron spectroscopy methods". *Journal of Electron Spectroscopy and Related Phenomenon*, 2014, 195, pp.145-154. https://doi.org/10.1016/j.elspec.2014.07.003.

[11] Marcano D.C., Kosynkin D.V., Berlin J.M., Sinitskii A., Sun Z., Slesarev A., Alemany L.B., Lu W., Tour J.M. "Improved synthesis of graphene oxide". *ACS Nano*, 2010, 4, pp. 4806-4814. https://doi.org/10.1021/nn1006368 .

[12] Stankovich S., Dikin D., Piner R.D., Kohlhaas K.A., Kleinhammes A., Jia Y., Wu Y., Nguyen B.T., Ruoff R.S. "Synthesis of graphene-based nanosheets via chemical reduction of exfoliated graphite oxide". *Carbon*, 2007, 45, pp.1558-1565. https://doi.org/10.1016/j.carbon.2007.02.034.

[13] Wang G., Yang J., Park J., Gou X., Wang B., Liu H., Yao J. "Facile synthesis and characterization of graphene nanosheets". *Journal of Physical Chemistry C*, 2008, 112, pp. 8192-8195. https://doi.org/10.1021/jp710931h.

[14] Chen J., Yao B., Li C., Shi G. "An improved Hummers method for eco-friendly synthesis of graphene oxide". *Carbon*, 2013, 64, pp. 225-229. https://doi.org/10.1016/j.carbon.2013.07.055.

[15] Barbakadze N.G., Tsitsishvili V.G., Korkia T.V., Amiridze Z.G., Jalabadze N.V., Chedia R.V. "Synthesis of graphene oxide and reduced graphene oxide from industrial graphite foil wastes". *Eur. Chem. Bull*., 2018, 7, pp.329-333. DOI: 10.1762/ecb.2018.7.329-333.

[16] Stankovich S., Dikin D.A, Dommett G.H., Kohlhaas K.M., Zimney E.J., Stach E.A., Piner R.D., Nguyen S.T., Ruoff R.S. "Graphene-based composite materials". *Nature*, 2006, 442, pp. 282–286. DOI: 10.1038/nature04969.

[17] Ramanathan T, Abdala A.A., Stankovich S., Dikin D.A., Herrera-Alonso M., Piner R.D., Adamson D.H., Schniepp H.C, Chen X., Ruoff R.S., Nguyen S.T., Aksay I.A., Prud'Homme R.K., Brinson L.C. "Functionalized graphene sheets for polymer nanocomposites". *Nature Nanotech*., 2008, 3, pp. 327–331 DOI: 10.1038/nnano.2008.96.

[18] Blake P., Brimicombe P. D., Nair R.R., Booth T. J., Jiang D., Schedin F., Ponomarenko L.A., Morozov S.V., Gleeson H.F., Hill E.W., Geim A.K., Novoselov K.S. "Graphene based liquid crystal device". *Nano Lett*., 2008, 8, pp. 1704–1708.

[19] Choi E-Y., Han T. H., Hong J., Kim E., Lee S.H., Kima H.W., Kim S.K. "Noncovalent functionalization of graphene with end-functional polymers". *J.Mater. Chem*., 2010, 20, pp.1907-1912. DOI: 10.1039/b919074k.

[20] Gonçalves C., Gonçalves I., Magalhães F., Pinto A. "Poly(lactic acid) composites containing carbon-based nanomaterials: A review". *Polymers*, 2017, 9, pp.1-37. doi:-10.3390/polym9070269.

[21] Porwal H., Grasso S., Reece M.J. "Review of graphene–ceramic matrix composites". *Advances in Applied Ceramics: Structural, Functional and Bioceramics*, 2013, 112, pp. 443-454. https://doi.org/01179/174367613X13764308970581

[22] Markandan A., Chin J.K., Michelle T., Tan T. "Recent progress in graphene based ceramic composites: a review". *Journal of Materials Research*, 2017, 32, pp. 84-106. https://doi.org/10.1557/jmr.2016.390 .

[23] Li F., Jiang X., Zhao J., Zhang S. "Graphene oxide: A promising nanomaterial for energy and environmental applications". *Nano Energy*, 2015, 16, pp. 488-515. https://doi.org/10.1016/j.nanoen.2015.07.014.

[24] Li Y., Ma F.M., Ding X., Wang H., Li P. "Silica/graphene oxide nanocomposites: Potential adsorbents for solid phase extraction of trace aflatoxins in cereal crops coupled with high performance liquid chromatography". *Food Chemistry*, 2018, 245, pp. 1018-1024. https://doi.org/10.016/j.foodchem.2017.11.070.
[25] Panatarani C., Muthahhari N., Rianto A., Joni I.M. "Purification and preparation of graphite oxide from natural graphite". *AIP Conf. Proc*., 2016, 1719,030022,6 pp. https://doi.org/10.1063/1.4943717 .
[26] Ambrosi A., Chua Ch.K., Khezri B., Sofer Z., Webster R. D., Pumera M. "Chemically reduced graphene contains inherent metallic impurities present in parent natural and synthetic graphite". *Proc. Nat. Acad. Sci. USA*, 2012, 109(32), pp.12899-12904. https://doi.org/10.1073/pnas.1205388109.
[27] Dimiev A.M., Eigler S. Graphene Oxide: Fundamentals and Applications, Wiley: Chichester, 2016, 432 p.
[28] Hu X., Yu Y., Zhou J., Song L. "Effect of graphite precursor on oxidation degree, hydrophilicity and microstructure of graphene oxide". *Nano: Brief Rep. Rev*., 2014, 9(3), 1450037, 8pp. DOI: 10.1142/S1793292014500374 .
[29] Kaniyoor A., Baby T.T., Ramaprabhu S. "Graphene synthesis via hydrogen induced low-temperature exfoliation of graphite oxide". *J. Mater. Chem*., 2010, 20, pp. 8467-8469. DOI: 10.1039/C0JM01876G.
[30] Chen T., Zeng B., Liu J.L., Dong J.H., Liu X.Q., Wu Z., Yang X.Z., Li Z.M. "High throughput exfoliation of graphene oxide from expanded graphite with the assistance of strong oxidant in modified Hummers method". *J. Phys., Conf. Ser*., 2009, 188, 012051, 5 p., https://doi.org/10.1088/1742-6596/188/1/012051
[31] Del Prado Lavin Lopez M., Valverde Palomino J.L., Sanchez Silva M.L., Romero Izquierdo A. In: Recent Advances in Graphene Research. 2016, INTECH, pp. 122-133. http://dx.doi.org/10.5772/63752.
[32] Sun L., Fugetsu B. "Mass production of graphene oxide from expanded graphite". *Mater. Lett*., 2013, 109, pp. 207-210. https://doi.org/10.1016/J.MATLET.2013.07.072.
[33] Yang H., Li H., Zhai J., Sun L., Yu H. "Simple synthesis of graphene oxide using ultrasonic cleaner from expanded graphite". *Ind. Eng. Chem. Res*., 2014, 53(46), pp.17878-17883. DOI: 10.1021/ie503586v.
[34] Gambhir S., Jalili R., Officer D.L., Wallace G.G. "Chemically converted graphene: scalable chemistries to enable processing and fabrication". *NPG Asia Mater*., 2015, 7, e186, 15 pp. https://doi.org/10.1038/am.2015.47.
[35] Aunkor M.T.H., Mahbubul I.M., Saidur R., Metselaar H.S.C., "The green reduction of graphene oxide". *RSC Adv*., 2016, 6, pp. 27807-27828. DOI: 10.1039/C6RA03189G.
[36] Muzyka R., Kwoka M., Smedowski L., Diez N., Gryglewicz G. "Characterization of graphite oxide and reduced graphene oxide obtained from different graphite precursors and oxidized by different methods using Raman spectroscopy". *New Carbon Mater*., 2017, 32(1), pp. 15-20. doi: 10.3390/ma11071050.
[37] Botas C., Perez–Mas A.M., Alvarez P., Santamaria R., Granda M., Blanco C., Menedez R. "Optimization of the size and yield of graphene oxide sheets in the exfoliation step". *Carbon*, 2013, 63, pp. 562-592. http://dx.doi.org/10.1016/j.carbon.2013.06.096.
[38] Alam S.N., Sharma N., Kumar L. "Synthesis of graphene oxide (GO) by modified Hummers method and its thermal reduction to obtain reduced graphene oxide (rGO)". *Graphene*, 2017, 6(1), pp. 1-18. DOI: 10.4236/graphene.-2017.61001.
[39] Rem W., Cheng H.M. "The global growth of grapheme". *Nature Nanotechnol*., 2014, 9, pp. 726-730. https://doi.org/10.1038/nnano.2014.229.
[40] www.mersen.com;http://www.toyotanso.com/index.html; http://www.geegraphite.com/; https://www.canada-carbon.com/; https://sealwiz.com/; https://www.graflex.ru/contacts/].
[41] Geim A.K., Novoselov K.S. "The rise of grapheme". *Nature Materials*, 2007, 6, pp. 183-191. http://dx.doi.org/10.1038/nmat1849

გრაფენის ოქსიდის და აღდგენილი გრაფენის ოქსიდის მიღება გრაფიტის ფოლგის ნარჩენებიდან

ნათია ბარბაქაძე[1*], ვლადიმერ ციციშვილი[1], თამარ ქორქია[1], ქეთევან სარაჯიშვილი[1], ლილი ნადარაია[2*], როინ ჭედია[1]

[1] *ივანე ჯავახიშვილის სახელობის თბილისის სახელმწიფო უნივერსიტეტი, პეტრე მელიქიშვილის სახელობის ფიზიკური და ორგანული ქიმიის ინსტიტუტი, ა. პოლიტკოვსკაიას ქ.31, თბილისი 0186*
E-Mail: chemicalnatia@yahoo.de; ტელ: (+995 599) 76-53-15
[2]*სტრუქტურული კვლევების ეროვნული ცენტრი, საქართველოს ტექნიკური უნივერსიტეტი. კოსტავას ქ. 77, თბილისი 0171*
***E-mail: likanad@gmail.com; ტელ: (995 593) 122035*

რეზიუმე. მრეწველობაში გრაფიტის ფოლგა მიიღება გრაფიტის ინტერკალირებით სხვადასხვა ნაერთებით, მათი შემდგომი თერმული შოკური დამუშავებით და მიღებული გაფართოებული გრაფიტის ფხვნილის კალანდირებით. სხვადასხვა ტექნოლოგიური პროცესების ნარჩენებისაგან ფხვნილების მიღება ხდება მათი

სველი და მშრალი დაფქვით. ენერგოდისპერსული რენტგენული ანალიზით დადგენილია, რომ ფხვნილი შედგება მხოლოდ ნახშირბადისა და ჟანგბადისაგან. ნაშრომში წარმოდგენილია გრაფიტის ფოლგის ნარჩენების ფხვნილისაგან გრაფენის ოქსიდის მიღება ჰამერსისა (~0°C; $KMnO_4$–$NaNO_3$–H_2SO_4) და ასევე გამარტივებული მეთოდით (~50°C; $KMnO_4$–H_2SO_4). გრაფენის ოქსიდის სინთეზი და მისი გამოყოფა სარეაქციო არედან განხორციელდა არსებული მეთოდების მოდიფიცირებით. ფხვნილის დაბალტემპერატურული დაჟანგვისას მიღებულ გრაფენის ოქსიდში C:O (ატ.%) თანაფარდობა აღწევს 61:38. მისი ასკორბინის მჟავით აღდგენის შემთხვევაში (ატ.%) თანაფარდობა მცირდება (C:O=81:19). რენტგენოდიფრაქციული ანალიზებით დადგენილია, რომ გრაფენის ოქსიდის პიკი გამოვლინდება 2Θ = 10.90°, რომელიც სრულიად ქრება აღდგენის პროცესში და აღდგენილი გრაფენის ოქსიდის დიფრაქციული მაქსიმუმი ფიქსირდება 2Θ=23.80°. გრაფენის ოქსიდის აღდგენა ჩატარდა ასკორბინის მჟავის, იოდწყალბადმჟავის, თუთიის ფხვნილის და ჰიდრაზინის მეშვეობით. აღდგენილი გრაფენის ოქსიდის მაღალტემპერატურული დამუშავებით (1000-1500°C) მიიღება დეფექტური სტრუქტურის მქონე გრაფენი.

Natural zeolites saturated with technogenic gasses, additives of building materials

Teimuraz Kordzakhia[1]*, Giorgi Tsintskaladze[1], Rajden Skhvitaridze[2], Irakli Giorgadze[2], Marine Zautashvili[1]

[1] *Iv.Javakhishvili Tbilisi State University; P.Melikishvili Institute of Physical and Organic Chemistry, (31 A.Politkovskaya str., 0186, Tbilisi, Georgia)*
[2] *Scientific Center "NanoDugabi", Georgian Technical University, (77 Kostava str., 0160, Tbilisi, Georgia)*
**E-mail: teimuraz.kordzakhia@tsu.ge; and phone number: +995591938185;*

Abstract. Increasing the volume of cement production in Georgia has fueled environmental and technical global problems. The Association Agreement with the European Union has created the necessity of developing the best available environmental environment in Georgian cement.

For the purpose of prevention of emission of CO_2, SOx, NOx in the atmosphere and proper global problems, such as "Thermal effect" and "acid rains", there has been offered sorbent trapping with zeolites - cleaning of technogenic oxides coming out of the kiln of cement clinker and afterwards by grinding of these saturated sorbents and utilizing them as a mineral additive zeolite modifying of cement innovative BAT nanotechnology methods.

The mechanism for detection of CO2, SOx, NOx gases with zeolithic adsorbents in semi-production conditions has been identified and studied by physical and chemical research (chromatography, so-called spectroscope, X-rayfactometric analysis). It also has been established that in the sample samples of cement samples, there is a substance in the material obtained from the subsequent Zeolite supplements.

Keywords: natural zeolite, cement, kiln for clinker, technogenic gasses, adsorption, infrared spectroscopy.

INTRODUCTION

Despite existing of lots of different means of neutralization of harmful components of gasses dissipated in the atmosphere (the main sources of which are energetic, chemical-metallurgical and cement enterprises) choosing of rational and effective cleaning methods is getting more and more actual. Because of becoming requirements stricter in relation to emission of stack gasses in the atmosphere [1, 2], it is necessary to develop cleaning technologies of stack gasses. One of the perspective methods of cleaning of stack gasses is a sorption method – by using natural zeolites.

Matter point of the problem

Nowadays the "main source" of emission of stack gasses and their components, such as **CO_2,SOx,NOx,** into the atmosphere, is a kiln of clinker in cement production.

Clinker raw charge contains on average 80% limestone - **$CaCO_3$.** In case of using coal as fuel, as a result of burning CO/**CO_2, SO_2/SO_3, and NO/NO_2** are moving to the stack gasses. Definitely: by the stack gasses of the clinker kiln emission of the following "harmful" technogenic compounds takes place: **742-825** kg/t **CO_2**; **1,15-9,18** kg/t **SOx**; **0,285-1,14** kg/t **NOx** [1], because of which cement production is deemed to be supporting creation of global problems "hot-house effect"/ "acid rains". The share of cement production in the emission of **CO_2** in environment is deemed to be 6-8% . At the same time these emitted technogenic substances are modifying mixtures of structural composition of cement-concrete and are supporting intensive solidification process. They are participating in creating crystallohydrates of complex, needle fiber habit (hydro calcium carboalluminate -**C_3A $3CaCO_3$ $31H_2O$** ettringite-**C_3A $3CaSO_4$ $31H_2O$**, thaumasite-**C_3S SO_4 $CO_3 15H_2O$**) and self (nano)- reinforcement, in the decrease of anisotropicity of concrete strength [2].

In Georgia high-functional cement-concrete is in demand, satisfaction of which is hindered by fragility of its structure, less stability to bending loads, i.e. anisotropicity of mechanical strength.

Natural zeolites, which Georgia is rich of (their supply exceeds 300 mln t), are characterized with macromolecular system, having well developed surface, activity of which is due to the molecular-sieve effect of micro and nanopores and also diffusion and sorption processes, have ability to take in technogenic compounds emitted during clinker burning **CO_2, SOx, NOx.** These gasses are ecologically harmful, but joining with zeolite by sorption and after utilization of this modified zeolite in the composition of cement they become structural components of cement-concrete – nano-modifying

compounds, because after mixing of cement they must form crystallohydrates of cement containing structural **CO_2, SOx, NOx**.

Earlier in production of cement there was offered by us perspectives of using zeolites as pozzolanic mineral addition [3,4]. There have been worked up technologies of different contents. Among them is the technology, which envisages drying of zeolite before grinding it together with clinker using the heat of stack gasses of the clinker kiln [5]. If we create certain conditions in the drying process of zeolite by the stack gasses, zeolite might trap **CO_2, SOx, NOx** by adsorption and stack gasses will be cleaned from them.

EXPERIMENTAL

In pilot conditions an experiment was conducted, for which zeolite containing clinoptilolite of fraction 5-10 mm was prepared. For identifying adsorbed oxides **CO_2, SOx, NOx in** the mentioned zeolite method of infrared spectroscopy was used. Infrared spectra were taken in far infrared and middle infrared bands on spectrophotometer „Agilent Technologies Cary 630 FTIR".

Probes were taken from the grid, which was placed in the pipe of the stack gas on the 7th, 14th, 21st and 27th day of working of the zeolitic filter. In the drawing below are given infrared spectra of these samples and initial zeolites.

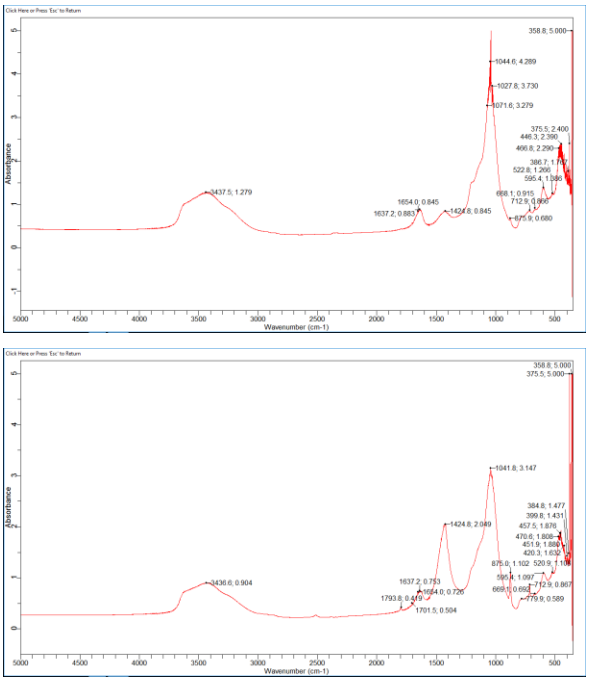

Drawing: Infrared spectra of aluminosilicate carcass of the taken probes from the initial (a) and zeolitic filters in far and middle infrared bands on the 28th (b) day of working.

As it is seen from the drawing the spectrum of the initial sample fully corresponds to the data given in literature [6,7], accordingly these are bands of tetrahedral deformational vibration inside aluminosilicate at 466 cm^{-1} and valence vibration at 1044.6 cm^{-1}, also bands of vibration between tetrahedrons accordingly are at 522.8, 595.4, 668.1, 712.9 cm^{-1}. Characteristic bands of natural minerals are: deformational of water at 1654.2 cm^{-1} and valence at 3437.5 cm^{-1} and vibration band of adsorbed carbon-ions at 1424.8 cm^{-1}. In infrared spectrum taken on the 7th day and especially on the 14th day the picture is changing –intensity of bands at 1424 cm^{-1} , 875 and 712 cm^{-1} , which correspond to CO_3^{-2}, NO_2^-, NO_3^-, SO_3^{-2} and SO_4^{-2}-ions accordingly [8,9]. Vibration frequencies of these ions are very close to each other and often their corresponding bands are overlapped. Also valence vibration band of Si-O-Si aluminosilicate at 1044 cm^{-1} coincides with vibration bands of SO_4^{-2} and NO_2^- ions [9], hence it is hard to fix absorbed ions exactly, though the general picture is clear. Intensity of bands of adsorbed ions in zeolitic filters from the clinker kiln is gradually increasing and reaches its maximum in the spectrum of the sample taken after the 28th day (drawing).

RESULTS

In the laboratory conditions we conducted adsorption of CO_2, N_2O and SO_2 separately on zeolites. Infrared spectra of these samples confirmed the results of the experiments performed in the pilot conditions.

In the laboratory and pilot conditions from adsorptive zeolitic tuff of **CO_2, SOx, NOx** oxides were prepared 6 samples, which in the amount of 20 mass% were mixed with cement composition. For the purpose of comparing the prepared 6 samples of "modified" cement there were prepared initial without additive **CEM I 52, 5** type and **20** mass% cements containing unmodified and modified zeolites. Testing was carried out by **EN 196** method, Results are represented in Table **1**.

Initial cement under study was serial "HeidelbergCement Georgia "of type **CEM I 52,5R**. It was mixed with 20mass% of initial natural zeolitic and adsorbed tuffs, by means of which it was turned into modified cement of **CEM II** type.

Mixing of the cement under study with **20** mass% zeolitic tuff is increasing water demand by 4.80%, slowing down the binding speed and is increasing cement strength (initial 2-7-day strength) by **0,50-2,30**%, also is increasing 28-day strength under binding by **10**% and decreasing 28-day strength under compaction by **4**%;

Mixing of the cement under study with **20** mass% **CO_2** adsorbed zeolitic tuff **is increasing its water demand only by 1%, is slowing down the binding**

speed, is increasing the cement strength under compaction by 7,60-14,80% and under bending by 32,80% at all stages;

Mixing of the cement under study with **20** mass% **SOx** adsorbed zeolitic tuff **is increasing its water demand only by 2,40%, is quickening the binding speed sharply, and is decreasing mechanical strength under bending/compaction by 26,50-38,50%;**

Table 1. Testing results of plain cements of CEM I 52, 5 type 20 mass% containing unmodified and modified zeolites

Cement composition, mass% +Plaster 5%		w/c, %	Physico-mechanical properties				
			Binding tems hr-min		Strength bending/compaction, mPa		
Zeolitic additive	Clinker		Start	Fin-ish	Day 2	Day 7	Day 28
Plaster	95	36.0	2-00	3-05	25.6	34.3	7.0 /54.8
Kl. (20%)	75	40.8	2-30	3-10	26.2	34.4	7.7 /52.6
Kl. (20%) +CO_2	75	37.0	2-40	3-40	29.4	39.4	9.3 /59.0
Kl. (20%) +SO_X	75	38.4	1-15	2-20	18.8	24.8	4.7 /33.7
Kl. (20%) +NO_X	75	38.4	3-00	4-10	32.0	43.2	8.2 /60.7
Kl. (20%) + (CO_2 +NO_X)	75	37.6	2-50	4-40	24.4	30.6	7.1 /47.8
Kl. (20%) + (CO_2 +SO_X)	75	38.4	1-00	2-35	29.6	35.2	6.2 /49.4
Kl. (20%) + (CO_2 +SO_X +NO_X)	75	42.0	1-35	2-40	28.0	27.6	8.1 /47.9

Mixing of the cement under study with **20** mass% **NOx is increasing its water demand only by 2,40%, is slowing down the binding time sharply at all stages, at all stages** –**most sharply by10,70-25,00 is increasing strength on compaction by 17,14% - strength on bending;**

Mixing of the cement under study with **20** mass% **CO_2+NOx** adsorbed zeolitic tuff, only by **1,60**% is increasing its water demand, is slowing down binding speed, by **12,70**%-is decreasing strength on compaction and by **1,40**% is increasing strength on bending;

Mixing of the cement under study with **20** mass% **CO_2+SOx** adsorbed zeolitic tuff, only by **2,40**% is increasing its water demand**, is increasing binding speed by 2 times, by 2,60-15,62**% is increasing the initial strength and by **9,80**% is decreasing **28-** day strength;

Mixing of the cement under study with **20** mass% **CO_2+SOx+NOx** adsorbed zeolitic tuff, is sharply increasing by **6% as its water demand, as well as binding capacity,by 9,37**% is increasing 2-day strength and **12,60**% is decreasing 28-day strength;

Cements of CEM II type containing zeolitic tuffs adsorbed with CO_2 and NOx are of the highest strength!

On all samples of studied cement was performed X-ray diffractometric analysis and we found that apart from the first sample all the other samples of cement alongside with Alite, Portlandite, Ettringite must contain mineral stratlingite **C_2ASH_8**, which is caused because of mixing and existing of zeolitic tuffs in cement;

№3 sample of cement unlike others contains calcium carbo aluminate **$C_3ACaCO_312H_2O$**, which can be caused by mixing in cement zeolitic tuff adsorbed with **CO_2**;

№5 unlike the rest of cement samples contains Calcium nitrate **Ca $(NO_3)_2$**, which might have been caused by mixing in cement zeolitic tuff adsorbed with **NOx.**

CONCLUSION

The performed work enables us to solve such global ecological problems as "thermal effect" and "acid rains" in the atmosphere by using zeolitic sorbents. Also by grinding such saturated sorbents and utilizing them as a mineral additive and further by zeolitic modifying of cement we can get cement-concrete of high strength

ACKNOWLEDGEMENT

The work was prepared with the support of the Ministry of Education and Science of Georgia and Shota Rustaveli National Science Foundation. Grant № AR 216800.

REFERENCES

[1] Schorcht F., Kourti I., Scalet B.M., Roudier S., Sancho L.D., JRC Reference Reports "Best Available Techniques (BAT) Reference Document for the Production of Cement, Lime and Magnesium Oxide", *Industrial Emissions Directive 2010/75/EU (Integrated Pollution Prevention and Control)*, 2013, pp.1-475.

[2] Tsintskaladze G., Skhvitaridze R., Keshelava V., Tsitsishvili V., Kordzakhia T., "Clinoptilolite Modified by Sulfur Oxides, as an Additive in Cements". *Georgian Engineering News (GEN)*, 2010, N2, v. 54, pp.109 – 111 (in Russian).

[3] Skhvitaridze R., Tsitsishvili V., Keshelava B., Tsintskaladze G. "The Use of Natural Zeolites of Georgia as Additives of

Building Materials", *Science and Technology*, 2014, N1, (715), pp. 98 – 102 (in Georgian).
[4] Skhvitaridze R., Giorgadze I., Verulava Sh., Shapakidze E., Gejadze I., Tsintskaladze G., Kordzakhia T. "Scientific Principles and Practice in the Use of Natural Mineral and Resources in the Georgian Cement Industry", *J."Cement International"*, 2018, v.16, #2, pp.50-57.
[5] Skhvitaridze R., Kordzakhia T., Tsintskaladze G., Giorgadze I., Verulava Sh., Skhvitaridze A., Kavtiashvili G. "Mode of Cement Producing". Georgia, Patent on invention **AP 2018 14402 A.** Inventors: published: Bulletin #9 (493), 05.10.2018
[6] Flanigen E., Khatami H., Szymanski H., "Infrared structural studies of zeolites frameworks. Molecular Sieve Zeolites", *Americ. Chem. Soc*, 1970, Table V, pp.460-488
[7] Tsitsishvili V., Tsintskaladze G., Charkviani M. "Effect of heat treatment on IR spectra of some synthetic and natural zeolites in the range of oscillation frequencies of a carcass". *Reports of Academy of Sciences of SSSR*, 1983, v.273, №6, pp.1434-1439.
[8] Nakamoto K., "Infrared Spectra of Nonorganic and Coordination Compounds", Publisher: Moscow Mir, 1966, 411p. (in Russian)
[9] Gordon A., Ford R., "Guide of Chemist", Publisher: Moscow, Mir, 1976, 541p. (in Russian).

ტექნოგენური აირებით გაჯერებული ბუნებრივი ცეოლითები სამშენებლო მასალების დანამატები

თეიმურაზ კორძახია[1]*, გიორგი წინწკალაძე[1], რაჟდენ სხვიტარიძე[2], ირაკლი გიორგაძე[2], მარინე ზაუტაშვილი[1]

[1] *ივ.ჯავახიშვილის თბილისის სახელმწიფო უნივერსიტეტი; პ.მელიქიშვილის ფიზიკური და ორგანული ქიმიის ინსტიტუტი (ა.პოლიტკოვსკაიას ქ.31, 0186, თბილისი, საქართველო)*
[2] *სამეცნიერო ცენტრი "ნანოდულაბი", საქართველოს ტექნიკური უნივერსიტეტი (კოსტავას ქ.77, 0160, თბილისი, საქართველო)*
**E-mail: teimuraz.kordzakhia@tsu.ge; +995591938185;*

რეზიუმე. საქართველოში ცემენტის წარმოების მოცულობის ზრდამ გაამწვავა გარემოსდაცვითი და ტექნიკური გლობალური პრობლემები. ევროკავშირთან ასოცირების ხელშეკრულებამ შექმნა ცემენტის ქართულ საწარმოებში გარემოსდაცვითი საუკეთესო ხელმისაწვდომი ტექნოლოგიების ათვისების აუცილებლობა.

ატმოსფეროში CO_2,SOx,NOx-ის ემისიის და შესაბამის გლობალურ პრობლემათა - „სითბური ეფექტის" და „მჟავური წვიმების" წარმოქმნის პრევენციის მიზნით შემოთავაზებულია ცემენტის კლინკერის ღუმლიდან გამომავალი ტექნოგენური ოქსიდების ცეოლითებით სორბციული დაჭერა - დასუფთავების და შემდგომში ამ გაჯერებული სორბენტების დაფქვით და მინერალურ დანამატად უტილიზაციით ცემენტის ცეოლითური მოდიფიცირებით ინოვაციური BAT ნანოტექნოლოგიური მეთოდები.

კვლევის ფიზიკურ-ქიმიური (ქრომატოგრაფია, ი.წ.სპექტროსკოპია, რენტგენულდიფრაქტომეტრული ანალიზი) მეთოდებით იდენტიფიცირებული და შესწავლილია ნახევრადსაწარმოო პირობებში ცეოლითური ადსორბენტებით CO_2,SOx,NOx აირების დაკავების მექანიზმი. ასევე დადგენილია შესწავლილი ცემენტის ნიმუშებში ამ აირებით გაჯერებული ცეოლითური დანამატების შეტანის შედეგად მიღებულ მასალაში სორბირებული აირების არსებობა.

STUDY OF POLYCYCLOALKANE HYDROCARBONS IN GEORGIAN PETROLEUM

Natela Khetsuriani*, Elza Topuria, Vladimer Tsitsishvili, Madlena Chkhaidze

TSU, Petre Melikishvili Institute of Physical and Organic Chemistry, 31 Politkovskaia, 0186, Tbilisi, Georgia
*E-mail: natixeco@yahoo.com

Abstract: Polycykloalkane Concentrates isolated from saturated hydrocarbons of the 200-350ºC fractions of Taribani Petroleum (Georgia) were studied by GC-MS. The concentrate preparation included the following steps of treatment of a crude oil: (a) distillation, (b) de-aromatization by liquid adsorption chromatography on silica gel, (c) Three-stage thermo-diffusion separation of iso-alkanes and cycloalkanes, and (d) thiourea adduct formation with cyclanes. In this presentation, a composition of one out of ten thermodiffusion fractions obtained will be discussed. The GC separation was achieved on a 200 m capillary column with Dimethylpolysiloxane with the use of the following temperature parameters: 40ºC at 2ºC/min to 280ºC (hold 70 min). Automated mass deconvolution and identification system (AMDIS) was used for data analysis; manual extraction of spectra was applied to insufficiently separated components. Complex study of mass spectral data and evaluation of gas chromatography retention index values led to the differentiation of isomers.
The relict compounds isoprenoids, polymethyl derivatives of decalines and also a series of adamantan derivatives, including the 2-n-buttile, 2-propyl and 1- methyl, 3-propyladamantanes that were identified in the petroleum for the first time.

Keywords: oil, saturated hydrocarbons, cycloalkanes, alkyladavantanes, thermo-difuzion, thiorea adduct formation, CG-MS metod, AMDIS.

INTRODUCTION

Georgian petroleum deposits are known from the ancient times. There are more than 1500 manifestations of oil and gas deposits. According to quantitative estimates of oil and gas resources (2002) it was determined that geological resource of oil in Georgia makes up to 850 million tons, including 400 million tons in the black sea shelf and the other 450 million tons on the land. Anticipated resource of gas is estimated up to 180 billion m^3 only on the land. As a result 1 gas, 1 gas (5.3 trillion cubic meters) and oil and 16 oilfields were discovered.

Regular studies of oils began in Georgia in the first half of the 20th century when the oil chemistry laboratory (1948) was established and these studies are being continued up to date. It was established that all known types of oils in Georgia were available. As an object of research the Taribani oil rich with paraffin hydrocarbons was selected. The Taribani oil was one of the long-known oils of the Red Wells, which were studied by the first researchers of Caucasian oils at the end of the 19th century. The oilfield is located in the southeast of Georgia, on the Shiraki Valley (Kakheti, the 12th licensed block). Taribani oil belongs to the tertiary period of formation, has different depth of bedding and age of the surrounding rocks. The oil sample was taken from the well # 23 at a depth of 2 345–2 374 m from the deposits of the upper Sarmat of the Eldar measure. This oil is paraffinic by nature (7%), although like all other Georgian oils, it contains a considerable amount of isoprenoid structures. The content of light fractions (55-200°C) makes up to 30%, sulfur – 0.2%, resins – 8.5%, asphaltenes – 6.2% [1].

The investigation was carried out by studying concentrates obtained from 200-350°C fraction of Taribani paraffinic oil.

EXPERIMENTAL

For preparation of concentrates from the oil the following stages of crude oil processing were used: distillation, dearomatization with silica gel, three-stage thermodiffusion separation of isoalkanes from cycloalkanes, and extraction of cycloalkanes from the obtained fractions with thiocarbamide. Ten thermodiffusion fractions were previously obtained from which the composition of mixture of the IX+X fractions was studied with the GC-MS method. IX+X factions were combined because of their similar group composition [2].

The combined fraction (IX+X) is concentrate of bridge structure polycycloalkanes of C_{10}-C_{16} composition. The results of study of this concentrate are presented in the previous works [3, 4].

In the present work the results of investigation of the composition of the VIII thermodiffusion fraction and extract obtained from this fraction with the help of thiocarbamide are reviewed. The GC-MS study had been performed in the GC-MS magnetic sector of mass spectrometer working in standard conditions [5]. Separation of concentrates was achieved by method of gas chromatography on 200 m GC capillary column with dimethylpolysiloxane in the programmed temperature conditions (from 40°C to 280°C at a speed of 2°C/min during 70 min). The appropriate chromatograms are given in Figures 1-4. The results of the analysis were obtained using automatic deconvolution and identification system (AMDIS) [6-10]. In case of poorly divided components the mass-spectra were processed manually. Complex study of MS data and GC retention indices made it possible to divide isomers in concentrates, which in itself is a great difficulty in the process of identification of compounds. The main components of the VIII thermodiffusion fraction, as it was expected, were **C_{11}-C_{22} isoprenoid alkanes**. Among them the predominant were **pristane C_{19}** and the **phytane C_{20}**, the well-known biomarkers of oil. **Cyclopentanes, cyclohexanes and decalines** were characterized by high intensity as well.

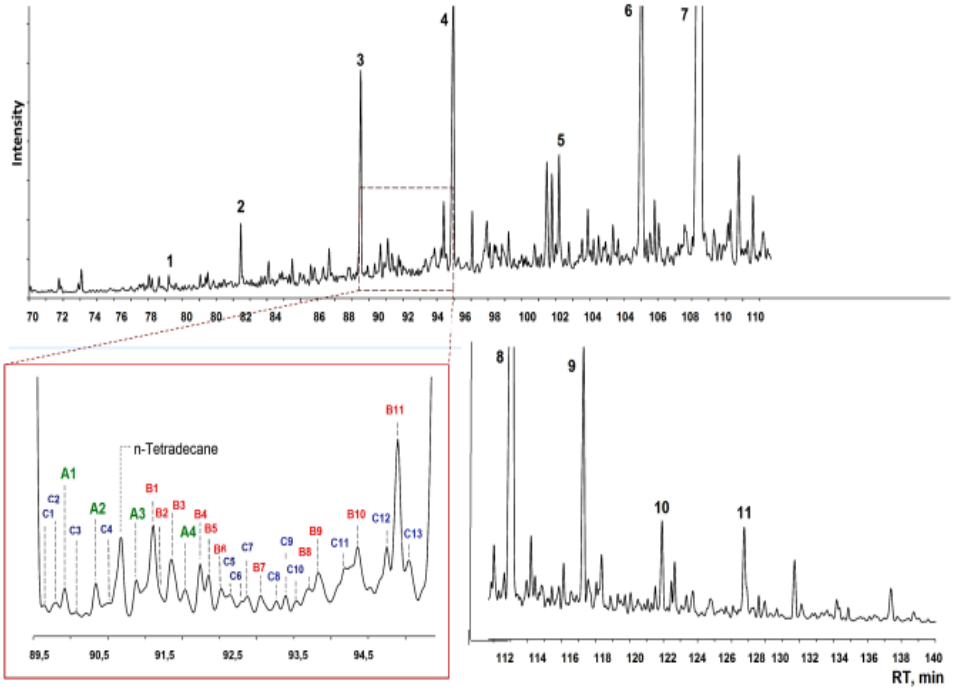

Figure 1. GC of concentrate VIII obtained after thermal diffusion: Isoprenoides: 1-Undecane 2,6-dimethyl-(C13); 2Dodecane 2,6-dimethyl-(C14); 3-Dodecane, 2,6,10-trimethyl-(C15); 4-Tridecane 2,6,9trimethyl-(C16); 5–Tetredecane 2,6,10-trimethyl-(C17); 6 – Pentadecane 2,6,10-trimethyl-(C18); 7 – Pristan-(C19); 8 - Pristan-(C20); 9 -Heptadecane 2,6,10,15-tetramethyl-(C21); 10 – Octadecane 2,6,10,15-tetramethyl-(C22); 11 – Nonadecane 2,6,10,15-tetramethyl-(C23).

Chromatogram of the VIII fraction is presented on Figure 1; the identified compounds are listed in Table 1. A segment of chromatogram (89-95, RT, min) of the VIII fraction is presented on Figure 3 and a list of compounds found in this segment is presented in Table 1.

Table 1. List of compounds found in this segment is presented(89 – 95RT, min)

A1	**3-methylhexyl-methylcyclopentane**
A2	**1,5-dimethylhexyl-methylcyclopentane**
A3	**3-methylhexyl-dimethylcyclopentane**
A4	**3-methylheptyl-methylcyclopentane**
B11	**n-octylcyclohexane**
B1, B3, B5, B8, B10	**cyclohexanes with C_9 substituents**
B2, B4, B5, B7, B9	**cyclohexanes with C_8 substituents**
C1-C9	**decalines with 4 C-atoms**
C10 – C11, C13	**decalines with C_4 substituents**
C12	**1-n-butyldecaline.**

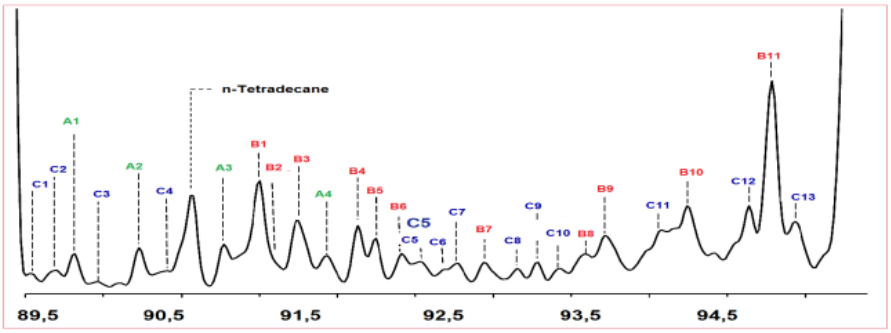

Figure 2. A segment of chromatogram (89-95, RT, min) of the VIII fraction

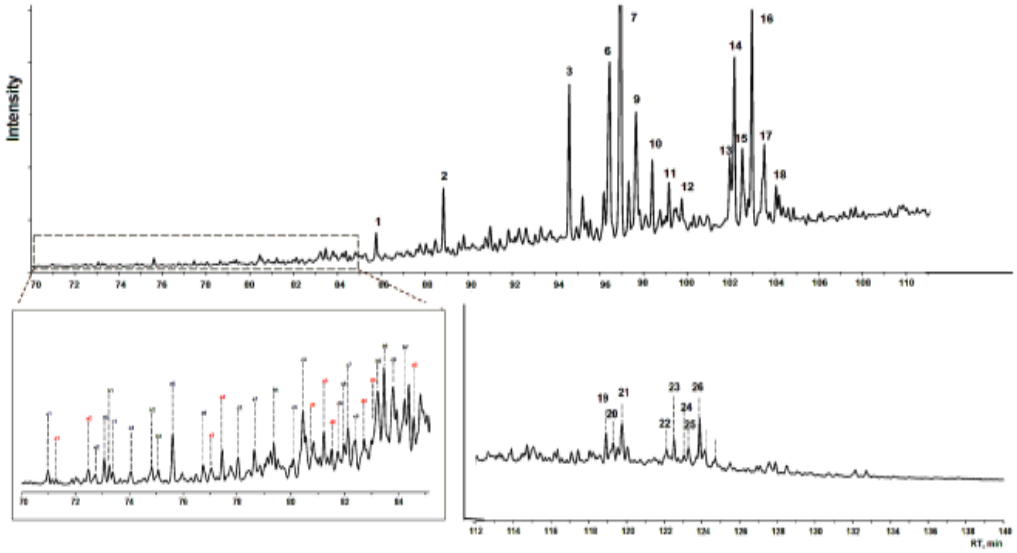

Figure 3. Chromatogram of extract obtained alter thiorena adduct formation in the VIII fraction
1-Bicycloalkane(C13); 2- Bicycloalkane(C14); 3,4,6,11, 13,15- Bicycloalkane(C15); 5,12,14,16,17 - Bicycloalkane(C16); 18 - Bicycloalkane(C17); 19-20 – Bicycloalkane (C20); 23,24,28 – Tricycloalkane (C19); 25-27 - Bicycloalkane(C21).

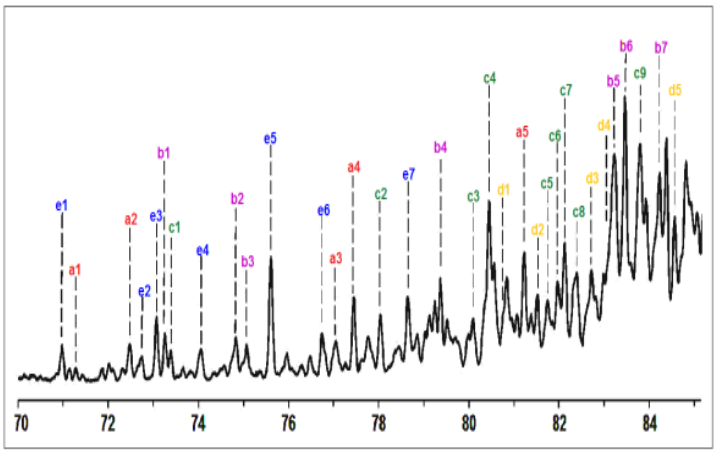

Figure 4. A segment of chromatogram (70 - 85, RT, min) of thiocarbamide extract

Separation of isoalkanes and cycloalkanes present in the thermodiffusion fraction was successfully carried out by formation of inclusion complex (adduct) of thiocarbamide with cycloalkanes and their extraction [11]. Because in chosen conditions the ability to give inclusion complex had only cycloalkanes [7] there were no n-alkanes in the obtained concentrate (extract). It contained **bicyclo**-and **tricyclo alkanes** which were separated on the 200 mm capillary column with dimethylpolysiloxane and the appropriate chromatogram was obtained (Figure 3). The list of compounds detected in the extract is presented in Table 2.

Table 2. List of hydrocarbons identified in this segment(70 – 85 RT, min)

a1	**3-Methyladamantane**
a2	**1,4-Dimethyladamantane**
a3	**1,2-Dimethyladamantane**
a4	**1,3-Dimethyladamantane**
a5	**2-Ethyladamantane**
d1	**1,3,5,6-Tetramethyladamantane**
d2	**1-Methyl-3-propyladamantane**
d3	**1,3-Diethyladamantane**
d4	**2-n-Butyladamantane**
d5	**1-n-Butyladamantane**
b1	**Tricyclo[4.3.1.1^{3,8}]undecane**
b2	**Tricyclo[6.3.0.0^{1,5}]undecane**
b3	**Tricyclo[6.2.1.0^{2,6}]undecane**
b4	**Tricyclo[5.2.2.0^{2,6}]undecane**
b5	**Tricyclo[7.3.0.0^{2,6}]dodecane,**
b6	**Tricyclo[7.2.1.0^{1,6}]dodecane**
b7	**Tricyclo[6.3.1.0^{4,12}]dodecane**
e1–e5	**Methyldecalines**
e6–e7	**Ethyldecalines**
c1	**1,3,4-Trimethyladamantane**
c2	**1,3,5-Trimethyladamantane**
c3	**1,3,4-Triethyladamantane**
c4	**1-Ethyl-2-methyladamantane**
c5	**Tricyclo[7.3.1.0^{5,13}]tridecane**
c6	**1-n-Propyladamantane**
c7	**1-Methyl-3-ethyladamantane**
c8	**2-Methyl-1-ethyladamantane**
c9	**2-n-Propyladamantane**

A segment of chromatogram (70-85, RT, min) of the extract is presented on Figure 6, and a list of hydrocarbons identified in this segment is presented in Table 2.

Among bicycloalkanes the content of the relict-type structures – the **long-chain derivative of perhydroindan – 1-(2-methyl, hexyl) perhydroin dan and polymethyl derivatives of decalin** – were determined [12]. In the same concentrate were determined protoadamantanes (the adamantanes predecessor compounds in petroleum) – **tricycloundecanes** (C_{11}), **homoadamantane** – tricyclo [4,3,1,1^{3,8})undecane having a seven-member cycle in its structure, **tricyclododecanes** (C_{12}) and **perhydrophenalene –** tricyclo [7,3,1,0^{5,13}]tridecane (C_{13}). The structures of **tricycloalkanes** with compact structures – polyedranes found in the extract are of particular interest. An efficient separation of these compounds became possible on the above mentioned 200 m capillary column. Typical structures and corresponding mass-spectra are presented on Figure 5-6. 18 hydrocarbons containing adamantan skeleton, including **dimethyl-, trimethyl-, tetramethyl-, ethyl-, methyl-ethyl-, diethyl-, propyl, methyl-propyl adamantanes,** were identified. It is noteworthy that **1-n-propyladamantane** and **n-buthyladamantane** were discovered in Taribani oil for the first time. On the spectrum (Figure 6) can be seen main peaks of a fairly large molecular ion radical ($C_4H_9^+$) and adamantil-cation (m/z 135)$^+$ [13].

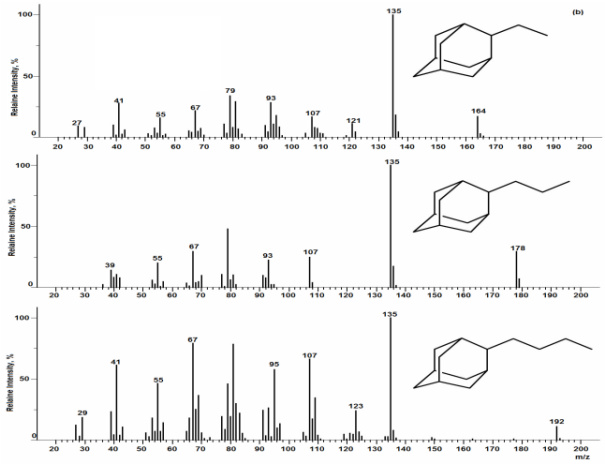

Figure 5. Mass spectra of (b) 2-Ethyl-(peak *a5*), 2-Propyl- (*peak c9*) and 2-Butyladamantanes (*peak d4*);

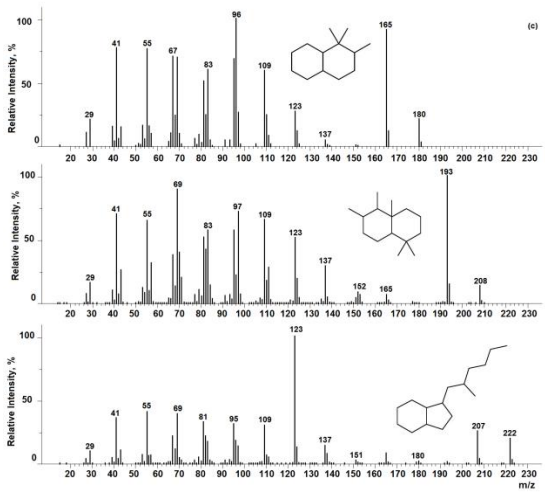

Figure 6. Mass spectra of (c) 1,1,2-Trimethyldecaline (*peak 1*), 1,2,3,7,7-Pentamethyldecaline (*peak 7*) and 1-(2-Methylhexyl)perhydroindane (*peak 16*).

The following way of fragmentation is similar to the spectra of adamantan monoalkyl derivatives. Experimental chromatographic retention time also corresponds to the estimated value of **2-n-buthyladamantane**. In the said concentrate was also established the presence of 1-n-propyl and of the **2-n-propyladamantane** and **1-methyl, 3-propyladamantane** for the first time.

CONCLUSION

Alkyladamantanes with substitute larger than ethyl radical were not found in petroleum prior to our investigation. This could be explained by their formation from tricyclic condenced hydrocarbons by isomerization when entering into contact with aluminosilicate rocks. It was considered that as in such conditions the higher derivatives of adamantane were not formed they could not be present in oils. But 1-n-, 2-n-propyl-, 1-methyl-3-propyl- and 2-n-buthyladamantanes were detected in Taribani oil.
The presence of these adamantine derivatives is difficult to explain because their probable predecessors were not detected in petroleum, or it can be proposed that they are products of destruction of higher molecular weight petroleum compound containing adamantine nucleus.

ACKNOWLEDGEMENT

The study was conducted at the department of spectrometric investigations of the USA Institute of Standards and Technology. We express our thanks to Anzor Mikaia, Carlos Gonzalez and the entire working group for carrying out this interesting work.

REFERENCES

[1] Topuria E.N., Usharauli E.A., Kortava L.M., Mchedlishvili I.J. Chemical typification of Taribani and Satskhenisi oils. Georg. Eng. News, 2003, No. 2, pp.175-180.
[2] Patent NU 1598 (ID # 11168/02), 29.09.2014.
[3] E.Topuria, E.Lekveishvili, N.Khetsuriani, I.Edilashvili. (2007) Investigation of Hydrocarbon - type content of middle and high-boiling fractions of Georgian oils by mass- and chromato-mass-spectrometry methods. Mass-spectrometry, volume 4, #3, pp. 197–226.
[4] Topuria E.N., Khetsuriani N.T.,(2011). Chromato-mass-spectrometric investigation of polycycloalkanes of middle fractions of Georgian oils.. IX International mass-spectrometric conference in petrochemistry, ecology and food chemistry - "Petromass" / Moscow, p.143-151.
[5] Elza N. Topuria, Natela T. Khetsuriani, Kirill V. Tretyakov, Carlos A. Gonzalez, Anzor I. Mikaia. (2013). GC- MS Study of the Composition of Saturated Hydrocarbons in High-Boiling Fractions of Georgian Oils. Eastern Analytical Symposium, Gaithersburg,USA, p.97.
[6] N.Khetsuriani, V.Tsitsishvili, E. Topuria, A.Mikaia.(2017). Study of Policiclic Aromatic Hydrocarbons of Norio Oil by GC-MS Method. Bulletin of The Georgian Academy if Sciences, vol.11, no.1, 2017, p.52-57.
[7] Nino Todua, Natela T. Khetsuriani, Elza N. Topuria, Levan A. Megutnishvili, Aleksey V. Mayorov, Anzor I. Mikaia. (2015). Pretreatment of oil samples for GCMS analysis of polycyclic aromatic Hydrocarbons and their hetero-analogs. 63rd Conference of Mass-spectrometry and Allied topics. St. Louis, Missouri, May 31-June 4.Journal of the American Society for Mass-spectrometry, vol. 26, suppl.1, p.83.
[8] S.M. Pyle et.al. (1997). J. Amer. Soc. Mass Spectrom. **7**: 183-190.
[9] Alford J.B., Peterson M.S., Green Ch.C. (2014). Impacts of Oil Spill Disasters on Marine Habitats and Fisheries in North America. CRC Press, 340 p.
[10] R.P.Rodgers, et.al. (2011). Anal. Chemistry. **83**: 4665-4687.
[11] V.Tsitsishvili, E.Topuria, N.Khetsuriani, M.Chkhaidze(2018). Policycloalkane Hydrocarbons in Taribani oil. **XI International Mass Spectrometry Conference on Petrochemistry, Environmental and Food Chemistry (Petromass 2018). Bled, Slovenia April, 15-18, p.7.**
[12] V.Tsitsishvili, E.Topuria, N.Khetsuriani, M.Chkhaidze (2018). Polycycloalkane Hydrocarbons in Taribani oil. **XI International Mass Spectrometry Conference on Petrochemistry, Environmental and Food Chemistry (Petromass 2018). Bled, Slovenia April, 15-18, p.7.**
[13] N.Khetsuriani, Elza Topuria, M.Chkhaidze, V.Tsitsishvili. Polycycloalcane hydrocarbons in Taribani oil. World Science, #9 (37), September 2018, pp.33-41.

პოლიციკლოალკანური ნახშირწყალბადების შესწავლა საქართველოს ნავთობებში

ნათელა ხეცურიანი*, ელზა თოფურია, ვლადიმერ ციციშვილი, მადლენა ჩხაიძე
თსუ, პეტრე მელიქიშვილის ფიზიკური და ორგანული ქიმიის ინსტიტუტი,
0186, თბილისი, პოლიტკოვსკაიას ქ#31
E-mail: natixeco@yahoo.com

რეზიუმე.
ტარიბანის ნავთობის 200-350°C ფრაქციიდან გამოყოფილი პოლიციკლოალკანების კონცენტრატი შესწავლილია ქრომატო-მას-სპექტრომეტრული მეთოდით. კვლევა განხორციელდა ნავთობების კვლევის კომპლექსური სქემის მიხედვით. წარმოდგენილ ნაშრომში განხილულია თერმოდიფუზიური დაყოფის მესამე საფეხურის VIII ფრაქციის ქიმიური შემადგენლობის შესწავლის შედეგები. აირ-თხევადი კაპილარული ქრომატოგრაფიის პროგრამირებული ტემპერატურის პირობებში მიღწეულია საკვლევი ფრაქციის ნახშირწყალბადების დაყოფა. მონაცემთა ანალიზისთვის გამოყენებული იყო ავტომატური მას-დეკონვოლუციისა და იდენტიფიკაციის სისტემა. ტარიბანის ნავთობში როგორც ყველა სხვა ქართულ ნავთობებში, იდენტიფიცირებულია რელიქტური იზოპრენოიდების (მათ შორის უმეტესწილად პრისტანის და ფიტანის), პოლიმეთილჩანაცვლე-ბული დეკალინების და ადამანტანის რიგის 18 ნახშირწყალბადი.
საკვლევ ნავთობში დეკალინებიდან აღსანიშნავია პერჰიდროინდანის გრძელჯაჭვიანი წარმოებულის, პროტოადამანტანებიდან – ჰომოადამანტანის და პერჰიდროფენანტრენის შემცველობის დადგენა. ადამანტანებიდან საგულისხმოა 1-ნ-პროპილადამანტანის, 2-ნ-პროპილადამანტანის, 2-ბუთილ-ადამანტანის, 1-მეთილ, 3-პროპილადამანტანების იდენტიფიცირება. ადამანტანის ამ წარმოებულების არსებობა პირველად იყო დადგენილი ნავთობში. სავარაუდოდ ნავთობში მათი არსებობა წარმოადგენს ადამანტანის ბირთვის შემცველი მაღალმოლეკულური ნაერთების დესტრუქციის შედეგად წარმოქმნილ სტრუქტურებს.

TAR-ASPHALTENIC COMPOUNDS OF GEORGIAN PETROLEUM

Natela Khetsuriani*, Esma Usharauli, Keto Goderdzishvili, Irina Mchedlishvili, Tamar Shatakishvili, Maka Kopaleishvili

TSU, Petre Melikishvili Institute of Physical and Organic Chemistry, 31 Politkovskaia, 0186, Tbilisi, Georgia
*E-mail: natixeco@yahoo.com

Abstract. When studying high-boiling compounds of oils characterized by an extremely complex composition and a large variety of molecules in them, methods for detection and identification of polycyclic condensed aromatic systems which are known to be a main structural blocks of tar-asphaltenic compounds are of certain interest. To study these systems of tar-asphaltenic compounds of oils we used a hydropyrolytic method of hydrocarbon fragmentation. In this paper are presented the results of GLC and mass spectrometric study of the products of hydropyrolysis of tars and asphaltenes from Norio (aromatic), Samgori (paraffinic) and Supsa (tarry) oils of Georgia having various chemical nature. Investigation of hydrocarbon composition of hydropyrolysates of tars and asphaltenes shows that they all contain the same aromatic structures. In these oils the structures of naphthalene, fluorene, diphenyl, phenanthrene, pyrene, chrysene, perylenes and their derivatives were identified.

Keywords: pertoleum, tars, asphaltenes, biomarkers, microelements

INTRODUCTION

Tar-asphaltenic compounds are a complex mixture of high-molecular weight substances with dark color present in crude oils and oil products in a dissolved state or in the form of colloidal systems. Their content in oils varies in very broad ranges – from a few tenths of a percent to tens of percent. All sulfurous and high sulfurous oils are highly tarry with a high content of asphaltenes as well. Tar-asphaltenic substances include tars, asphaltenes, carbenes, carboids, asphaltogenic acids and their anhydrides.

Tars and asphaltenes are high molecular weight heteroatomic complex compounds of petroleum. Their content in petroleum can reach up to 25-50% by weight. The role of tars and asphaltenes in all processes from extraction to refining of petroleum is extremely high.

The term “Asphaltenes” appeared in 1937 when Boussingault defined them as a distillation residue of bitumen: insoluble in alcohol and soluble in turpentine (Boussingault, 1937). Today, asphaltenes are defined as the heaviest components of petroleum fluids that are insoluble in light n-alkanes such as n-pentane (nC5) or n-heptane (nC7) but soluble in aromatics such as toluene. These polydisperse molecules consist mostly of polynuclear aromatics (PNA) with different proportions of aliphatic and alicyclic moieties and small amounts of heteroatoms (such as oxygen, nitrogen, sulfur) and heavy metals (such as vanadium and nickel, which occur in porphyrin structures). Heavy tars and waxes can co-precipitate with asphaltenes and their amount is variable depending on the method of separation. Asphaltenes and tars isolated from a crude oil according to ASTM-D2007 are shown. They differ in color and texture. Asphaltenes are black, shiny, and friable solids; while tars are dark brown, shiny, and gummy [1-2].

The high-boiling aromatic hydrocarbons of petroleum are complex hybrid compounds, in which along with the aromatic structures there are four-, five- and six-membered cycloalkane rings and a large number of different alkyl substituents. This makes it difficult to study the above hydrocarbons and prevents detection of their individual chemical structures.

While the composition and properties of tar-asphaltenic substances have been studied in some detail, the structure of their molecules has not been fully investigated. However, according to the generally accepted opinion, the main structural blocks of molecules of tars and asphaltenes are polycyclic, predominantly aromatic, condensed systems [3-4].

It is noteworthy that in the study of complex organic compounds like steroids and other ones the method of thermal degradation proved to be quite successful in determining their basic structural elements [5]. We investigated the possibility of using thermal destruction methods to identify and determine

aromatic fragments of high-boiling compounds of petroleum. An autoclave hydropyrolytic method of hydrocarbon fragmentation was elaborated. Development of the method and a choice of the hydropyrolysis regimen were carried out on the basis of the study of hydropyrolysates of a number of individual polycycloaromatic hydrocarbons with various structures [6].

Material and methods.

All used chemicals were of analytical grade. AFP silica gel (activated Fine-Porous silica gel) – Manufacturer: Labstatus Ltd, (Ukraine); Petroleum ether (Sigma-Aldrich International GmbH; Germany); Dioxsane (Sigma-Aldrich International GmbH; Germany); Benzene (Garlo Erba; Germany); n-Heptane (Sigma-Aldrich International GmbH; Germany); Methods of GLC and mass spectrometry; standard method for isolation of asphaltenes from petroleum with n-heptane [11]. Reference standards: fenantrens, pyrenes, chrysenes, perylenes (Sigma-Aldrich International GmbH, Germany);

To study these systems of tar-asphaltenic compounds of oils we used a hydropyrolytic method of hydrocarbon fragmentation. In this paper are presented the results of GLC and mass spectrometric study of the products of hydropyrolysis of tars and asphaltenes from Norio (aromatic), Samgori (paraffinic) and Supsa (tarry) oils of Georgia having various chemical nature, differing significantly in their physical and chemical properties. Physical and chemical characteristics of these oils – in Table 1.

Table 1. Physical and chemical characteristics of Georgian Petroleum

Characteristics	Oilfield		
	Norio	Samgori	Supsa
Depth of bedding, m	1400	2830	3350
Density at 20^{0C}, kg/m^3	900.0	837.0	943.0
Viscosity at 20^{0C}, sS	19.0	3.0	22.0
Cloud Point,^{0}C	-45.0	3.0	15.0
Flash Point,^{0}C	15.0	-10.0	40.0
Content in mass, %			
Sulfur	0.23	0.17	0.42
Tar	8.58	7.0	14.4
Asphaltenes	1.22	0.95	4.19
Paraffin	0.82	6.8	3.1
Cocking ability	3.93	1.0	10.7
Ash content	0.011	0.018	0.043
Yield of fractions in mass, %			
Up to 200^{0}C	22.7	30.0	13.42
Up to 350^{0}C	48.5	65.7	40.9

Hydropyrolysis was carried out at temperature of 450 ^{O}C, hydrogen pressure - 7 MPa and duration of the process – 4 hours. Hydropyrolysates were extracted with dioxane. Hydropyrolysates of tars and asphaltenes were analyzed by gas-liquid chromatography (GLC) and mass spectrometry. GLC analysis of hydropyrolysates of tars and asphaltenes showed that they are almost identical by composition, contain the same aromatic structures, and differ from each other only in terms of the quantitative ratio of these structures. The structures of naphthalene, fluorene, diphenyl, phenanthrene, pyrene, chrysene and their derivatives were identified. The group composition of hydrocarbons in the hydropyrolysates of tars and asphaltenes of oils under investigation is shown in Table 2. The concentration value is normalized to the sum of the concentrations of these compounds. Examination of the data of mass-spectrometric analysis shows that on the mass-spectra clearly distinguished groups of peaks of characteristic ions of polycyclic aromatic hydrocarbons can be observed.

Table 2. Group composition of hydropyrolysates of tars and asphaltenes of Georgian Petroleum

Types of hydrocarbons	Source compounds and composition of the appropriate hydropyrolisates, % *mass*					
	Norio		Samgori		Supsa	
	Tar	Asp.	Tar	Asp	Tar	Asp.
Naphthalenes	4,3	4,2	3,7	3,5	4,3	4,4
Biphenyles	1,8	1,7	1,5	1,4	1,5	1,6
Dihydrofluo-renes	3,2	3,7	4,5	3,8	6,7	3,2
Fluorenes	2,2	2,0	1,8	1,7	2,2	2,3
Phenanthrenes	7,9	7,8	4,3	4,0	7,6	7,7
Dihydropyrene	13,7	10,7	7,0	9,0	10,1	11,0
Pyrenes	11,9	15,1	8,0	13,5	13,0	15,0
Chrysenes	13,2	13,1	11,3	13,0	12,0	12,8
Dihydropery-lenes	7,8	7,7	8,0	11,0	8,9	9,0
Perylenes	7,8	9,0	13,0	12,2	9,9	10,4
Benzchrysenes	4,2	3,7	5,6	5,2	3,8	3,0
Anthracenes	2,1	2,6	6,7	4,5	3,0	2,4
Dihydrobenz-pyrenes	3,3	2,8	2,4	2,6	2,5	2,6
Benzperylenes	2,1	1,5	2,4	2,2	1,3	1,6
Dihydrobenzpe-rylenes	1,3	1,1	1,4	1,2	0,9	0,9
Phenanthro-phenanthrenes	1,0	1,1	2,2	1,5	0,9	1,4
Phenanthryl-phenanthrenes	0,3	0,6	0,4	0,7	0,8	1,2
Dibenzperylene	1,0	0,5	0,9	0,4	0,3	0,5

Mass spectrometric analysis of hydropyrolysates of samples under investigation shows that they all contain the same structures. Naphthalenes, biphenyls, fluorenes, phenanthrenes, pyrenes, chrysenes, perilenes, benzchryzenes, benzperylenes are identified. A high content of phenantrenes, pyrenes, chrysenes and perylenes, and as well of aromatic structures with a large number of rings in the condensed system should be noted.

The data presented in Table 2 show that the qualitative composition of the hydropyrolysates of all investigated tars and asphaltenes is the same. The structures of naphthalene, phenanthrene, pyrene, and chrysene have been identified in them in considerable amounts, which is quite similar to the results of GLC analysis of hydropyolysates (Fig. 3). However,

according to the mass spectrometry data aromatic structures with a large number of rings in the condensed system (perylene, benzphenanthrene, etc.) are also found in hydropyrolysates.

The characteristic groups of peaks of molecular and fission-fragment ions, as well as the presence of intensive peaks of double charged ions, confirm the highly condensed aromatic nature of these compounds and allow to determine their molecular masses and the degree of hydrogen unsaturation. However, the exact nature of cycles binding in the condensed system, the place of attachment of substituents cannot be determined by mass spectra and are selected from a number of possible structures, as the most probable [7-9].

Mass spectrometric analysis showed that in the hydropyolysates among the aromatic hydrocarbons there predominate unsubstituted and methyl-substituted structures, the complete dealkylation of which seemingly did not occur during hydropyrolysis. This is evidenced by the distribution of the molecular masses presented in Table 2 and the character of distribution of the intensities of the peaks of the characteristic fission-fragment ions. The high probability of (MH)+ and (M-CH3)+ processes established by the nature of these distributions, indicates the polymethylsubstituted structure of these compounds. Probable structures of polycyclic aromatic hydrocarbons identified in hydropyolysates of tars and asphaltenes are shown on Table 3.

Table 3. Probable structures of polycyclic aromatic hydrocarbons identified in tars and asphaltenes

Phenanthrene	Pyrene	Chrysene	Perylene	Anthracenes	Benzperylenes - I
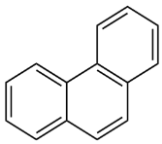	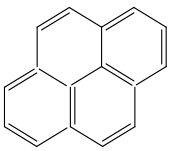	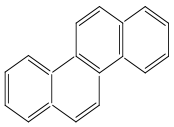	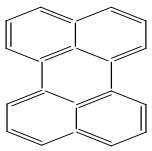	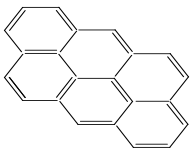	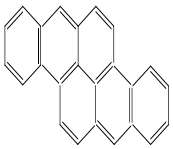
Benzchrysenes	Dihydroperylenes – I	Dihydroperylenes	Benzperylenes – II	Dibenzperylenes	Chrysene
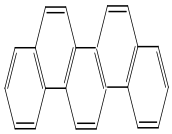	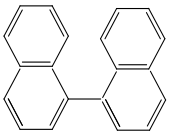	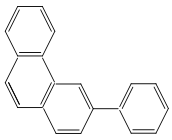	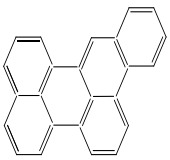	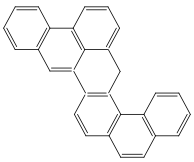	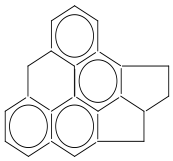

Thus, data obtained from the mass spectrometric study of hydropyolysates of tars and asphaltenes of Norio, Samgori and Supsa crude oils, together with confirmation of the GLC analysis results gives more capacious information on the composition of the substances under investigation. The content of aromatic structures with a large number of rings in the condensed system (perylenes, benzpyrenes, antantrenes) is found in them along with naphthalene, phenanthrene, pyrene, chrysene, etc.

Hydrocarbon composition by GLC and mass spectra of hydropyolysates of tars and asphaltenes of Norio, Samgori and Supsa crude oils shows that they all contain the same aromatic structures. Significant amounts of phenanthrenes, pyrenes, chrysenes, perylenes and their alkyl- and naphthene derivatives are identified in them. The content of aromatic structures with a large number of rings in the condensed system is also quite big, although their largest part consists of compounds with the degree of hydrogen unsaturation according to the formula C_nH_{2n+x}, where $x \leq 30$.

To determine the geological age of the crude oils under investigation the content of microelements was studied [10]. The content of microelements in ash residues were studied by methods of photochemical oxidation and spectrometry. The ratio V/Ni <1 shows that these oils belong to tertiary types of oils, which can be explained by conditions of accumulation of the initial organic matter and the corresponding geochemical origin.

Biomarkers of Georgian (Samgory, Norio and Supsa) oils are presented on the Figure:

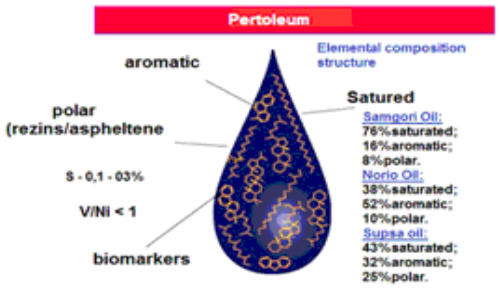

Conclusions.

- It is determined that tars and asphaltenes from Norio, Samgori and Supsa crude oils contain the same aromatic structures.
- Naphthalenes, biphenyls, fluorenes, phenanthrenes, pyrenes, chrysenes, perilenes, benzchryzenes, benzperylenes are identified.
- Distribution of microelements in oils is studied. It is found that these oils are tertiary types of oils (V/Ni <1).
- Biomarkers of Norio, Samgori and Supsa oils are determined.

REFERENCES

[1] Gousl.L. & Firoozadabi.A.(2002).Measuring Asphaltenes and Resins, and Dipole Moment in Petroleum Fluids, AiChE Journal, vol.48, #11, pp.2646-2663.

[2] James G.Speght. (2014) The Chemistry and Technology of Petroleum, 934p.

[3] Sergienko S.R. , Taimova B.A., EI Talalaev(1979) High-Molecular-Weight Compounds of Crude Oil, Nauka, Moscow. 412p.

[4] Pokonova U.V. - LGU, 1980) Chemistry of High-Molecular Oil Compounds, Leningrad, 170p.

[5] Jan Ake A., Lisboa B.P., Sjöpvall J.(1968). Studies on the Metabolism of C19 - Steroids in Rat Liver: 3. Isolation and Biosynthesis of 5α - Androstanetriols in Rat Liver Microsomes. European Journal of Biochemistry, 6(2), c. 317-324.

[6] Usharauli E.A., Melikadze L.D., Kortava L.M., Kogan L.O., Brodskii E.S. (1987). Hydropyrolytic determination of aromatic fragments of high boiling compounds of oils. Neftechimia. v. XXVII, # 4, p. 481-488.

[7] Brodskii, E.S., Lukashenko, I.M., Kalinkevich, G.A., Savchuk, S.A., "Identification of petroleum products in environmental samples using gas chromatography and gas chromatography–mass spectrometry", J. Anal. Chem. 57(6), 486 (2002).

[8] Brodskii, E.S., Shelepchikov, A.A., "Three-dimensional ion mass chromatograms of hydrocarbon and heteroatomic compound types", Mass-spektrometria 9, 197 (2012) (in Russian).

[9] Brodskii E.S. (1985). Mass-spectrometric analysis of hydrocarbons and heteroatomic compounds of oils. In "Methods of investigation and composition of aromatic compounds of oils and bitumen". M., Nauka, p. 57-119.

[10] Melikadze L.D., Goderdzishvili K. G. (1971). Photochemical concentration of ash-forming elements in crude oil and oil products. Elsevier, v.11, issue 2, pp.120-124.

[11] ASTM D3279-07. (2007). Standard Test Method for n-Heptane Insolubles, Philadelphia PA, Available from http://www.astm.org/Standards/D3279.htm *(1) Petroleum Asphaltenes*. Available from: https://www.researchgate.net/publication/221926634_Petroleum_Asphaltenes [accessed May 05 2018].

საქართველოს ნავთობების ფისოვან-ასფალტენური ნაერთები

ნათელა ხეცურიანი, ესმა უშარაული, ქეთო გოდერძიშვილი,ირინა მჭედლიშვილი, თამარ შატაკიშვილი, მაკა კოპალეიშვილი

თსუ, პეტრე მელიქიშვილის ფიზიკური და ორგანული ქიმიის ინსტიტუტი, 0186, თბილისი, პოლიტკოვსკაიას ქ#31 E-mail: natixeco@yahoo.com

რეზიუმე. ნავთობის მაღალმდუღარე ნაერთების შესწავლისას, რომლებიც ხასითდება მეტად რთული შედგენილობით და მოლეკულების ფართო მრავალფეროვნებით, განსაკუთრებულ ინტერესს წარმოადგენს ფისოვან–ასფალტენური ნაერთების ძირითადი სტრუქტურული ბლოკების - პოლიციკლური კონდენსირებული არომატული სისტემების – აღმოჩენის და იდენტიფიკაციის მეთოდები. ნავთობის ფისოვან–ასფალტენური ნაერთების შესწავლისას ჩვენ მიერ გამოყენებული იყო ნახშირწყალბადების ფრაგმენტაციის ჰიდროპიროლიზური მეთოდი. წინამდებარე სტატიაში მოყვანილია საქართველოს სხვადასხვა ქიმიური შედგენილობის ნავთობებიდან: ნორიოს (არომატული), სამგორის (პარაფინული) და სუფსის (ფისოვანი) ნავთობებიდან მიღებული ფისოვან–ასფალტენური ნაერთების ჰიდროპიროლიზის პროდუქტების აირ–თხევადი ქრომატოგრაფიის და მასს–სპექტრომეტრული ანალიზის შედეგები. ფისოვან–ასფალტენური ნაერთების ჰიდროპიროლიზის პროდუქტების ნახშირწყალბადოვანი შედგენილობის შესწავლამ აჩვენა, რომ ისინი შეიცავენ ერთნაირ არომატულ სტრუქტურებს. ზემოაღნიშნულ ნავთობების ფისოვან-ასფალტენურ ნაერთებში იდენტიფიცირებულია ნაფტალინი, ფლუორენი, დიფენილი, ფენანტრენი, პირენი, ქრიზენი, პერილენი და მათი წარმოებულები.

Investigation of petroleum from new wells of Eastern Georgia

Natela Khetsuriani*, Esma Usharauli, Keto Goderdzishvili, Elza Topuria, Irina Mchedlishvili

TSU, Petre Melikishvili Institute of Physical and Organic Chemistry, 31 Politkovskaia, 0186, Tbilisi, Georgia, *E-mail: natixeco@yahoo.com

Abstract. Investigation of new wells of Satskhenisi oil (#7, #11, #12, #13, #14) and Manavi oil (#11, #12) was carried out. By IR spectroscopy it was established that Satskhenisi oil belonged to naphtheno-aromatic type and Manavi oil – to paraffinic type of oils. According to distribution of trace elements V, Fe, Ni, Co, Mo, Cu, Pb, Sn, Zn, Sr, Ba, Ti and the ratio V/Ni <1, these oils refer to tertiary types of oils, which is explained by conditions of accumulation and geochemical transformation of the original organic compounds. Using simulation chromatographic distillation of Manavi oil from the #12 well were obtained naphtha and diesel fractions. In naphtha by method of gas-liquid chromatography were identified individual paraffinic, naphthenic and aromatic hydrocarbons and in diesel fraction – individual n-paraffinic hydrocarbons. Physical and chemical characteristics, chemical nature and high yield of light fractions outlines perspective for obtaining of high quality energy purpose oil products like gasoline, petroleum solvents, aviation and diesel fuels and several brand petroleum oils from this new wells of petroleum deposits.

Keywords: Petroleum, Tar, Asphaltens, nafta, Diesel, microelements

INTRODUCTION

The main energy source in the world's economy is petroleum products of which are used by all other branches of industry and which provides 1/3 of the world's energy demand. According to the data obtained in 2018, the world's reserves of petroleum amount to 7,471.5 billion barrels on land and 160 billion barrels on the seabed.

One of the main problems among the challenges facing humanity in the 21st century is to solve the issue of energy security. Countries that have sufficient oil and gas resources can ensure their energy security, develop their economy and strengthen their independence.

Georgia, in terms of its geological structure, belongs to two oil and gas bearing territories: the Black Sea region and the Caspian province. According to the calculations of foreign and Georgian specialists, the expected oil resources in Georgia make 2 billion 350 million tons, and of gas - 180 billion m^3. Even in case of development of 40-50% of this potential resource, the country's budget will receive a profit of several hundred billion dollars.

It was established that according to the physical and chemical parameters Georgian oils belong to unique, low-sulfur, high-quality oils and from the point of view of processing they are quite an interesting raw material. Studies of these oils have shown that in Georgia there are almost all known types of oils that differ from each other by their chemical nature (paraffinic, naphthenic, naphtheno-aromatic, aromatic, etc.). Through the study of oils and their physical, chemical and geochemical parameters using uniform integrated methods, it is possible to plan the production of commercial oil products for energy purposes of local industry and agriculture, which is of great importance for the determination of the country's energy resources and their rational management [1-5].

The goal of the work was investigation of new wells of petroleum from Satskhenisi and Manavi oilfields for their certification. Satskhenisi oilfield is located at the eastern part of Gare-Kakheti oil region in the north wing of Norio-Khashmi anticlinal at a distance of 30 km to the north-east from Tbilisi. Satskhenisi anticlinal is composed of Maikop and Miocene sedimentary structures [6] and Manavi oilfield is located to the south from the Kakheti Range at a distance of 60 km from Tbilisi, to the north-south of the dome of the Ninotsminda oil-bearing anticline with corresponding sedimentary structures consisting of oil-containing Upper Cretaceous paleogenic sediments.

In connection with the rehabilitation of Satskhenisi oil production and for the purpose of certification of Georgian oils five new wells (№№ 7, 11, 12, 13, 14) of Satskhenisi oil with depth of occurrence 1040-1400m have been studied [7, 8]. Physical and chemical characteristics and the possibility of obtaining commercial oil products were investigated. Physical and chemical characteristics of the investigated oils are shown in Table 1.

Table 1. Physical and Chemical Characteristics of Satskhenisi crude oil

Parameter	Satskhenisi crude oil		
	Well #7	Well #11	Well #12
Density at 20^{0}C, kg/m^3	760,5	808,2	787,1
Density at 15^{0}C, kg/m^3	764,5	812,0	791,0
Molecular weight, ^{0}API	53,59	42,76	47,38
Kinematic viscosity 20^{0}C, cSt	0,9232	2,27	1,25
Ash content, %	0,0011	0,0021	0,0013
Asphaltenes, %	0,024	0,08	0,038
Resins, %	0,8	1,8	1,2
Paraffines, %	0,045	1,05	0,5
Sulfur, %	0,1	0,1	0,1
Mechanical impurities, %	0,004	0,19	0,071
Acidity, mg KOH per 1g of oil	0,65	1,3	0,78
Acid number	0,032	0,059	0,035
Pour point, ^{0}C	>-30	>-30	>-30
V/Ni ratio	<1	<1	<1
Yield of light fractions, %			
Under 200^{0}C	61,0	54,0	63,0
Under 320^{0}C	90,0	84,0	86,0

The results showed that all these crude oils are characterized by low density (765.0–816.0 kg/m^3 at 15°C), viscosity (0.92 - 2.48 cSt), small amount of paraffins (0.04–1.1%), sulfur (0.1%), and tar and asphaltenes (0.24-2.27%). Distillation curves of crude oils of all five wells showed that they are characterized by high content of light fractions boiling below 320 °C with a yield of 80-92%.
Temperature-distillation chart shows that similarly to previously produced crude oils new wells of Satskhenisi oilfields are characterized by high content of light fractions. Temperature-distillation chart of oils from the new wells with initial boiling point below 320 C is shown in Figure 1.

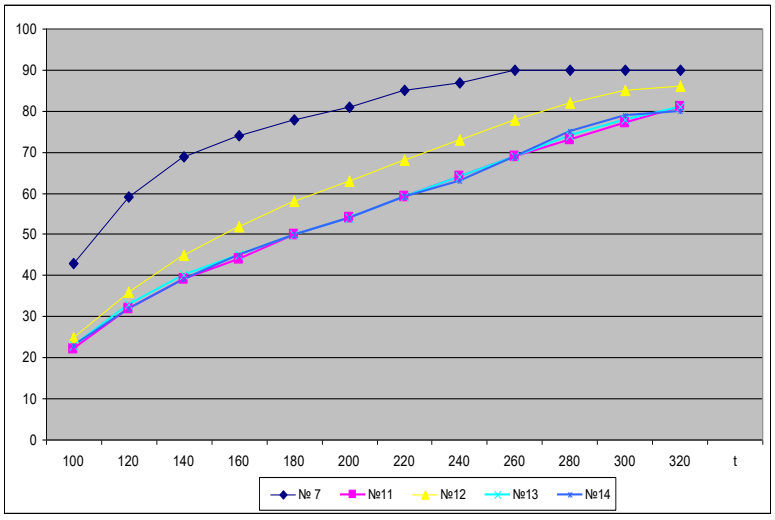

Figure 1. Temperature-distillation chart of oils from new wells of Satskhenisi oilfield

At present, general accepted approach for carrying out comprehensive studies of composition of oils is a method of infrared spectrometry. The structural and group composition of crude oils and their components is determined by intensity of characteristic absorption bands in IR spectra using common baseline with fixed points at 1850 and 650 cm^{-1}. Content of methylene groups (CH_2) in average molecule is assessed by absorption band at 720 cm^{-1}, content of methyl groups (CH_3) – by the absorption band at 1380 cm^{-1}, of sulfoxide groups (SO) by the band at 1030 cm^{-1} and of carbonyl group (CO) in the region of 1720-1700 cm^{-1} with respect to C = C aromatic bonds by absorption band at 1600 cm^{-1}.

We have studied the results of infrared spectrometric analysis of crude oils from new wells,

which was performed on a Perkin Elmer Spectrum spectrometer (model 10.4.2). The infrared spectra of all studied oils are presented in Figure 2.

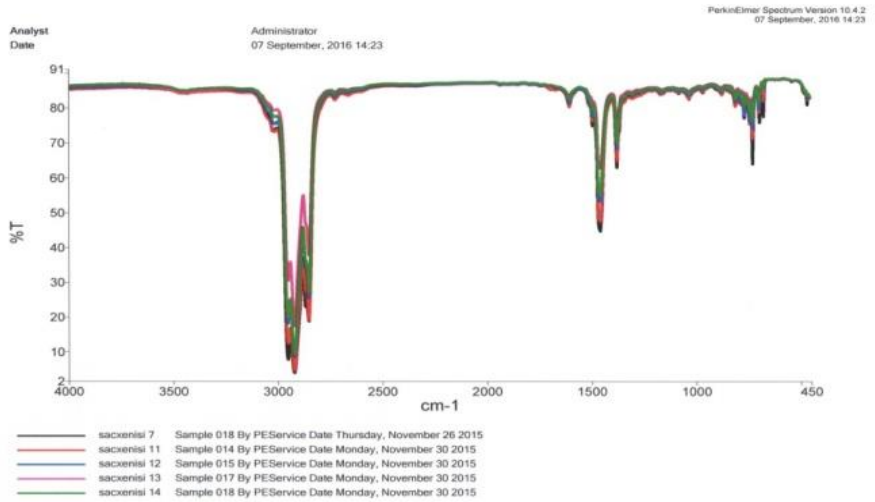

Figure 2. The IR spectra of all studied crude oils

IR spectra of all wells (№7, №11, №12, № 13, №14) of Satskhenisi oilfield are virtually identical. On spectra of fractions bands corresponding to alkanes (728 cm^{-1}), naphthenes (1030 cm^{-1}) and arenes(1500 cm^{-1}) can be clearly distinguished. This result, along with physical and chemical characteristics of the investigated oils, suggests that oils of new wells of Satskhenisi oilfield have similar chemical composition and belongs to the naphthene-aromatic type of oils.

Due to the high yield of light fractions of the Satskhenisi oil, the light commercial oil products — naphtha, kerosene and diesel fuels — were isolated and investigated. The study of the above mentioned commodity oil products showed that they meet the requirements of the relevant standards.

Oil production in wells #11 and #12 is carried out by the company Canargo Energy Corporation. Reserves of wells make 130 million barrels of oil and 59 billion cubic pounds of 2C gas (NSA). Perforation interval is 4680–4953 m. Physical and chemical characteristics of the crude oil from the Manavi oilfield are shown in Table 2.

The oil under study is characterized by medium density, high yield of light fractions (68%) and low content of sulfur and tar-asphaltenic compounds (8.92%), paraffin content is 6.1%. Simulation of complete distillation of crude oil was performed on a Sim Dis chromatograph, Auto System XL, manufactured by Perkin Elmer, according to ASTM D 2887 standard [9]. The crude oil under study is characterized by a high content of light fraction, the residue above 500°C is 12.5%. The distillation curve for Manavi oil is shown in figure 3.

Table 2. Physical and Chemical Characteristics of Manavi Petroleum

Parameter	Manavi Petroleum	
	Well #11	Well #12
Density at 20^0C, kg/m^3	826,0	822,5
Density at 15^0C, kg/m^3	829,6	826,5
Molecular weight, ^{0}API	39.6	40,0
Kinematic viscosity 20^0C, cSt	3,4	3,15
Ash content, %	0,0141	0,0098
Asphaltenes, %	1,86	2,7
Tar, %	7,07	8,12
Paraffines, %	6,5	6,2
Sulfur, %	0,18	0,17
Mechanical impurities, %	0,02	0,01
Acidity, mg KOH per 1g of oil	0,23	0,20
V/Ni ratio	<1	<1
Yield of light fractions, %		
Under 200^0C	30,0	32,0
Under 320^0C	65,0	67,4

.

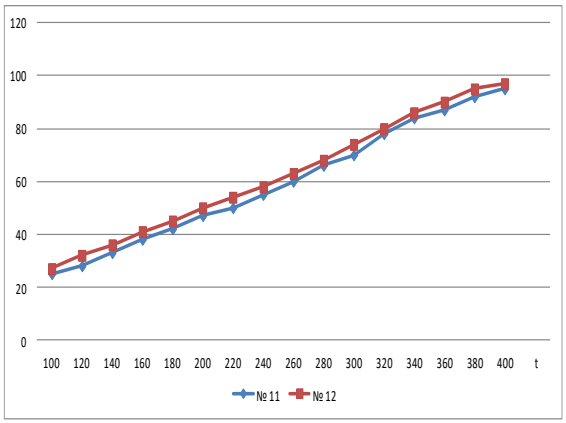

Figure 3. Distillation curves for Manavi oil, wells #11 and #12

An infrared spectrometric analysis of oils from new wells, carried out on a Perkin Elmer Spectrum spectrometer, model 10.4.2., showed that the IR spectra of the wells are almost identical. The intensity of the absorption bands of 721.4 cm^{-1} and 1377 cm^{-1} characterizes the content of methyl and methylene groups in paraffin hydrocarbons. The presence on the spectrum of the band 1600cm^{-1} characterizes the content of aromatic hydrocarbon. It has been determined that crude oils of the new wells of the Manavi oilfield have the same chemical composition and refer to the paraffin type of oils.

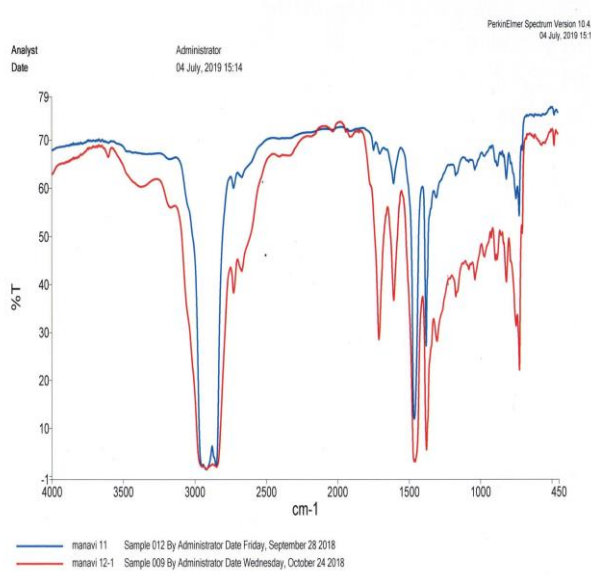

Figure 4. IR spectra of Manavi Crude Oil

From the results of the study, it turned out that due to the low content of sulfur, tar-asphaltenic compounds and high yield of light fractions, the Manavi oil was high-quality paraffinic oil.

The naphtha fraction isolated from the Manavi crude oil (35–180°C) was studied by the gas chromatography method "PON A" [10]. The elemental and group hydrocarbon composition, molecular weight, relative density, saturated vapor pressure and octane number were determined (Table 3). Individual paraffinic, naphthenic and aromatic hydrocarbons and their derivatives were also identified.

The physical-chemical indices of diesel fractions with different boiling points are shown in table 5. The study showed that the refractive index, density and kinematic viscosity increase with an increase in the boiling point of the diesel fraction. Fractions are characterized by a high diesel index and cetane number (table 4).

Table 3. Characteristics of the naphtha fraction

The name of indicators					*Magnitude*
Density at 20°C, kg/m³					736,0
Molecular weight					101,998
Vapor pressure, psi					1,7
Octane number					73,51
Distillation	s.b. 31°C	10% 70°C	50% 110°C	90% 156°C	b.e. 200°C
Content - C					86,118
Content - N					13,882

Group composition		
Groups	Output, % mass.	Yield,% vol.
Paraffin	24,027	25,972
n-paraffin	27,531	29,344
Olefins	-	-
Naphthenes	32,231	30,932
Aromatics	15,753	13,362
Unknown	0,459	0,399
Amount	100,0	100,0
Under 200°C	30,0	32,0
Under 320°C	65,0	67,4

Table 4. Physical and chemical characteristics of diesel fractions

Fraction, °C	**Manavi Petroleum, Well #11**		
	140-320, °C	**140-350, °C**	**180-350, °C**
Gutput, %	42.1	47.0	37.0
Density at 20°C, kg/m³	814.2	820.8	834.0
n_D^{20}	1.4528	1.4560	1.4682
Kinematic viscosity 20°C, cSt	2.61	3.2	4,5
Diesel index	64.4	63.3	64.7
Cetane number	57.0	55.0	50.6
	Manavi Petroleum, Well #12		
Gutput, %	42.9	49.0	40.0
Density at 20°C, kg/m³	819.0	822.3	835.0
n_D^{20}	1,4580	1.4640	1.4682
Kinematic viscosity 20°C, cSt	2.8	3.3	4.6
Diesel index	64.7	63.5	61.6
Cetane number	58.0	55.6	51.8

In the carbamide concentrate of the diesel fraction 180–320ºC, the distribution of n-paraffin hydrocarbons was studied by a gas-liquid chromatography (Table 5). In this table are shown the identified n-paraffin hydrocarbons C_9–C_{26}, with a maximum content of tetradecane ($C_{14}H_{30}$).

The distribution of trace elements V, Fe, Ni, Co, Mo, Cu, Pb, Sn, Zn, Sr, Ba, Ti in Satskhenisi and Manavi oils was also studied. Trace elements were isolated using the developed in the laboratory of petroleum chemistry photochemical method of extracting the concentrate of ash elements from petroleum and petroleum products, which has found wide application in other scientific research organizations.

Table 5. Paraffin hydrocarbons

Hydrocarbon names	*Molecular weight, g/mol*	***Relative concentration***	
		Manavi #11	Manavi #12
Nonane	164.40	0.14	1.33
Decane	142.29	2.34	3.80
Undecane	156.31	5.86	7.60
Dodecane	170.34	8.61	8.33
Tridecane	180.40	10,87	9.00
Tetradecane	199,39	12,40	10.77
Pentadecane	221.42	10.37	9.88
Hexadecane	232.41	8.77	7.26
Heptadecane	240.48	7.80	7.05
Octadecane	254..5	6.61	6.73
Nonadecane	268.52	5.70	4.87
Eicosane	282.55	4.78	4.24
Heneicosane	296.58	4.21	4.76
Docosane	310.60	3.98	4.33
Tricosane	324.38	3.88	3.70
Tetracosane	338.65	2.65	2.73
Pentacosane	352.69	1.20	1.70
Hexacosane	366.72	0.79	1.36

Consequently, on the basis of the study it was concluded that distribution of V, Fe, Ni, Co, Mo, Cu, Pb, Sn, Zn, Sr, Ba, Ti microelements and the ratio V/Ni <1 indicate that these oils are of tertiary type, which can be explained by conditions of accumulation of initial organic substance and by relevant geochemical origin [11].

The results of the study

The oils of the new wells of the Satskhenisi and Manavi oilfields, located quite close to each other in the region of the Kakheti Range were studied. Physical, chemical and geochemical parameters, as well as functional groups by IR spectrometry, were determined. It has been established that Satskhensi oil refers to naphthene-aromatic, and Manavi oil to paraffin types of oils.

According to the distribution of trace elements V, Fe, Ni, Co, Mo, Cu, Pb, Sn, Zn, Sr, Ba, Ti and the ratio V/Ni <1, these oils refer to tertiary types of oils, which is explained by the conditions of accumulation of the original organic matter and corresponding geochemical origin.

By low content of sulfur, tar-asphaltene compounds and high yield of light fractions, Satskhensi and Manavi crude oils are high-quality raw material for production of commercial oil products for energy purposes – gasolines, high-quality organic solvents, aviation and diesel fuels and various petroleum oils for local industry and agriculture.

REFERENCES

[1] Chemistry of oil and gas. A.I Bogomolov, A.A. Gaile and others. Publishing house Khimia, 1995, 448p. ISBN: 5-7245-1023-5. (in Russian)

[2] Modern methods for investigation of crude oils. Leningrad, “Nedra, 1984, 430p.

[3] N.Khetsuriani, E.Usharauli, E.Topuria, I.MchedliShvili. Use of mass-spectrometry for investigation of aromatic structure of high-boiling compounds of oil. IX International massspectrometry conferece in Petrochemistry, ecology and food Chemistry “Petromass2011”. Moscow, 2011, pp.128-131.

[4] James G. Speight. Handbook of Petroleum Analysis. First published: February 2015, 368 pages. ISB 978-1118369265. DOI: 10.1002/9781118986370.

[5] V.G.Tsitsishvili, N.T.Khetsuriani. Georgian Crude Oil and Bitumen Deposits. Proceedings of the International Mass Spectrometry Conference on Petrochemistry and Environmental “PETROMASS 2014”, 2014, 1-4 September, Tbilisi, Georgia, pp.13-14.

[6] http://www.gogc.ge/ge/oil-production

[7] E.P. Gventsadze, P.P. Busel. To the investigation of Georgian oil deposits. Proceedings of the Georgian National Academy of Sciences, Chemical Series, 1978, v. 4, #1, h. 66-75.

[8] E.A. Usharauli, E.N. Topuria, Q.G. Goderdzishvili, I.J.Mchedlishvili, N.T. Ketsuriani. Investigation of crude oil from Satskhenisi oil deposit. Transactions of Petre Melikishvili Institute of Physical and Organic Chemistry 2015, p.131-135.

[9] ASTM D2887. Standard Test for Boiling Range Distribution of Petroleum Fraction by Gas-Chromatography.

[10] ASTM D 3710 Standard Test Method for Boiling Range Distribution of Gasoline and Gasoline Fractions by Gas-Chromatography.

[11] L.D. Melikadze, Q.G. Goderdzishvili, G.I. Zulfigarli. To the investigation of trace elements in Georgian oils. Tbilisi, “Mecniereba”, 1976, 98p.

აღმოსავლეთ საქართველოს ახალი ჭაბურღილების ნავთობების კვლევა

ნათელა ხეცურიანი*, ესმა უშარაული, ქეთო გოდერძიშვილი, ელზა თოფურია, ირინა მჭედლიშვილი

თსუ, პეტრე მელიქიშვილის ფიზიკური და ორგანული ქიმიის ინსტიტუტი, 0186, თბილისი, პოლიტკოვსკაიას ქ#31, *E-mail: natixeco@yahoo.com

რეზიუმე. ჩატარდა საცხენისის ახალი (# 7, # 11, # 12, # 13, # 14) ჭაბურღილების და მანავის ახალი (# 11, # 12) ჭაბურღილების ნავთობების კვლევა. იწ სპექტროსკოპიის მეთოდით დადგინდა ამ ნავთობების ფიზიკურ–ქიმიური და გეოქიმიური პარამეტრები. დადგენილია, რომ საცხენისის ნავთობები მიეკუთვნება ნაფტენო-არომატული ტიპის ნავთობებს, ხოლო მანავის ნავთობები - პარაფინულ ტიპის ნავთობებს. ნავთობებში მიკროელემენტების V, Fe, Ni, Co, Mo, Cu, Pb, Sn, Zn, Sr, Ba, Ti განაწილება და V/Ni <1, თანაფარდობა, მიუთითებს რომ აღნიშნული ნავთობები მიეკუთვნებიან მესამეული ტიპის ნავთობებს, რაც აიხსნება საწყისი ორგანული ნაერთების წარმოშობით და შესაბამისი გეოქიმიური გარდაქმნით. მანავის #12 ჭაბურღილის ნავთობის სიმულაციური ქრომატოგრაფიული დისტილაციის გამოყენებით მიღებულია ნაფტას და დიზელის ფრაქციები. ნაფტაში აირ–თხევადური ქრომატოგრაფიის მეთოდით იდენტიფიცირებულია ინდივიდუალური პარაფინული, ნაფტენური და არომატული ნახშირწყალბადები, ხოლო დიზელის ფრაქციაში – ინდივიდუალური ნ–პარაფინული ნახშირწყალბადები. შესწავლილი ნავთობების ფიზიკურ–ქიმიური მახასიათებლები, ქიმიური ბუნება და მსუბუქი ფრაქციების მაღალი გამოსავალი სახავს ახალი საბადოს ნავთობებიდან მაღალი ხარისხის ენერგეტიკული დანიშნულების სასაქონლო ნავთობპროდუქტების - ბენზინები, ნავთობური გამხსნელები, საავიაციო და დიზელის საწვავები და სხვადასხვა მარკის ნავთობური ზეთები - მისაღებად.

Resol oligomer on the basis of adamantane type bisphenol

Givi Papava*, Nazi Gelashvili, Nora Dokhturishvili, Eter Gavashelidze, Nanuli Khotenashvili, Riva Liparteliani

Petre Melikishvili Institute of Physical and Organic Chemistry at Iv. Javakhishvili Tbilisi State University. 31, A.Politkovskaia str., Tbilisi, Georgia, 0186.
*givi.papava31@mail.ru, Tel.+995 559 70 55 61

Abstract. Heat-resistant and thermostable polymers, that is the polymers possessing three-dimensional structure, especially those with rigid space lattice have been widely used. Most significant representatives of polymers of this class are the phenol-formaldehyde polymers. Methylol derivative on the base of adamantine type bisphenol was obtained. Interaction of 2,2-bis-(4-oxyphenyl)adamantane with formaldehyde was investigated in n-propyl alcohol, at 115-135^{o}C temperature interval, in the presence of ammonia as the catalyst. Some kinetic regularities of reaction of interaction of adamantane type bisphenol and formaldehyde were studied. It was proved that the reaction proceeded according to the second order. Activation energy and reaction rate constants were calculated. Studies to determine the effect of various factors on the rate of conversion, at the interaction of formaldehyde and 2,2-bis-(4-oxyphenyl) adamantane proved that the most optimal term for the process is its carrying out at 125^{0}C in n-propyl alcohol, at molar ratio of starting components 1:8, in the presence of 2 mass % ammonia used as a catalyst (with respect to bisphenol), at the reaction duration 10 hrs and initial concentration of bisphenol – 0.6 mol./l. IR-spectroscopy was used to study the process of thermal hardening of methylol derivative of bisphenol at isothermal terms, on the air. On the base of the IR-spectral data the mechanism of the process of hardening of methylol derivative of bisphenol can be presented as follows: at the initial stages the methylene ether bonds are formed. Then, at high temperatures, these bonds suffer destruction and the infusible and insoluble product is formed, which is confirmed by the decrease of intensity of absorption band in the region 825 cm $^{-1}$. Resite with adamantane grouping suffers intense decomposition in temperature interval 450-550^{o}C. Adamantane-containing resite suffers decomposition without formation of coke residue, which enables us to recommend it for making heat-eliminating covers. High thermal indices of a polymer on the base of methylol derivative of 2,2-bis-(4-oxy phenyl) adamantane, enables us to use it as the binder for the creation of heat and thermally stable materials.

Keywords: cycloparaffins, resol, oligomer, bisphenol, adamantine

INTRODUCTION

Heat-resistant and thermostable polymers, that is the polymers possessing three-dimensional structure, especially those with rigid space lattice have been widely used. Most significant representatives of polymers of this class are the phenol-formaldehyde polymers [1-4].

Recently, to increase some indices (heat- and thermal stability, strength at impact loads et al) various bisphenols were used for the synthesis of phenol formaldehyde polymers. It enabled us to decrease cross-linking of macromolecules, which makes significant effect on physical-mechanical and other indices of polymers [5-8].

Thanks to the very interesting set of properties of other type polymers which contain cycloparaffin card type groupings [9-13] we considered interesting and expedient to lead investigations in the sphere of phenol formaldehyde polymers with adamantane type card groupings

EXPERIMENTAL

First stage of the study deals with the synthesis of methylol derivatives of adamantane-containing bisphenol. Initial component of the synthesis was 2,2-bis-(4-oxy- phenyl) adamantane (as the phenol component) and alcoholic solution of formaldehyde.

To realize successfully the reaction of synthesis, and to determine optimal terms of the reaction, we considered proper to investigate some kinetic regularities of the process.

Interaction of 2,2-bis-(4-oxyphenyl) adamantane with formaldehyde was investigated in n-propyl alcohol, at 115-135^{o}C interval, in the presence of ammonia as the catalyst, at the molar ratio of bisphenol to formaldehyde 1:4.

Schematically the reaction can be presented as follows:

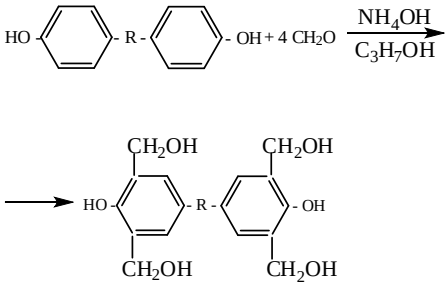

Bisphenol II

where R =

Control over the reaction process was realized according to the quantity of the used formaldehyde [14].

Figure 1 offers kinetic curves of condensation reaction of bisphenol with formaldehyde at various temperatures. It was found that at 115-135°C temperature interval, up to the high rate of conversion, the rate constants preserved constant values during the reaction, and were calculated by the Arrhenius quadratic equation.

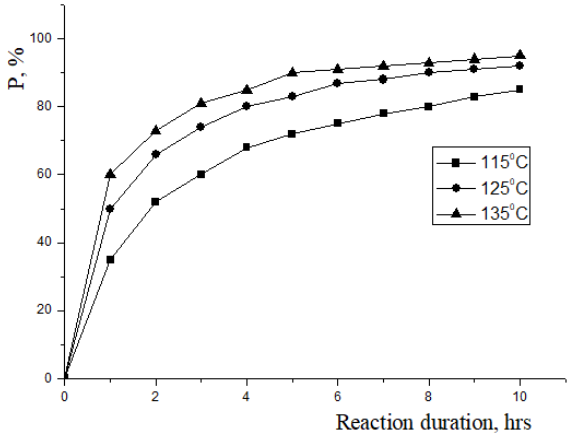

Fig. 1. Kinetic curves of interaction of formaldehyde and 2,2-bis(4-oxyphenyl)-adamantane at 115-135°C. P - conversion rate.

Direct linear relation of logarithm of the rate constant at inverse absolute temperature refers to the second order reaction. Activation energy of the given reaction calculated from this relation (dependence) according to Arrhenius equation equals to $69.6 \cdot 10^3$ J/mol.

We studied the effect of various factors on the process of reaction, and namely those of temperature and reaction length, quantity and nature of the catalyst, type of reaction medium, concentration and ratio of initial reagents.

As is seen from the kinetic curves (Fig. 1), by the increase of temperature, the rate and speed of conversion are increased. Conversion rate increases also at the increase of reaction duration. Reaction is mainly accomplished in 3 hours. 135°C is the limiting temperature value, over which conversion of methylol groups occurs.

Kinetic curves of the reaction are significantly affected by the quantity and nature of the catalyst. At the increase of catalyst quantity (ammonia) from 1 to 2 mass %, with respect to bisphenol, the conversion rate at 135°C in 10 hours increases from 80 to 94%. Further increase of quantity of the catalyst doesn't affect the rate of conversion.

Reaction progress is also affected by the nature of the catalyst. By the increase of catalyst activity (pyridine, triethyl amine, ammonia) the conversion rate increases and in 10 hrs reaches 27,50; 83,10 and 86.25 %.

To determine the effect of nature of the reaction medium, the reaction was carried out in various organic solvents: in n-paraffin, n-butanol, 1,2-ethyleneglycol, 1,4-butyleneglycol and glycerin. Experiments showed that in 5 hours of the reaction the conversion rate equaled to 88,00; 85.05; 93.00 and 95.50, correspondingly. The best results were obtained when the solvents glycerin and ethylene glycol were used.

But to carry out the process of reaction in these solvents is not expedient, since separation of the reaction product is extremely complicated.

It was shown that at the increase of starting concentration of bisphenol from 0.1 to 0.6 mol./l in the reaction mixture, the maximum fractional conversion is increased and by the end of 10 hrs it equals to 70.50 and 94.50%, correspondingly.

At the interaction of formaldehyde and 2,2-bis-(4-oxyphenyl)adamantine, the formaldehyde to bisphenol ratio 4:1 is optimal. At this ratio of starting components we studied all the above referred regularities.

We have studied the effect of formaldehyde amount exceeding the equimolecular on the rate of formation of methyl derivative and bisphenol fractional conversion. Experiments were carried out by the use of various starting quantities of formaldehyde. Various molar ratios of bisphenol to formaldehyde, namely such as 1:4, 1:8 and 1:16 were tested, correspondingly.

Experiments showed that by the increase of formaldehyde quantity over the equimolecular one, rate and speed of bisphenol conversion markedly increased.

Studies to determine the effect of various factors on the rate of conversion, at the interaction of

formaldehyde and 2,2-bis-(4-oxyphenyl)adamantane proved that the most optimal term for the process is its carrying out at 125^{0}C in n-propyl alcohol, at molar ratio of starting components 1:8, in the presence of 2 mass % ammonia used as a catalyst (with respect to bisphenol), at the reaction duration 10 hrs and initial concentration of bisphenol – 0.6 mol./L.

Methyl derivative of 2,2-bis-(4-oxyphenyl)adamantane was separated from the reaction mixture by precipitation in water or by evaporation of the solvent under vacuum at 60^{o}C temperature. The isolated product is solid powder, with yellowish hue, well soluble in acetone, alcohol, dioxan, dimethyl formamide, insoluble in aromatic hydrocarbons and water.

RESULTS

X-ray diffraction studies showed that in distinct from 2,2-bis-(4-oxyphenyl)- adamantane, its methyl derivative is of amorphous structure.

According to the data of analysis, hydroxyl groups equal to 6.08 %; molecular mass determined by ebulioscopy - 586; methylol group content - 25.56%. These data well conform to the calculated values of these indices for tetra methyl derivative of 2,2-bis-(4-oxyphenyl)adamantane, esterified by the use of propyl alcohol.

According to the above referred scheme formation of reaction products is confirmed by the data of IR spectroscopy. Spectra of methyl derivative show the absorption band in the zone of 1030 cm^{-1}, which is characteristic to valence fluctuation of methylol groups. But the spectra fixes also an absorption band in the regions 1085 and 1110 cm^{-1}, which is characteristic to simple ether bonds, which refers to esterification of methyl groups by propyl alcohol. IR spectra of absorption show also the absorption bands in the regions 1380 and 3360 cm^{-1}, characteristic to valence and deformation fluctuations of phenol hydroxyl hydrogen bonds of the polymer.

Absorption bands in the regions of 2880 and 2970 cm^{-1} are characteristic to valence fluctuations of methyl groups, while the band at 1600 cm^{-1} corresponds to aromatic ring.

Irrespective of the fact that methylol groups in the process of formation of bisphenol methyl derivative undergo esterification, it affects significantly their reaction activity. They are thermo-reactive and suffer hardening at heating.

Figure 2 presents thermogravimetric curve of hardening of methyl derivative of 2,2-bis-(4-oxyphenyl)adamantane. Figure 2 shows that bisphenol methyl derivative at heating up to 400^{o}C on the air, the mass is decreased by 32%. Decrease of the mass up to 400^{o}C should be attributed mainly to the hardening process, which apparently takes place up to 400-470^{o}C. But, alongside with the hardening process, destruction processes are started at the above stated temperatures. At 560^{o}C the whole polymer is evaporated, without coke residue formation. Behavior of methylol derivative of adamantane-containing bisphenol should be attributed to polycyclic adamantane grouping.

Taking into consideration the results of thermogravimetric analysis we can state that in the temperature range 150-400^{o}C the decrease of mass is mainly conditioned by polycondensation processes. Above this temperature, the destruction processes are prevailing. Considering this fact the further thermal hardening was carried out by using these data.

Process of thermal hardening of methylol derivative of 2,2-bis-(4-oxyphenyl)adamantane was investigated in isomeric conditions, on the air, at temperatures 150, 200, 250, 300^{o}C (Figure 3).

At heating of methylol derivative of bisphenol of 2,2-bis-(4-oxyphenyl)adamantane for five hours the intensity of absorption band in 1030 cm^{-1} , characteristic to free non-esterified methylol group – decreases significantly. This is apparently connected with condensation of methylol groups and with the formation of ether bond -CH_2-O-CH_2-. Intensity of absorption band is decreased significantly in the region of 3360 cm^{-1} and absorption bands in 3550 cm^{-1} characteristic to valence fluctuations of phenyl hydroxyl groups, participating in the formation of dimer hydrogen bonds - are increased.

Analogous changes were observed in deformation fluctuations of phenol hydroxyl in the regions of 1360, 1380 cm^{-1}.

Figure 3 shows that by the increase of hardening temperature in isothermal conditions up to 250^{o}C, at the starting section of the curves, the mass decrease rate is higher. At the increase of length of heating, intensity of decrease slows down for a continuous time. Up to 250^{o}C decrease in mass apparently is conditioned by conversion of methylene ether groups, at a less degree, by conversion of methylol groups with the isolation of low molecular reaction products. The process of hardening apparently proceeds up to deeper rate of completion, which can be explained by the formation of the products with less rigid spatial, three-dimensional structure, conditioned by large size adamantane grouping.

In IR spectra of the product of thermal treatment of methylol derivative of 2,2-bis-(4-oxy-phenyl)adamantane, carried out at 200^{o}C, in isothermal conditions, the intensity of absorption bands at 1085 and 1110 cm^{-1}, corresponding to simple ether bonds, greatly decreases. Destruction of these bonds takes place and infusible and insoluble product, resite is formed. Intensity of the absorption band at 825 cm^{-1} characteristic to extra-planar deformation fluctuations of two siding =CH groups of benzyl nucleus suffer significant decrease, which apparently refers to the formation of new bonds.

DISCUSSION

On the base of the IR-spectral data the mechanism of the process of hardening of methylol derivative of bisphenol can be presented as follows: at the initial stages the methylene ether bonds are formed. Then, at high temperatures, these bonds suffer destruction and the infusible and insoluble product is formed, which is confirmed by the decrease of intensity of absorption band in the region 825 cm^{-1}.

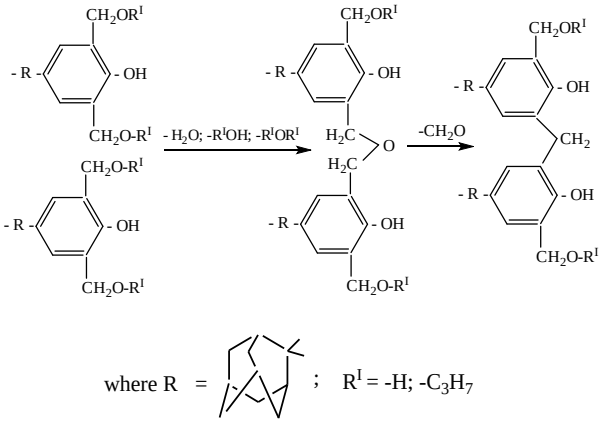

At thermal treatment of tetra-methylol derivative of 2,2-bis-(4-oxyphenyl)adamantane, at 250°C, on the air, at isomeric conditions, the IR spectra show the adsorption band corresponding to the aldehyde group, at 1660 cm^{-1}, which is explained by partial oxidation of methylene group, and a band of absorption in the region of 1680 cm^{-1}, which is characteristic to quinoid groups, and is accompanied by a decrease of absorption band intensity in 2880 and 2970 cm^{-1}, corresponding to valence fluctuations of $–CH_2$- groups, apparently is associated with the changes in adamantane structure.

According to the thermogravimetric curve (Fig. 2), at thermal hardening of methylol derivative of adamantane-containing bisphenol, mass decrease takes place and increases up to 400°C. As it was stated above, mass decrease mainly takes place at the expense of the process of hardening. Presence of adamantane grouping contributes to the decrease of effect of steric factors on the process of thermal hardening, as a result of which degree of completeness shifts towards high values. In common phenol formaldehyde polymers, at the early stage of reaction the process of hardening stops due to rigidifying of the structure and formation of frequent cross-linking, which is a result of a decrease of a degree of completeness at comparatively early stage.

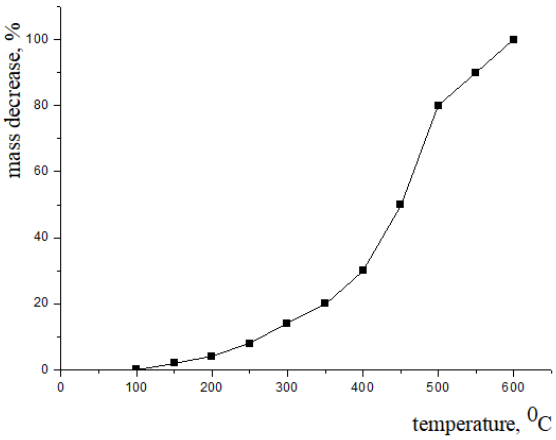

Fig. 2. Dynamic thermogravimetric curve of methylol derivative of 2,2-bis (4-oxyphenyl)adamantane (heating speed 5°C /min, on the air).

At thermal treatment of methylol derivative of 2,2-bis-(4-oxy phenyl)adamantane, at 300°C, in isomeric conditions, on the air, IR spectra of the product of hardening show absorption band in the region of 1600 cm^{-1} (characteristic to the formed condensed aromatic hydrocarbons) and the increase of absorption band intensity in the region of 1720 cm^{-1} (characteristic for carboxyl groups formed by oxidation of carbonyl groups).

Behavior of phenol hydroxyl groups at thermal treatment in the temperature range 250-300°C should be emphasized. Absorption bands at 3360 and 1389 cm^{-1}, characteristic for valence and deformation fluctuations of phenol hydroxyls, linked by polymer hydrogen bonds, suffer great changes. Their intensity is decreased, while the intensity of the bands at 3550 and 1360 cm^{-1}, belonging correspondingly to valence and deformation fluctuations of phenol hydroxyl, participating in the formation of dimer hydrogen bonds - increase. This refers to regrouping of polymer hydrogen bonds towards those of dimers, characterized by high resistance.

We have stated above that presence of card groups increases thermal indices of other class polymers. To evaluate thermal stability of adamantane-containing bisphenol aldehyde polymer, we prepared resite of the corresponding polymer.

Resite was prepared as follows: weighted amount of a methylol derivative sample was heated to 180-200°C 10-15 min prior their melting. When the melt started hardening, it was subjected to thermal treatment at 250°C within 1 hour. Preliminary experiments, by extraction of dispersed sample of resite from boiling acetone within 5 hours, showed that it didn't contain low molecular products and that thus the hardening process was practically brought to the end.

We carried out thermogravimetric and thermo-mechanical studies of resite. Structural changes

taking place at thermal treatment were evaluated according to the data of IR-spectroscopy.

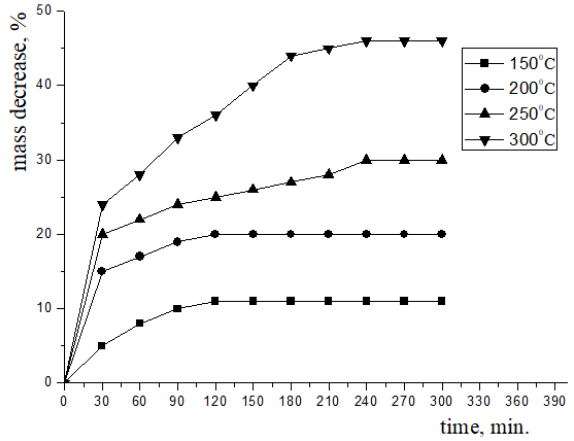

Fig. 3. Mass decrease at thermal hardening of methylol derivative of 2,2-bis (4-oxyphenyl)adamantane on the air, in isothermal conditions, at temperatures: 150 (1), 200 (2), 250 (3) and 300°C (4).

Resite, obtained by hardening of methylol derivative of 2,2-bis-(4-oxyphenyl)adamantane, in distinct from common phenyl formaldehyde resites, as is shown by thermogravimetric studies, up to 300°C doesn't reveal mass decrease practically, while in case of common phenol formaldehyde resite, the mass decrease in this case equals to 10%. Resite with adamantane grouping suffers intense decomposition in temperature range 450-550°C, and for common resite, this interval falls within 400-500°C. Adamantane-containing resite suffers decomposition without formation of coke residue, which enables us to recommend it for making heat-eliminating covers.

Thermomechanical studies of adamantane-containing resite showed that the polymer revealed insignificant deformation (~ 2%) when it was treated up to the temperature of thermal decomposition. At the temperature about 500°C the increase of deformation is observed, which apparently is connected with resite destruction.

High thermal indices of a polymer on the base of methylol derivative of 2,2-bis-(4-oxy phenyl)adamantane, enables us to use it as the binder for the creation of heat and thermally stable materials. Glass-reinforced plastic on the base of methyl derivative of 2,2-bis-(4-oxy phenyl)adamantane, according to its dielectric and mechanical characteristics significantly exceeds glass reinforced plastics on the base of common phenol formaldehyde oligomers, currently produced in industrial conditions.

Methylol derivative on the base of adamantine type bisphenol was obtained. Some kinetic regularities of reaction of interaction of adamantane type bisphenol and formaldehyde were studied. It was proved that the reaction proceeded according to the second order. Resite with adamantane grouping suffers intense decomposition in temperature interval 450-550°C.

Adamantane-containing resite suffers decomposition without formation of coke residue, which enables us to recommend it for making heat-eliminating covers. High thermal indices of a polymer on the base of methylol derivative of 2,2-bis-(4-oxy phenyl) adamantane, enables us to use it as the binder for the creation of heat and thermally stable materials.

REFERENCES

[1] Dagher HJ, Iqbal A, Bogner B . Polymers & Polymer Composites 2004; Vol 12, No 3.

[2] Conner, Anthony H.; Lorenz, Linda F.; Hirth, Kolby C. 2002. Accelerated cure of phenol-formaldehyde resins : studies with model compounds Journal of applied polymer science. Vol. 86 (2002): Pages 3256-3263.

[3] Luukko, P., Alvila, L., Holopainen, T., Rainio, J. & Pakkanen, T.T., "The Effect of Alkalinity on the Structure of Phenol-Formaldehyde Resol Resins", J. Appl. Polym. Sci. 82 (2001) 258.

[4] Turunen, M., Alvila, L., Pakkanen, T.T. & Rainio, J., "Modification of phenol-formaldehyde resol resins by lignin, starch and urea", J. Appl. Polym. Sci. 88 (2003) 582.

[5] Doroshenko Yu.E.. Korshak V.V., Sergeev V.A.. Phenol formaldehyde polymers. Effect of bisphenol structure on polymer properties. Plast. Masses, 1965, No 8, p. 9-11.

[6] Sergeev V.A., Korshak V.V., Shatikov V.K. Thermally reactive polymers on the base of various structure phenols and formaldehyde. High Mol. Comp., 1967 A-9, No 9, p. 1925-1956.

[7] Korshak V.V., Sergeev V.A., Shatikov V.K., Soverov A.A., Nazmutdinova I.Kh. et al. Phenolphthalein containing thermally reactive copolymers. High Mol. Comp., 1968, A-10, p. 1085-1091.

[8] Hoagland M.E., Duling L.N. Adamantane Copolycarbonates. – U.S. Patent 351 6969, 1970.

[9] Duling L.N. Schneider L.D., Gary I. Adamantane Pol

[10] Deiscoll G.L. Polyesters of adamantane diols and aromatic tetra carboxylic acid di -anhydrides – U.S. Patent 3497472, 1970.

[11] Beridze L.A., Papava G.Sh., Tsiskarishvili P.D., Kutateladze M.K. Mixed aromatic polyesters with card type groupings. Proceedings of Acad.Sci. Georgia, Chemical Series, 1981, v.7, No 2, p. 136-141.

[12] Thompson R.N., Duling L.N. Polysulfonate polymer from adamantane bisphenols. – U.S. Patent, 1973 3738965.

[13] Papava G.Sh., Sergeev V.A., Vinogradova S.V., Abnerova S.V., Maisuradze N.A., Korshak V.V., Tsiskarishvili P.D., Shitikov V.K. Some kinetic regularities of reaction of bisphenols of nornornane type with formaldehyde. High Mol. Comp., 1974, v. 16, No 11, p.844-845.

[14] Walker G. Formaldehyde. Moscow, Goskhimizdar, 1957, p.423.

რეზოლური ოლიგომერი ადამანტანის ტიპის ბისფენოლის საფუძველზე

გივი პაპავა*, ნაზი გელაშვილი, ნორა დოხტურიშვილი,
ეთერ გავაშელიძე, ნანული ხოტენაშვილი, რივა ლიპარტელიანი

*თსუ, პეტრე მელიქიშვილის ფიზიკური და ორგანული ქიმიის ინსტიტუტი, 0186, თბილისი, პოლიტკოვსკაიას ქ#31, *givi.papava31@mail.ru,* Tel.+995 559 70 55 61

რეზიუმე. თერმომედეგი და თერმოსტაბილოური პოლიმერები, რომლებსაც აქვთ სამგანზომილებიანი, ხისტი სივრცითი სტრუქტურა, ფართოდ გამოიყენება. ამ კლასის პოლიმერებიდან განსაკუთრებით მნიშვნელოვანია ფენოლ-ფორმალდეჰიდური პოლიმერები. მათ მისაღებად ჩვენს მიერ, ადამანტანის ჯგუფის შემცველი ბისფენოლების საფუძველზე სინთეზირებული იყო ამ ბისფენოლების მეთილოლწარმოებულები. შესწავლილი იყო 2,2-ბის-(4-ოქსიფენილ)ადამანტანისა და ფორმალდეჰიდის ურთიერთქმედების რეაქცია ნორმალური პროპილის სპირტის არეში, 115-135^{0}C ტემპერატურულ ინტერვალში, კატალიზატორის - ამიაკის თანაობისას. შესწავლილი იყო რრეაქციის ზოგიერთი კინეტიკური კანონზომიერება. დადგენილ იქნა, რომ რეაქცია არის მეორე რიგის. გამოთვლილი იყო აქტივაციის ენერგია და რეაქციის სიჩქარის მუდმივები. შესწავლილი იყო ფორმალდეჰიდისა და 2,2-ბის-(4-ოქსიფენილ)ადამანტანის ურთიერთქმედებისას სხვადასხვა ფაქტორების გავლენა გარდაქმნის სიჩქარეზე და დადგენილ იქნა რეაქციის ოპტიმალური პირობები: რეაქციის ტემოერატურა 125^{0}C , სარეაქციო არე ნ-პროპანოლი, საწყისი კომპონენტების მოლური თანაფარდობა 1 : 8, 2 მას.% კატალიზატორის - ამიაკის თანაობისას (ბისფენოლის მიმართ), რეაქციის ხანგრძლივობა 10 საათი, კომპონენტების საწყისი კონცენტრაცია - 0,6 მოლი/ლ. იზოთერმულ პირობებში, ჰაერზე, ბისფენოლის მეთილოლწარმოებულების გამყარების პროცესის შესწავლისათვის გამოყენებული იყო ი.წ. სპექტროსკოპიული ანალიზი მეთოდი. ი.წ. სპექტროსკოპიული ანალიზის მონაცემების საფუძველზე, ბისფენოლის მეთილოლწარმოებულების გამყარების პროცესი შეიძლება წარმოვიდგინოთ შემდეგი სახით: საწყის სტადიაზე წარმოიქმნება მეთილენეთერული ბმები. შემდეგ, მაღალ ტემპერატურაზე, ბმები განიცდიან დესტრუქციას და წარმოიქმნება ულღობადი და უხსნადი პროდუქტი, რაც დასტურდება 825 სმ -1 უბანში შთანთქმის ზოლის ინტენსივობის შემცირებით. ადამანტანის ჯგუფის შემცველი რეზიტი 450-550^{0}C ტემპერატურის ინტერვალში განიცდის ინტენსიურ დაშლას და ამ დროს არ წარმოქმნის კოქსს, რაც გვაძლევს იმის უფლებას, რომ რეკომენდებულ იქნას თბოდამცავი საფარველის შექმნისათვის. 2,2-ბის-(4-ოქსიფენილ)ადამანტანის მეთილოლწარმოებულების საფუველზე მიღებული პოლიმერის მაღალი თერმული მაჩვენებლები საშუალებას გვაძლევს, რეკომენდებულ იქნან ისინი რათა ისინი გამოყენებულ იქნან როგორც შემკვრელი თბო- და თერმომედეგი მასალების შესაქმნელად

Radiation resistant materials

Givi Papava, Marina Gurgenishvili*, Ia Chitrekashvili, Zurab Tabukashvili, Zurab Chubinishvili

Petre Melikishvili Institute of Physical and Organic Chemistry at Iv. Javakhishvili Tbilisi State University. 31, A.Politkovskaia str., Tbilisi, Georgia, 0186.
*marina.gurgenishvili@yahoo.com, Tel. +595 571 17 62 56

Abstract. Polymers and the composites on their base are widely used in various branches of science and technology, including nuclear one. There are a series of works where composites are considered for their application in the specific spheres such as absorption of thermal neutrons. There is no universal material, which can be used in any exploitation condition. On the basis of resole type matrixes -bisphenol formaldehyde oligomers, we have obtained polymer composites in which thermally modified natural sorbents, diatomite and boron carbides were used as fillers. Diatomite contains active amorphous silica and it is light, porous, cheap material. Matrix of polymer composites –resole type thermo-reactive oligomer, is the chemical-and radiation resistant material. Boron carbide is the universally known reactor material. The composite that does not contain a component that captures thermal neutrons, practically doesn't weaken neutron flux. At the increase of content of such component in the samples we observe marked weakening of flux density. Of course, at the long-term exploitation terms these indices will undergo deterioration due to burning-out of boron from the composition, but the rate of deterioration will depend on the radiation source capacity. It should be stated that all those composites are thermally stable up to 400^0C . Alteration of diatomite and boron carbid concentration does not affect practically therno-physical and mechanical properties of the composites. Long-term testing of the samples at the above given neutron energy and current density, (integral dose equalled to $5{,}04.10^{12}$ n/cm$^{2)}$ showed that mechanical strength of the composites at bending (it is more sensitive parameter towards irradiation) practically is not altered. Mass loss was not significant either. This refers to the fact that the accumulated dose is not enough yet for destruction of polymer matrix and for changing of macro-properties of the filler mineral.

Keywords: radiation, composition, bisphenol, neutron, diatomite

INTRODUCTION

Polymers and the composites on their base are widely used in various branches of science and technology, including nuclear one [1,2]. In special literature we come accross a series of works where such composites are considered for their application in the specific spheres such as absorption of thermal neutrons [3-5], namely in the sphere of the constructions for biological protection, which are the sources of neutron irradiation amd are the inseparable parts of the aggregates. There is no universal material of this type, which can be used in any exploitation condition . Such materials are selected according to specific technical requirements. Therefore expansion of nomenclature of such materials is a rather urgent task.

With this in view, on the basis of resole type matrixes -bisphenol formaldehyde oligomers, we have obtained polymer composites in which thermally modified natural sorbent, diatomite and boron carbides were used as fillers.

Thermally modified diatomite is interesting since it contains active amorphous silica and is light, porous, cheap material. Such composites could be used in various environment conditions, in the constructions of facilities for collective protection against various origin and intensity ($E_n < 0{,}5$ eV) thermal neutrons. As is known, materials used in the facilities for collective protection against thermal neutrons ought to satisfy a series of demands. They must be characterized by the necessary mechanical strength, capacity to absorb neutrons, high radiation, chemical and thermal stability and must be characterized by the stability of these parameters in the exploitation process.

Matrix of polymer composites –resole type thermo-reactive oligomer, is the chemical-and radiation resistant material [1, 6]. The very characteristics of diatomite used for upgrading of resole type oligomer's mechanical and physical properties markedly exceed the characteristics of the matrix, while the component that regulates the capacity for neutron absorption of the composites – boron carbide, is the universally known reactor material [7, 8].

EXPERIMENTAL

We used Kisatibi (Georgia) origin diatomite as the starting material, up to 50 mcm dispersion boron carbide (B_4C) and modified diatomite of the same dispersion. To obtain the polymer matrix we used bisphenol, which contained norbornane type groups : 4,4'-(2-norbornyliden)-diphenol, 4,4'-(hexahydro-4,7-methylenindan-5-yliden)-diphenol and 4,4'-(decahydro-1,4,5,8-dimethylennaft-2-yliden)-diphenol.

Oligomers were obtained through interaction of bisphenols with formaldehyde:

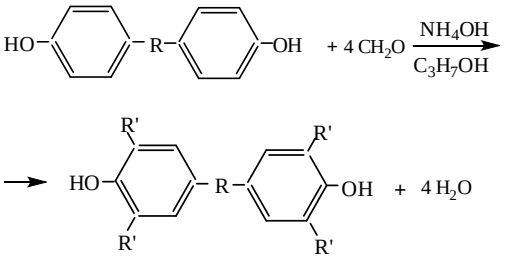

R' = -H ; $-CH_2OH$; $-CH_2OC_3H_7$

Reaction was carried out in isopropyl alcohol. Butyl mercaptan was used as a catalyst. After completion of the reaction isopropyl alcohol was isolated from the mixture by distillation. The obtained methylol derivative was dried under the vacuum at 50-60^{0}C. Study of thermal modification process of diatomite was performed over the electro-vacuum device. Diatomite content was determined by the chemical method. Spectroscopic study was carried out by UR-20 type device.

We used cylindrical as well as prism type samples obtained by compression compounding of composites. Their testing for the capacity to absorb thermal neutrons and long-term exposure of samples to radiation to such neutrons was carried out on the device of neutron-activation analysis (E_n=0,025eV, N_o=2,5.10^6 n/cm^2.sec), according to the specially developed method. Measuring error equaled to 10-16%. We observed that the bigger the absorption coefficient, the higher the accuracy of measuring. Mechanical strength of the samples was measured on Dynstat.

On the basis of the carried out studies we determined optimal terms for thermal modification of diatomite, its composition and properties. Technology for obtaining composites was developed, some physical-mechanical and radiation properties of the obtained composites were studied in a rather wide range of composite component concentrations.

Bisphenol-aldehyde oligomers are formed at the interaction of norbornan type card groups methylol derivatives, which are transformed into oligomers. At their further hardening they form resites. Mechanism of oligomer hardening can be presented according to the following scheme:

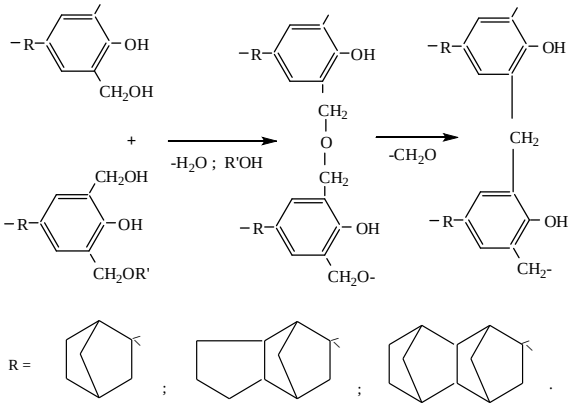

R' = C_3H_7 -

In the composite diatomite is not a neutral component. On its surface, as well as in its pores there are active functional silanole groups ≡Si=OH, which interact with reactive methylol groups of resole oligomers. This interaction can be presented in the following form:

$$\equiv Si - OH + HOCH_2 - \rightarrow \equiv Si- O - CH_2 - + H_2O$$

Chemical bond is created between diatomite and resole, which is stable and conditions high physical and mechanical properties of the composite. IR spectroscopy studies proved that at this time absorption bands characteristic for –OH groups at the 3750 cm^{-1} zone completely disappear. Resole oligomers of diatomite macro pores at the compression treatment of composites undergo structuring and macromolecules are formed, which due to their big size are unable to leave the pores without rupture of chemical bonds of the created structured oligomers. This, to a certain extent conditions high physical-mechanical indices of the created composite.

Boron carbide does not form chemical bond with the matrix, but its grains have high specific surface and because of it, they jointly with the weak molecular bond forces with polymers, are capable to create high mechanical clutch forces. Therefore, joint application of the modified diatomite and boron carbide provides obtaining of the composites possessing high indices.

RESULTS

Natural diatomite contains 3,5-8,0% associated water. Dehydration process is carried out by heating on the air, at 150 ^{o} C, within 1,5 hour. Table 1 offers composition of thermally modified diatomite in oxide form at optimal conditions (450 ^{o} C, 4 hr).

Table1. Chemical composition of thermally modified diatomite in oxide form (mass%)

#	Composition	mass%
1	SiO_2	92,03
2	Al_2O_3	4,05
3	CaO	1,27
4	Fe_2O_3	1,05
5	MgO	0,12
6	R_2O	0,18
7	Losses at heating	1,3

x) R = K, Na, etc.

As is seen, at thermal modification the chemical composition of diatomite suffers changes. At this moment organic admixtures are burnt and porosity increases from 75% to 85%. Macropore capacity changes within 0,7-2,4 cm3/g, 0,3-1,6 mcm effective radius. Presence of such filler in the boron-containing composite will probably contribute to long-term exploitation of constructions, since such residual pores will partially absorb helium which is released at the $^{10}B(n.\alpha)^{7}Li$ reaction, which will exclude swelling of the material and hence, deterioration of its properties.

Table 2 offers initial component composition of the considered polymer composites. On the basis of these compositions, by the compression compounding, we prepared the samples, which were used in further studies.

Table 2. Initial component composition of polymer composites, mass%

№	Resole	Thermally modified diatomite	Boron carbide
1	60	5	35
2	60	10	30
3	50	20	30
4	50	10	40
5	40	20	40
6	40	30	30
7	20	30	50
8	20	20	60

Table 3 offers some charactetistics of polymer composites. As is seen from the Table data, optimal physical-mechanical characteristics are inherent to the composites containing up to 40 mass % thermoreactive oligomers. Their mechanical strength at bending reaches 95 MPa. Therefore for the future studies we selected only the composites which contain matrices of this concentration.

Table 3. Some characteristics of composites

Characteristics	Composition №			
	1	2	3	4
Fluidity, mm	160-200	150-195	130-190	140-200
Resiliency kJ/m^2	10.0	8.5	12,0	10,0
Strength at bending, MPa	60,0	60,0	90,0	80,0
	5	6	7	8
Fluidity, mm	120-190	110-180	90-160	100-170
Resiliency kJ/m^2	13,0	12,0	7,0	7,5
Strength at bending, MPa	95,0	95,0	70,0	70,0

DISCUSSION

Table 4 offers the results obtained in the process of testing of these compositions for absorption capacity with respect to thermal neutrons. Just for the comparison Table offers two composites. Both compositions contained 40 mass% polymer matrix. In one of them the remaining 60 mass% was thermally modified diatomite, and in the other – boron carbide.

Table 4. Influence of composite composition on absorption capacity of thermal neutrons x

Sample composition	Thickness, mm	Test duration min	Rate of irradiation decrease
40 mass% TRO+ 60 mass.% TMD	6	20	1.05
40 mass% TRO + 30 mas.% TMD+ 30% B_4C	5	20	17
40 mass.% TRO + 20 mass% TMD + 40% B_4C	5	20	23
40 mass% TRO + 60 mass.% B_4C	6	20	39

x)TRO- thermo-reactive oligomer; TMD-thermally modified diatomite.

As is seen from the Table data the composite that does not contain a component that captures thermal neutrons, practically doesn't weaken neutron flux. At the increase of content of such component in the samples we observe marked weakening of flux density. Of course, at the long-term exploitation terms these indices will be deteriorated due to burning-out of boron from the composition, but the rate of deterioration will depend on the radiation source capacity. It should be stated that all those composites are thermally stable up to 400^{0}C temperature. Alteration of diatomite and boron carbid concentration does not affect practically therno-physical and mechanical properties of the composites.

Long-term testing of the samples at the above given neutron energy and current density, (integral dose equalled to $5{,}04.10^{12}$ n/cm$^{2)}$ showed that

mechanical strength of the composites at bending (it is more sensitive parameter towards irradiation) practically is not altered. Mass loss was not significant either. This refers to the fact that the accumulated dose is not enough yet for destruction of polymer matrix and for changing of macro-properties of the filler mineral.

CONCLUSION

Processes for obtaining of the resole type bisphenol-formaldehyde oligomer and for thermal modofication of natural diatomite have been studied. Polymer compositions are considered, which contain 20-60% oligomer, 5-30 mass% thermally modified diatomite and 30-60% boron carbid. It was proved that the composites containing 40 mass% matrix are characterized by optimal mechanical indices. They are thermally stable up to 400 ^{0}C temperature. Composites capacity to absorb thermal neutrons (E_n=0,025eV) depends on boron carbid concentration in it. By the increase of boron concentration in the composites from 30% to 60%, neutron current intensity decreases 17-40-fold. At the effect of integral dose of thermal neutrons - 5.10^{12} n/cm^2 , the mechanical strength of the composites practically doesn't suffer changes.

REFERENCES

[1] Ivanov V.S. Radiation Chemistry of Polymers, L., "Khimia", 1988

[2] Sudareva N.A. et al. Polymer Materias as Conservers of Radiation Wastes. Atom Energy, vol.74, # 2, 1993

[3] Kozlov V.F. Reference Book for Radiation Security. M., "Energoizdat" 1991.

[4] Plastic Mass for Neutron Absorption, Patent. ДД№3000574. Cl..G 21 F1/12 . 1992.

[5] Material for Thermal Neutrons Absorption, Patent of Japan. N3-6587884. Cl..G 21 F1/12. 1993.

[6] Method for obtaining thermally stable resole type tars. Papava G.Sh, Abnerova S.V. Sergeev V.A., Shitikov V.K., Tsiskarishvili P.D.,Vinogradova S.V., Korshak V.V.,Gribova I.A. Author's Certificate, USSR, № 454813 (1974).

[7] Radiation effects of the glass silicia. Proceedings of the "12th International Conference on Radiation Physics and Chemistry of Inorganic Materials". Tomsk, Russia, September 23-27, 2003.

[8] Brief Reference Book for Engineers- Physicists.Comp. by Fedorov N.D M.,1961.

რადიაციულად სტაბილური მასალები

გივი პაპავა, მარინა გურგენიშვილი*, ია ჩიტრეკაშვილი, ზურაბ თაბუკაშვილი, ზურაბ ჩუბინიშვილი

*თსუ, პეტრე მელიქიშვილის ფიზიკური და ორგანული ქიმიის ინსტიტუტი, 0186, თბილისი, პოლიტკოვსკაიას ქ#31, *marina.gurgenishvili@yahoo.com* ტელ. +595 571 17 62 56

რეზიუმე. პოლიმერები და მათ ბაზაზე მიღებული კომპოზიციები ფართოდ გამოიყენება მეცნიერების სხვადასხვა დარგში და ტექნოლოგიაში, ბირთვულის ჩათვლით. მრავალი ნაშრომია ცნობილი, სადაც განხილულია კომპოზიციები და მათი გამოყენება სპეციფიურ სფეროებში, როგორიცაა მაგალითად თერმული ნეიტრონების აბსორბციისათვის მათი გამოყენება. დღემდე არაა ცნობილი ისეთი უნივერსალური მასალა, რომლის გამოყენებაც შესაძლებელი იქნებოდა ნებისმიერი ექსპლუატაციის პირობებში. რეზოლის ტიპის მატრიცების -ბისფენოლ-ფორმალდეჰიდური ოლიგომერების საფუძველზე, ჩვენს მიერ მიღებულია პოლიმერული კომპოზიტები, რომლებშიდაც შემავსებლად თერმულად მოდიფიცირებული ბუნებრივი სორბენტი დიატომიტი და ბორის კარბიდი იყო გამოყენებული. დიატომიტი შეიცავს აქტიურ ამორფულ სილიციუმს, მსუბუქი, ფოროვანი და იაფი მასალაა. პოლიმერული კომპოზიციების მატრიცა - რეზოლის ტიპის თერმორეაქტიული ოლიგომერი არის ქიმიურად და რადიაციისადმი მედეგი მასალა. ბორის კარბიდი კი ცნობილია, როგორც უნივერსალური, რეაქტორებში გამოყენებული მასალა. კომპოზიტი, რომელიც არ შეიცავს ისეთ კომპონენტს, რომელიც იჭერს თერმული ნეიტრონებს, პრაქტიკულად ვერ ასუსტებს ნეიტრონების ნაკადს. ასეთი კომპონენტის შემცველობის გაზრდისას შეინიშნება ნეიტრონების ნაკადის სიმკვრივის შესუსტება. რასაკვირველია, ხანგრძლივი ექსპლუატაციის პირობებში ეს მაჩვენებლები შესუსტდება. კომპოზიციიდან ბორის მოცილების სიჩქარე დამოკუდებულია რადიაციის წყაროს სიძლიერეზე. დადგენილია, რომ ყველა ეს კომოზიტი თერმომედეგია 400^{0}C-ზე მაღალ ტემპერატურაზე. დიატომიტისა და ბორის კარბიდის კონცენტრაციის შემცირება პრაქტიკულად არ ახდენს გავლენას კომპოზიტების თერმო-ფიზიკურ და მექანიკურ თვისებებზე. ნიმუშების ხანგრძლივი პერიოდის განმავლობაში გამოცდამ გვიჩვენა, რომ კომპოზიტების მექანიკური სიმტკიცე ღუნვაზე პრაქტიკულად არ იცვლება. მასის დანაკარგი არ იყო მნიშვნელოვანი. ეს მიუთითებს იმ ფაქტზე, რომ აკუმულირებული დოზა არაა საკმარისი პოლიმერული მატრიცის დესტრუქციისათვის და მინერალური შემავსებლის მაკრო თვისებების ცვლილებისათვის.

Antianemic therapeutic-prophylactic drug

Leila Japaridze*, Tsiala Gabelia, Eter Salukvadze, Nana Osipova, Tamar Kvernadze, Omar Lomtadze

Petre Melikishvili Institute of Physical and Organic Chemistry at Iv. Javakhishvili Tbilisi State University. 31, A.Politkovskaia str., Tbilisi, Georgia, 0186.
**Corresponding lelojaparidze@gmail.com*

Abstract. Research goal was obtaining of ant stress, ecologically clean preparation with high bio-accessibility (bio-digestibility) and low toxicity intended for oral administration, and determination of prospects of its use in the area of live-stock farming (namely pig breeding). Manufacturing method of mentioned preparation is elaborated, which foresees the use of freshly-prepared iron carbonate paste synthesized via interaction of $FeCl_2 \cdot 4H_2O$ and $NaHCO_3$ as a source of main active component – Iron (II); interaction of iron carbonate and cobalt chloride with complex formation with monosaccharide D-Fructose having hemo-stimulating properties; concentrating of complex solutions up to syrup consistency; its extraction from reaction area in the free state using alcohol-ether mixture, its treatment with acetone, ether, and drying in vacuum conditions; infraction of complex mixtures containing certain quantities of Fe(II) Fructose and Co(II) Fructose with aqueous Askan-clay (through ultrasonic material dispersion); preparation of water suspension, its drying, grinding, manufacturing of solid form of preparation for oral administration. The preparation manufactured by mentioned method contains (in mass %): Fe(II)-Fructoze 15.75-31.6, [Fe(II)-3.75-7.5], Co(II)-Fructose 0.28, [Co(II)-0.07], natural Askan-clay 68.2-36.5.The offered method provides getting of highly digestible, functional targeted product with maximum content of Fe(II). Therapeutic and preventive efficiency of manufactured preparation was tested on animals under study, namely on store pigs (toxicity of preparation was preliminary tested on laboratory white rats). Experiment result was expressed in getting rid of complications (iron deficiency anemia, diarrhea-dyspepsia) caused by stress factors related to termination of breast feeding of store pigs and food change, as well as in their normal growth and development, normal blood chemistry values and live weight gain.

Keywords: Antianemic Fe(II)-complex, Bentonite, Application in pig breeding, Metal deficiency anemia

INTRODUCTION

Metal deficiency anemia in animals is caused by deficit of indispensable microelement of vital importance – iron. Iron deficiency anemia in newly-born pigs is predetermined by significant difference between growth rates of newly-born pigs and quantity of microelements delivered with mother's milk. Due to iron deficiency takes place functional disturbance of hematogenic (blood-forming) organs, there is observed the low level of hemoglobin and erythrocytes, vulnerability towards different diseases (diarrhea, body dehydration etc.). Against the background of anemia diseased pigs experience development of immunodeficiency, suppression of erythropoiesis, takes place development of secondary diseases of digestive, breathing and other organs. Based on the above mentioned it can be said that anemia is a general pathological process of many body organs and system as a whole. As a result pig-breeding branch experiences significant economic damage. In the major part of large pig-farming enterprises pig anemia reaches 100%, while mortality index attains 10-15% [1-5].

Based on the above mentioned it is topical to offer a preparation for pig-breeding branch, which will supply animals with additions containing biologically active microelements, aminoacids, hydrocarbons, vitamins etc. under conditions of intensive growth and metabolic processes developing with speed-limit in organism that is characteristic for pigs.

Use of non-traditional natural mineral additions, as the cheap source of calcium, phosphorus, silicium, magnum and other indispensable micro- and macroelements easily digestible for animals is especially important. Various adsorbents, including natural minerals – zeolites, glauconites, bentonites, marls etc., are added to animal ration with a mentioned purpose. Priority is always given to food additions prepared on the basis of cheap, local natural raw materials.

Research goal was the manufacturing of antianemic preparation containing biogenic microelements Fe(II) and Co(II), hemo-stimulating organic compound D-fructose (Fru) and natural mineral, bentonite-Askan-clay used as an adsorbent, as well as its testing in live-stock farming (pig-breeding) for treatment and prevention of stress conditions related to termination of breast feeding of store (young) pigs.

Separation from mother pig is the most critical moment of piggies' life – from the birth till a killing. In case of early termination of breast breeding period (26^{th} day from the birth) two stress-factors – separation from mother breast and food change have significant negative impact on animals. The mentioned negative development may cause recurrence of iron deficiency anemia (that was no more registered after two-times injection of iron-containing injection solution to piglets). There are frequent manifestations of complications in functioning of gastrointestinal tract (dyspepsia-diarrhea). As a result takes place deterioration of general physical-physiological and blood chemistry values of animals [6-13].

Experimental part

At the first stage Fe(II),Co(II))-D-Fru complexes are synthesized separately, under conditions of constant stirring, as a result of interaction between corresponding salts and monosaccharide D-fructose. Fe(II),Co(II)-D-Fru complexes are obtained in the alkaline medium (pH = 10-11). It should be noted that the yield of the complex Fe (II) with fructose, obtained resulting from interaction of iron source FeCl2.4H2O and D-fructose is low and equals to 74.34%. 25.66 % of total iron quantity is in the oxidized Fe(III) condition [14]. It is known that iron (III) ions, in contradistinction from iron (II) ions are characterized by low bio-accessibility [15]. In order to manufacture the targeted product with maximum content of Fe(II) the method is developed that envisages the use of freshly prepared $FeCO_3$ as an iron source.

$FeCO_3$ was obtained through the interaction of hot saturated solutions of $NaHCO_3$ and $FeCl_2.4H_2O$-, under conditions of constant stirring. Reaction runs with gas emission (CO_2). After sedimentation, the water was removed from a formed precipitation through decantation. It is washed out thoroughly first by flowing water and then by distilled water, up to removal of chlorine ions. Green-colored iron (II) carbonate is obtained that is kept under water layer (in order to avoid the bivalent iron ions oxidation to trivalent ones).

Solutions of synthesized complexes are concentrated up to sirup consistency in the vacuum-evaporator at 60°C. Extraction of the complexes in the pure form from the reaction site is made by the mixture of alcohol-ether solutions. Complexes are washed out by acetone, ether, and finally are dried using the lyophilisation method.

The second stage implies the bentonite-Askan clay drying at 90-100°C, down to a constant weight, its swelling by the distilled water (ratio clay : water = 1:5), paste preparation (moisture 25%). After 24 hours 20% of hydrochloric acid is added to a swelled, paste consistency Askan-clay (alkaline bentonite, pH of which is 9,15) in order to equate its acidity to 3.5 (according to preliminary researches conducted under conditions of different pHs it is established that a maximum adsorption at the Askan-clay surface is reached in the range of pH = 3.5-5.0. So, the mixtures of iron (II) and cobalt (II) complexes are entered into the prepared paste (pH = 3.5), which is treated for 1 hour via ultrasound dispersion method at 22 kHz. Then the distilled water is added. Water suspension is obtained. Suspension is dried at 60-70°C, is grinded in the ball mill and is sieved in 6400 hole/cm^2 sieve. Finally, the solid form of antianemic medical and preventive preparation for oral administration is obtained. The composition of the preparation is given in Table 1.

Table1. Antianemic preparat for oral administration, mass. %

Preparative Form	Component	Content
Preparation for oral administration	Fe(II)Fructose	15.75-31.6
	D-Fructose	12.0-24.1
	Fe(II)	3.75-7.5
	Co(II)Fructose	0.28
	D- Fructose	0.21
	Co(II)	0.07
	Natur.Askanclay	68.2-36.5

Manufacturing of medical and preventive preparation against animal anemia foresaw synthesis of Fe(II) and Co(II)-fructose complexes separately, under different temperature conditions, as a result of interaction of corresponding salts and D-fructose; infriction of mixture containing certain quantities of obtained complexes (through ultrasonic material dispersion) with Askan-clay water suspension paste, drying of obtained product, grinding, and manufacturing of solid form of preparation for oral administration. It is noteworthy that the yield of Fe(II) fructose obtained as a result of interaction of $FeCl_2 \cdot 4H_2O$ (used as iron source) and D-fructose is low and equals to 74.34%. 25.66% of total iron quantity is in oxidized Fe(III) condition [14]. It is known that Fe(III) ions in contradistinction from Fe(II) ions are characterized by low bio-accessibility (bio-digestibility) [15]. With the purpose of preparation of Fe(II) targeted product with a maximum content there is elaborated a method, which foresees the use of newly prepared $FeCO_3$- as the iron source.

$FeCO_3$ was obtained through interaction of hot saturated solutions of $NaHCO_3$ and $FeCl_2.4H_2O$-, under conditions of constant stirring. Reaction runs with emission of gas (CO_2). By means of decantation water is removed from the deposit formed after sedimentation. Afterwards it is washed thoroughly first with flowing water, and then by distilled water up to removal of chlorine ions. As a result, green-colored iron(II) carbonate is obtained, which is kept under water layer (in order to get rid of oxidation of bivalent iron ions into trivalent ones).

Studies related to determination of medical and preventive efficiency of preparation manufactured according to abovementioned method and in regard to weight change of animals being investigated was conducted in private pig-breeding farm located in Zahesi Village (farmer G. Tsiklauri), on 29 store pigs of three nests. On the basis of the agreement biochemical studies of blood samples were carried out in the laboratory of the Institute of Veterinary Medicine at Georgian Agrarian University (here should be noted that the preparation was primarilytested on toxicity in laboratory conditions, on 20 white rats. It was established that preparation with 3.75-7.5% content of iron (II) is non-toxic).

Experimental pigs were divided into three groups according to analogue principle for testing of manufactured preparation. With the purpose of preparation selection 20-day pigs were fed (along with mother's milk) once a two days by 0.25-0.5 grams of preparation dissolved in water (along with 250 grams of liquid food). Starting with 26^{th} day they were nourished everyday with 0.5-1.0 gram per 450 grams of food in the form of solid addition. Food addition for I group of pigs (12 piggies) contained 7.5-9.0% of elementary iron, II group (12 piggies) – 3.75-7.5%, while the food for III group of animals (5 piggy's) didn't contain any additions.

In order to determine the effect of antianemic solid preparation on the organism a control slaughter of 2-month pigs (n = 3) after 1, 6 hours from preparation administration and in the end of study – on the 40^{th} day was conducted. The test material for pathanatomical and histological analyses was taken from subdermal tissue, muscles, differently-located lymphatic glands and parenchymal organs. Initial fixation of material was made in 10% formaldehyde solution (formalin), with its further transfer to 15% solution. Material was formed in paraffin. Hematoxylineozine solution was used slice taking. In case of necessity Sudan-3 was used for study of fatty degeneration and lipids.

Results and discussion

As a result of systematic observations over store pigs there were established that antianemic preparation has a positive impact on animals, and there was no negative development, in particular, no expected deterioration of general physical-physiological condition and blood chemistry values caused by stress-factors related to termination of breast breeding period (Table 2).

Table 2. Relative efficiency of antianemic preparation on biochemical indiceof store (young) pigs, I– preparation with 7.5-9.0% content of Fe(II), n=12; II– preparation with 3.75-7.5% conten of Fe(II), n=12; III–control group, n=5

Group	Age, days			
	20	30	40	50
	hemoglobin in the blood, g/l			
I	96.5	101.3	109.6	112.2
II	102.0	109.1	118.0	120.5
III	82.3	84.3	86.1	88.3
	Erythrocytes in the blood, 10^{12} l			
I	7.2	7.4	7.7	7.9
II	7.5	7.8	8.1	8.5
III	5.0	5.3	5.4	5.6
	Iron(II) in the blood, mkmol/l			
I	25.8	26.0	26.5	26.8
II	27.2	28.5	27.9	28.5
III	19.5	19.6	20.3	22.6

According to pathanatomical and histological studies in an hour after preparation intake the micro-morphological structure of pig body was preserved, slightly expressed serous fluid, single leucocytic infiltration and slightly expressed vascular response in the form of hyperemia were registered in venous capillaries. Micro- and macro-morphological indicators in the heart, kidneys and lungs were within the norm, and no abnormalities were registered in them.

In the end of the research, at the 40^{th} day, the morphological structure of lymphatic nodes and organs were within a norm. According to micro- and macro-morphological researches it was established that the preparation use don't cause any changes in dermal, subdermal tissue and internal organs and organism response to the preparation is within the norm.

It should be noted that slightly expressed capillary hyperemia registered in the derma itself and in regional lymphatic nodes, and perivascular infiltration that was not observed in 6 hours after preparation intake, cannot be the result of manifestation of preparation toxicity, its dermal accumulation and other adverse effects. The mentioned fact is most likely the indicator of stress reactions caused by manipulations on pigs (blood taking for analysis, food change).

High therapeutic and preventive effect of targeted product is predetermined by:

- Chelate complex with high content of indispensable microelement – Fe(II) with hemo-stimulating compound D-fructose [16-17];
- Complex of cobalt – ultra component promoting iron accessibility (digestibility) with D-fructose [18-19];
- Adsorbent – local, ecologically clean, non-toxic, natural Askan-clay, thanks to which the preparation acquires the ability of double, parallel action – hemo-stimulating metal complexes fill a deficit of microelements in the organism, while Askan-clay, at the expense of high adsorbing, catalytic and prolonging properties will adjust functioning of gastrointestinal tract. At the same time, it will provide gradual, planned release of microelement complexes from clay surface (which is naturally released from organism), and eliminates or reduces to the minimum a side effect permanently accompanying anemia [19-20];
- Bioaccessibility of preparation is also improved by treatment of Askan-clay and metalcomplex-containing system via ultrasonic material dispersion method, with dispersion of preparation particles sized up to nanosize under conditions of 22 kHz (the mentioned method is used for improvement of pharmacological and therapeutic properties of medicinal products and is considered as a new prospective direction of medicine [21-23].
- Manufactured preparation is kept in a dark, hermetically sealed vessel. Medical and preventive composite preparation for metal deficit has to contain 7.5-9.0% of iron (II). In case of different iron concentration takes place the correction of mentioned content.

According to studies carried out using adsorption-desorption processes, infrared-spectrophotometric, thermographic, complexonometric titration, photometric analysis [24-26] and other physical and chemical methods there was shown that synthesized iron-fructose complex contains maximum quantity of bivalent iron. Adsorption of metal complexes on the clay surface is of physical nature that predetermines prolonging properties of preparation. According to studies carried out on rotation viscosimeter Reotest-2 in the pH=2.5-3.0 range (acidity of gastric juice of store pigs) the offered preparation meets the requirements applied to reological and structure-forming parameters of medicinal products.

Conclusions

So, the antianemic medical and preventive preparation with 3.75-9.0% content of iron(II) is not toxic, it ischaracterized by hemo-stimulating. antistress properties that provides stable liveweight gain of store pig s in comparison with control analogues (Table 2, 3). As is seen from the Table, the preparation with 3.75-7.5% content of Fe(II**)** is the optimal one.

Table 3. Impact of preparation manufactured according to offered way on live weight of young pigs (20-120 days), I – preparation with 7.5-9.0% content of Fe(II), n=12, II – preparation **with 3.75-7.5% content of Fe(II), n=12; III – control group, n=5**

Group	Pigs age, days					
	20	30	40	50	60	120
	live weight, kg					
I	4.50± 0.2	7.30± 0.2	9.55± 0.4	13.22± 2.42	16.85± 2.29	100.20 ±3.5
II	4.90± 0.3	7.80± 0.3	9.80± 0.4	13.58± 2.5	17.3±2. 40	102.0 ±3.1
III	4.00± 0.3	6.80± 0.4	8.00± 0.4	12.50± 2.45	15.80± 2.5	98.45± 2.8

Acknowledgement

Authors express gratitude for funding the Grant project #FR/436/6-480/14 of Shota Rustaveli National Science Foundation, within a framework of which the study was conducted.

References:

[1] Mikhailova O.A., Tendencies of the Word Swine breeding development. *Herald of Agrarian Science,* 2018 , 3*6-45*.
[2] Bushev A.V., Anemia in young pigs. Bushev A.V., Ten E.V., 2007**,** *"Farm livestock veterinary*", 2003**,** no. *10, 45-49* p. (in Russian).
[3] Misik A., Pig breeding industry development in countries worldwide. *Svinovodstvo (Pig breeding)*,2006, no.*1,18-20* (in Russian).
[4] Nikoladze M.G**.,** Diagnostics and prevention of pigs anemia and immune deficiency, *Abstract of diss. of cand. of veterinary sciences,* 2003,Vitebsk, *19 p*. (in Russian).
[5] Biryukov M.V**.,** Iron deficiency anemia of pigs, *Svinovodstvo (pig breeding),* 2013, no. 5**:** *45-49* (in Russian).
[6] Kairov V.P., Growth and development of early weaned pigs under action of biologically active agents (additions), *Herald of Gorky State Agrarian University,* 2010, *47,no. 1, 63-67.*

[7] Avilov Ch.K., Impact of stress-factors on resistance of pig organism, *Veterinary of farm animals*, 2006 , no. *6 , 46-47*(in Russian).
[8] Barannikov V.A**.**. Live weight dynamics and growth intensity of pigs as a result of use of antistress preparations, *Proceedings of Kuban State Agrarian University*, 2012**,** *1, 39, 90-92* (in Russian).
[9] Kopteva Yu.S., Metabolism and productivity of store pigs when using probiotic complex under conditions of industrial technology, *Abstract of diss. of cand. of biological sciences*, 2011, (in Russian).
[10] Lamarin A.A., Pig diseases, Lamarin A.A., Bolocky I.A., Barankov A.I, Reference book. Teaching aid, SPb., *Lan*, 2008, *640* p. (in Russian).
[11] Khodyreva I.A., Sadomov N.A,Store pigs intestinal micro-biocenosis correction using the preparations of microbiological synthesis, *Belarusian State Academy of Agriculture, Gorky, Mogilev district, Republic of Belarus* . 2013**,** pp.*15-20* (in Russian).
[12] Kokorev V.A., Optimization of mineral nutrition of farm animals. *Zootechnia*, 2013, no. *7***,** pp.*12-16* (in Russian).
[13] Shulaev G.M., Dobry V.N., Bioplexes of microelements in composition of premixes for store pigs, *Svinovodstvo (Pig breeding)*, 2003, no. 6, pp. *30-34* (in Russian).
[14] Gabelia Ts, L. Japaridze, E. Salukvadze, L. Kashia, S. Urotadze**.**. Determination of Fe(II)/Fe(III)-ions ratio in the iron-fructose complex, *Bulletin of Georgian National Academy of Sciences*, 2009, vol. *35*, no. *1, 36-39* (in Georgian).
[15] Stuklov N.I., E.N. Semyonova, Treatment of iron deficiencyanemia, What is more important, efficiency or tolerability? " *Journal of International Medicine*",2013, vol. *2*, no. *1***,** pp. *47-55* (in Georgian).
[16] Gabelia Ts., L. Japaridze, E. Salukvadze, L. Kashia, S. Urotadze, Synthesis and study of iron (II)-fructose complex, *Bulletin of Georgian National Academy of Sciences, chemical series*, 2008**,** vol. *34*, no. *4***,** pp. *401-404* (in Georgian).
[17] Salukvadze E., L. Japaridze, C. Gabelia, O. Lomtadze, Antianemic preparation on the basis of chelate complex of metals and natural alumosilicates, *Chemistry of coordination compounds: actual problems of analytical chemistry, 16-17 November,* 2017 , Baku, *56-57* (in Russian).
[18] Gabelia Ts., L. Japaridze, E. Salukvadze, S. Urotadze, Method for medication manufacturing on the basis of Askan-clay, *GE P 2014, 6144* B (in Georgian).
[19] Gabelia Ts., L. Japaridze, E. Salukvadze, L. Kashia, K. Ebralidze, Study of reological properties of Co-fructose-Askangel, *Herald of Georgian National Academy of Sciences, chemical series*, 2009,vol. *35*, no. 3, pp. *337-339* (in Russian).
[20] Japaridze L., Ts. Gabelia, E. Salukvadze, N. Osipova, T. Kvernadze, K. Ebralidze Obtaining and study of modified Askan clay, *Bulletin of Georgian National Academy of Sciences, chemical series*, 2017, vol. *43*, no.1**,** pp. *93-96* (in Georgian).
[21] *Coffey, Rebecca August, 20 Things You Didn't Know About Nano-technology, 2012, Discover , 31,6.*
[22] *Laurence, Jeremy, Scientists develop nanoparticle method to help tackle major diseases, 2012, (18 November).*
[23] Japaridze L, Ts. Gabelia, E. Salukvadze, N. Osipova, T. Kvernadze, O. Lomtadze, Iron Carbonate synthesis Method Aimed at obtaining Antianemic Preparation, *5th International Conference "Nanotechnologies"*, 2018**,** Tbilisi, *80-81*.
[24] Japaridze L., Ts. Gabelia, E.Salukvadze, O. Lomtadze, Investigation of metal-complex compositions by the metal-indication method, *Chemistry of coordination compounds: actual problems of analytical chemistry*, 2017**,**16-17 November, Baku**,** pp. *56-57*.
[25] Beshkenadze I., M. Gogaladze, N. Klarjeishvili, O. Lomtadze, G. Chagelishvili, L. Gogua. Results of the Study of $M_2^{I}{\cdot}M^{II}{\cdot}L_2{\cdot}nH_2O$ Type Citrates, *Annals of Agrarian Science*, 2018, *16***,** pp.*7-11*.
[26] Beshkenadze I., A. Chagelishvili, M. Gogaladze, G. Chagelishvili, N. Klarjeishvili, I. Lomtadze, Z. Molodinashvili, Study of Physiological Activity of Microelements and Glutamine Acid-containing Chelate Citrates, *Annals of Agrarian Science*, 2017, *15* **,** pp. *243-246.*
[27] Japaridze L., C. Gabelia, E Salukvadze, O. Lomtadze, G. Kozmanashvili, Study of Metal-Complexes Composition by Metal-Indicatory Method, *Bulletin of the Georgian National Academy of Sciences*, 2018**,** vol.*12*, no. *2, 45-49.*

ანტიანემიური სამკურნალო-პროფილაქტიკური საშუალება

ლეილა ჯაფარიძე*, ციალა გაბელია, ეთერ სალუქვაძე, ნანა ოსიპოვა, თამარ კვერნაძე, ომარ ლომთაძე

ივანე ჯავახიშვილის სახ. თბილისის სახელმწიფო უნივერსიტეტის პეტრე მელიქიშვილის ფიზიკური და ორგანული ქიმიის ინსტიტუტი, 0186

რეზიუმე. კვლევის მიზანს შეადგენდა პერორალურად მისაღები, ანტისტრესული, მაღალი ბიოათვისებადობის, დაბალი ტოქსიურობის, ეკოლოგიურად სუფთა პრეპარატის მიღება, მეცხოველეობის სფეროში (მეღორეობა) მისი გამოყენების პერსპექტივის განსაზღვრა. შემუშავებულია აღნიშნული პრეპარატის მიღების მეთოდი, რომელიც მთავარი მოქმედი კომპონენტის- რკინა (II) წყაროდ ითვალისწინებს ახლადმომზადებული, $FeCl_2.4H_2O$ და $NaHCO_3$ ურთიერთქმედებით სინთეზირებული რკინის კარბონატის

პასტის გამოყენებას. რკინის კარბონატის და კობალტის ქლორიდის ურთიერთქმედებას ხსნადი კომპლექსების წარმოქმნით ჰემომასტიმულირებელი თვისებების მონოშაქრ D-ფრუქტოზასთან. კომპლექსების ხსნარების დაკონცენტრირებას სიროპის კონსისტენციამდე. სარეაქციო არედან თავისუფალი სახით ექსტრაგირებას სპირტ-ეთერის ნარევით, დამუშავებას აცეტონით, ეთერით, გაშრობას ვაკუუმის პირობებში. განსაზღვრული რაოდენობების შემცველი Fe(II) ფრუქტოზის და Co(II) ფრუქტოზის კომპლექსების ნარევის შეზელას (ულტრაბგერითი დისპერგირების გზით) წყლიან ასკან-თიხასთან. წყალსუსპენზიის მომზადებას, გაშრობას, დაფქვას, პრეპარატის პერორალურად მისაღები, მყარი ფორმის მომზადებას. აღნიშნული ხერხით მომზადებული პრეპარატი შეიცავს მას.%: ლიგანდს D- ფრუქტოზას- 24,2-29,0; რკინას (II)- 7,5-9,0; კობალტს (II)- 0,007; ბუნებრივ ასკან-თიხას 68,3-62,0. შემოთავაზებული მეთოდი უზრუნველყოფს Fe(II) მაქსიმალური შემცველობის, მაღალთვისებადი, ფუნქციონალური მიზნობრივი პროდუქტის მიღებას. მომზადებული პრეპარატის თერაპიული და პროფილაქტიკური ეფექტურობა მოსინჯული იყო საკვლევ ცხოველებზე- მოზარდ გოჭებზე. (წინასწარ პრეპარატის ტოქსიურობა გამოცდილი იყო ლაბორატორიულ თეთრ ვირთხებზე). ექსპერიმენტის შედეგი გამოიხატა მოზარდი გოჭების მეძუძურობის დასრულებასთან და საკვების ცვლილებასთან კავშირებული სტრესული ფაქტორებით გამოწვეული გართულებების (რკინადეფიციტური ანემია, დიარია-დისპეპსია), თავიდან აცილებაში, ცხოველების ნორმალურ ზრდა- განვითარებაში, სისხლის ბიოქიმიურ მაჩვენებლებში და ცოცხალი მასის ნამატში.

Complexes of Biometals with Anesthetic Substance

Koba Amirkhanashvili*, Nani Zhorzoliani, Lela Metreveli, Vladimer Tsitsishvili
Petre Melikishvili Institute of Physical and Organic Chemistry of Ivane Javakhishvili Tbilisi State University, 31 Politkovskaia str., 0186,Tbilisi Georgia, amirhan@hotmail.com ,

Abstract. Nickel(II) and Cobalt(II) complexes of lidocaine (2-diethylamino-N-(2,6-dimethylphenyl)acetamide, (Lid),or Novocain-4-amino-2-(diethylamino)ethyl ester monohydrochloride(Nov) with general formula $(LidH)_2[MeX_4]\cdot 2H_2O$,$(NovH)_2[MeX_4]\cdot 2H_2O$,were X-NCS´,CI´,Br´ have been synthesized and characterized by chemical composition, IR spectra, thermoanalytical TG-DTG/DTA and X-ray diffraction methods. Their solubility in water and organic solvents has been studied. The structure of the compounds is proposed based on infrared absorption spectrum analysis, X-ray diffraction analyses and the literature data: In compounds, the central ion coordination with acidoligands generates tetrahedral anion, while the ligands in the form of protonated cations remain in an outer coordination field.

Keywords: Coordination compounds, lidocaine, ligands, metal ions, novocain, pharmacological applications,

Transition metals play important roles in biological processes and the field of knowledge concerned with the application of inorganic chemistry to therapy or diagnosis of disease is medicinal inorganic chemistry . The introduction of metal ions or metal ion binding components into a biological system for the treatment of diseases is one of the main subdivisions in the field of bioinorganic chemistry. Nowadays, the bioinorganic chemists target the heterocyclic ligands and their metal complexes to study their pharmacology as the main focus of research [1-5]. A wide range of biological activities such as antibacterial, antifungal, antitumor and antiviral activities are exhibited by the nitrogen-containing organic compounds and their metal complexes. Transition metal complexes offer two distinct advantages as DNA-binding agents [6-10].

Among the metal ions regarded as coordination centers of potential anticancer agents, platinum and ruthenium ions are commonly explored. However, there is an emerging curiosity in the synthesis of cheaper first-row coordination compounds as efficient DNA binders with potential cytotoxic activity. Hence, herein the attention is focused primarily on the research concerning with a few pharmacological activities of the cheaper and easily available firstrow coordination compounds V(IV), Co(II), Ni(II), Cu(II) and Zn(II) complexes. Moreover, these metal ions are the essential elements present in the biological intracellular environment of living organisms. They are most abundantly found trace elements present in biological systems together with iron and olso most of the metalloproteins have these elements . These metal ions are nowadays present in several inorganic pharmaceuticals used as drugs against a variety of diseases, ranging from antibacterial and antifungal to anticancer applications [11-15].

Study of biometal-complexes with organic ligands has one more significant aspect: traditionally for treatment of microelement deficency in organisms, inorganic salts or mixes of those salts and bioorganic compounds are used. They are characterized by low bio-permeability. Parallel to therapeutic effects, undesirable side effects may develop by receiving metal ions in excess. In contrast, coordination compounds are characterized by good water-solubility and stability in wide pH range; they do not produce aggressive free radicals; due to prolongation effect, they provide proper quantity of microelements. Thus, scientists came to obvious conclusion: microelements should be introduced into living organism primarly by coordinately bound structure with biometals.Organisms have developed strategies to extract transition metals from the environment and use the metals in electron-transfer reactions, reaction of small molecules, Levis-acid catalysis and the generation of reactive organic radicals. Among biometal-coordination compounds their complexes with anesthetics are significant. It is well known that modern medicine can't be imagined without anesthetics (Novocain, trimecaine, lidocaine et eal); In regards of chemistry, these compounds are potential ligands, containing donor atoms and atom groups. Lidocaine, Novocain and Trimecaine belong to the family of drugs called local anesthetics. [16-

18]; This medicine prevents pain by blocking the signals at the nerve endings in the skin. This medicine does not cause unconsciousness as general anesthetics do when used for surgery. Lidocaine [2-diethylamino-N-(2,6-dimethylphenyl) acetamide]: Very versatile anesthetic that is used for topical, regional, neuraxial, and intravenous anesthesia[19-20] Lidocaine solutions are widely used for cardiac arrhythmias. A 2013 review on treatment for neonatal seizures recommended intravenous lidocaine as a second line treatment, if phenobarbital fails to stop seizures.[21].Lidocaine stabilizes the neuronal membrane by binding to and inhibiting voltage-gated sodium channels,thereby inhibiting the ionic fluxes required for the initiation and conduction of impulses and effecting local anesthesia.Trimecaine and Lidocaine hydrochloride are used as local anesthetics for infiltration and conductor anesthesia[22]. Novocain (Procaine)-4-amino-2-(diethylamino)ethyl ester monohydrochloride is a local anesthetic of the ester type that has a slow onset and a short duration of action. It is mainly used for infiltration anesthesia, peripheral nerve block, and spinal block.[23]. Novocain is readily absorbed following parenteral administration and is rapidly hydrolyzed by plasma cholinesterase to aminobenzoic acid and diethylaminoetanol. A vasoconstrictor may be added to the solution of Novocain to promote local hemostasis, delay systemic absorption and increase duration of anesthesia. Spiral anesthesia with Nov is contraindicated in patients with generalized septicemia: sepsis at the proposed injection site; certain diseases of the cerebrospinal system ,e.g.meningitis, syphilis and a known hypersensitivity to the drug, drugs of a similar chemical configuration or aminobenzoic acid or its derivatives. Trimecaine has two main application fields. The first one is local anesthesia (topical ,infiltrational, topical mucosal and inhalational,spinal and Bier´s intravenous).The other field is prophylaxis and therapy of ventriculous arrhythmia on myocardial infarction and in cardiosurgery. It is also used for prophylaxis of sympathic reaction during tracheal intubation.

Synthesis of coordination compounds and study of their properties by modern physical-chemical methods is one of the most important tasks in chemistry. These data enrich and contribute to the development of inorganic, physical, analytical chemistry. Coordination compounds are found in living organisms too. They contain complex-forming agents and ligands by specific ratio. Disruption of this balance results in development of pathological processes in organism. Therefore, alongside with chemical interests, study of coordination compounds is important not only for explaining biochemical processes in living organisms but also for making of new therapeutic preparations.There is no vital process, branch of science or technology without involvement or application of coordination compounds. In living organisms, complex-forming agents are biometals: Zn, Fe, Co, Mn, Mg, Cu,Cr and others are vital elements that play significant role in metabolism by creating natural conditions for heart muscle and nervous system functioning. They are part of enzymes and serve as catalysts of biochemical reactions of phospholipids, collagen, peptides hydrolysis. They participate in redox processes. Biometals in chelate forms function as stimulators that contribute growth-development, propagation, productivity, and resistance to diseases of living organisms [17]. Due to antioxidant, antiseptic properties some synthezied metal complex-formations are successfully used in medicine for anemia, tuberculosis, metal-deficiency diseases treatment, in agriculture –as ecologically safe admixes. Recent research provided great potential for coordination compounds in the creation of anti-diabetes, anti-cancer preparations [24-29].

EXPERIMENTAL OR MATERIALS & METHODS

Research infrastructure for project implementation

1.Transition metals salt:

$Ni(NCS)_2$,$Co(NCS)_2$,.KNCS,$NiCI_2 \cdot 6H_2CoCI_2 \cdot 6H_2O$, $NiBr_2$,$CoBr_2$,HBr.

2.Organic ligands: Lidocaine (Lid·HCI) and Novocain(Nov·HCI).

3.Ethanol-96%,Methanol-98,4%,Benzol-C_6H_6,Efir-$(C_2H_5)_2O$.

Anesthetic preparation; Lidocaine and Novocain are present in the European Pharmacopoeia in two forms: The free base, not very stable and characterized by a very low solubility in aqueous solution and the chloride salt, characterized by a very high soluble in aqueous and used generally for the preparation of injection solutions. To modify and improve solubility, stability and therefore efficacy of the free base, Lidocaine is usually made available as salts.

Interest in synthesis and study of new coordination compounds containing various safe organic ligands is determined by their diverse application. We pursue to achive one part of the objective: to synthesize and study coordination compounds of biometals and local anesthetics.

All solvents and reagents were obtained from commercial sources and were used as received: without further purification.

Interest in synthesis and study of new coordination compounds containing various safe organic ligands is determined by their diverse application. We pursue to achive one part of the objective: to synthesize and study coordination compounds of biometals and local anesthetics. All Coordination Compounds were characterized by the:

Fourier transform infrared spectra of the starting (Lid and Lid·HCl·H_2O; Nov and Nov·HCl·), reference (Lid·HNCS, Nov·HNCS), and complexes were recorded on a Agilent Cary 630 FTIR spectrometer over the wavenumber range 4000 – 500 cm^{-1} using KBr pellets. Elemental analyses were performed using a Labertherm CHN elemental analyser. Melting points have been measured on the Dynalon SMP_{10} device.

Thermal resistance of the complexes were studied on Derivatograph Paulic F.,Paulic I.,Erdey L.X-ray Diffractometer Dron-4–To detect crystalline samples of compounds with X-ray-diffraction parameters and structure.

RESULTS

The experiment was carried out in water, water-ethanol solutions and various organic solvents or in their mixtures. The optimal parameters (solvent, pH of solution, temperature) were established for the original method of syntheses.

Ni(II) and Co(II) complexs of lidocaine (**1,2**),and Novocain(**3,4**) are prepared in water-methanol solution (pH=5-6) with 1:2:4 molar ratio of the nickel chloride ($NiCl_2·6H_2O$),Cobalt chloride($CoCI_2·6H_2O$) , lidocaine, Novocain and potassium thiocyanate (KSCN). The prepared mixture was filtered, placed on a magnetic stirrer with heating for a while, and then left at room temperature for slow evaporation; After 3-4 days green crystals were formed. The resulting complexes were washed with ether and dried in air. Anal Calculated for **1**, $C_{32}H_{50}N_8O_4S_4Ni$: C 48.18;
H 6.32; N 14.04;S 16,08;Ni 7,36. found: C 47.92;
H 6.09; N 14.01;S 15,84;Ni7,26 Isolated yield 68%. Chemical formula of pale green crystals is a $(LidH)_2[Ni(NCS)_4]·2H_2O$.

Anal.Calculated for **2**, $C_{32}H_{50}N_8O_4S_4Co$:C 48.16; H 6.31; N 14.04;S 16,07;Co 7,38. found: C 47.81; H 6.28; N 13.94;S 16,12;Co 7,48. Isolated yield 69%. Chemical formula of blue crystals are a $(LidH)_2[Co(NCS)_4]·2H_2O$.

Anal.Calculated for **3**, $C_{30}H_{46}N_8O_6S_4Ni$:C 44.94; H 6.00; N 13.98;S 15,99;Ni 7,32. found: C 44.51; H 5,54; N 14,01;S 15,16;Ni 6,98. Isolated yield 65.5%. Chemical formula of green crystals are a $(NovH)_2[Ni(NCS)_4]·2H_2O$.

Anal.Calculated for **4**, $C_{30}H_{46}N_8O_6S_4Co$: C 44.93; H 5.78; N 13.97;S 15,99;Co 7,35. found: C 44.62; H 5.61; N 13.42;S 15,37;Co 7,08. Isolated yield 64% Chemical formula of blue crystals are a $(NovH)_2[Co(NCS)_4]·2H_2O$..

Ni(II) and Co(II) complexes of lidocaine (**5**),and (**6**) are prepared in water-ethanol solution (pH=5-6) with 1:2 molar ratio of the nickel chloride ($NiCl_2·6H_2O$),Cobalt chloride($CoCI_2·6H_2O$) and lidocaine. .After 6-7 days green crystals(**5**), dark blue crystals(**6**) were formed at room temperature. The resulting complexes were washed with ether and dried in air. Anal.Calculated for **5**, $C_{28}H_{50}N_4O_4Cl_4Ni$:C 47.55; H 7.12; N 7.92;Cl 20,05;Ni 8,30. found: C 47.42; H 7,06; N 7,54;Cl 19,83 Ni 8,11. Isolated yield 70%. Chemical formula of green crystals are a $(LidH)_2[NiCl_4]·2H_2O$.

Anal.Calculated for **6**, $C_{28}H_{50}N_4O_4Cl_4Co$:C 47.54; H 7.12; N 7.92;Cl 20,04;Co 8,33. found: C 47.34; H 7.02.; N 7.82;Cl 19.84;Co 8,18. Isolated yield 72%.. Chemical formula ofdark blue crystals are a $(LidH)_2[CoCl_4]·2H_2O$.

Ni(II) and Co(II) complexes of lidocaine (**7**) and (**8**) are prepared in water-ethanol solution (pH=5-6) with 1:2:4 molar ratio of the nickel bromide ($NiBr_2$),Cobalt bromide($CoBr_2$) lidocaine and HBr.Green compounds of (**7**)**,** and blue of (**8**) grew after ten days.

Anal.Calculated for **7**, $C_{28}H_{50}N_4O_4Br_4Ni$:C 38.00; H 5.69; N 6.33;Br 36,11;Ni 6,63. found: C 37.72; H 5,41; N 6,18;Br 36,10 Ni 6,12. Isolated yield 64, 6%. Chemical formula of green crystals are a $(LidH)_2[NiBr_4]·2H_2O$.

Anal.Calculated for **8**, $C_{28}H_{50}N_4O_4Br_4Co$:C 37.99; H 5.69; N 6.33;Br 36,10;Co 6,66. found: C 37,27; H 5,18;N 6.12;Br 35,98;Co 6,29.Isolated yield 65%. Chemical formula of cherry color crystals are a $(LidH)_2[CoBr_4]·2H_2O$.

Microelemental analysis and melting temperature determination proved composition and identity of synthesized compounds.Their solubility in water and organic solvents has been studied.

The corresponding chemical formulas, melting points and their solubility in water and organic solvents are given in Table 1.

Table1.Results of measuring of melting point and solubility for prepared compounds

№	Solubility			Melt. T°C
	H_2O	C_2H_5OH	CH_3COCH_3	
1	Slig.sol.	+	+	188
2	Slig.sol	+	+	176
3	Slig.sol.	+	+	184
4	Slig.sol.	+	+	181
5	Soluble	+	+	112
6	Soluble	+	+	109
7	Soluble	+	+	110
8	Soluble	+	+	103

DISCUSSION

In the process of searching for new biologically active complexes in the role of ligands, anesthetic preparations with pharmacological and therapeutic potential were selected. According to the chemical structure, local anesthetics are divided into two groups: esters and amides. Novocain is an ester, and lidocaine belongs to the amide group. The presence of amide group causes the properties of substances to enter into hydrolysis reactions under the action of acids and alkalis. The presence of a tertiary nitrogen atom of organic bases (tertiary aliphatic amino group) limits the basic properties of ligands and the ability to enter into complexation reaction. Diring experiments it was established that Lidocaine complexes were synthesized more easily, than Novocaine complexes.

Compared with lidocaine, ester bonds are unstable, quickly destroyed, have a short duration and show a weak complexing ability.Preparation of complexes had been investigated in various metal-ligand stoichiometric ratios. It was established that at any initial metal-ligand ratio composition of complex compounds is respectively 1: 2. The Lid·HCl and Nov·HCl complexes of Ni(II) and Co(II) were synthesized and characterized by elemental analysis, IR spectra,thermoanalytical TG-DTG/DTA and X-ray diffraction methods.

The IR spectrum of the lidocaine free base showed sharp adsorption peaks at 3249 cm^{-1} due to amide N–H stretch, at 1667 cm^{-1} due to amide C=O stretch, and at 1506 cm^{-1} due to aromatic C=C bending vibrations. The benzene ring in lidocaine molecule helps produce the peak at about the 3030 cm^{-1} due to aromatic C–H stretch vibrations, other weak but resolved peaks are observed at 1476 and 1293 cm^{-1} due to amide band and III vibrations, as well as a peak in the fingerprintregion at 765 cm^{-1} due to deformations of 1,2,3-trisubstituted aromatic ring.[30]

As in the long-standing work on the IR spectra of lidocaine salts and modern publications [31,32,29,33] no attempt was made to disentangle and assign the generally poorly resolved C–H stretching bands near 3000 cm^{-1} arising from the N-ethyl substituents ($\nu_{asym}(CH_2)$ near 2930 ± 10 cm^{-1}, $\nu_{asym}(CH_3)$ near 2960 ± 10 cm^{-1}, and $\nu_{sym}(CH_3)$ near 2870 ± 10 cm^{-1}) and the methyl substituents of the phenyl ring usually giving prominent bands near 2925 and 2865 cm^{-1} as well as variable intensity bands near 2975 and 2945 cm^{-1}. Perhaps the band at 2800 cm^{-1} in the spectrum of lidocaine free base can be assigned to $\nu_{sym}(CH_2)$ for the methylene group at the nitrogen atom with a stretching frequency usually lowered from its value in hydrocarbons near 2850 cm^{-1}, but this effect is completely eliminated when the nitrogen acquires a positive charge in amine salts.

The IR spectra of lidocaine salts and complexes show adsorption peaks due to NH^+ stretching vibrations. The IR spectrum of lidocaine hydrochloride monohydrate, all eight peaks and shoulders at 2640 2460 cm^{-1} noted in [34] are observed, but for complexes these peaks have higher frequencies, as is the case with salts of strong acids .In addition, in complexes, NH^+ stretching peaks overlap with C–H stretching bands. Following the authors of [34], we locate the center of gravity of the NH^+ band and ignore the C–H stretching bands summarizing the vibration frequencies in lidocaine, its salts and complexes .

The IR spectrum of Lid·HCl·H_2O also demonstrates two narrow peaks at 3460 and 3390 cm^{-1} due to O– stretching vibrations in hydrogen-bonded water molecules, these peaks are also visible in the spectra of lidocaine complexes. It is believed that the IR is a tool that allows identification of the formation of hydrogen bond interactions, by the shift of the bands of the functional groups involved in the formation of the hydrogen bonds. However, this tool does not always lead to correct results. For example, according to the IR study [34], the lidocaine hydrohexafluoroarsenate is essentially free of hydrogen bonding, but the X-ray analysis [30] is in conflict with this conclusion.

The IR spectrum of the lidocaine thiocyanate, Lid·HCNS, shows very strong peak at 2068 cm^{-1} corresponding to the first fundamental frequency [35]of the thiocyanate C–N stretching, and weak peaks of the second (396 cm^{-1}) and third (770 cm^{-1}) fundamental frequencies. According to data of Bertini & Sabatini [36], in IR spectra of substituted thiocyanate complexes the C–N stretching assumes characteristic forms and values: >2100 cm^{-1} and sharp for S-bonded thiocyanates, and ≤2100 cm^{-1} and broad for N-bonded ones. The second and third fundamental frequencies are also sensitive to the type of bonding: 450-490 and 760-880 cm^{-1} for N-bonded thiocyanates, 400-440 and ≈700 cm^{-1} for S-bonded thiocyanates. In the Ni(II) complex **1** the first fundamental frequency is 2124 cm^{-1}, which indicates S-bonding, but the peak is rather narrow (<4 cm^{-1} at half height), as well as the second and third fundamental frequencies are 480 and 810 cm^{-1}, respectively, and this indicates N-bonding. The same inconsistency occurs for the Co(II) complex **2.**The IR-spectroscopic researches of the **5,6,7,8** complexes indicate that Co(II) and Ni(II) coordinate directly with acidoligands(Me-hal bond) in the complexes.The evidence of that is existence of just one adsorption band of 425 and 430 cm^{-1} in the IR-spectra of complexes. Molecule of Lidocaine as cation forms outer sphere as a result of protonating(3410 and 3446cm^{-1}) of trio nitrogen atom.

By the analysis of IR spectrum of pure novocaine(procaine)[37],one can notice the presence of several distinctive bands, characteristic to vibrational modes of functional groups, as follows: a doublet consisting of two sharp N-H stretching bands at3345 and 3314 cm-^{1},a–NH_2 scissoring band at 1604 cm-^{1}and –NH_2 wagging and twisting bands in the 850-750 cm-^{1}spectral range. The band around 3200 cm-^{1}can be assignedto ammonium ions (due to the fact that procaine was use das a chlorohydrate) The spectrum also shows a C-N stretching band in 1360-1250 cm-^{1}range characteristic for aromatic amines. The presence of a tertiary amino group is sustained by the -N-CH_2 stretching band around 1170 cm-^{1}.The two most polar bonds in esters are the C = O and C-O respectively, which produce distinctive bands in the spectrum around 1700 cm-^{1}and 1200 cm-^{1}, respectively. Being an aromatic ester, it is expected that aromatic C = O stretching appears at lower wavenumbers than the ones characteristic for aliphatic ones (which absorb near1750 cm-^{1}), in this case at 1692 cm-^{1}.Ontheotherhand, the C-O stretching can be attributed to the intense band around 1250 cm-^{1}[38].Studying the spectra of compounds **3,4** does not make it possible to conclude that the connection between the metal and novocaine occurs.Here,the ligand is protonated and acts as a cation and the vibration band in the140-400cm-^{1}region corresponds to the stretching vibrations of the tetrahedral anion $[M(NCS)_4]^{2-}$.

To study the thermal stability and the sequence of the thermal process, the following compounds were studied:$(LidH)_2[Ni(NCS)_4]\bullet 2H_2O$ **(1)**,$(LidH)_2[Co(NCS)_4\cdot 2H_2O$**(2),**$(LidH)_2[NiCI_4]\cdot 2H_2O$ (**5**),$(LidH)_2[CoCI_4]\cdot 2H_2O$(**6**). The heating velocity was V=10°/sec. The thermogrames are characterized by the DTG curve of the endo and exo-effects, which is due to their physical-chemical transformations. [39].Thermal decomposition of each complex starts with dehydration, and than the decomposition of organic parts goes. The thermal dehydration of the complexes takes place in one, or two steps. At the first endo effect within 170-180 ° C temperature interval, dehydration of the complexes takes place. The following endo-effects on 250° -280°C (Ni(II) complexes(**1)** mass loss is 66,36%,calculated 67,68%; Co(II) complexes(**2**) mass loss is 62,92%,calculated 63,26%),on 300°-320°C(Ni(II) complexes(**5**) mass loss is 66,92%,calculated 66,26%; Co(II) complexes(**6**) mass loss is 65,57%,calculated 65,80%) correspond to the oxidation of two molecules of the organic ligand of lidocaine. A strong exoelectric effect on 540° -560°C ((**1)** mass loss is 87,39%,calculated 87,78%;(**2**) mass loss is 92,22%,calculated 92,38%),on 600°-620°C((**5**) mass loss is 92,22%,calculated 92,38%;(**6**) mass loss is 90,83%,calculated 91,37%) cleaves acid ions. The decomposition mechanism and the thermal stability of the complexes under investigation were determined on the basis of their structures. Metal oxides were obtained as the final decomposition product(650-700 ° C) which is confirmed by chemical analysis on metals.

The crystal structure of bis(lidocaine) tetrathiocyanonickelate(II)dihydrate $(LidH)_2[Ni(NCS)_4]\cdot 2H_2O$-(**I)** was performed in an Oxford Diffraction Gemini-R Ultra, Ruby CCD diffractometer. The structure was solved using SHELXL2017/1 program [40-41]

Complex-(**1)** crystallizes in the monoclinic space group $P2_1/c$ with a = 18.3509(5), b = 7.6532(2), c = 14.9585(4) Å, β = 109.964 (2)°, V = 1974.57 (9) Å^3, and Z = 2. Coordination of the Ni^{2+} ion with ligands generates octahedral anion $Ni[(NCS_4)\cdot 2H_2O]^{2-}$ with N-bonded thiocyanates, while two protonated cations $LidH^+$ remain in an outer coordination field.Oxygen atoms of water molecules lie on a straight line O–Ni–O and are spaced from the central atom by the same distance of 2.0987(9) Å, but nitrogen atoms in the $Ni[N_4O_2]$ octahedron are located at different distances from the central nickel atom , and the angles between the N–Ni–N bonds slightly deviate from 90 degrees with a minimum of 87.89(4)^o for angle $N1^i$–Ni–N2 and a maximum value of 92.11(4)^o for angles N1–Ni–N1 and N1–Ni–N2.

.

CONCLUSIONS

The study of biometal coordination compounds in this direction is not only et a theoretical significance, but also potential application in the metallotherapeutic and contemporary chemical-pharmaceutical industry. Actuality of synthesis and study of new coordination compounds containing various safe organic ligands is conditioned by their diverse application. We pursue to resolve one part of this big problem: to obtain and study coordination compounds of transitional- and bio-metals and local anesthetics, in particular: Novocaine and Lidocaine. The Lid·HCI, or Nov·HCI complexes of Ni(II) and Co(II) with general formula $(LidH)_2[MeX_4]\cdot 2H_2O$, $(NovH)_2[MeX_4]\cdot 2H_2O$, were X = Cl, NCS, have been synthesized and characterized by elemental analysis, IR spectra, , thermoanalytical TG-DTG/DTA and single-crystal X-ray diffraction methods. Thermal decomposition of each complex proceeds stepwise.

. The structure of the compounds is proposed based on infrared absorption spectrum analysis, X-ray diffraction analyses and the literature data: In compounds, the central ion coordination with acidoligands generates tetrahedral anion, while the ligands in the form of protonated cations remain in an outer coordination field [42-43]..

Bis(lidocaine) tetrathiocyanonickelate(II) dihydrate $(LidH)_2{\cdot}Ni{\cdot}(NCS)_4{\cdot}2H_2O$ crystallizes in the monoclinic space group $P2_1/c$ with a = 18.3509(5), b = 7.6532(2), c = 14.9585(4) Å, forming structure of molecular crystal with slightly distorted $Ni[(NCS)_4(H_2O)_2]^{2-}$ octahedrons symmetrically associated with two $LidH^+$ ions by hydrogen bonds.

ACKNOWLEDGMENTS

We acknowledge to Shota Rustaveli National Science Foundation of Georgia (SRNSFG) for financial support.(Project 18-3889).

REFERENCES

[1]. Selvaganapathy M., Raman N. "Pharmacological Activity of a Few Transition Metal Complexes: A Short Review". *Journal of Chemical Biology & Therapeutics*, 2016, vol. 1, issue 2, pp. 108-125. doi:10.4172/2572-0406.1000108.

[2]. Dabrowiak J.S. Metals in Medicine (Inorganic Chemistry: A Textbook Series). John Wiley & Sons: Chichester UK, 2009, 320 p.

[3]. Thompson K.H. Encyclopedia of Inorganic Chemistry. John Wiley & Sons: Chichester UK, 2011.

[4]. Roat-Molane R.M. Bioinorganic Chemistry: A Short Course. John Willey & Sons: Chichester UK, 2007, 541 p.

[5]. Williams R.J.P.. "Bio-inorganic chemistry. Its conceptual evolution". *Coordination Chemistry Review*, 1999, vol. 100, p. 573-610.

[6]. Hossain M., Bashar A., Khan N., Roy P.K., Ali S., Farooque A. "Preparation, physical characteriza tion and antibacterial activity of Ni(II), Co(II), Cd(II), Zn(II) and Cr(III) Schiff base complex compounds''. *Bangladesh. Science Journal of Chemistry*, 2018, vol.6, issue 2, pp.17-23.

[7]. Yadav M., Debasis Behera. ",Synthesis, characterization and biological activity of Mn(II), Fe(II), Co(II), Ni(II), Cu(II), Zn(II) and Cd(II) complexes of N-thiophenoyl-N′-phenylthiocarbohydrazid". *Journal of Chemistry. Department of Applied Chemistry, Indian School of Mines (India)*. 2012, vol. 2013, article ID 721397, 8p. doi: 10.1155/22013/721397.

[8]. Guerra W., Silva-Caldeira P.P., Tezenzi H., Pereira-Maia E.C.. "Review. Impact of metal coordination on the antibiotic and non-antibiotic activities of tetracicycline-based drags". *J. Coordination Chemistry Reviews*, 2016, vol. 327-328. pp. 188-189. Doi: 10.1016/j.ccr 2016.04.009.

[9]. Khoo T. J., Bin Break., M.K., Crouse K.A., Tahir M.M., Ali A.M. et. al. ''Synthesis and biological activity of two Schiff base ligands and their Ni(II), Cu(II), Zn(II), Cd(II) complexes derived from S-4-picolyldithiocarbazate and X-ray cristal structure of Cd(II) complex''. *J. Inorganic Chem. Acta*, 2014, vol. 413, pp. 68-76.

[10]. Gurunath S., Kurdekar, Sathisha Mudigoudar Puttanagouda, Naveen V.Kulkarni, Srinivasa Budagumpi,Vidyanand K.Revanhar. ,,Synthesis, characterization,antibiogram and DNA binding studies of novel Co(II),Ni(II),Cu(II) and Zn(II) complezes of Schiff base ligands with quinolone core". *Medicinal Chemistry Research*, 2011, vol. 20, issue 4, pp. 421-429.

[11]. Patel K.S., Patel J.C., Dholariya H.R., Patel V.K., Patel K.D. "Synthesis of Cu(II), Ni(II), Co(II), and Mn(II) complexes with ciprofloxacin and their evaluation of antimicrobial, antioxidant and anti-tubercular activity". *Indian Journal of Scientific Research*, 2012, vol. 2, issue 3, p.49-59. doi: 10.4236/ojmetal.2012.23008.

[12]. Barnes K.R., Cisplatin Lippard S.I. "Related anticancer drugs, recent advances and insighrs", in:. Sigel A., Sigel H. (Eds) Metal Ions in Biological Systems'', Marcel Dekker: New York, 2004, vol.42, pp.143-177,.

[13]. Ang W.H., Dyson P.J. "Classical and non-classical ruthenium-based anticancer drugs: Towards targeted chemotherapy''. *European Journal of Inorganic Chemistry*, vol. 2006, issue 20, pp. 4003-4018. Doi:10.1002/ejic.200690041.

[14]. Devi J., Batra N. "Synthesis, characterization and antimicrobial activities of mixed ligand transition metal complexes with isatinmonohydrazone Schiff base ligands and heterocyclic nitrogen base". *J. Spectochim Acta A Mol. Bimol. Spectosc*. 2015, vol. 135, pp.710-719.

[15]. Shen S., Chen H., Zhu T., Ma X., Xu J., Zhu W. et al. "Synthesis, characterization and anticancer activities of transition metal complexes with a nicotinhydrazone ligand". *Oncology Letters*, 2017, vol.13, issue 5, pp 3169-3173.

[16]. Bertram G., Susan B., Anthony J. Basic & Clinical Pharmacology.Twelfth Edition. Lange Basic Science, 2012, 1248 p.

[17]. Katzung B.G., Masters S.B., Trevor A.J. Basic & Clinical Pharmacology. McGraw-Hill Medical: New York, 2012, 1248 p.

[18]. Mashkovsky M.D. Lekarctvennie Sredstva (Medicines). Medicina: Moskow, vol. 1, 1994, 715 p. (in Russian).

[19]. Alster T., Garden J., Fitzpatrick R., Rendon M., Sarkany M., Adelglass L. "Lidocaine/ tetracaine peel in topical anesthesia prior to laser-assisted hair removal: Phase-II and Phase-III

study results". *USA J. Dermatology Treatment*, 2014, vol. 25, pp.174-196.

[20]. Wilhelm I.R., Tzabazis A., Likar R., Sittl R., Griessinger N. "Long-term treatment of neuropathic pain with a 5% lidocaine medicated plaster". *European Journal Anesthesiology*, 2010, vol. 27, pp.169-182.

[21]. Slaughter L.A., Patel A.D. Slaughter J.L. "Pharmacological treatment of neonatal seizures: a systematic review". *Journal of Child Neurology*, 2013, vol. 28, no 3, pp. 351–64. doi:10.1177/0883073812470734.

[22]. Ordabayeva S.K. Pharmaceutical Chemistry of Aromatic Compounds. Curriculum. Shymkent, 2018, 270 p. (in Russian))

[23]. Reynolds J.E.F. Martindale – The Extra Pharmacopoeia, 30th Edition. Pharmaceutical Press: London, 1993, 1016 p..

[24]. Barta Hollo B., Magyari J., Armakovic S., Bogdanovic G.A., Rodic M.V., Armakovic S.J., Molnar J., Spengler G., Leovaca V.M., Meszaros Szecsenyi K. "Coordination compounds of hydrazine derivative with Co(II),Ni(II),Cu(II) and Zn(II):syntehesis,characterization,reactivity assessment and biological avaluation". *New Journal of Chemistry*, 2016, vol. 40, issue 7, pp.5885-5895.

[25]. Braga D., Chelazzi L., Dichiarante E., Chierotti M.R., Gobetto R. "Molecular salts of anesthetic lidocaine with dicarboxylic acids:solid-state properties and a combined structural and spectroscopic study". *Torino,Italy.American Chemical Society,Crystal Growth Design*, 2013, vol. 3, pp. 2564-2572. Doi: 10.1021/cg400331hI.

[26]. Puglia C., Saprietro M.G., Bonina F., Castelli F., Zammataro M., Chiechio S. "Development, characterization and in vitro and in vivo evaluation of benzocaine and lidocaine-loaded nanostructired lipid carriers". *University of Catania, Italy.Journal of Pharmacceutical Science*, 2010, vol. 100, issue 5, pp. 1892-1899. Doi: 10.1002/jps.22416.

[27]. Robinson J.K., Hanke C.W., Sengelmann R.D., Siegel D.M. Surgery of Skin. (Eds Bhatia A.C., Rohrer T.E). Elsevier: Amsterdam, 2005, 872 p.

[28]. Reed K.L., Malamed S.F., Fonner A.M. "Local anesthesia. Part 2: Technical considerations". *Anesthesia Progress*, 2012, vol. 59, no 3, pp. 127-137. Doi: 10.2344/0003-3006-59.3.127

[29]. Tabrizi L., McArdle P., Erxleben A., Chiniforoshan H. "Nickel(II) and cobalt(II) complexes of lidocaine: Synthesis, structure and comparative in vitro evaluations of biological perspectives". *European Journal of Medicinal Chemistry*, 2015, vol. 103, pp. 516-529. Doi: 10.1018/j.ejmech. 2015.09.018

[30]. Hanson A.W., Röhrl M. "The crystal structure of lidocaine hydrochloride monohydrate". *Acta Cryst*., 1972, vol. B28, pp. 3567-3571. Doi: 10.1107/SO567740872008350

[31]. Powell M.F. "Lidocaine and lidocaine hydrochloride". *Analytical Profiles of Drug Substances*, 1986, vol. 15, pp. 761-779.

[32]. Badawi H.M.; Förner W., Ali S.A. "The molecular structure and vibrational, 1H and 13C NMR spectra of lidocaine hydrochloride monohydrate". *Spectrochim. Acta Part A Mol. Biomol. Spectrosc*., 2016, vol. 152, pp. 92–100.

[33]. Sridhar M.A., Indira A, Prasad S., Cameron T.S. "Crystal structure of lignocaine tetrabromozincate, $(C_{14}H_{22}ON_2)_4$ $(ZnBr_4)_2$" *Zeitschrift für Kristallographie*, 1997, vol. 212, no 10), pp. 391-392.

[34]. Neville G.A., Regnier Z.R. "Hydrogen bonding in lidocaine salts. The NH+ stretching band and its dependence on the associated anion". *Canadian Journal of Chemistry*, 1969, vol. 47, pp. 4229-4235.

[35]. Jones L.H.. "Infrared spectrum and structure of the thiocyanate ion". *Journal of Chemical Physics*, 1956, vol. 25, no 5, pp. 1069-1072. Doi: 10.1063/1.1743101

[36]. Bertini I., Sabatini A. "Infrared spectra of substituted thiocyanate complexes. The effect of the sustituent on bond type". *Inorganic Chemistry*, 1966, vol. 5, no 6, pp. 1025–1028. Doi: 10.1021/ic50040a017

[37]. Fuliaș A., Ledeți I., Vlase G., Popoiu C., Hegheș A., Bilanin M., Vlase T., Gheorgheosu D., Craina M., Ardelean S., Ferechide D., Mărginean O., Moș L. **"**Thermal behaviour of procaine and benzocainePart II: compatibility study with somepharmaceutical excipients used in solid dosage forms". *Chemistry Central Journal (Romania)*, 2013, vol. 7, pp. 140-152. doi: 10.1186/1752-153X-7-140.

[38]. Silverstein R.M., Webster F.X., Kiemle D. Spectroscopic Identification of Organic Compounds. John Wiley & Sons: New York, 2005.

[39]. Machaladze T. ,Thermal Analysis'. Georgian Technical University: Tbilisi, Georgia, 2006, 91 p. (in Georgian).

[40]. Rigaku Oxford Diffraction, 2015 (https://www.rigaku.com/en/products/smc/crysalis).

[41]. SHELXSL2017/1, Program for the solution of crystal structures, G. M. Sheldrick, University of Göttingen, Germany, 2017

[42]. Zhorzholiani N.B., Metreveli L.A., Amirkhanashvili K.D., Lomtadze O.G. Study of Tetra-Acid Complexes with Anesthetic

Preparation. 5th International Conference ,,Nanotechnologies",N a no-2018, November 19-22,2018, Tbilisi, Georgia,pp.185-186. ISBN 978-9941-28-320-8.

[43]. Tsitsishvili V., Zhorzholiani N., Amirkhanashvili K. "Synthesis and crystal structure of trimecaine hexachlorostannate(IV) monohydrate". *International Journal of Scientific Engineering and Science*., 2018, vol. 2, issue 2, pp. 4246-4254. https://www.academia.edu//36284704.

ბიოლითონთა კომპლექსები ანესთეზიურ ნივთიერებებთან

კობა ამირხანაშვილი*, ნანი ჟორჟოლიანი, ლელა მეტრეველი, ვლადიმერ ციციშვილი

პეტრე მელიქიშვილის ფიზიკური და ორგანული ქიმიის ინსტიტუტი,ივანე ჯავახიშვილის ბილისის თბილისის სახელმწიფო უნივერსიტეტი;პოლიტკოვსკაიას 31, 0186, თბილისი,საქართველო.
amirhan@hotmail.com, 995 77 420062

რეზიუმე. ეთანოლწყალხსნარებში გარდამავალი ლითონის მარილისა და ანესთეზიურ პრეპარატ ლიდოკაინის (Lid·HCI) ან ნოვოკაინის(Nov·HCI) ნებისმიერი თანაფარდობისას,სუსტ მჟავა არეში ხდება ლიგანდის პროტონირება და მიიღება შემდეგი შედგენილობის კოორდინაციული ნაერთები: $(LidH)_2[MeX_4]\cdot 2H_2O$, $(NovH)_2[MeX_4]\cdot 2H_2O$, სადაც M-Co(II),Ni(II),X-NCS′,CI′,Br′.სინთეზირებული კომპლექსების შედგენილობა და ინდივიდუალობა დადგენილია მიკროელემენტური ანალიზით.შესწავლილია მათი ხსნადობა წყალსა და ორგანულ გამხსნელებში. ნაერთთა თერმული დაშლა იწყება დეჰიდრატაციით(170-180°C),ხოლო ორგანული ლიგანდი იჟანგება 560-620°C ტემპერატურულ ინტერვალში.დაშლის საბოლოო პროდუქტი ლითონთა ოქსიდებია. X-ray დიფრაქტომეტრიის პარამეტრების გათვალისწინებითა და .შთანთქმის ინფრა-წითელი.სპექტრების შესწავლის საფუძველზე დადგენილია მათი აღნაგობა: ნაერთებში ცენტრალურ იონთან კოორდინირებს აციდოლიგანდები და წარმოქმნის ტეტრაედრულ ანიონს,ხოლო ლიგანდები პროტონირებული კატიონის სახით გარე კოორდინაციულ სფეროშია. ჩატარებულია ლიდოკაინისა და $(LidH)_2[Ni(NCS)_4]\cdot 2H_2O$ შედგენილობის მონოკრისტალის სრული რენტგენოსტრუქტურული ანალიზი და დადგენილია მათი სტერეოქიმია.ნაერთი კრისტალდება მონოკლინურ სინგონიაში.მოლეკულური სტრუქტურა ფორმირდება ოქტაედრული $[Ni(NCS)_4(H_2O)_2]^{2-}$ იონისა და ორი სიმეტრიულად განლაგებული $LidH^+$ კატიონისაგან.